

FILE 62

(1)

AD-A206 241



DTIC
ELECTE
APR 04 1989
S D
D. C.

DISTRIBUTION STATEMENT A
Approved for public release
Distribution Unlimited

DEPARTMENT OF THE AIR FORCE
AIR UNIVERSITY

AIR FORCE INSTITUTE OF TECHNOLOGY

Wright-Patterson Air Force Base, Ohio

89 4 03 045

①

AFIT/GA/ENY/88D-05

DTIC
S ELECTRIC D
APR 04 1989
D &

FRACTIONAL-ORDER FEEDBACK

IN LINEAR SYSTEMS

THESIS

Kevin D. Klonoski
Captain, USAF

AFIT/GA/ENY/88D-05

Approved for public release; distribution unlimited

AFIT/GA/ENY/88D-05

FRACTIONAL-ORDER FEEDBACK IN LINEAR SYSTEMS

THESIS

Presented to the Faculty of the School of Engineering
of the Air Force Institute of Technology

Air University

In Partial Fulfillment of the
Requirements for the Degree of
Master of Science in Astronautical Engineering

Kevin D. Klonoski, B.S.

Captain, USAF

March 1989

Approved for public release; distribution unlimited

Accession For	
NTIS CRA&I	<input checked="checked" type="checkbox"/>
DTIC TAB	<input type="checkbox"/>
Unannounced	<input type="checkbox"/>
Justification	
By	
Distribution /	
Availability Codes	
Dist	Avail and/or Special
A-1	

Preface

The original intent of this effort was to produce a fractional order sensor for use in monitoring structural vibrations. As the work progressed it was expanded to include analog simulation and proof-of-concept for fractional-order feedback. This goal was achieved. Incorporating fractional-order circuits into active feedback control systems will provide many advantages for controls engineers.

Many thanks to my advisor, Lt Col Ron Bagley. I don't know if I can ever thank you for your patience, understanding and commitment. Dr. Torvik, thank you for insulating me from the repercussions that could have been there for not finishing on time. Thank you, Maj Kolesar for your comments on the A/D recorder. It was the key to our success.

To members of my family (the Fischer clan) and Emmanuel Lutheran Church, thanks for your prayers and support. Special thanks to Wil Schonscheck for weekly putting life into proper perspective.

To my wife and kids: Nita, your patience, encouragement and love were there when I needed them most. Nathan and Katie, teenagers deserve more than a dad whose nose is buried in a book except when telling you to clean your room and wash dishes. Josh and Gabe - Daddy will finally be able to play soccer with you again.

Finally, the real credit belongs to Jesus Christ who's given me all I have and sees me through the trials - even though at times the battles seem overwhelming. Through Him, the final victory's ours.

Table of Contents

	Page
Preface	ii
List of Figures	v
List of Tables	viii
List of Symbols	ix
Abstract	xii
I. Introduction	1
Problem Statement	2
Approach	2
Scope	3
Assumptions	4
II. Background	6
Evolution of Fractional Calculus	6
Physical Application	8
Summation	10
Potential Sources of Development	11
III. Theory	14
IV. Experimental Procedure	24
Overview	24
Domino Ladder Circuit Fabrication	25
Domino Ladder Circuit Performance Evaluation	28
Domino Ladder Circuit and Analog Combination	35
Domino Ladder Circuit and Analog Verification	36
Fractional Order Equation Synthesis	47
Open- and Closed-Loop Simulation	53
Total Cycle Simulation	58
Final Configuration Testing	66
V. Analysis of Results	70
Introduction	70
Circuit Validation	70
Open and Closed Loop Simulation Problems	78
Theoretical Tools	
Mittag-Leffler Expansion Method	86
Laplace Transform Method	87
Additional Comments	87

VI. Conclusions and Recommendations	92
Summary	92
Areas for Further Study and Development	93
Equipment Improvements	95
Appendix A: Laplace Transform Method for Predicting Time Response Theoretically	96
Appendix B: Fortran Source Code - Laplace Transform Method ...	112
Appendix C: Mittag-Leffler Expansion Method for Predicting Time Response Theoretically	136
Appendix D: Matrix _x ® Code for Mittag-Leffler Method	140
Appendix E: Oldham-Zoski Fractional-Order Differentiating Circuit Design Method	145
Appendix F: Detailed Equipment Set-up and Procedures	150
Appendix G: Oldham - Zoski Circuit Validation Data	167
Bibliography	205
Vita	208

List of Figures

Figure	Page
1. T-Cell Ladder Circuit	16
2. Abbreviated Ladder Circuit	18
3. Oldham-Zoski Circuit Schematic	21
4. Oldham-Zoski Circuits Constructed on Breadboard	26
5. Example of Phase Calculation Parameters	30
6. Circuit 1 Gain Characteristics	31
7. Circuit 1 Phase Angle Characteristics	32
8. Circuit 2 Gain Characteristics	33
9. Circuit 2 Phase Angle Characteristics	34
10. Op-amp and Oldham-Zoski Circuit Combination for $D_t^{1/2}(x)$	36
11. Harmonic Oscillator - Analog Configuration	37
12. Amplitude Checkout Circuit Using Harmonic Oscillator	38
13. Initial $D_t^{3/2}(x)$, $D_t^{1/2}(x)$ Gains Using Theoretical Predictions.	39
14. $D_t^{3/2}(x)$, $D_t^{1/2}(x)$ After Gain Adjustments	40
15. $D_t^{3/2}(x)$, $D_t^{1/2}(x)$ Gain Check at $\omega^2 = 3.5$ rad/sec	41
16. Configuration for $D_t^{3/2}(x)$, $D_t^{1/2}(x)$ Using Only One Fractional Order Circuit	43
17. Results of Integrating $D_t^{3/2}(x)$ to Obtain $D_t^{1/2}(x)$ Directly ...	44
18. Analog Configuration for Producing $D_t^{3/2}(x)$, $D_t^{1/2}(x)$ Using Two Fractional Order Circuits	45
19. $D_t^{3/2}(x)$, \dot{x} , $D_t^{1/2}(x)$ Comparison Using Two Fractional Order Circuits	46
20. Pace® TR48 Analog Computer	47

Figure	Page
21. Patch Cords and Input Jacks	48
22. General Second Order Analog Configuration	51
23. Potentiometer Schematic and Circuit Symbol	52
24. Open-Loop System With Comparator Isolation of $D_t^{1/2}(x)$ Input .	55
25. Closed-Loop System With Comparator Isolation of $D_t^{1/2}(x)$ Input	56
26. Initial Open- and Closed-Loop Response	57
27. Theoretical Open-Loop Response	59
28. Theoretical Closed-Loop Response	60
29. Total-Cycle Analog Configuration	61
30. Complete Open-Loop Total-Cycle Simulation	63
31. Open-Loop Response After Step Function Removal	64
32. Closed-Loop Response After Step Function Removal	65
33. Final Open-Loop Configuration	66
34. Final Closed-Loop Configuration	67
35. Experimental vs Theoretical Comparison for the Open-Loop Configuration	68
36. Experimental vs. Theoretical Comparison for the Closed-Loop Configuration	69
37. Noisy Output Signal When Interfacing the Oldham-Zoski Circuit With the Analog Computer Through a Summing Junction	73
38. Long Leads on Discrete Components	74
39. Theoretical Response Without $s^{-1/2}$ Initial Value Terms	79
40. $1/2$ Derivative Response With Input Not Isolated at $t=0$	82
41. $1/2$ Derivative Response With Input Isolated at $t=0$	83
42. Response to Sinusoidal Forcing Function with $\omega^2 = 3.5$	84

Figure	Page
43. Comparison of Asymptotic Limit Selection for the Laplace Transform Response Method	89
44. Comparison of Mittag-Leffler Expansion And Laplace Transform Reponse Predictions	90
45. Circuit Response With Improper Coefficient Set-up	91
46. Contour Integral Definition for Laplace Transform Method	98
47. Analog Interface Configurations for the Oldham-Zoski Circuit. for Different Fractional Operators	148
48-65 Circuit 1 Validation	169-186
66-83 Circuit 2 Validation	187-204

List of Tables

Table	Page
1. Design and As-Fabricated Oldham-Zoski Circuit Values..	27
2. Circuit Gains - Predicted Versus Experimental Oldham-Zoski - Analog Interface Configuration 4.....	148
3. Details for Realizing the Four Different Analog Computer Interface Configurations for the Oldham-Zoski Circuit	148
4. Circuit 1 Performance Validation Data	168
5. Circuit 2 Performance Validation Data	168

LIST OF SYMBOLS USED

A	- Amplitude of a sinusoidal function
a_i	- Mittag-Leffler expansion parameter for the i_{th} characteristic root
(A)	- Vector of a_i 's
C	- Capacitance, capacitor
c_1	- Visco inertial damping coefficient
c_2	- Viscous damping coefficient
c_3	- Visco inertial damping coefficient
(D)	- Vector of half-derivative operators
dB	- Decibel
D_n	- Minority carrier diffusion coefficient
$D_t^{1/2}(x)$	- One-half derivative of x (viscoelastic)
$D_t^{3/2}(x)$	- Three-halves derivative of x (visco inertial)
E	- Electric potential
$E_{1/n}$	- Mittag-Leffler Expansion Operator
f_M	- Lower frequency limit
f_m	- Upper frequency limit
G	- Geometric capacitance ratio, domino ladder circuit
g	- Geometric resistance ratio, domino ladder circuit
h	- Numeric integration step size
i, j	- $(-1)^{1/2}$; used interchangeably depending on the the background source of the expression
k	- Stiffness coefficient
m	- Mass; nearest integer

n_p	- Excess minority carrier density
n_{p0}	- Excess minority carrier density at equilibrium
r	- Parameterization of Laplace variable along integration path
R	- Resistance, resistor; radius parameterization of Laplace variable in polar coordinates
s	- Laplace transform variable
\hat{s}	- The square-root of the Laplace transform variable
t	- Time
t_{ps}	- Time interval between axis crossings for determining the phase shift difference of two sinusoidal functions
T	- Total period of a sinusoidal function
u	- The real part of the complex variable \hat{s}
$u(t)$	- Forcing or control input function (function of time)
v	- Velocity; imaginary part of complex variable \hat{s} ; voltage
x	- Position
\dot{x}	- Rate
\ddot{x}	- Acceleration
\mathcal{X}	- Laplace transform of x
z	- Vertical distance, continued fraction variable
α	- Ratio of fluid velocity to fluid density; fractional-order power in continued-fraction development
γ	- Offset of inverse Laplace integration path from the imaginary axis
$\Gamma(\)$	- Gamma function (generalized factorial)
\mathcal{E}	- Applied electric field
λ	- Characteristic root, eigenvalue
$[\Lambda]$	- Matrix of characteristic values
μ_n	- Minority carrier mobility

- μ - Mean-value, composite Simpson integration routine
- ρ - Fractional derivative order, $-1 < \rho < 1$; radius parameter in
polar parameterization of s
- σ - The real part of the Laplace transform variable
- τ - Integration variable
- τ_n - Minority carrier lifetime
- ω - Imaginary part of Laplace transform variable; frequency
- \mathfrak{z} - Integrand substitution variable
- $\mathfrak{L}\{ \}$ - Laplace transform operator

Abstract

SUMMARY: Feedback of the $1/2$ and $3/2$ derivatives as well as x and \dot{x} is demonstrated for a second-order system defined by the differential equation:

$$m\ddot{x} + c_1 D_t^{3/2}(x) + c_2 \dot{x} + c_3 D_t^{1/2}(x) + kx = u(t)$$

Three methods of producing the fractional derivative or integral of an input signal are investigated. The method selected employs a circuit developed at Trent University, Ontario, Canada for use in electrochemistry research. The circuit performs the mathematical operation $d^\nu(\cdot)/dx^\nu$ for $-1 < \nu < 1$; negative values of ν represent integration. The results presented show the circuit accurately differentiates a sinusoidal input for a frequency range spanning 0.01 Hz to 10.0 Hz.)

The second-order differential equation above is simulated on an analog computer. An optimal $u(t)$ is then used for feedback modification of the original open-loop system. Improved system performance resulted.

A Laplace transform method and a Mittag-Leffler expansion provide analytical predictions of the system's response. The output of the two methods is identical. Comparison of the theoretical predictions with the experimental data shows excellent agreement with respect to the initial transient behavior and asymptotic behavior of the steady-state response for both the open- and closed-loop systems. *Kypros, Texas (K-1)*

FRACTIONAL-ORDER FEEDBACK IN LINEAR SYSTEMS

I. Introduction

$$\frac{d^{\nu}[f(x)]}{dt^{\nu}} \quad (1)$$

Members of the scientific and engineering community have little difficulty in recognizing Eq (1) as the ν th derivative of a function of the variable x with respect to time. But how many will pose the question L'Hospital asked Leibniz in 1695, "What if ν be one-half?". Leibniz replied that it will "lead to a paradox", but added, "someday it would lead to useful consequences" (1:115). (For an historical development of fractional calculus the reader is directed to reference 1.)

Fractional derivatives have indeed proven useful in the analysis of a wide variety of physical systems (2:126). In the context of this research, fractional derivatives are capable of describing the behavior of viscoelastically-damped structures (3:348,4:209). The spacecraft and

in their designs. This expanding interest has motivated an investigation of active control requirements for viscoelastically-damped systems. The stability of feedback in such systems has been addressed (3:351). However, implementation of such a control system requires development of a feedback method (6) and a sensor or instrument capable of producing the fractional derivative or integral of electrical signals.

Problem Statement

Current methods of providing the fractional derivative of an input signal require either digital processing or resistor-capacitor circuit ladders containing many components. In addition, the resistor-capacitor circuit ladder is designed for a fractional order of one-half (7:39). The goal for this research was to produce a general fractional differentiator/integrator which serves as the key component in an active control system for viscoelastically-damped structures.

Approach

Three parallel areas of investigation were examined in an attempt to identify a device:

- 1) Excess charge carriers in doped semiconductors undergo a diffusion process in passing through the semiconductor lattice. Bagley and Torvik showed fractional derivatives of order one-half are common to diffusion processes (8:2). The application of a focused monochromatic light beam generates a localized excess concentration of charge carriers

in the semiconductor material and results in voltage changes as the excess carriers diffuse away from the source (9:54). Measurement of this voltage might provide a possible source of a fractional derivative.

2) Oldham identified a fractional integrating circuit of order one-half in his textbook on fractional calculus (10:149). This circuit has several characteristics which preclude it as an optimum choice. However, in developing the theory for this circuit, reference was made to Wall's work in continued fractions which can be used to represent Laplace transforms of functions (11:355). This method might permit the development of ladder circuits of fractional order, since s^α is the Laplace transform definition of a fractional derivative.

3) Finally a continued investigation of the literature to identify other scientific fields that might have fabricated or used such a device for research will be undertaken. Electrochemistry and geophysics are two fields in which fractional derivatives have found use (2:126,10:154).

Scope

The desirable attributes of the device include: i) Operation over a wide range of frequencies (especially .01 to 200 Hz - the frequencies of interest to many structural engineers), ii) small size, relatively few components, passive in nature and inexpensive to manufacture, and iii) generalization to any fractional order.

Evaluation of device performance will be accomplished in three phases:

Phase 1. A function generator is used to apply a sinusoidal input signal of varying frequency to the device. The observed output should match the expected magnitude and phase behavior of a $1/n$ th-order fractional differentiator/integrator.

Phase 2. An analog computer simulation of a second-order system incorporates the device to supply the fractional derivative terms of the system. Solution techniques for this type of system exist (12,13:141), and experimental agreement within 10% of the predicted response is established as the success criteria for this phase.

Phase 3. This thesis parallels the development of optimal fractional-order feedback theory by Capt Rich Walker (6). The parameters developed for feedback by application of his modified linear quadratic regulator will be applied to the system referred to in Phase 2. The ability of the feedback method to produce improved, stable control system performance will be the criterion for success in this phase.

Assumptions

This research takes on only proof-of-concept development. Circuits, if built, will consist of discrete components fabricated on breadboards. No attempt to use integrated circuit resistors and capacitors will be made. Perfection of circuits and device operation will be left as a follow-on task. Feedback will be accomplished through manual adjustment of attenuators on the analog computer and not through automatic means. Most systems exhibiting behavior that can be

modeled with fractional derivatives involve the half-order derivatives. Initial investigation will consist of half-order devices that can be generalized to $1/n$ th-order devices. While many materials exhibit stress-strain and damping characteristics that can be modeled by fractional derivatives, no effort will be made to tie the system simulated on the analog computer to a physical system, or specific material.

II. Background

Evolution of Fractional Calculus

Beginning in 1695, when L'Hospital first posed the fractional derivative question, many noted scientists and mathematicians have focused their attention toward developing the foundation of fractional calculus. In 1823 Neils Henrik Abel used fractional calculus to formulate a solution to the tautochrone problem. This was the first recorded application of fractional calculus (1:121). Beginning in 1832 Joseph Liouville published several papers dealing with fractional derivatives (1:116). G.F. Bernhard Riemann developed a theory for fractional integration which was published posthumously in 1876 (1:116). But neither Riemann nor Liouville were able to provide definitions for Eq (1) which could be generalized for any ν , positive or negative, and for a sufficiently wide class of functions. Henri Laurent published what many consider the foundation paper in fractional calculus in 1884. In this paper, Laurent produced a definition of fractional operations which also applied to integer values of ν and followed precisely the rules of integer calculus for differentiation and integration (1:118). Finally in 1936, with the theory of fractional operations well defined, Harold T. Davis developed a notation for fractional operations which will be used throughout the remainder of this paper (1:117):

Let ν be a positive real number, $cD_x^{-\nu} f(x)$ will denote integration of order ν of function f along the x axis from c to x . Similarly, the operator $cD_x^{\nu} f(x)$ denotes differentiation of order ν with terminal limits c and x . (1:117)

The mathematical interpretation of the integration operator in the time domain:

$${}_c D_t^{-\nu} [f(t)] = \frac{1}{\Gamma(\nu)} \int_c^t (t-\tau)^{\nu-1} f(\tau) d\tau \quad (2)$$

One would assume that the definition of fractional differentiation would involve replacing ν by $-\nu$ in Eq (2). However, this produces a divergent integral. To obtain a fractional derivative, first integrate to the correct fractional order between 0 and 1 and then use conventional differentiation to obtain the desired result:

$${}_c D_t^{\nu} [f(t)] = {}_c D_t^{m-\rho} [f(t)] = \frac{d^m}{dt^m} \left[\frac{1}{\Gamma(\rho)} \int_c^t (t-\tau)^{\rho-1} f(\tau) d\tau \right] \quad (3)$$

Where m is the least integer greater than ν , $\nu = m-\rho$, and $0 < \rho \leq 1$ (1.116).

Except for a small class of functions, Eqs (2) and (3) are not computationally convenient to use. However, if both expressions are treated as convolution integrals, the fractional operators have simple definitions in the Laplace domain:

$$\mathcal{L} \{ {}_c D_t^{-\nu} f(t) \} = s^{-\nu} \mathcal{L} \{ f(t) \} \quad (4)$$

$$\mathcal{L} \{ {}_c D_t^{\nu} f(t) \} = s^{m-\rho} \mathcal{L} \{ f(t) \} \quad (5)$$

It is through the use of these Laplace transform operators that fractional calculus proves to be most useful (2.126).

Physical Application

Abel used fractional calculus to determine the shape of a wire in a vertical plane which would cause a bead placed on the wire to take the same amount of time to reach the lower end no matter where the bead was originally placed (1:121). In 1921 P.G. Nutting noted stress relaxation properties in viscoelastic materials could be modeled by fractional powers of time rather than the traditionally expected decaying exponential (2:126). This development led A. Gemant in 1938 to propose time differentiation of fractional order for modeling stiffness and damping properties of viscoelastic materials (2:126). In 1966, M. Caputo suggested fractional derivatives might be used to model the behavior of geological strata (2:126). In 1970, V. O. Shestopol employed fractional calculus to describe the mechanism of deformation in tungsten and platinum at high temperatures (2:126). Other areas of physical application include creep and stress relaxation, creep buckling, and techniques for fitting experimental data. (2:126 - This reference is an excellent source for a historical perspective of the application of fractional calculus to damping.)

Beginning in 1979, R. Bagley and P. Torvik published a series of articles developing a method for modeling the behavior of viscoelastic materials by using fractional derivatives in a finite element formulation. The stress-strain curve for viscoelastic materials is dependent, not only on the applied load, but also on the frequency at which the load is applied. Previous methods of modeling this phenomena were computationally difficult to use for anything but steady-state conditions or predicted non-causal behavior -- both of which made

transient analysis of viscoelastic systems impractical (14:741). Bagley showed that a fractional derivative model, incorporating three to five parameters, could be used to accurately describe the behavior of many viscoelastic materials over a large range of frequencies (2:128). Approximately 130 materials have been characterized in this manner (2:130). Subsequent research verified the damping characteristics of viscoelastic materials could also be modeled in a similar fashion (15:83). In 1985, Bagley and Torvik showed finite element methods could incorporate fractional calculus, effectively increasing the usefulness of fractional calculus to the structural analyst (14:743).

When a model effectively describes a physical system over an entire range of operating conditions, one might expect the model to also predict behavior for conditions outside of range tested. One of the areas of recent interest in engineering is the damping requirements of large space structures. The excellent damping properties of viscoelastic materials make them highly suitable candidates for use in such structures. The space environment cannot be simulated in ground-based testing. A model that can predict performance outside of testable conditions is necessary. Bagley and Torvik present a strong argument for accepting the fractional calculus model as such (2:134).

Requirements for these structures will no doubt include some combination of active and passive control for station-keeping and other mission requirements. If viscoelastic materials are integral to these structures, it seems likely that the control system should include and adapt the fractional-order model. Three questions immediately arise --

can fractional orders of displacement be sensed; is there a constitutive control law for fractional-order feedback in these systems; and, is such feedback stable ?

Steven B Skaar, et al, addressed the stability of fractional order feedback in simple physical systems and outlined conditions necessary to guarantee a stable system (3). The paper discussed the characteristics of a fractional-order sensor and suggested a circuit comprised of lead-lag transfer functions (3:355). However, the authors stated more study was required to develop the idea. In addition, the paper addressed the form of the feedback control law. The feedback must be a function of the vibration frequency and must be of the same order as the equations of motion. In other words, if the material properties are best described by the one-half and three-halves derivatives, the feedback should be of the same form (3:356).

Capt Rich Walker went further in his 1988 AFIT Master's Thesis, defining an optimal linear quadratic feedback control law. His research showed that linear feedback of the fractional- and integer-order terms of a second-order system could both improve performance and guarantee stability. One of the assumptions made in his paper was the existence of a sensor or device which would provide the fractional-order input signals to the controller (6).

Summation

Models exist, using fractional derivatives, which accurately describe and predict the behavior of viscoelastic systems. The use of viscoelastic systems in large space structures would provide a number of benefits. A control law exists for feedback control of systems

containing these viscoelastic materials. This law improves system performance and produces stable systems. To implement this control law, a device is required which produces the fractional-order derivative of an input signal. This is the justification of the work to follow in this thesis.

Potential Sources of Development

A rigid flat plate on the surface of a Newtonian fluid produces motion in the fluid which can be described by the diffusion equation (8:2):

$$\frac{\partial v}{\partial t} = \alpha \frac{\partial^2 v}{\partial z^2} \quad (7)$$

v = transverse velocity profile in the fluid

z \equiv vertical distance from the surface of the plate

α \equiv ratio of fluid viscosity to fluid density

t \equiv time

Simply stated, the time rate of change of the fluid is proportional to the second derivative of velocity with respect to distance from the surface of the plate. Bagley and Torvik show that the solution of this equation is a fractional derivative of order one-half (8:2). Similar solutions can be found for other parabolic differential equations. One would expect that any diffusion process would result in fractional-order solutions.

The goal is to find a diffusion process where current, voltage, or charge carriers, excited by an electrical or mechanical signal, diffuse

through some medium. The Haynes-Shockley experiment, circa 1949, is used to create excess charge carriers in semiconductor materials by the application of a focused monochromatic light source. These excess charge carriers then diffuse through the semiconductor lattice and can be measured at some distance from the source of the excitation (9:56). One might expect the charge measured to be related to the input source by some type of diffusion process. This will be one area of investigation.

Another type of diffusion process provides a second possible device candidate. Electrochemists analyze solutions for electro-reducible species with a two-electrode cell configuration. When the potential (voltage) of one of the electrodes is lowered, electro-reduction occurs at this electrode which creates a time-dependent faradaic current. The half-order integral (semiintegral) of this current is proportional to the bulk concentration of the solution's oxidizer. The first method used to obtain the semiintegral involved recording the current versus time response of the system; the result was then digitally processed.

K. Oldham developed a resistor/capacitor ladder circuit that produced the analog semiintegral when hard-wired into the reduction apparatus. This innovation significantly reduced the sample processing time of the analysis. Oldham states this technique has now become the preferred method (7:39). One difficulty with Oldham's circuit is the number of cells (resistor/capacitor combinations) required to produce an accurate output. Another is its limitation to half-order fractional operations, instead of general fractional orders.

The theory of continued fractions developed by Wall (11) was significant in Oldham's development. Use of this theory might possibly lead to the synthesis of a passive component circuit which will produce a generalized fractional-order output. This will be the alternative area of investigation.

III. Theory

A specialized form of the continuity equation for excess minority carriers in semiconductors is (9:56):

$$\frac{\partial n_p}{\partial t} = - \frac{n_p - n_{p0}}{\tau_n} - \mu_n \epsilon \frac{\partial n_p}{\partial x} + D_n \frac{\partial^2 n_p}{\partial x^2} \quad (8)$$

where $n_p \equiv$ excess minority carrier density (free electrons) in p-type semiconductor

$n_{p0} \equiv$ excess minority carrier density at equilibrium

$\mu_n \equiv$ minority carrier mobility

$\epsilon \equiv$ applied electric field

$D_n \equiv$ minority carrier diffusion coefficient

$\tau_n \equiv$ minority carrier lifetime.

This equation arises from pulsing the semiconductor surface with focused beam of monochromatic light of the proper wavelength to generate excess carriers. The term $(n_p - n_{p0})/\tau_n$ represents the generation rate per unit volume due to the excitation pulses. The carrier lifetime, τ_n , represents the average time a minority carrier exists before recombining with a hole. This parameter is a direct measure of the number of impurities and imperfections in the semiconductor lattice. The greater the number of imperfections, the shorter the lifetime.

The solution to Eq (8):

$$n_p(x,t) = \frac{N}{(4\pi D_n t)^{1/2}} \exp \left\{ - \left[\frac{x^2}{4D_n t} + \frac{t}{\tau_n} \right] \right\} \quad (9)$$

where $N \equiv$ number of carriers generated per unit volume (9:55).

The term $N/(4\pi D_n t)^{1/2}$ is in the characteristic form of the result associated with a half-order derivative operation. However, the exponential term multiplying it gives a decaying exponential appearance to the excess minority carrier population. If the exponents could be set approximately equal to zero, the negative voltage from the free electrons would be inversely proportional to the half-order derivative of the number of free electrons generated per unit volume. In an analog simulation, the strength of the input pulse would be proportional to the voltage of the input signal. The rate at which the carriers decay at the measurement point, x , would be related to the half-order derivative of the input. This criteria requires that two conditions be satisfied since all the terms in the exponent are positive. That is,

$$\begin{aligned} x &\ll 0 \\ t &\cong 0.001\tau_n \end{aligned} \quad (10)$$

The first condition requires that the charge measurement be made close to the excitation site. Inserting a probe close to the excitation site would affect the semiconductor properties, invalidating Eq (8).

Typical lifetimes in silicon and germanium are on the order of 10^{-9} seconds (9:849). Thus, the maximum effective time in which to accomplish the measurement would be 10^{-6} seconds. The lowest operating frequency

of the device would then be in the Megahertz range. Most structural engineers are interested in frequencies three to four orders of magnitude smaller than this. Some other method is needed; this diffusion process is not a suitable candidate.

The ladder circuit, illustrated in Figure 1, which consists of T-cells composed of resistors and capacitors, closely approximates a half-order integrator if the number of cells are on the order of 100 (10:154). Several related articles also simulate half-order operations with simpler circuitry (7:41,16:253). These other methods were also limited to half-order operations.

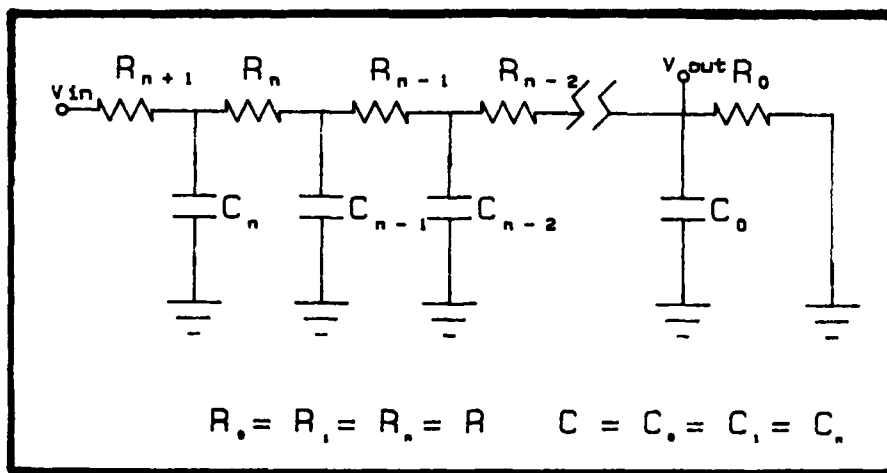


Figure 1. T-Cell Ladder Circuit

One reference detailed the representation of certain functions using continued fractions (11). One function was of particular interest:

(11)

$$\int_0^{\infty} \frac{e^{-u} du}{(1+zu)^{\alpha}} = \frac{1}{1 + \frac{az}{1 + \frac{z}{1 + \frac{(a+1)z}{1 + 2z} \dots}}}$$

The expression on the right hand-side of Eq (11) is called a continued fraction (11:349). If the following substitutions are made:

$$\begin{aligned} u &= st \\ z &= (RCs)^{-1} \\ du &= sdt \end{aligned} \quad (12)$$

the term on the left becomes:

$$s \int_0^{\infty} \frac{e^{-st} dt}{\left(1 + \frac{st}{RCs}\right)^{\alpha}} = (RC)^{\alpha} s \int_0^{\infty} \frac{e^{-st} dt}{(RC + t)^{\alpha}} \quad (13)$$

This form looks like a Laplace transform. If the substitution $\tau = RC + t$ is made, the following transform results:

$$(RC)^{\alpha} s \int_0^{\infty} \frac{e^{-st} dt}{(RC + t)^{\alpha}} = e^{-RCs} (RC)^{\alpha} \Gamma(1-\alpha) s^{\alpha} \quad (14)$$

From Section II, s^{α} is recognized as the Laplace transform of the fractional derivative of order α .

The continued fraction, with $(RCs)^{-1}$ substituted for z , is the impedance expression for the circuit illustrated in Figure 1. For a given circuit, the impedance relation is written:

$$\frac{\mathcal{E}(s)}{i(s)} = z(s) \quad (15)$$

As an example, Figure 2 illustrates an abbreviated version of the ladder circuit, and the impedance relation becomes:

$$z(s) = R_1 + \frac{1}{\frac{1}{R_0} + C_0 s} \quad (16)$$

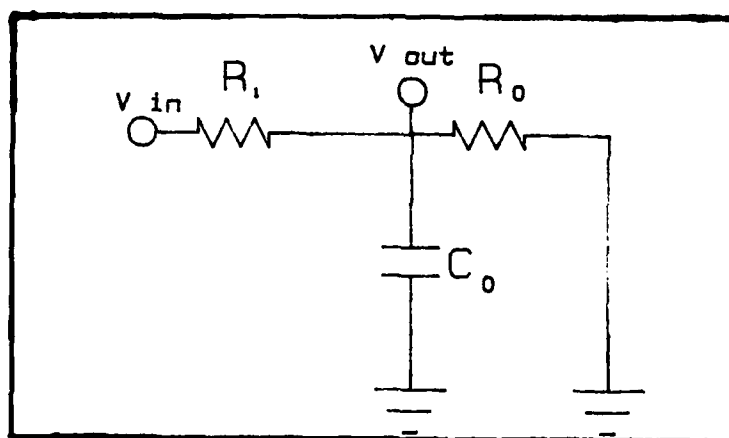


Figure 2. Abbreviated Ladder Circuit

Dividing both sides by R_1 and multiplying the fraction by unity gives:

$$z(s) R_1^{-1} = \frac{\frac{1}{R_1 C_0 s}}{1 + \frac{1}{R_0 C_0 s}} \quad (17)$$

The continued fraction is not yet in the form shown in Eq (11), but

by inverting both sides of Eq (17) and substituting Eq (15) for $z(s)$:

$$\frac{i(s)R_1}{\mathcal{E}(s)} = \frac{1}{1 + \frac{1}{\frac{R_1 C_1 s}{1 + \frac{1}{R_0 C_0 s}}}} = e^{RCs} (RC)^\alpha \Gamma(1-\alpha) s^\alpha \quad (18)$$

But this is true only if the resistors and capacitors in the circuit have values such that:

$$R_{n-m} = \frac{\Gamma(m+a)}{\Gamma(1+a)} \frac{1}{m!} R ; \quad C_{n-m} = \frac{\Gamma(1+a)}{\Gamma(m+a)} (m-1)! C \quad (19)$$

where $n \equiv$ the number of cells in the circuit and m goes from 0 to n

This finally produces an expression:

$$i(s) R = e^{RCs} (RC)^\alpha \Gamma(1-\alpha) s^\alpha \mathcal{E}(s) \quad (20)$$

This expression states the voltage drop across the first resistor is the fractional derivative of the input voltage multiplied by a constant. However, the term e^{RCs} is a delay term. If the substitution is made to transform s into the frequency domain, then for

$$s = j\omega \quad (21)$$

the delay term becomes a function of frequency, implying the phase shift of the circuit is not constant, but also is a function of frequency. This circuit was fabricated and tested. The Bode gain plot had the proper gain slope, but the circuit had a phase shift of 45 ± 5 degrees over less than a decade of frequency.

Further investigation of the literature provided an article describing a circuit which produced fractional derivative (or integral) output (17). The authors claimed the circuit operated successfully in the millisecond to several hundreds of seconds range. Since frequency is the inverse of time, this performance characteristic translated into frequencies spanning a range of 0.01 to 1000 Hz. However, the circuit had only been used with constant and ramp input signals. One of the assumptions used in designing the circuit was that the input current was constant. Because the circuit is a linear device, it should be useful in processing sinusoidal signals. Again, the circuit contains chains of resistors and capacitors, but this time the cells are connected as illustrated in Figure 3. The following narrative provides the rationale for why the circuit works:

If an input current is passed through the network a potential $E(t)$ is generated across the j th pair of components. The magnitude of the current is related to the component values of R_j and C_j by:

$$i(t) = \frac{E_j(t)}{R_j} + C_j \frac{d}{dt} [E_j(t)] \quad (22)$$

which can be inverted (by Laplace transformation):

$$E_j(t) = \frac{1}{C_j} \int_0^t i(t-\tau) \exp \left[-\frac{\tau}{R_j C_j} \right] d\tau \quad (23)$$

τ being an integration variable. Since $i(t)$ is common to all pairs it follows the potential across the entire circuit is:

$$E(t) = \int_0^t i(t-\tau) \sum_{j=-n}^{+N} \frac{1}{C_j} \exp \left[-\frac{\tau}{R_j C_j} \right] d\tau \quad (24)$$

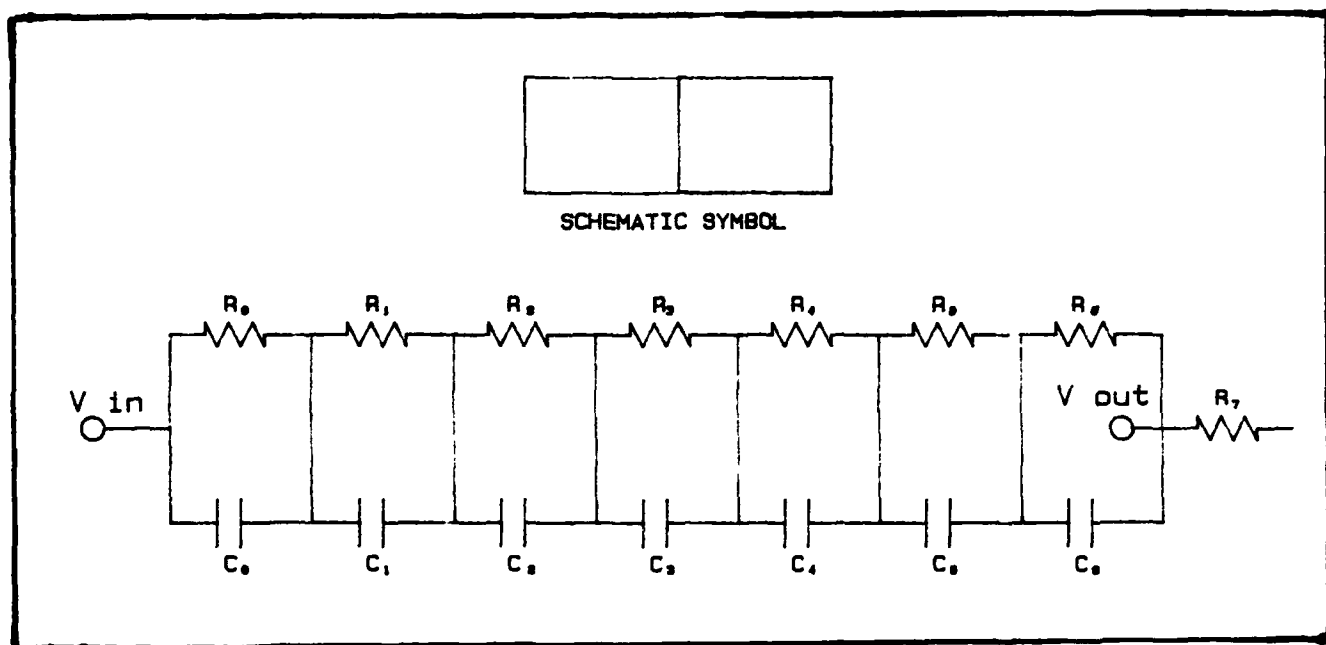


Figure 3. Oldham-Zoski Circuit Schematic

Adjacent resistors are now stipulated to differ in value by a constant factor, as do the capacitor values, although the progression ratios are not necessarily equal. Thus:

$$R_j = g^{-j} R_0 \quad \text{and} \quad C_j = G^{-j} C_0 \quad (25)$$

where G and g are geometric ratios, both > 1 . A parameter ν is defined relating G to g :

$$\nu = \frac{\ln G}{\ln g} \quad (26)$$

and Eq (24) can be recast

$$E(t) = \frac{R_0^\nu}{C_0^{1-\nu}} \int_0^t \frac{t(\tau)}{\tau^\nu} \sum_{j=-n}^{+N} \frac{\tau G^j g^j}{R_0 C_0} \exp \left[-\frac{\tau G^j g^j}{R_0 C_0} \right] d\tau \quad (27)$$

In the limit as n and N approach infinity and G and g approach unity:

$$E(t) = \frac{\pi \csc(\nu\pi) R_0^\nu}{\Gamma(1-\nu) \ln(Gg) C_0^{1-\nu}} \int_0^t \frac{i(t-\tau)}{C \tau^\nu} d\tau \quad (28)$$

and by using the Riemann-Liouville definition of a fractional integral as in Section II (17:27):

$$E(t) = \frac{\pi \csc(\nu\pi) R_0^\nu}{\Gamma(1-\nu) \ln(Gg) C_0^{1-\nu}} \frac{d^{\nu-1} [i(t)]}{dt^{\nu-1}} \quad (29)$$

Therefore, the input voltage is proportional to the integral of the current through the circuit. From the principle of continuity the input current equals the output current. If a resistor is connected in series with this circuit, the voltage across the resistor, $E_R(t)$ is related to the input voltage $E(t)$:

$$E_R(t) = i(t) R = \frac{\ln(Gg) C_0^{1-\nu}}{\pi \csc(\nu\pi) R_0^\nu} \frac{d^\nu E(t)}{dt^\nu} \quad (30)$$

The voltage across this resistor is the $1/\nu$ th derivative of the input voltage. Additional details of this circuit - henceforth referred to as the Oldham-Zoski circuit (OZ) - are contained in Appendix E (including fabrication and interface details).

The theory for simulating a second-order equation, including half-order terms supplied by the OZ circuit, is developed in Section IV under the subheading Analog Simulation. Basically, given a set of initial conditions and a set of coefficients for a second-order system, the response, as a function of time, can be obtained on the analog computer.

Finally, there is a need to evaluate experimental results and be confident in their accuracy. Two techniques will be used to predict the theoretical results of the open and closed loop simulations. First, a Laplace transform method which will be used to evaluate the residues and a contour integral in the s plane. Second, a Mittag-Leffler expansion which will be used to expand the homogeneous solution of the differential equation as an infinite series in the time domain. Details of the Laplace transform method are included in Appendix A. Appendix C details the Mittag-Leffler expansion.

IV. Experimental Procedure

Overview

This section details eight distinct tasks:

1) Circuit design and fabrication. The details of realizing the half-order derivative circuit are presented.

2) Circuit Performance Evaluation. A signal generator was used to produce a sinusoidal signal of varying frequency as the input to the half-order circuit. The output of the circuit was compared to the input signal to ensure the proper phase and magnitude relationships existed.

3) Circuit Gain Adjustment for Analog Simulation. To obtain a zero amplitude offset of the derivative signal, several operational amplifiers and a potentiometer were combined with the half-order circuit.

4) Half-Order Analog Performance Evaluation. A harmonic oscillator circuit was programmed on an analog computer. Its output was introduced into the circuit and op amp half-order combinations to ensure proper phase and magnitude performance.

5) Fractional-Order Equation Synthesis. Using the physical variable method, a second-order differential equation, including half- and three-halves order terms, was programmed on an analog computer.

6) Open- and Closed-Loop Simulation. The performance results and comparison with the analytic prediction are presented. As with all experiments there were some discrepancies. The source and resolution of these discrepancies is discussed.

7) Total-Cycle Simulation. With the system totally at rest, a step input was introduced into the system to establish the initial conditions tested. This task identified adjustments to correctly model the initial-value problem.

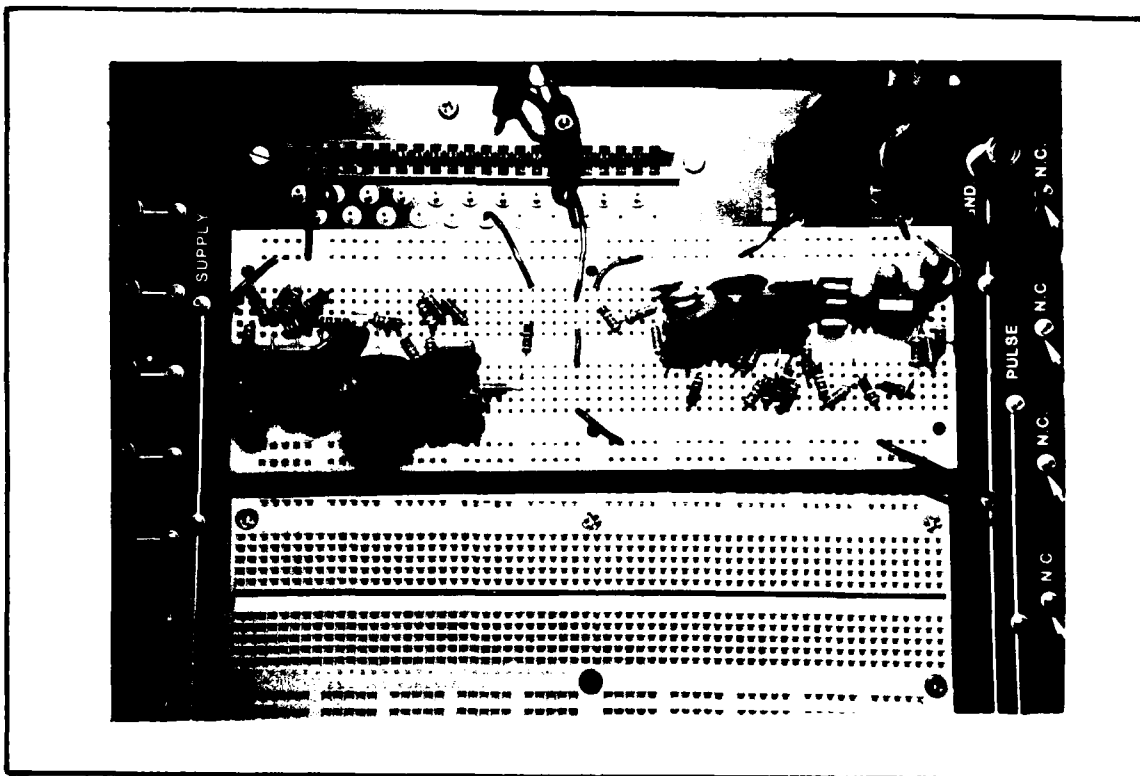
8) Final Configuration and Performance Evaluation. The lessons learned from the total-cycle simulation were applied to an initial-value configuration. The final results are discussed.

This section provides a general functional description of the procedures used in each task without going into a detailed step-by-step description of the equipment configuration and operation. Learning to operate the equipment correctly required a significant effort during this research. Therefore, where appropriate, references are made to Appendix F which contains a detailed description of the equipment configuration and operation.

Circuit Design and Fabrication

For this application a half-order differentiating Oldham-Zoski circuit will be designed and fabricated. Appendix E details the method of determining the component values listed in Table 1. This circuit is shown schematically in Figure 3. Resistors and capacitors within 2% of the design values listed in the table were used. This is consistent with the Oldham-Zoski article (17:35). A photograph of the completed circuits is shown in Figure 4. The as-fabricated component values are also listed in Table 1. These are not off-the-shelf values, but were

obtained by serial and parallel combination of discrete components. This was necessary as the design values were not commercially available. Trial and error combinations of components were evaluated until a combination within 2% of the desired value was obtained.



*Figure 4. Oldham-Zoski Circuits Constructed
on Breadboard*

Table 1. Design and As-Fabricated Oldham-Zoski Circuit Values

Circuit 1: Design Range .01-1000 Hz (7 Cells - per 17:32)						
Design Values				As-Fabricated Values		
R(M Ω)	C(μ F)	τ (s)	f(Hz)	R(M Ω)	C(μ F)	f(Hz)
25.4	10.0	254.56	0.0039	25.403	10.11	0.0039
9.88	3.891	38.46	0.0260	9.89	3.89	0.0260
3.84	1.514	5.823	0.1717	3.827	1.536	0.1708
1.50	0.589	0.8814	1.134	1.504	0.588	1.131
0.582	0.2292	0.1334	7.496	0.5821	0.2289	7.507
0.226	0.0892	0.0213	46.95	0.2258	0.0899	49.26
0.0882	0.0347	0.00306	326.8	0.0895	0.0344	333.3
0.00172	0.0270	0.00005	21533.	0.0017	0.0268	21744.
0.00363				0.0036		
Circuit 2: Design Range .01-100 Hz (6 Cells)						
Design Values				As-Fabricated Values		
R(M Ω)	C(μ F)	τ (s)	f(Hz)	R(M Ω)	C(μ F)	f(Hz)
12.7	20.0	254.56	0.0039	12.705	20.12	0.0039
4.942	7.782	38.46	0.0260	4.936	7.84	0.0258
1.923	3.028	5.823	0.1717	1.925	3.046	0.1706
0.7482	1.178	0.8814	1.134	0.7471	1.176	1.138
0.2911	0.4584	0.1334	7.496	0.2931	0.4600	7.418
0.1133	0.1784	0.0213	46.95	0.1133	0.1781	48.50
0.02204	0.1388	0.00306	326.8	0.0221	0.1380	327.5
0.04670				0.0462		

After completion of component selections, the combinations were placed on an E&L Instruments Elite 1 circuit board and rechecked to ensure the values matched the measured values. This step is highly recommended because several combinations were determined to be outside the tolerance limits when installed. Two circuits were built, Circuit 2 was designed and fabricated with twice the capacitance and half the resistance of Circuit 1. Circuit 1 was used to provide the half derivative, and Circuit 2 provided the three-halves derivative in the analog simulations.

Circuit Performance Evaluation

The simplest criteria to apply in identifying a fractional derivative of order one-half is its Bode plot. A gain of 10dB per decade and a constant phase shift of 45 degrees characterizes a half-order derivative (18:226). Experimentally determining a circuit's Bode plot requires a sine wave generator, a recording or display device, and a counter/timer. The method employed connects the output of the Tektronix function generator (model FG506) to the input of the circuit under test. The output of the circuit under test is connected to either a Hewlett-Packard Analog/Digital recorder (model 7090A) or a Tektronix oscilloscope (model SC504); a Tektronix counter/timer (model DC509) is connected to the output of the function generator. The output voltage is then compared to the input voltage, and the gain is calculated. The gain at a given frequency (ω) is given by:

$$\text{Gain}_{|\omega = \text{constant}} = 20 \log_{10} \left(\frac{\text{output voltage}}{\text{input voltage}} \right) \quad (31)$$

The phase shift is calculated by determining the time interval (t_{ps}) between the t-axis crossings of the input and output voltages and comparing it to the total period (T) of the sine wave as illustrated in Figure 5.

$$\text{Phase Shift (deg)} = \frac{180^\circ}{\pi} \left[\frac{t_{ps}}{T} \right] \quad (32)$$

This procedure is repeated for a number of frequencies in the performance range of the circuit. The data was then plotted, as illustrated in Figures 6-9, and the slope of the gain plot and the magnitude of the phase plot are compared to the 10dB/decade gain slope and 45 degree phase shift criteria. A detailed equipment list and test procedure is contained in Appendix F.

Experimental values of 10 ± 1 dB/decade for the gain and 45 ± 5 degrees for the phase shift were established as the initial pass/fail criteria for the circuit. These values were a first attempt at establishing such a criteria. Since both circuits tested satisfied this criteria and performed adequately on the analog computer, these parameters appear to be a valid performance criteria.

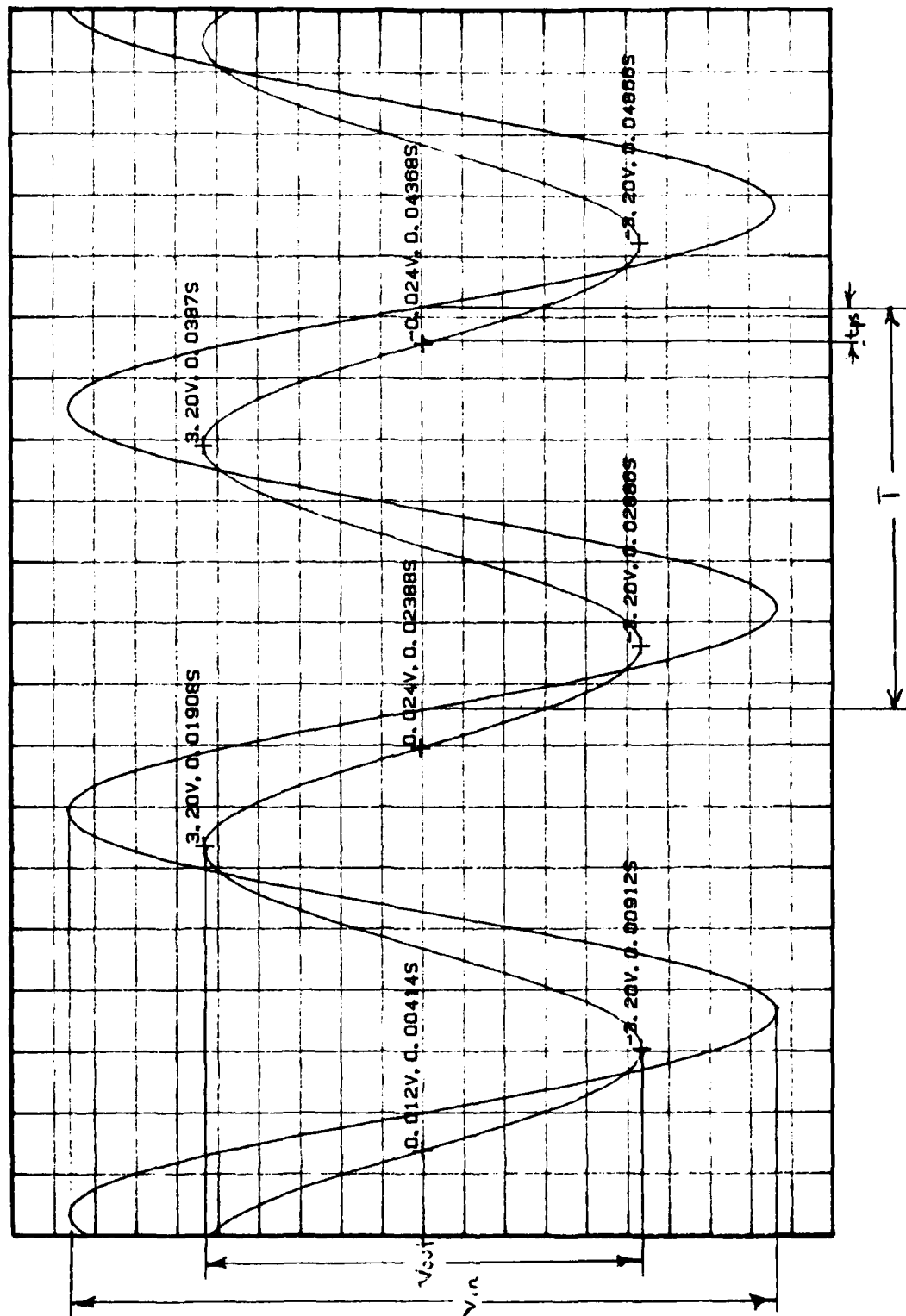


Figure 5. Example of Phase Calculation Parameters

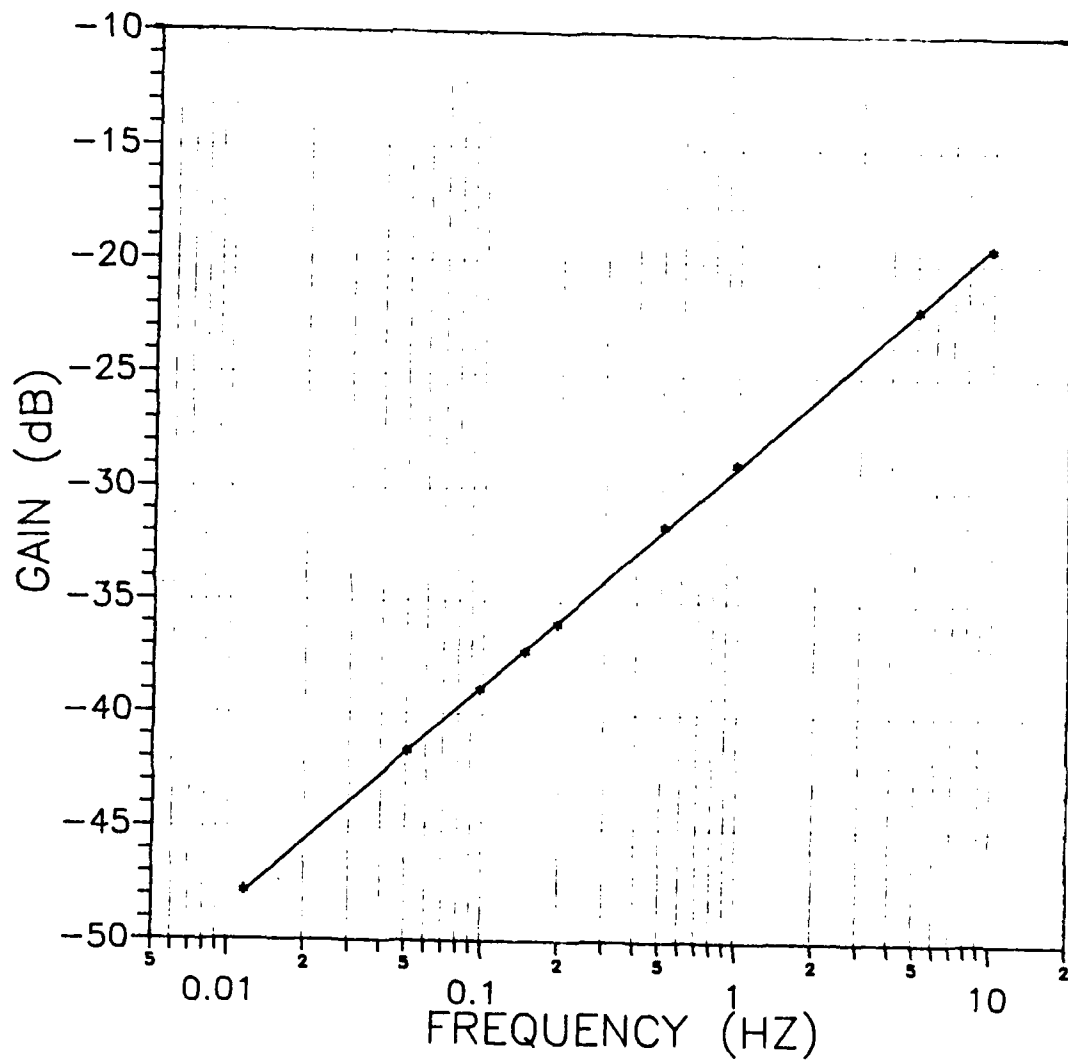


Figure 6. Circuit 1 Gain Characteristics

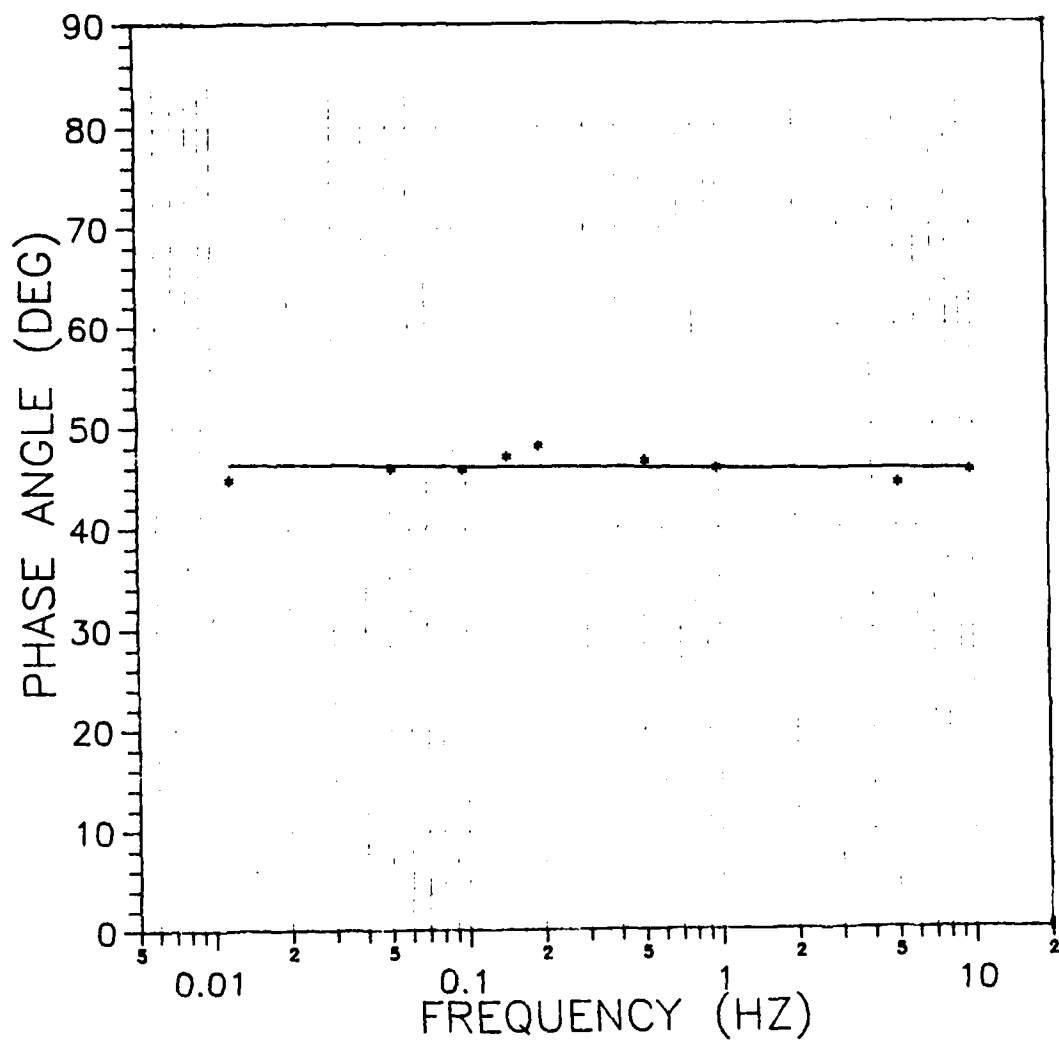


Figure 7. Circuit 1 Phase Angle Characteristics

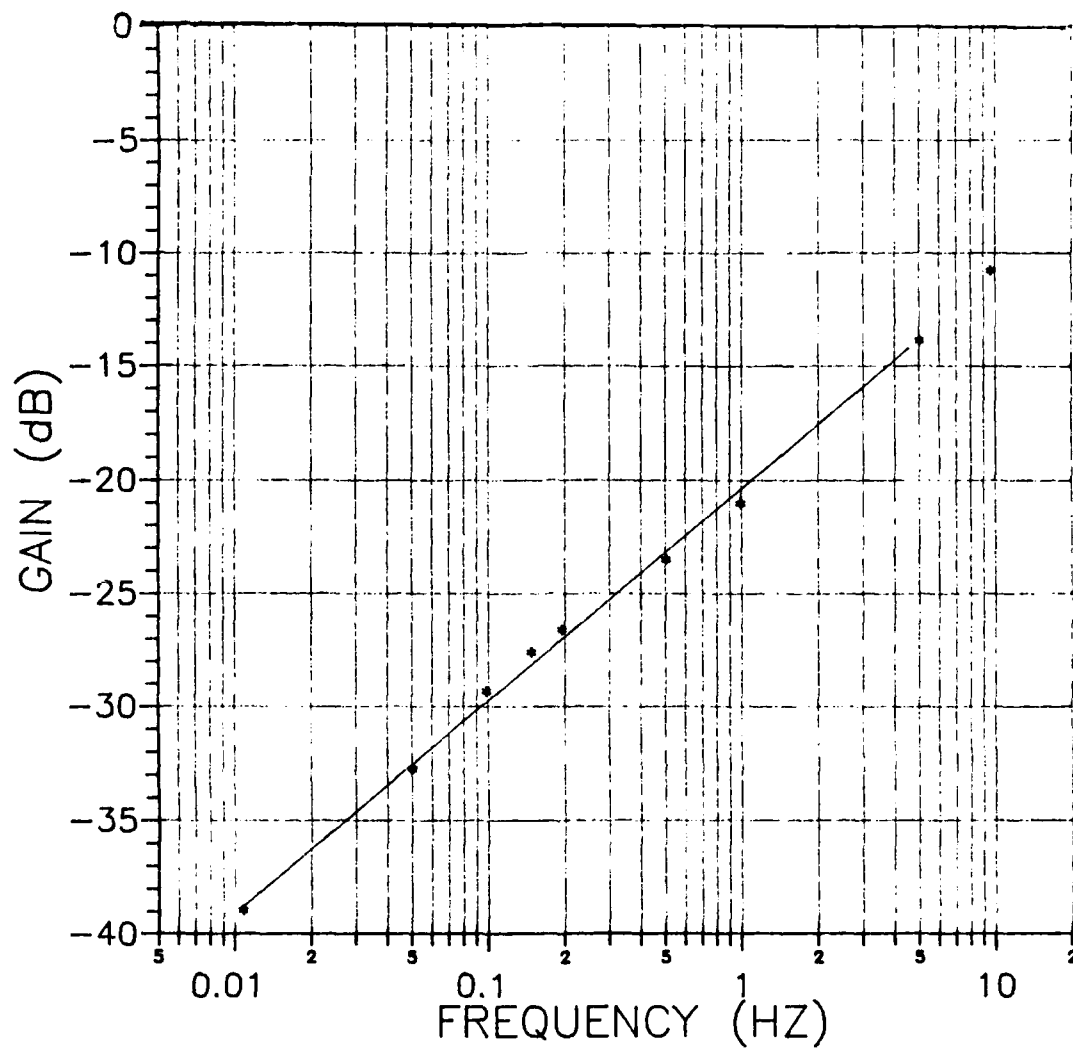


Figure 8. Circuit 2 Gain Characteristics

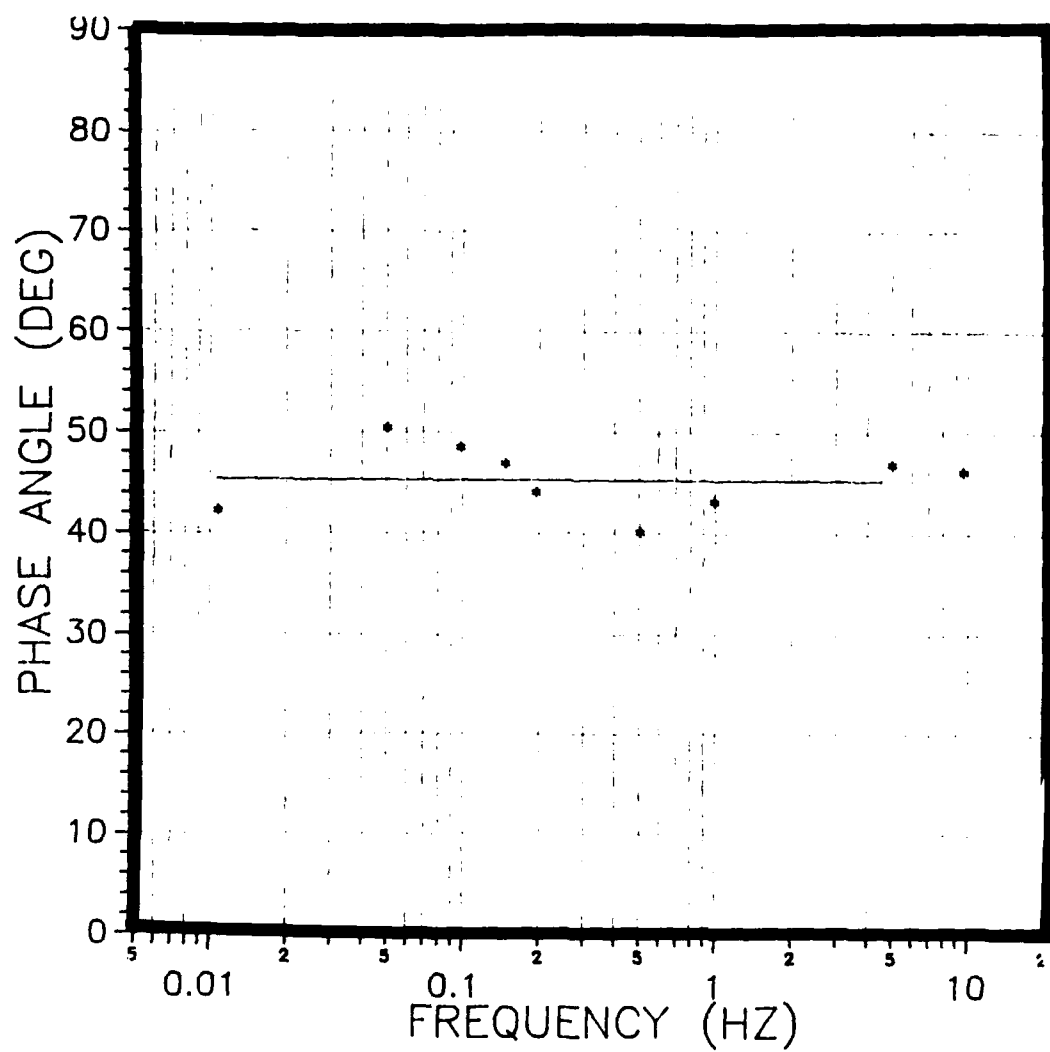


Figure 9. Circuit 2 Phase Angle Characteristics

Circuit Gain and Adjustment for Analog Simulation

The change in gain and phase of the differentiating circuit's output arises from the mathematical definition of the steady-state derivative of a sine function:

$$\frac{\partial^{\nu}}{\partial t^{\nu}} (A \sin \omega t) = A \omega^{\nu} [\sin(\omega t - \nu\pi/2)] \quad (33)$$

When the input amplitude is unity, the magnification factor of the output amplitude with regards to the input amplitude is ω^{ν} - which is a function of the frequency. If the Oldham-Zoski circuit is to function as a true differentiator, this amplitude magnification factor at $\omega = 1$ rad/sec must be $1^{\nu} = 1$. Figure 6 and Figure 8 show clearly that this is not the case for either of these circuits. Therefore, both circuits must be combined with operational amplifiers to ensure that the gain plot has a value of zero dB at $\omega = 1$ radian/sec.

The Oldham-Zoski article defines relationships for the amplification required for a given circuit design (17:30). For Circuit 1 a gain of 26.53 (pure number, not dB) was predicted; the gain for Circuit 2 was 13.54. To realize this on the analog computer, two amplifiers with gains of 10 and a potentiometer in series with each half-order circuit were required as shown in Figure 10. More information on the gain calculations for each circuit is contained in Appendix E.

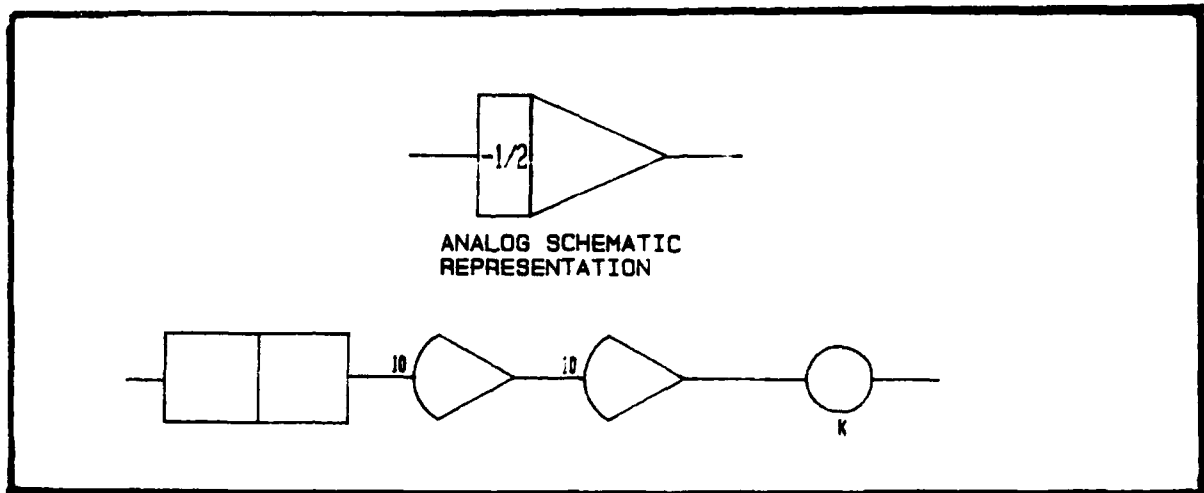


Figure 10. Operational Amplifier and Oldham-Zoski Circuit Combination for $\bar{O}_t^{(2)}(x)$

Half - Order Circuit Analog Performance Evaluation

Theory does not always match real life, and verification of the gains was required prior to simulating a second-order system. A sine wave with $\omega = 1$ radian/sec was used to perform the verification. A harmonic oscillator was programmed with a frequency of 1 radian/sec (see Figure 11 and reference Appendix F for details regarding the programming of a harmonic oscillator on the analog computer) . The oscillator's output served as the input to the half-order circuit being evaluated. The input amplitude and the output amplitude were plotted using the Hewlett-Packard A/D recorder (model 7090A - see Figure 12). A comparison is made, and adjustments, if necessary, are determined by the relationship:

$$\frac{\text{actual output amplitude}}{\text{input amplitude}} = \frac{1}{\text{adjustment factor}} \quad (34)$$

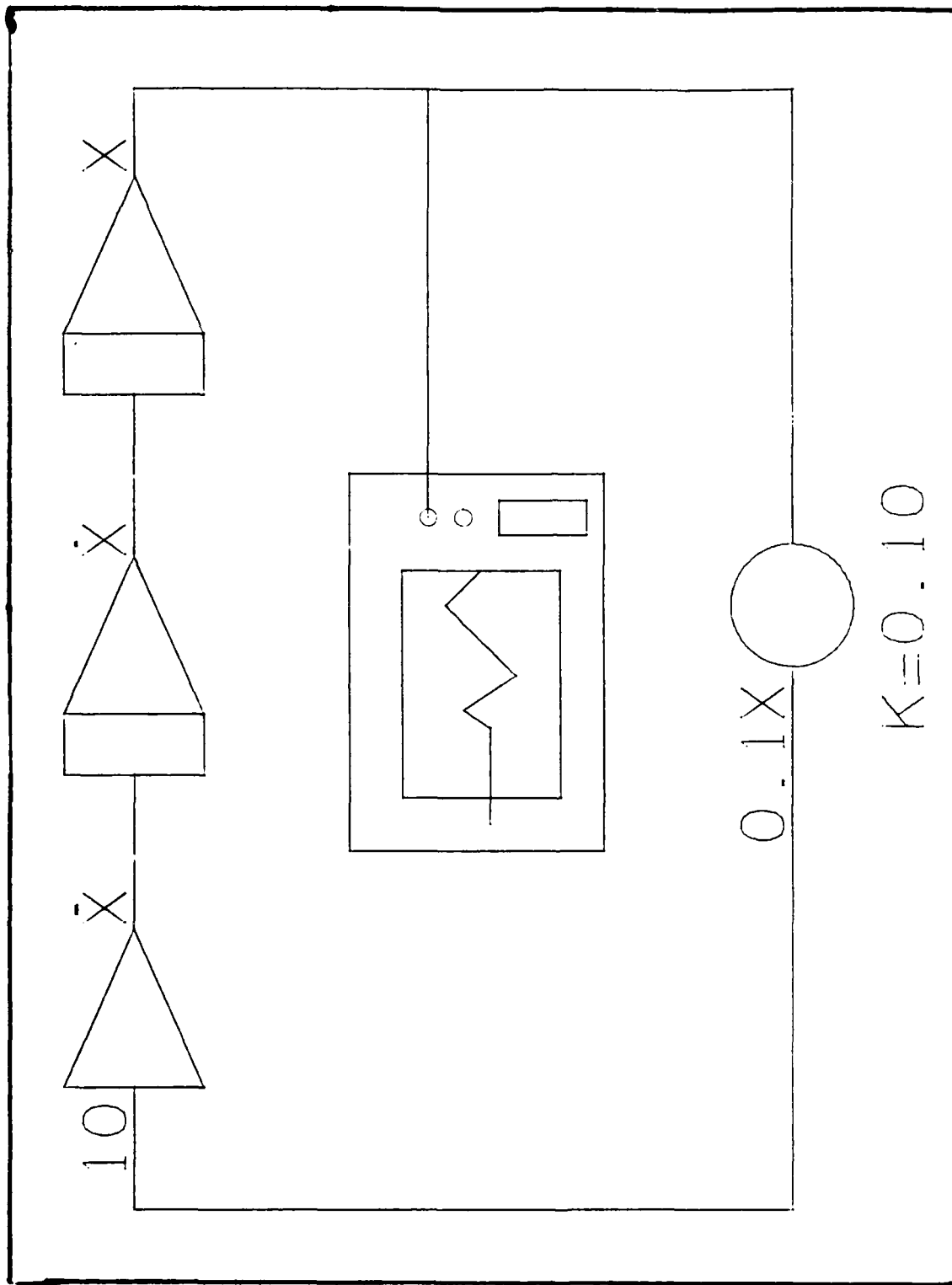


Figure 11. Harmonic Oscillator - Analog Configuration

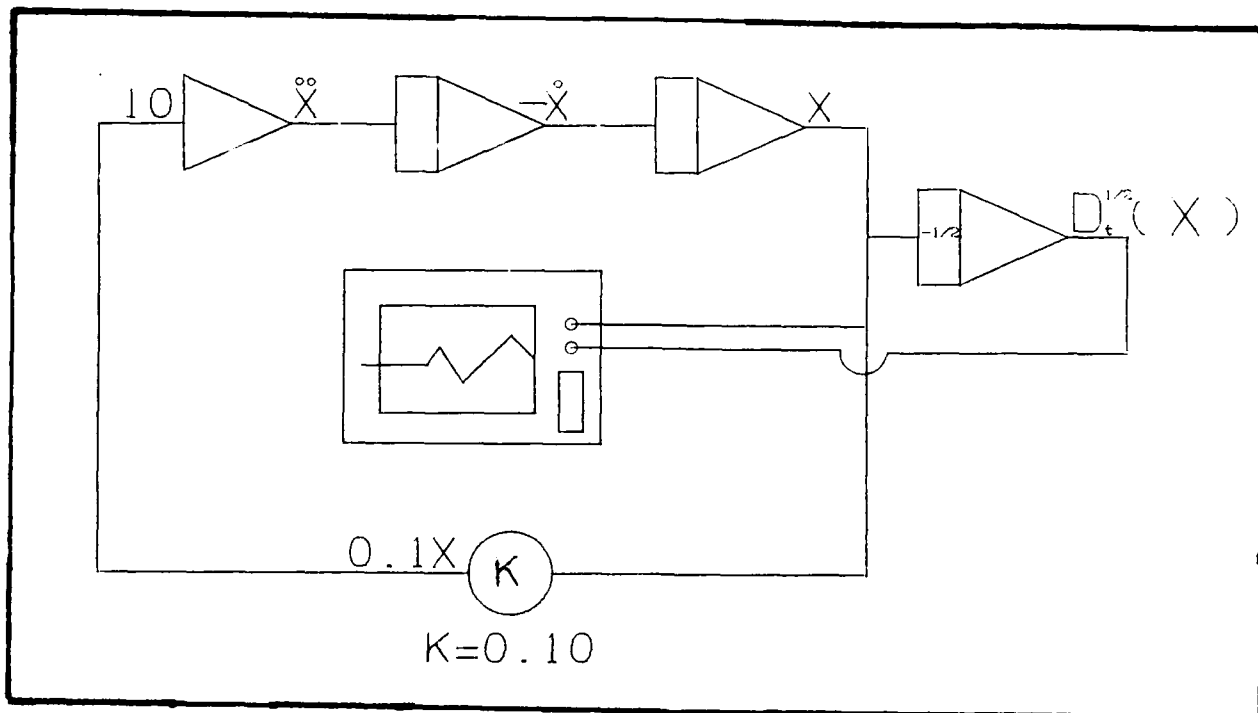


Figure 12. Amplitude Validation Circuit Using Harmonic Oscillator

The initial potentiometer setting for the half-order circuit was modified by multiplying its value by the adjustment factor. The process was repeated until the adjustment factor was approximately one. An example of this process is depicted in Figures 13 and 14.

Although the circuits are tuned to perform correctly at $\omega = 1$ radian/sec, their behavior at other frequencies requires evaluation. As a check, the frequency of the harmonic oscillator was changed to $\omega^2 = 3.5$ radians/sec. From Eq (33) the predicted magnification factor for the output amplitude at this frequency should be $(3.5)^{1/4}$ or 1.37. Figure 15 shows the experimental result of 1.35. The combination of this check, and the original circuit validation, bolstered confidence in the half derivative circuits prior to attempting the analog simulations.

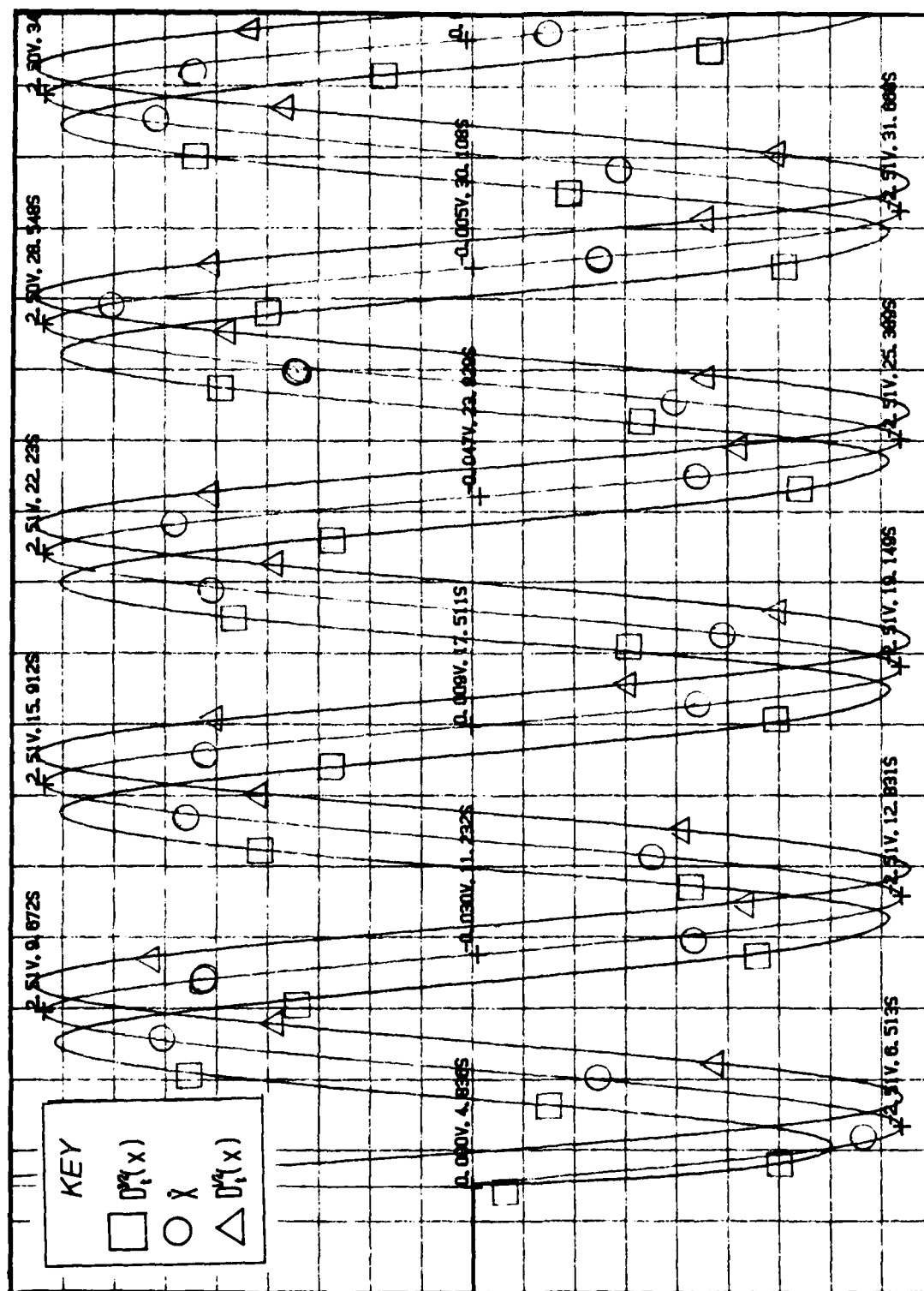


Figure 13. Initial $U_1^q(x)$ Using Theoretical Predictions

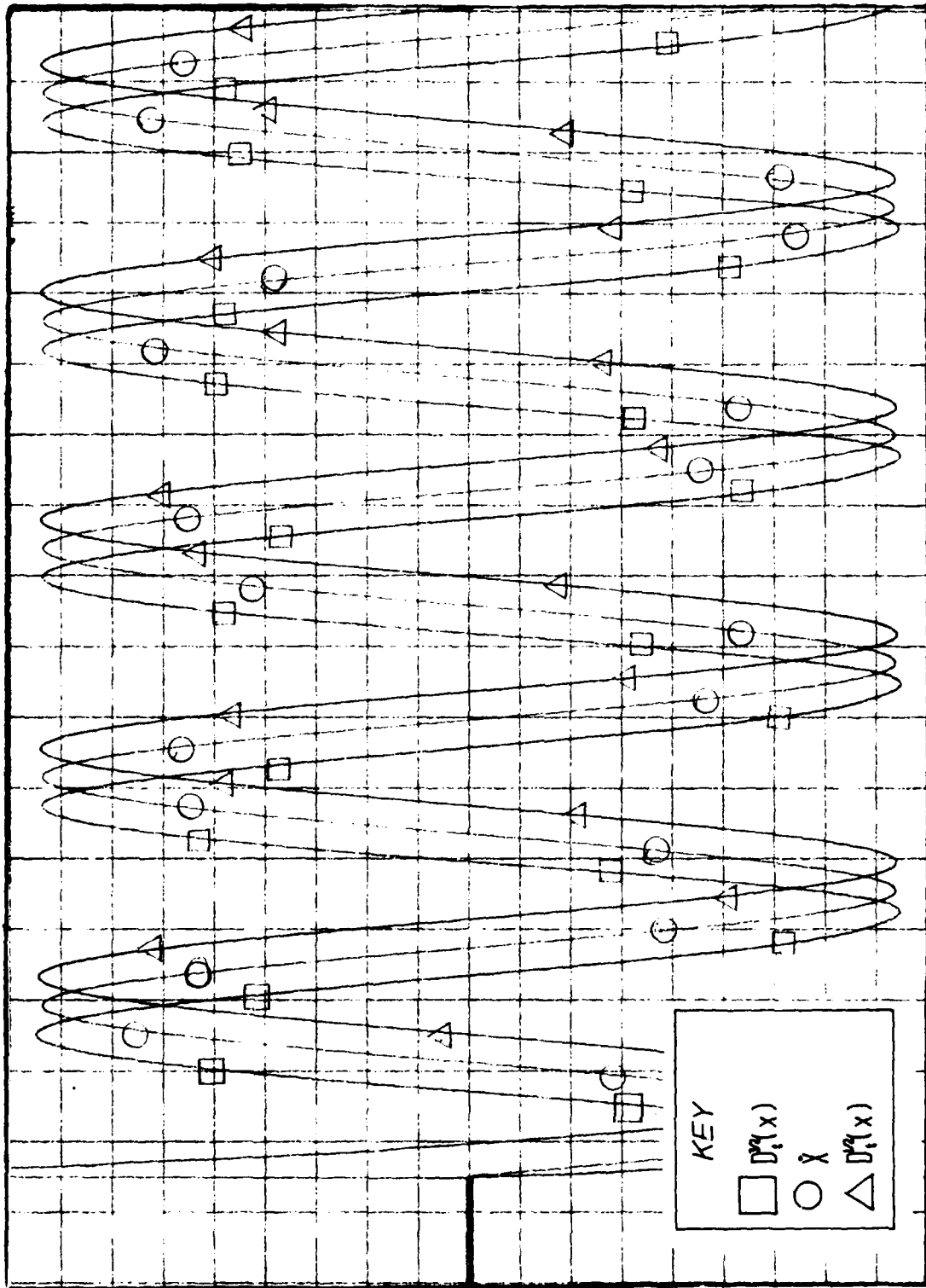


Figure 14. $D_1^q(x)$, $D_1^q(x)$ After Gain Adjustments

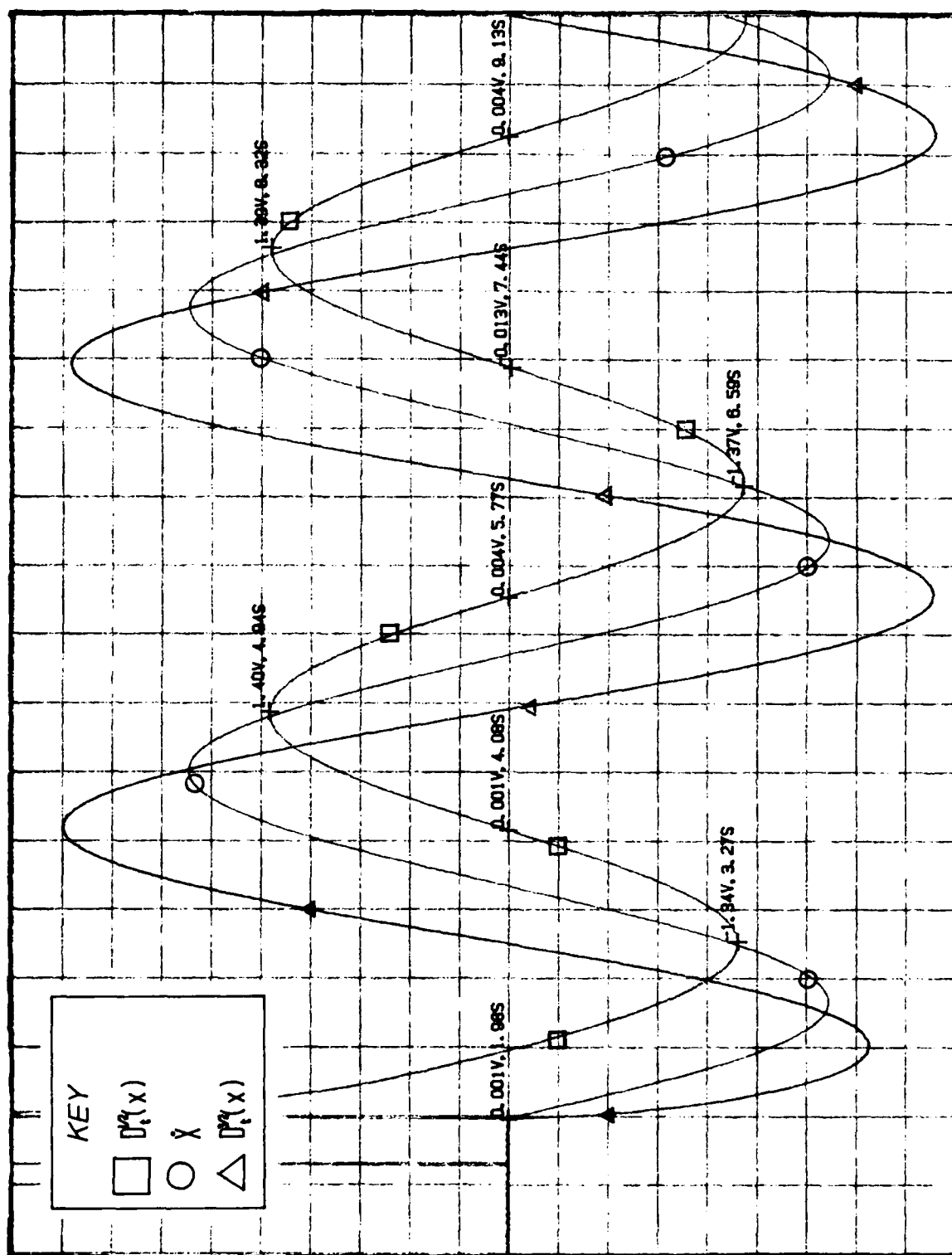


Figure 15. $D_i^q(x)$. $D_i^q(x)$ Gain Check at $\omega^2 = 3.5 \text{ rad/sec}$

It would be desirable if both the $1/2$ and $3/2$ derivatives could be obtained by using a single half-order circuit. Using the Oldham-Zoski circuit to differentiate the x signal to provide $D_t^{3/2}(x)$, and then connecting the $D_t^{3/2}(x)$ output to a full integer integrator should produce the $D_t^{1/2}(x)$ signal. All analog integrators are checked at the factory to ensure their output falls within a range that matches the performance of the others. Using only one half-order circuit to provide the signal for both $D_t^{1/2}(x)$ and $D_t^{3/2}(x)$ eliminates concerns with performance matching two half-order circuits. To test this concept the harmonic oscillator was tuned to $\omega = 1$ radian/sec, its x signal was differentiated to obtain $D_t^{3/2}(x)$, then integrated to obtain $D_t^{1/2}(x)$. This circuit configuration is pictured in Figure 16, and the results are plotted in Figure 17. The peak-to-peak amplitude for each cycle is correct, and the phase shift is also correct. However, there is an underlying ramp in the signal, indicating a bias voltage exists in the $D_t^{3/2}(x)$ signal. Several possible causes were identified, (see Section V) and fixes were implemented. Even then, the ramp could not be totally eliminated.

Incorporating a second half-order differentiator to produce $D_t^{1/2}(x)$ from the x (displacement) signal solved much of the problem. With the system configured as shown in Figure 18, the $D_t^{3/2}(x)$, x , and $D_t^{1/2}(x)$ signals are shown in Figure 19. The proper relationships now exist. Section V includes a discussion of the problems associated with using a single circuit to produce both fractional derivatives.

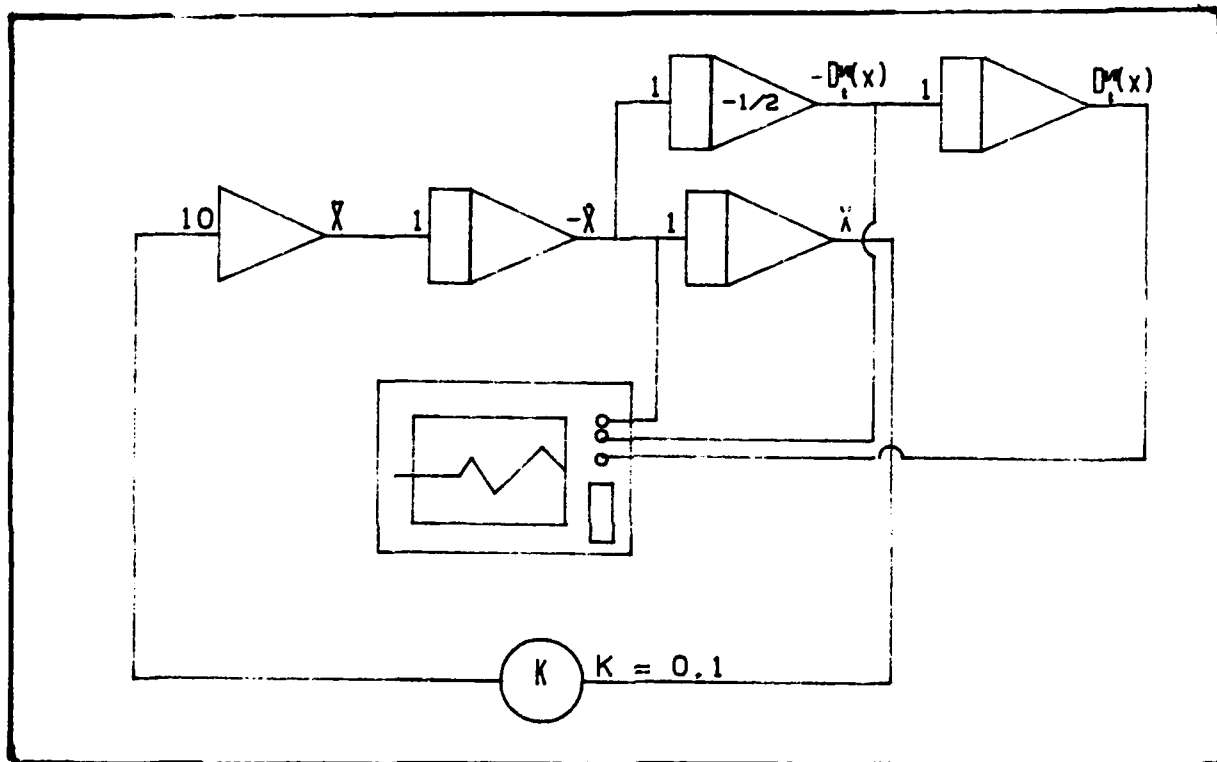


Figure 16. Configuration for $D_t^{\lambda}(x)$, $D_t^{\lambda}(x)$ Using Only One Fractional Order Circuit

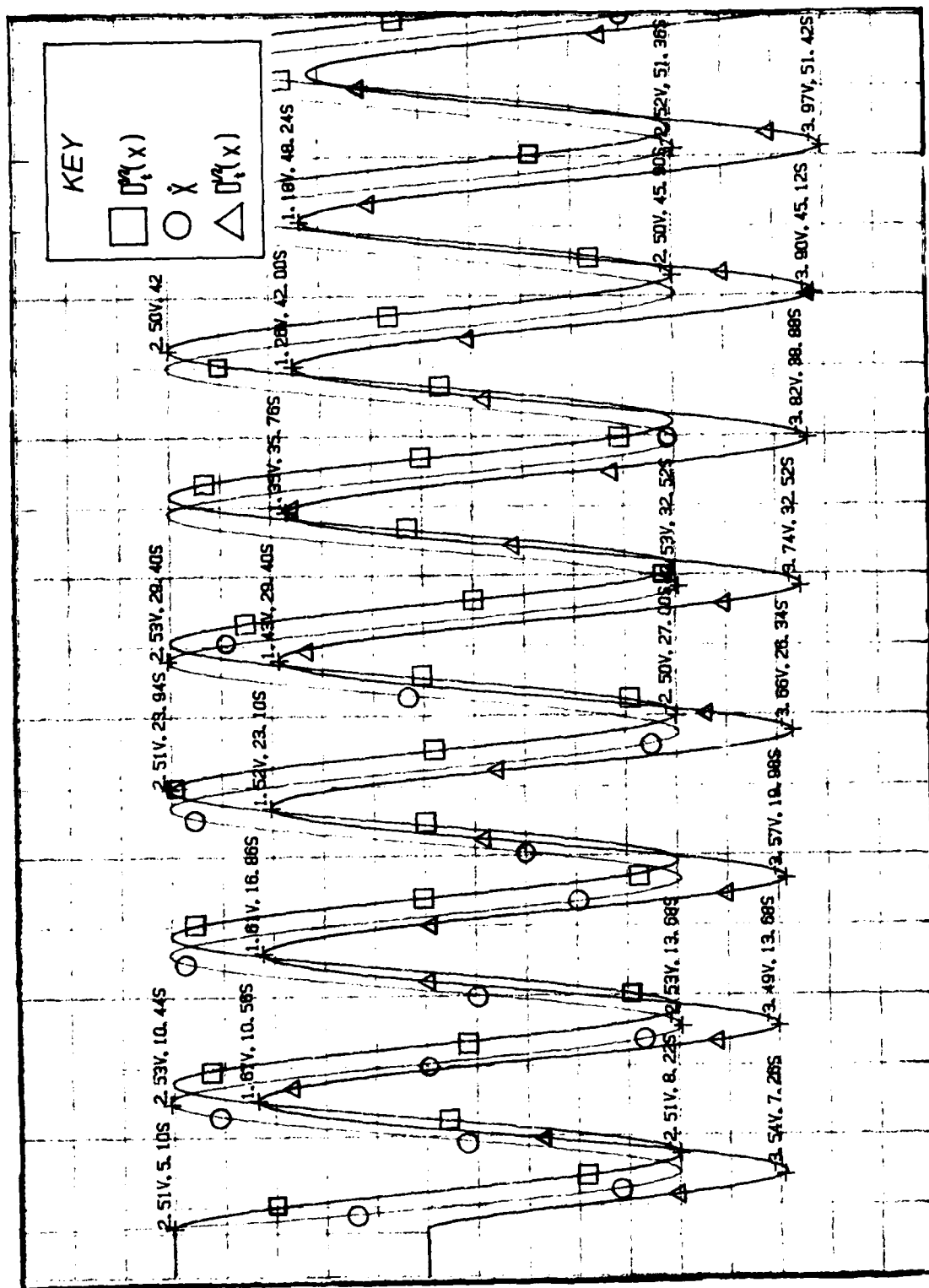


Figure 17. Results of Integrating $U_1^m(x)$ to Obtain $U_1^m(x)$ Directly

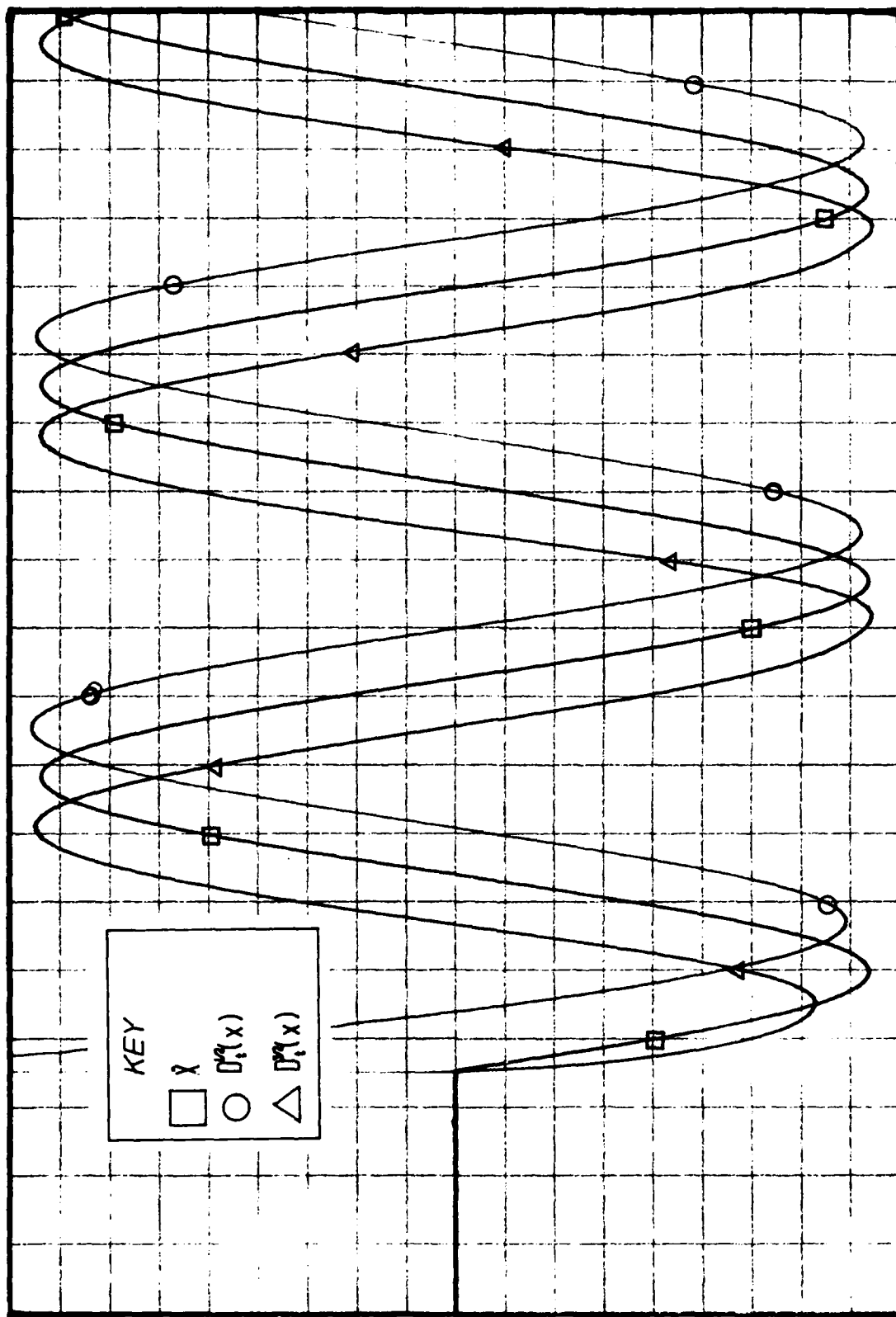


Figure 19. $D_1^\alpha(x)$, \tilde{x} , $D_1^\alpha(x)$ Comparison Using Two Fractional Order Circuits

Fractional-Order Equation Synthesis

The EAI analog computer (PACE, model TR[®] 48) depicted in Figure 20 is a solid-state second-generation computer. Components available for patching into simulations include operational amplifiers capable of summing, inverting, multiplying, and integrating; potentiometers for precision multiplication; comparators for switching logic; function switches for applying various input (forcing) functions; and a digital voltmeter for readout purposes. Each component has input and output jacks which accept patch cords with banana plug terminations (see Figure 21), permitting interconnection of components for modeling a variety of systems. Appendix F contains detailed descriptions of these components and their uses.

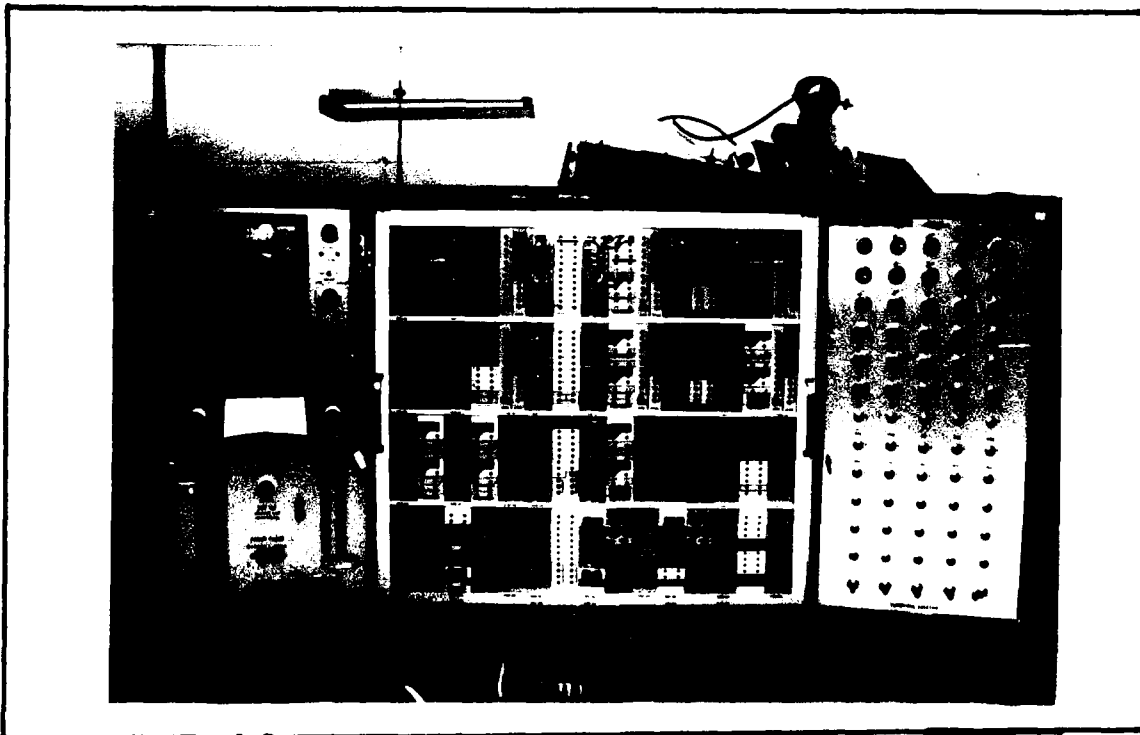


Figure 20. Pace TR48 Analog Computer

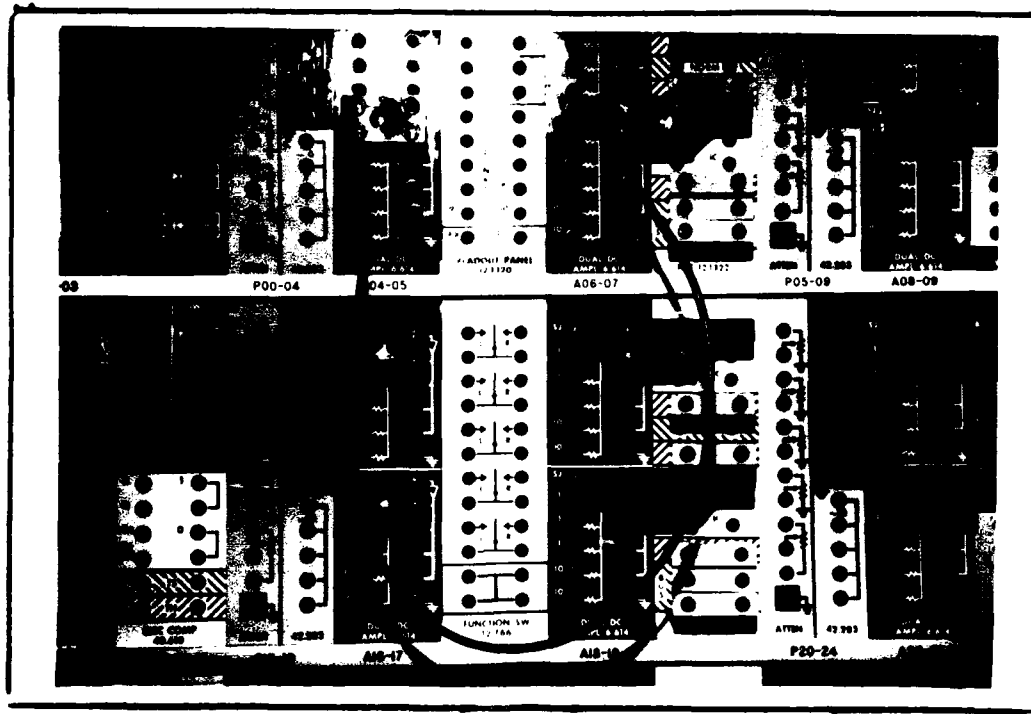


Figure 21. Patch Cords and Input Jacks

A general second-order differential equation containing half-order derivatives can be written as follows:

$$m\ddot{x} + c_1 D_t^{3/2}(x) + c_2 \dot{x} + c_3 D_t^{1/2}(x) + kx = u(t) \quad (35)$$

where

- $m \equiv$ system mass
- $c_2 \equiv$ viscous damping coefficient
- $k \equiv$ system stiffness coefficient
- $c_1 \equiv$ viscoinertial damping coefficient
- $c_3 \equiv$ viscoelastic damping coefficient
- $u(t) \equiv$ system control or forcing function

The \ddot{x} , \dot{x} , and x terms are acceleration, velocity, and position. The two additional terms, $D_t^{3/2}(x)$ and $D_t^{1/2}(x)$, are respectively, the three-halves and one-half derivative of position with respect to time.

Eq (35) can be rewritten such that the acceleration is a function of the other terms:

$$\ddot{x} = m^{-1} \left\{ f(t) - c_1 D_t^{3/2}(x) - c_2 \dot{x} - c_3 D_t^{1/2}(x) \right\} \quad (36)$$

The three-halves derivative can be obtained by differentiating \dot{x} or integrating x by order one-half, and is mathematically defined in the time domain:

$$D_t^{3/2}(x) = \frac{d^{-1/2}[\dot{x}(t)]}{dt^{-1/2}} = \left[\Gamma(1/2) \right]^{-1} \int_c^t \dot{x}(\tau) (t-\tau)^{-1/2} d\tau + D_t^{3/2}(x(0)) \quad (37)$$

Likewise the one-half derivative can be obtained from either \dot{x} or x , and it is defined as:

$$D_t^{1/2}(x) = \frac{d^{-1/2}[\dot{x}(t)]}{dt^{-1/2}} = \left[\Gamma(1/2) \right]^{-1} \int_c^t \dot{x}(\tau) (t-\tau)^{-1/2} d\tau + D_t^{1/2}(x(0)) \quad (38)$$

The initial conditions on both fractional derivatives are identically zero according to Bagley (12). The other three time-dependent quantities in the equation:

$$\dot{x} = \int_c^t \ddot{x}(\tau) d\tau + \dot{x}(0) \quad (39)$$

$$x = \int_c^t \dot{x}(\tau) d\tau + x(0) \quad (40)$$

and $f(t)$, an arbitrary time-dependent forcing function which is produced in a separate circuit on the analog computer.

In addition all terms in Eq (35) can be written using \ddot{x} :

$$\begin{aligned} \ddot{x} = m^{-1} & \left\{ f(t) - c_1 \left[\Gamma(1/2) \right]^{-1} \int_c^t \ddot{x}(\tau) (t-\tau)^{-1/2} d\tau \right. \\ & \left. - c_2 \left[\int_c^t \ddot{x}(\tau) d\tau + \dot{x}(0) \right] \right. \\ & + c_3 \left[\Gamma(1/2) \right]^{-1} \int_0^t \left[\int_0^t \ddot{x}(\tau) d\tau + \dot{x}(0) \right] (t-\tau)^{-1/2} d\tau \\ & \left. - k \int_0^t \left[\int_0^t \ddot{x}(\tau) d\tau + \dot{x}(0) \right] d\tau \right\} \end{aligned} \quad (41)$$

This form of the equation motivates modeling this second-order system on the analog computer. That is one operational amplifier acts as \ddot{x} and is a summer into which all the other terms serve as input. The output of \ddot{x} is then connected to an integrator, which produces as its output, \dot{x} . This output is then connected to another integrator, and its output is x . Use of a half-order fractional differentiators can produce the $D_t^{3/2}(x)$ and $D_t^{1/2}(x)$ as previously explained. Thus, all the terms necessary to produce \ddot{x} are available and the output of the system (x) can be directed to a display or recorder for observation. A schematic representation of this circuit is found in Figure 22.

It should be noted the operational amplifiers on the model TR48 are inverting amplifiers. That is the output of the amplifier has the opposite sign of the input. For example, when \dot{x} is put through an amplifier configured as an integrator, the output is $-\dot{x}$ instead of \dot{x} . To obtain the correct signs, both the $D_t^{3/2}(x)$ and \dot{x} signals must be passed through inverters to obtain the correct sign.

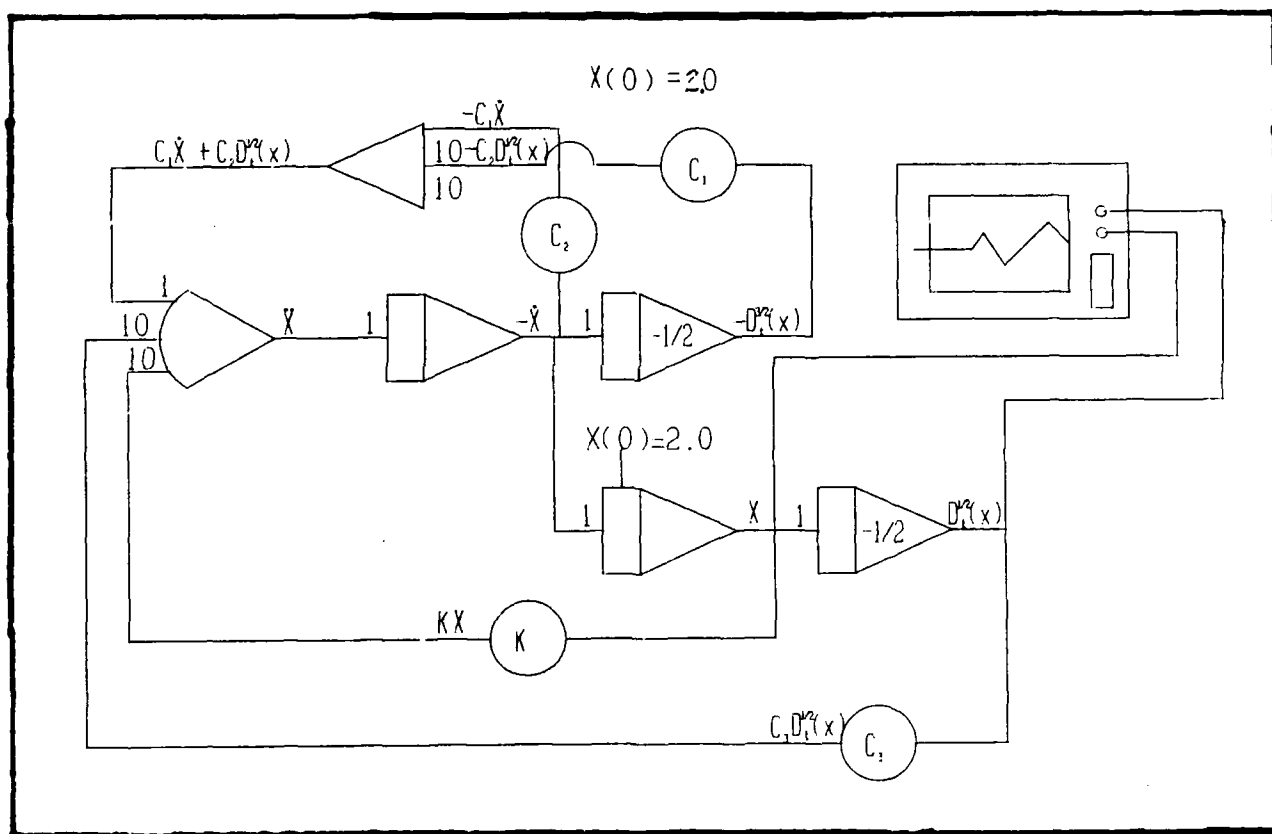


Figure 22. General Analog Computer Configuration for a Second-Order System

Each operational amplifier on the TR48 has four input jacks; two are unity-gain jacks and the other two amplify the input signal by a factor of ten. These factor of ten jacks will hereafter be denoted $\times 10$. To provide the correct coefficients (c_1 , c_2 , c_3 , and k) the output signal for each derivative term must be connected to a potentiometer (Figure 23).

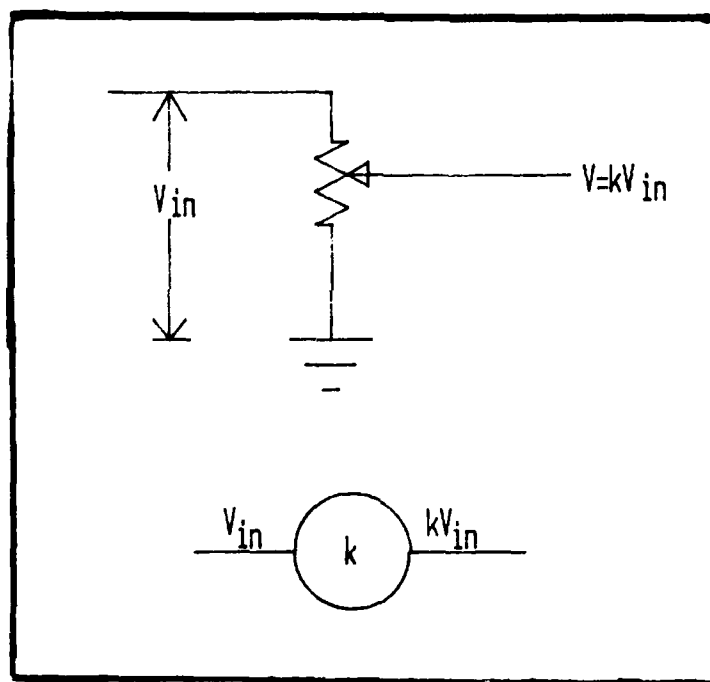


Figure 23. Potentiometer Schematic
and Circuit Symbol

Each potentiometer is adjustable in $1/10000$ th increments to provide a specific fraction of the amplitude of the input signal. For example, if c_1 were 0.2500, the output of the three-halves derivative would have to be connected to a potentiometer set at 0.2500. However, if c_1 were 1.2500, the three-halves derivative would have to be connected to a $\times 10$ input jack on the \ddot{x} summer. Specific details for establishing the proper signs and magnitudes of the coefficients are presented in Appendix F.

Open- and Closed Loop Simulation

The first task was to determine a set of coefficients that would result in frequencies within the operational band of the half-order circuits on hand. At the time the coefficients were developed, the circuit designed by the continued fraction method was the one under consideration. This circuit had a frequency range spanning 0.05 to 0.40 Hz. This range was then evaluated to determine a set of open- and closed-loop coefficients compatible with the circuit's performance. The equation developed was:

$$\ddot{x} + 2D_t^{1/2}(x) + x = u(t) \quad (42)$$

where $u(t)$ is the control force (zero for the open-loop equation).

It should be noted that this criteria is consistent with the Bagley-Torvik model for a viscoelastically-damped structure which has a stress-strain relationship modeled by the addition of a half-order term (13:137).

Using the linear quadratic feedback theory developed in Capt Walker's thesis (6), the optimal feedback for this system was determined to be:

$$u(t) = 1.6324 D_t^{3/2}(x) - 2.891 \dot{x} + 3.1556 D_t^{1/2}(x) - 0.4142x \quad (43)$$

resulting in the closed loop equation:

$$\ddot{x} - 1.6324 D_t^{3/2}(x) + 2.891 \dot{x} - 1.1556 D_t^{1/2}(x) + 1.4142x = 0 \quad (44)$$

Figure 24 illustrates a schematic for the open-loop equation, and Figure 25 depicts the schematic for the closed-loop equation.

The initial condition on x for both the open- and closed-loop cases was originally set at 2.5, volts and in the final stages of the experiment, it was set at 2.0 volts. Stepping down the -10 volt reference voltage on the attenuator module, through a potentiometer, then into the IC jack on the x operational amplifier established this initial condition. This voltage acts as the initial disturbance for studying the response of the system. Again, referencing Figures 24 and 25, both half-order circuits are isolated from the initial conditions by comparators. When the "OP" button is pushed to start the simulation the comparators connect the input to the one-half and three-halves-order circuits. This was accomplished to conform to the necessary initial conditions established by Bagley for all fractional order derivatives (12). The analog computer was operated according to the detailed

description discussed in Appendix F, and the output is recorded on the Hewlett-Packard recorder (model 7090A). Figure 26 is a sample output; it illustrates the x response for both the open- and closed-loop systems.

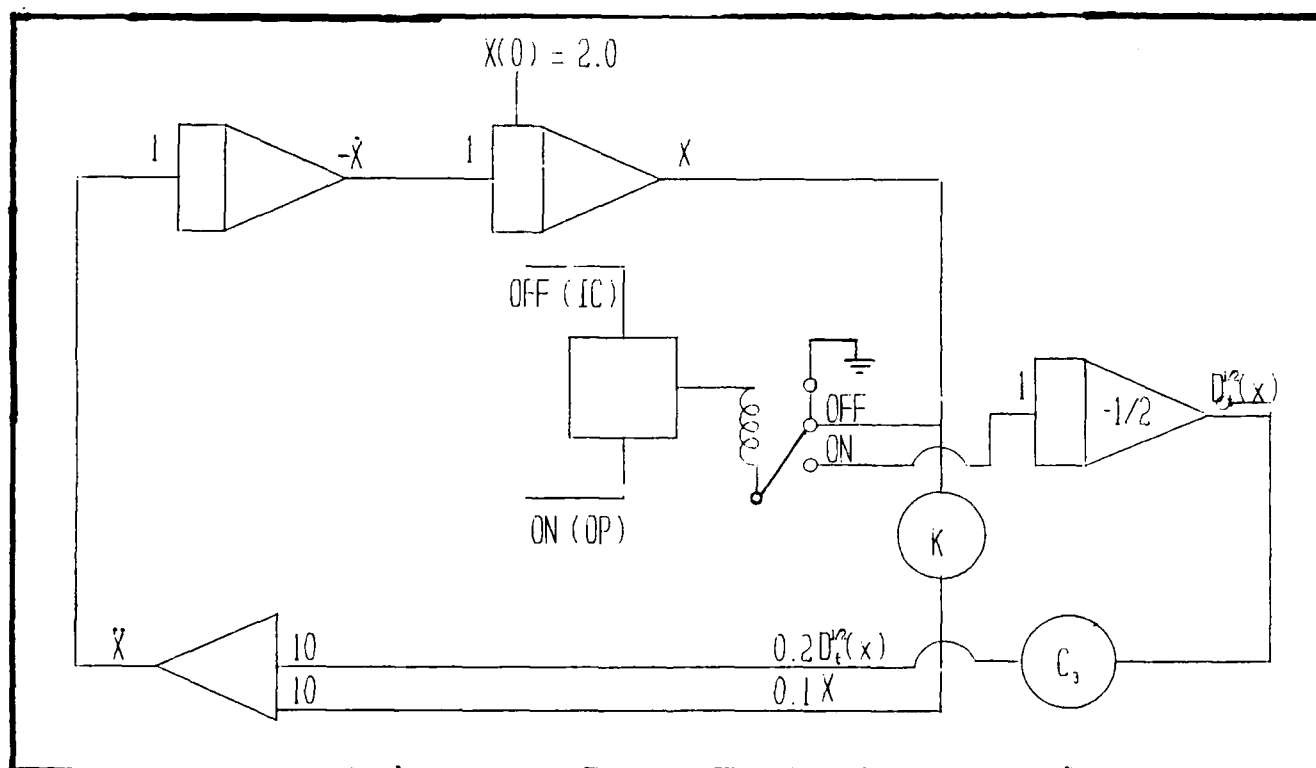


Figure 24. Open-Loop System with Comparator Isolation of $D_t^2(x)$ Input

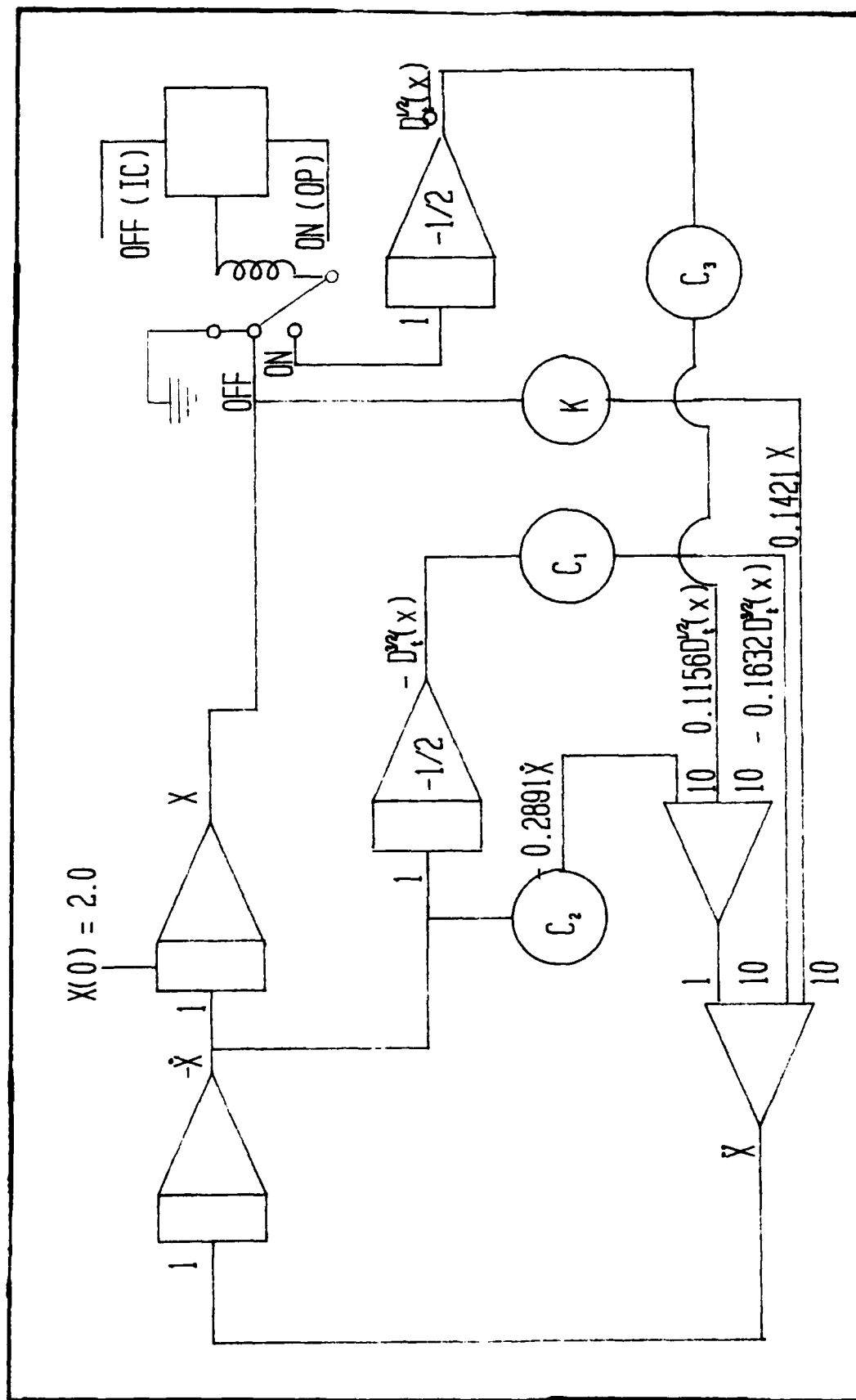


Figure 25. Closed-Loop System with Comparator Isolation of $D_1^2(x)$ Input

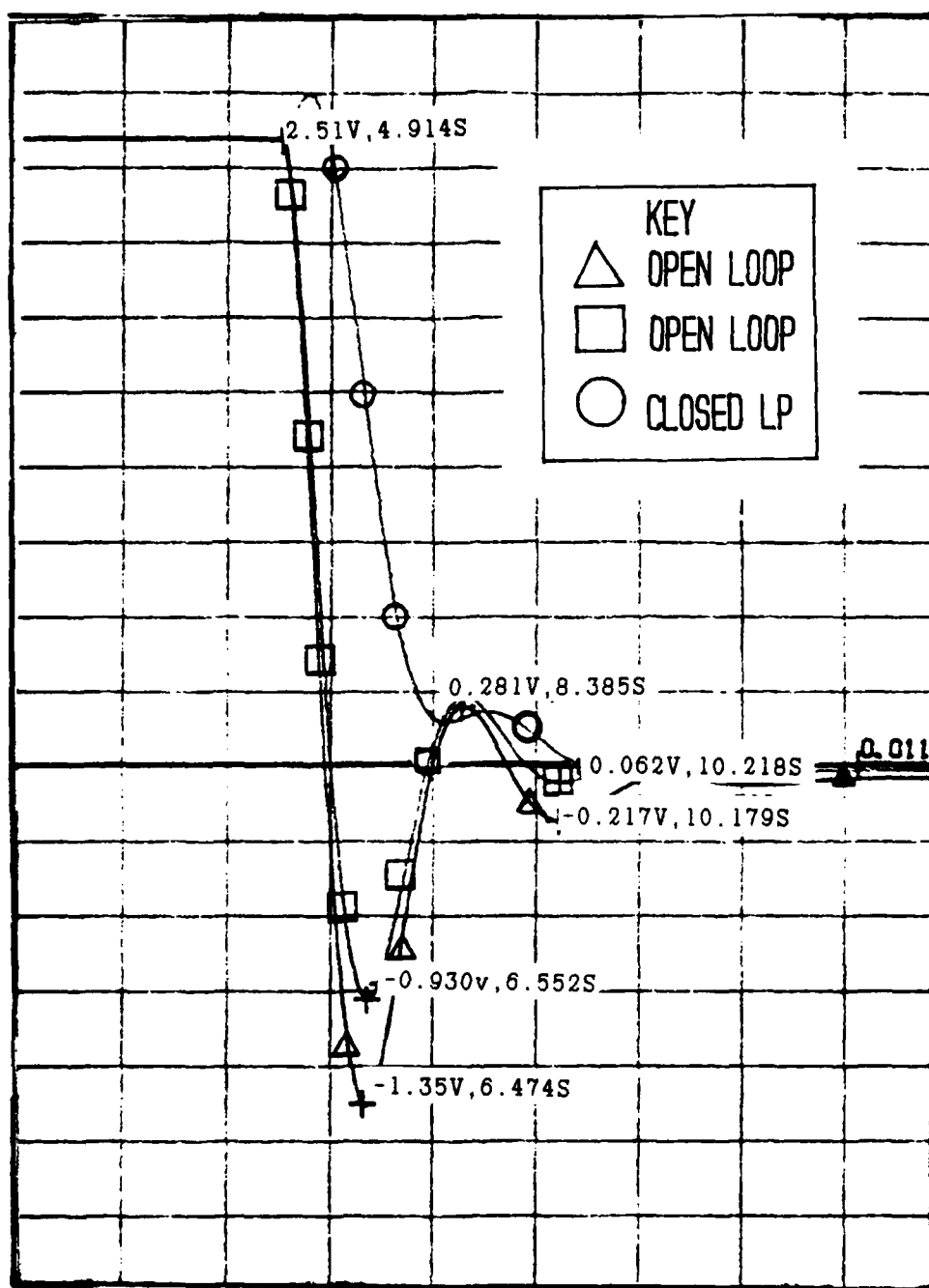


Figure 26. Initial Open- and Closed-Loop Response

Two theoretical methods for predicting the open- and closed-loop responses were developed in parallel with the experimental effort. One method involved Laplace transforms, and it is detailed in Appendix A. The other uses a Mittag-Leffler expansion in the time domain, and it is detailed in Appendix C. Both methods produced exactly the same response for the open- and closed-loop cases. Therefore, only the Laplace transform response will be shown for comparison (Figure 27 for the open-loop and Figure 28 for the closed-loop response). It is easy to recognize the initial discrepancies between the experimental results and the theoretical predictions. In the open-loop case the analytic methods predict a very heavily damped response that never crosses the horizontal axis and approaches zero from above. The experimental results crossed the horizontal axis, approached zero from below and decayed rapidly. The same type of disparity was observed on the closed-loop system. Although feedback made the system more responsive, it became necessary to resolve the discrepancy between theory and experiment.

Total-Cycle Simulation

The previous configuration modeled the open- and closed-loop cases as initial-value problems. This procedure starts with the system at rest. By using a function switch (described in Appendix F), a step voltage was applied to the circuit (Figure 29).

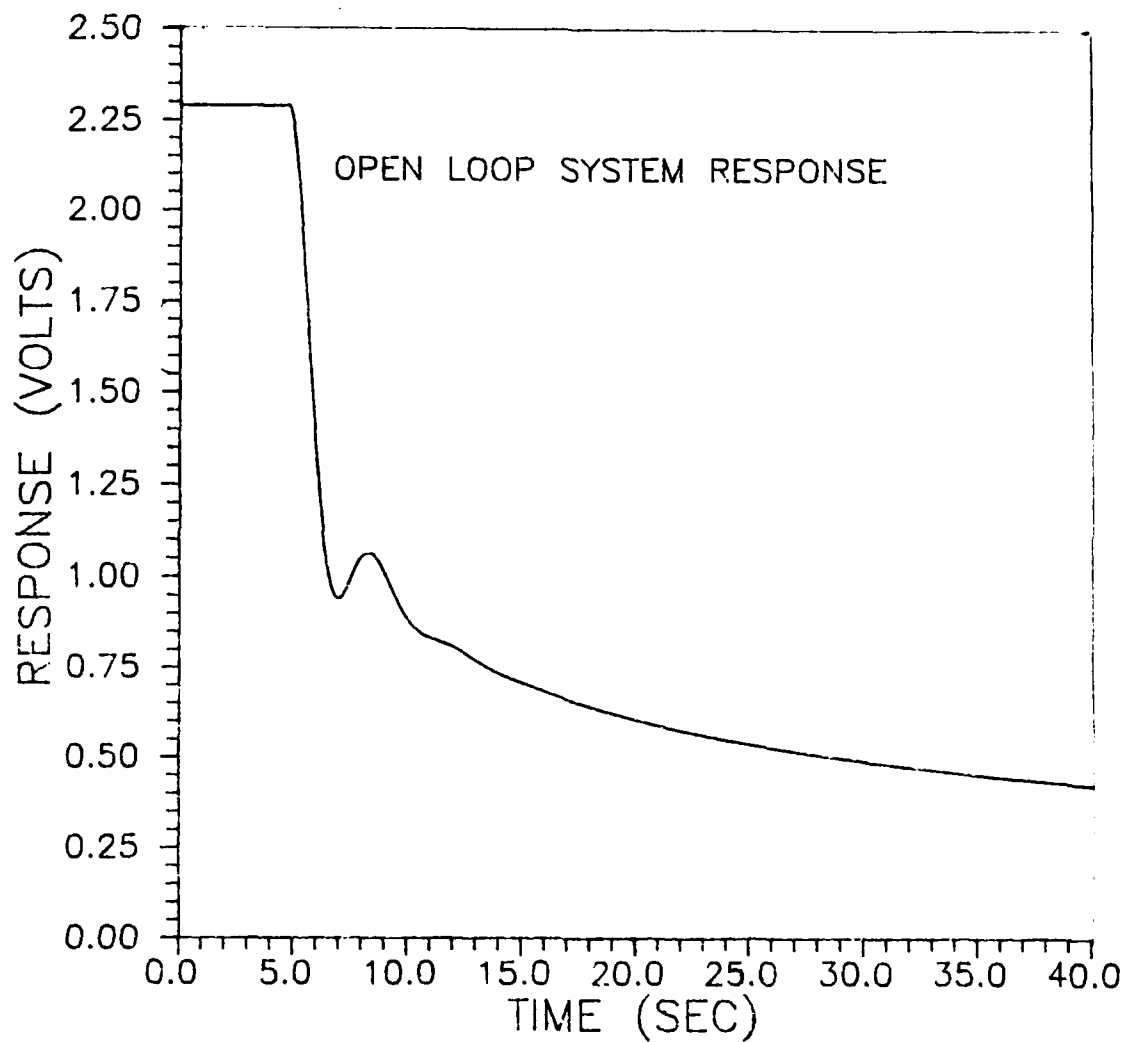


Figure 27. Theoretical Open-Loop Response

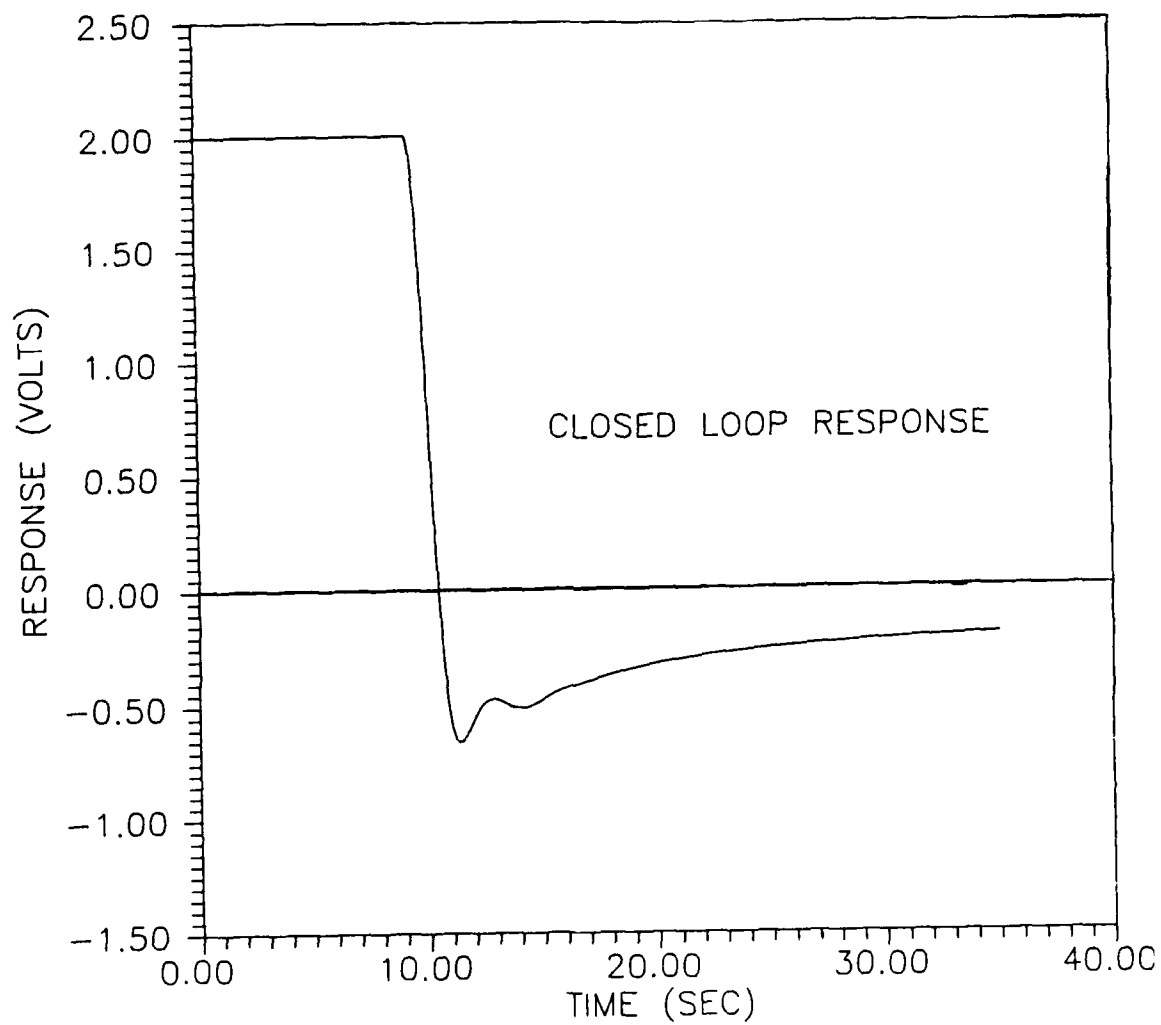


Figure 28. Theoretical Closed-Loop Response

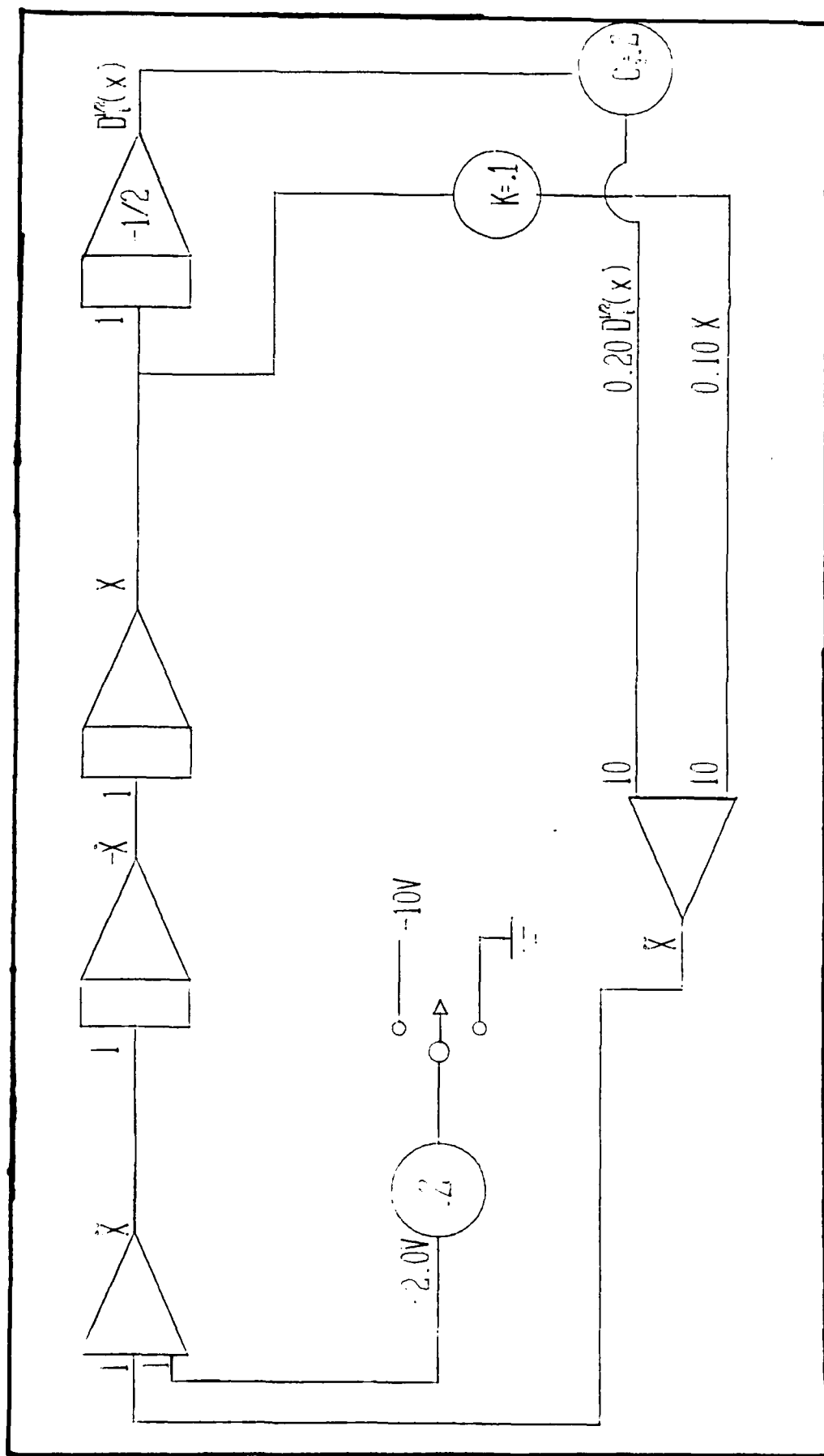


Figure 29. Total-Cycle Analog Configuration

The circuit undergoes a transient response, eventually coming to rest at a displacement value approximately equal in magnitude to the size of the step function. This steady system state is nearly the same as that modeled in the original configuration by placing an initial condition on x . The one difference in this case is that the fractional-order derivatives are not isolated from their inputs. When the function switch was toggled, the step function was removed. This section of the response curve approximates the response modeled by the theoretical predictions. The result of this total-cycle simulation is shown in Figure 30. Figure 31, for the open-loop case, and Figure 32, for the closed-loop case, represent the second half of the Total-Cycle Simulation. The experimental response compares favorably with that modeled by the initial-value problems. Section V (Analysis) draws conclusions concerning the modifications required to the initial-value problem configuration to more correctly model the initial conditions.

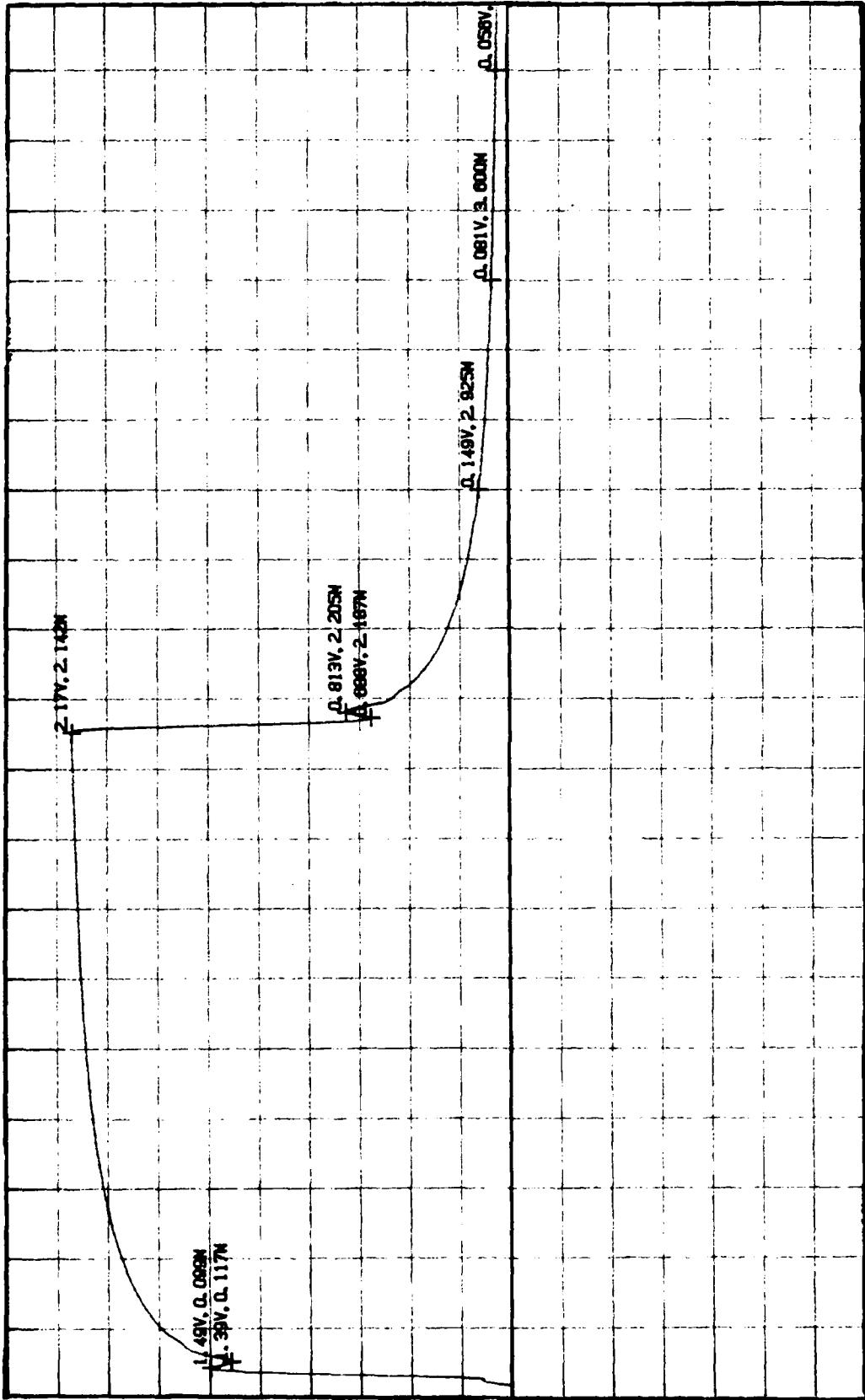


Figure 30. Complete Open-Loop Total-Cycle Simulation

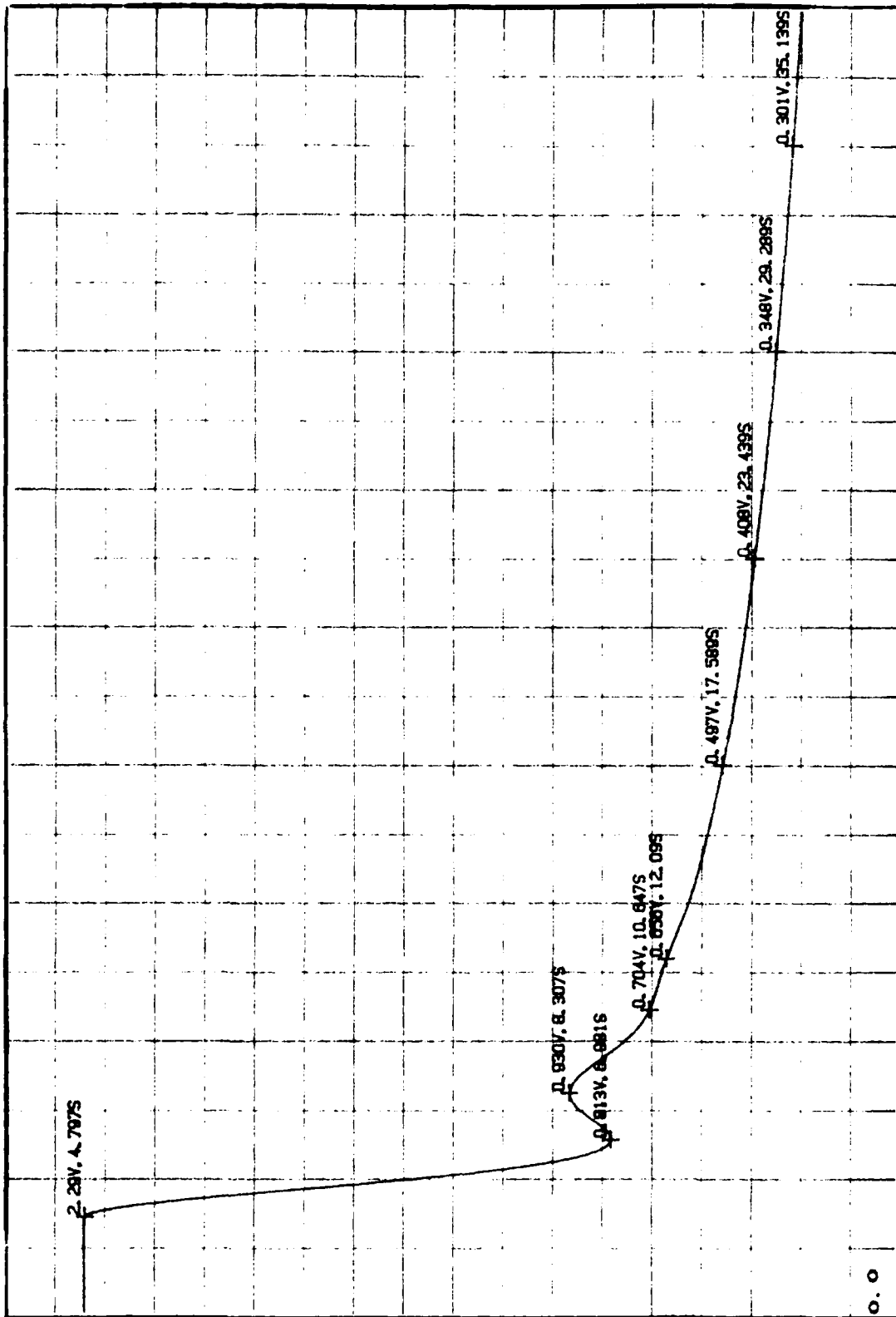


Figure 31. Open-Loop Response After Step Function Removal

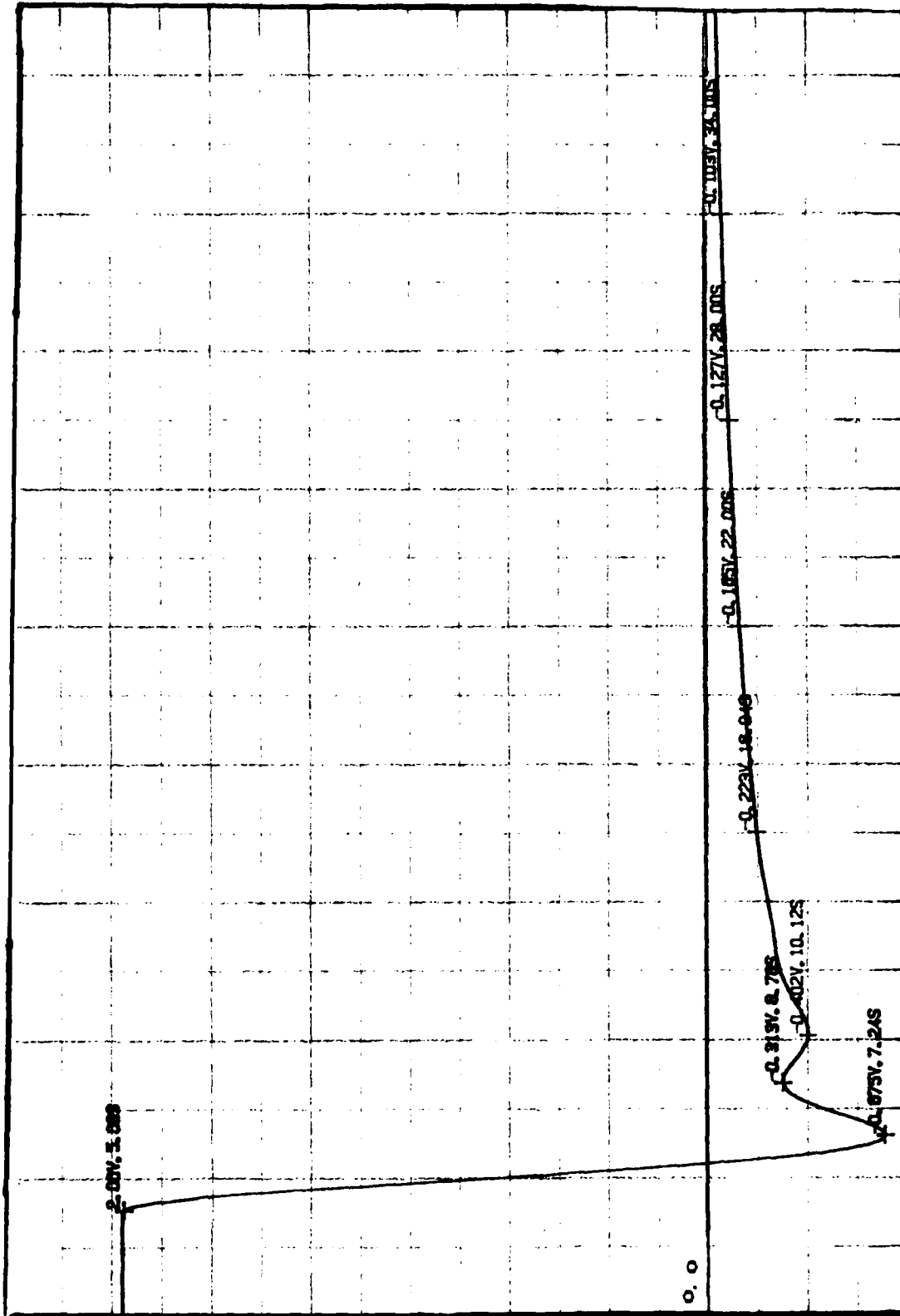


Figure 32. Closed-Loop Response After Step Function Removal

The final configurations for both open- and closed-loop initial-value problems are pictured in Figures 33 and 34, respectively. There are two changes made from the original initial value configuration. First, both half-order circuits are not isolated, but allowed to charge their capacitors to whatever value is consistent with their input. Secondly the "x" summer was isolated from its input using a comparator (Appendix F) until the "OP" button was pressed. Final results for both open- and closed-loop cases are compared with the theoretical predictions in Figures 35 and 36. The minor discrepancies are discussed in the analysis section.



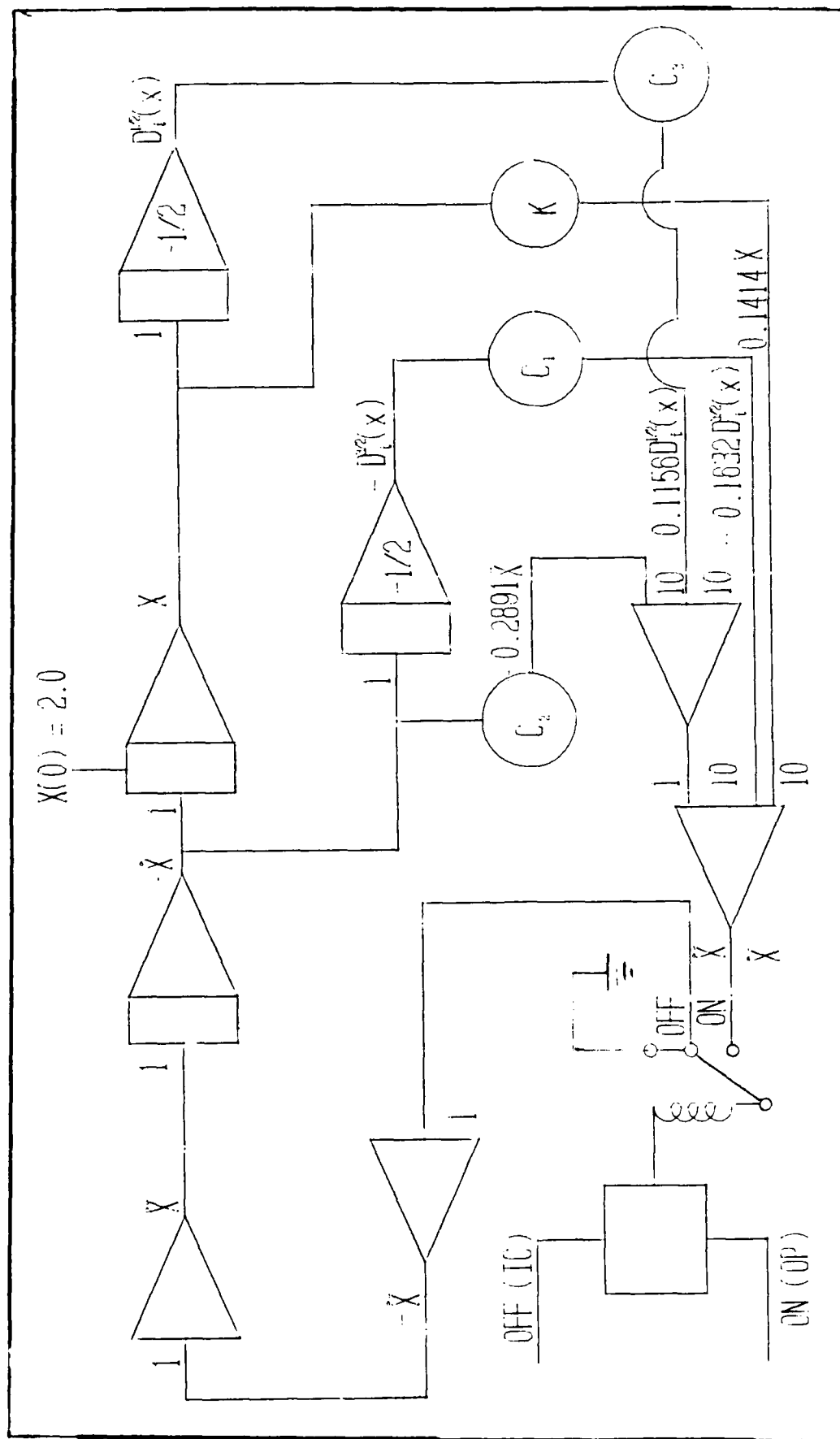


Figure 34. Final Closed-Loop Configuration

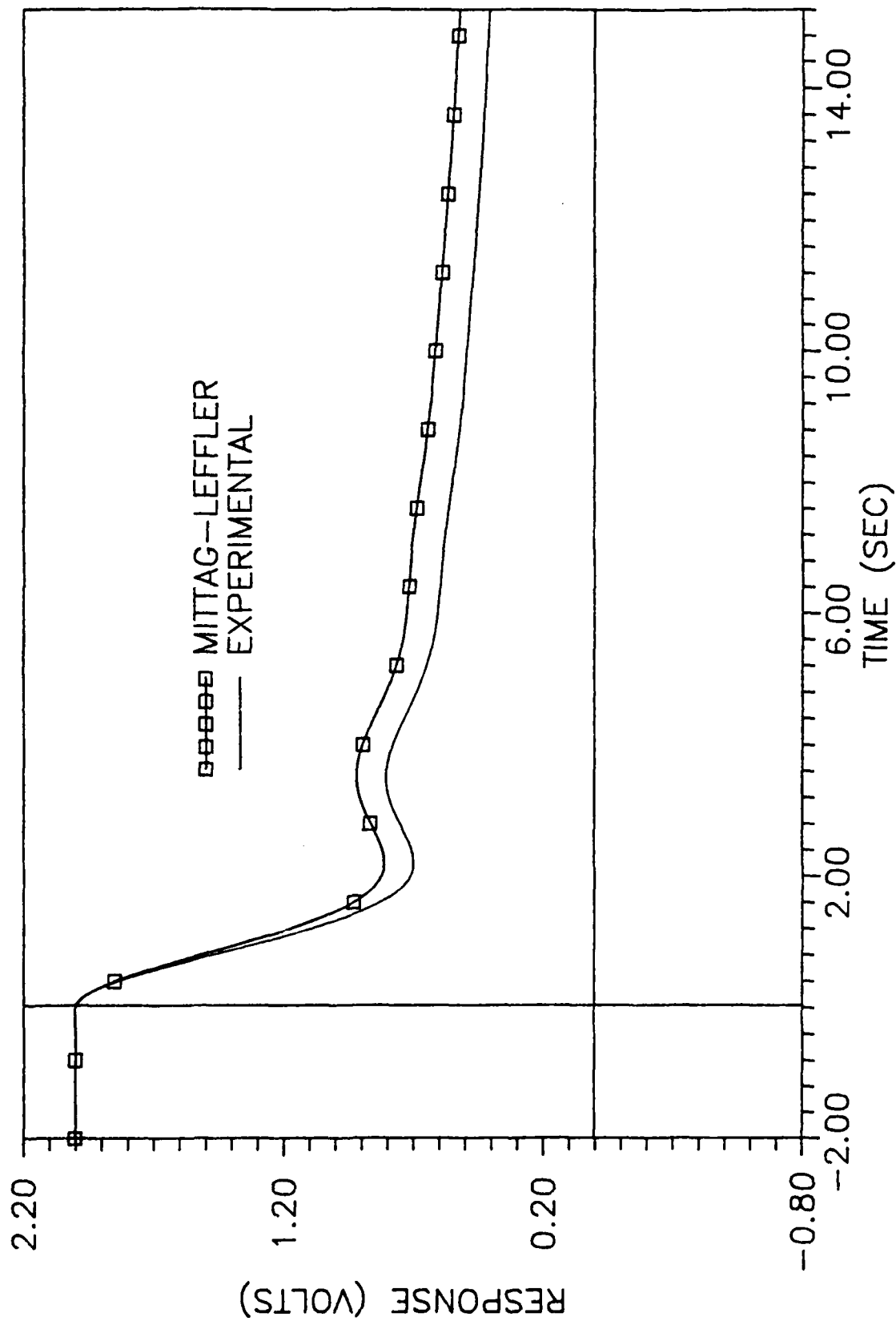


Figure 35. Experimental versus Theoretical Comparison for the Open-Loop Configuration

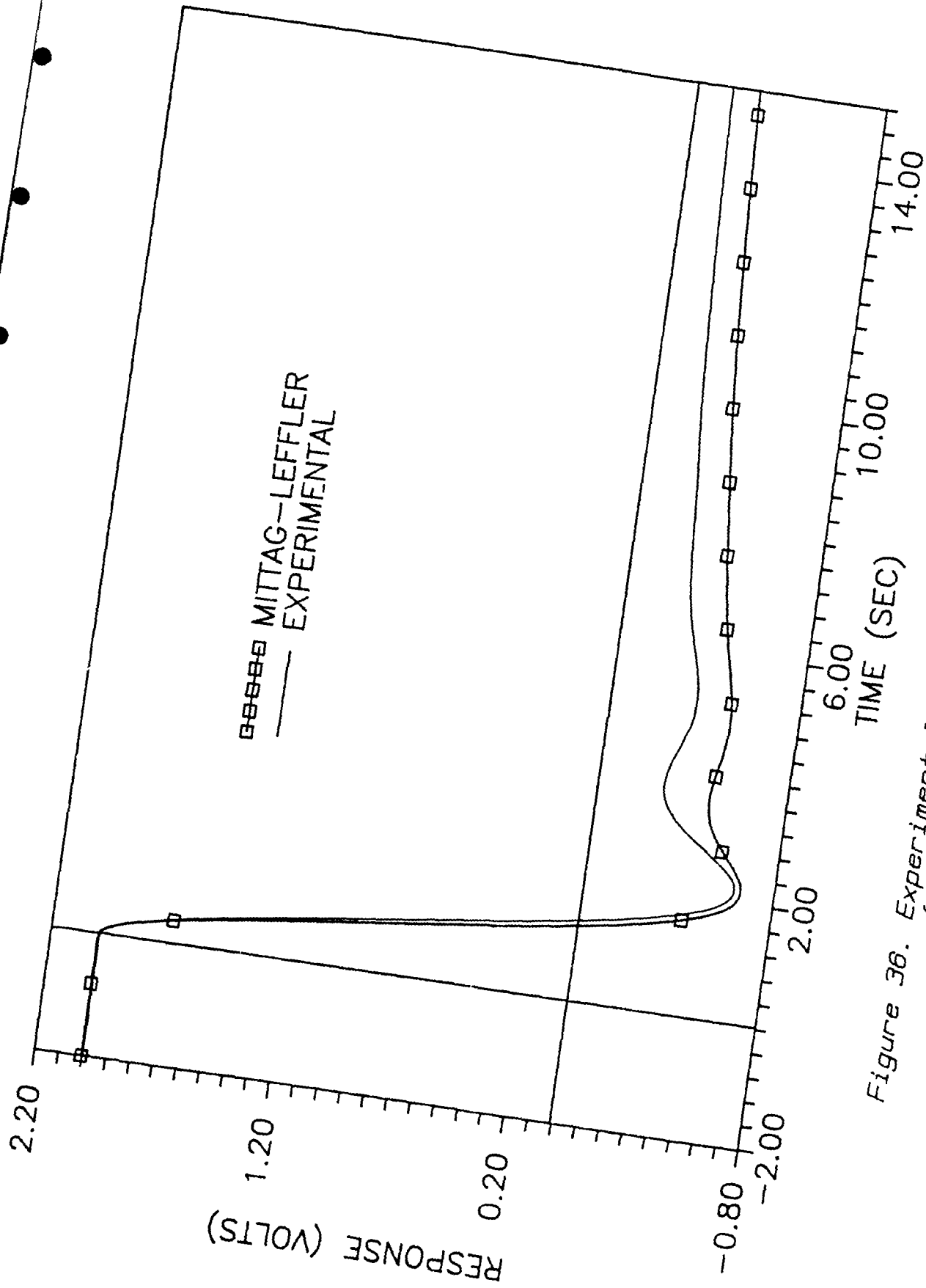


Figure 36. Experimental versus Theoretical Comparison for the Closed-Loop Configuration

V. Analysis of Results

Introduction

This section deals only with anomalies and unexpected results encountered during the research. Tasks which closely matched theoretical predictions are covered in the conclusion section; it is sufficient to state they functioned as expected. The discussion is divided into three parts; problems in the circuit validation, problems with simulation results, and disadvantages associated with using the analytical tools. In each area, the problems are defined, possible causes listed, and solutions presented.

Circuit Validation

The voltage level output from the Tektronix function generator was not constant over the frequency range tested. At low frequencies, (0.05 Hz) the output voltage was several volts lower than at higher frequencies. The function generator is designed to terminate into a 50 Ω impedance load. The Oldham-Zoski circuit impedance is much higher than this, especially at low frequencies where the majority of the current passes through the resistors. By placing a 50 Ω resistor in parallel with the circuit, the impedance remained close to 50 Ω . The variation of circuit impedance with the frequency at which the circuit was tested was not observed to adversely affect the performance of the test configuration. Slight differences were noted in the start-up transient response of the input and output signals as a function of frequency.

These transient characteristics are repeatable for a specific circuit and frequency. In addition, the amplitude of the input signal remained between 8.00 and 8.10 volts for all frequencies tested (Appendix G contains the circuit verification data). These slight variations were judged to be acceptable.

When using the oscilloscope and counter/timer combination to determine magnitude and phase angle, the results were not repeatable to the accuracy desired (± 1 dB/decade gain slope and ± 5 degrees phase shift). The slope of the Bode magnitude plot would vary from 9.1 to 11.25 dB/decade, and the phase angle varied from 37 to 43 degrees as a function of frequency. The oscilloscope was not capable of tracking the output of the fractional order circuit using just one magnitude range. Constant adjustment was required. It became necessary to check the adjustments twice at each frequency to ensure that the controls had not been bumped when changing from one channel to the other. The trigger control on the counter/timer which is tuned to detect a signal crossing through the zero voltage level was extremely sensitive. Because of the need for frequent adjustments, the confidence in these results was low.

It became necessary to attempt verification of the circuit on the analog computer. The three-halves derivative functioned correctly on the analog, when implemented. The phase was approximately 43 degrees, and the magnitude could be adjusted correctly. However, running the output of the three-halves derivative through an integrator to produce the one-half derivative produced the sinusoid-ramp combination

illustrated in Figure 17. The peak-to-peak amplitude of the sine wave had the correct magnitude, but the underlying ramp function indicated a bias voltage at the input of the operational amplifier.

The source of the bias could not be readily identified. With visual observation of the phase and magnitude, it was impossible to determine small biases on the output signal or to observe the transient adjustment of the circuit to an input signal. To further complicate matters, the original method of connecting the fractional-order circuit to the operational amplifier was accomplished by inserting a banana plug directly into the summing junction of the operational amplifier. This procedure avoided adding resistance to the circuit by connecting into one of the input resistors of the operational amplifier. When the signal passed through the operational amplifier, it produced the extremely noisy output signal illustrated in Figure 37.

Many possible causes were identified with the original circuit configuration. First, there was concern with the many potential sources of stray voltages and inductances. The operational amplifiers were not commonly grounded; this situation enhanced possible ground potential biases between components. The long patch cords connecting the circuit board to the analog computer passed in close proximity to the analog computer's power supply. The long leads on the discrete resistors and capacitors were not trimmed, resulting in a circuit similar to that depicted in Figure 38. These items were corrected by grounding the circuit board and operational amplifiers together, trimming component leads so that the components were flush-mounted to the circuit-board,

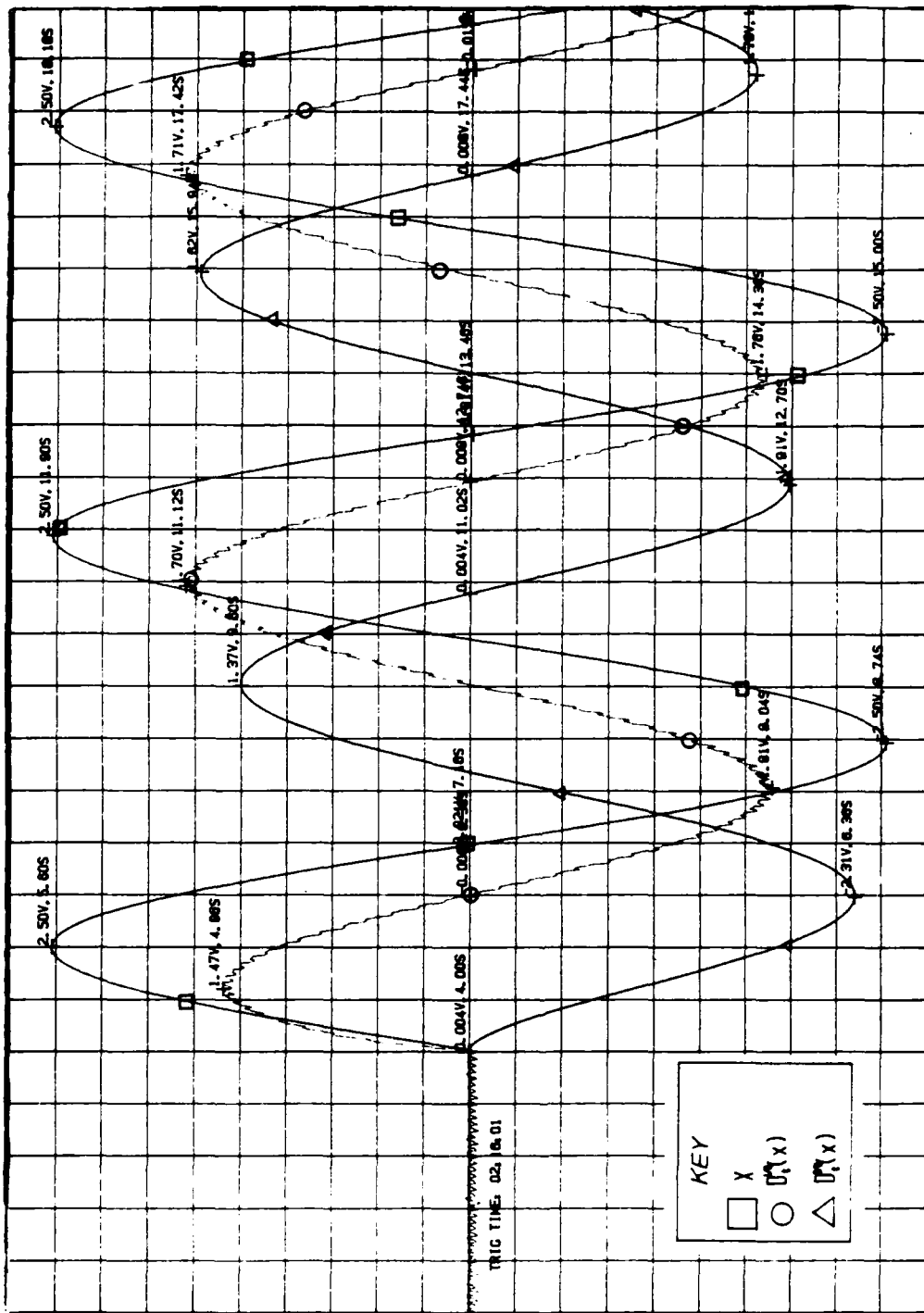


Figure 37. Noisy Output Signal When Interfacing the Oldham-Zoski Circuit With the Analog Computer Through a Summing Junction

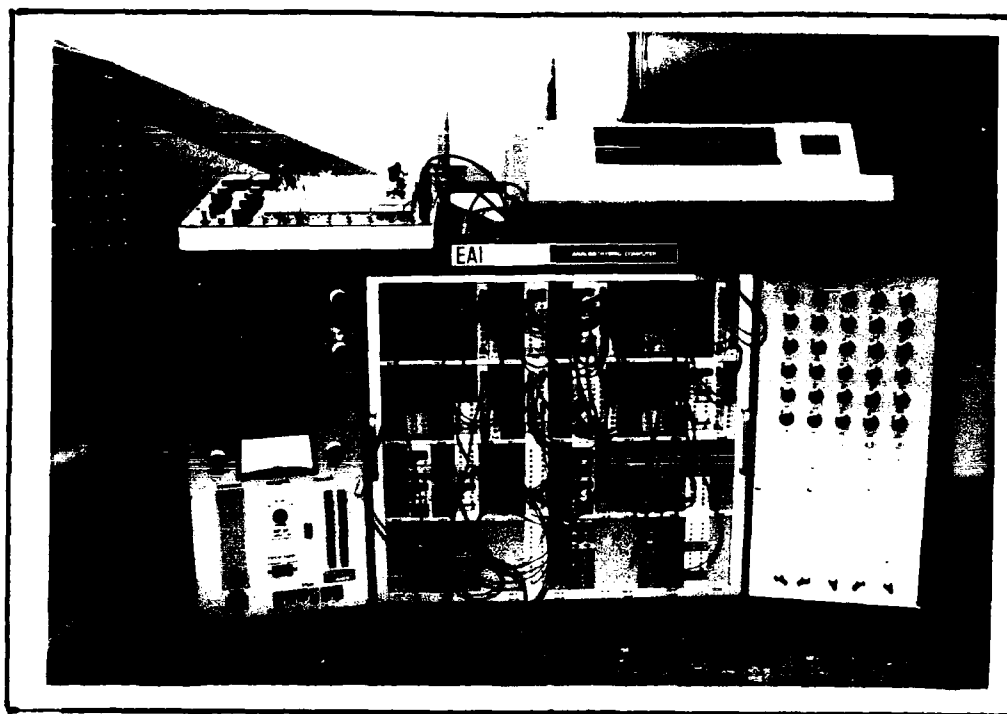


Figure 38. Long Leads on Discrete Components

and using coax cables to connect the circuit-board to the analog computer. Reducing the final resistance value in the half-order circuit by $10K\Omega$ and patching its output into a $X10$ input jack ($10K\Omega$ resistance) on the operational amplifier, instead of the summing junction, eliminated the noisy signal.

The most significant change was the use of the Hewlett-Packard analog-digital recorder (model 7090A). It eliminated problems associated with the start-up transient. Appendix G contains the plots of the circuit validation; the start-up transient is seen to be smooth with no discontinuities. The analog-digital recorder greatly simplified data collection and analysis; set-ups became routinely simple, and digitized values of interest on the output plot could be annotated directly on the plot through the use of a built-in routine.

The method of supplying the one-half derivative was altered to eliminate the ramp. A second half-order circuit was constructed with capacitors having twice the value of the capacitors used in the first circuit and resistors having half the value of those used in the original circuit (the time constant remaining the same).

The performance comparisons of the circuits produced an unexpected result. When second-order effects are considered, a capacitor is modeled as a lossless capacitance in parallel with a resistance (19). When combined into a typical Oldham-Zoski cell, the second-order model then has a capacitance in parallel with two parallel resistances. One would predict the circuit with the lowest capacitance to be the circuit with the best phase characteristics. Comparison of Figures 7 and 9 show this is indeed the case. When designing future circuits an effort should be made to make the capacitor values as small as feasible. The use of an impedance bridge to measure the 'quality' of the capacitances is also recommended.

The circuit produced a phase angle of 43 degrees when connected to the analog computer, but only 37-38 degrees when measured by the oscilloscope and analog-digital recorder. Examination of the input circuitry on the analog-digital recorder showed a 1M Ω resistor connected in series with the input. To correct this situation the circuit was connected to ground, instead of connecting the half-order circuit directly to the input of the recorder. The recorder was then put in parallel with the last resistor of the half-order circuit. This configuration produced a phase angle of 43 degrees.

Finally, the ramp in the one-half derivative that resulted from integrating the three-halves derivatives requires analysis. With the Hewlett-Packard analog-digital recorder, small amplitude biases were observed in the output of both half-order circuits. The input from the function generator was also observed to be biased. It appeared this was the reason for the anomaly. A closer evaluation proved differently. For example, in the validation plot (Appendix G) for Circuit 1 at $f = 0.1451\text{Hz}$ ($\approx \omega = 1$), the ratio of the input amplitude (peak-to-peak) to the output amplitude is 63.32. However, the ratio of total offset is:

$$\frac{\left(\left| \text{positive peak} \right| - \left| \text{negative peak} \right| \right)_{\text{INPUT}}}{\left(\left| \text{positive peak} \right| - \left| \text{negative peak} \right| \right)_{\text{OUTPUT}}} = 22.85 \quad (45)$$

This analysis indicates only 0.0025 volts of the bias is attributable to the input bias, while the total bias is 0.007 volts. Using this rough, first-order method, the actual bias voltage of the circuit is:

$$\left(\frac{0.007 - 0.0025}{2} \right) = 0.00225 \text{ volts} \quad (46)$$

The gain of Circuit 1, when connected to the analog is 25.6. This should result in an actual bias on the output of the differentiator of 0.060 volts. This value is small when compared with the 2.0-volt initial-value, but when integrated over time, this value would produce a significant ramp. The actual calculation of the bias voltage required to produce the ramp observed is:

$$\left(\frac{-0.07 \text{ v}}{(45.12 - 98.88) \text{ s}} \right) = -0.013 \text{ volts/sec} \quad (47)$$

The bias observed was actually much less than that predicted by this first-order method. It is noted that Circuit 1 is biased positively while the one-half derivative exhibits a negative bias. The operational amplifiers involved are inverters; therefore, the bias does have the correct sign.

Does this bias affect the simulation, and is it an error that increases with time? The output of the one-half and three-halves derivatives is connected to the summer and results in an amplitude error of the opposite sign of the particular fractional derivative; that is $\ddot{x} = -D_t^{3/2}(x) - D_t^{1/2}(x) + \dots$. If the one-half derivative is larger than nominally predicted, and it should be, then \ddot{x} is slightly smaller than it should be. Thus \dot{x} is smaller than it would be if the bias was not there, and the same argument applies to x . When x is differentiated by the fractional-order circuit the result is a slightly smaller $D_t^{1/2}(x)$ input, compared to the case where the bias was not present. In other words, with feedback, the error is stable and does not grow with time.

Upon completion of the second fractional-order circuit design, the circuit was connected to the harmonic oscillator for an amplitude check with $\omega = 1$ radian/sec. The harmonic oscillator's output amplitude was not stable, and decayed with time. The first thought was to remove the fractional-order circuit to see if it might be the cause. With this done, the amplitude continued to decay. Three new operational

amplifiers were selected, the circuit was rewired, and the problem persisted, indicating it was not an operational amplifier problem. A second analog computer was placed into service, thinking the power supply was bad on the first unit, but the decay still continued. It was then noticed that everytime someone used a computer-printer in the room, the voltage would experience a step-function loss of amplitude. Waiting until the demand decreased on the electrical supply circuit before operating the analog computer solved the problem. The whole analog computer functioned better; the potentiometers were not as noisy and easier to set. The operating schedule was shifted to occur late at night when the electrical supply was more stable.

Open- and Closed-Loop Simulation Problems

Figure 26 shows the initial open- and closed-loop responses obtained experimentally. Figures 27 and 28 depict the results predicted for the simulation by the Laplace transform method. The frequency, amplitude, and axis crossings vary significantly from that observed experimentally. A second Laplace transform prediction was made (Figure 39), deleting the $s^{-1/2}$ terms when transforming the half-order derivatives (see Appendix A). This response was almost entirely due to the residue, there was very little contribution from the integral along the branch cut. The result was in close agreement with the experimental data, however, it did not agree with the initial-value problem work reported by Bagley (12) which required the $s^{-1/2}$ terms.

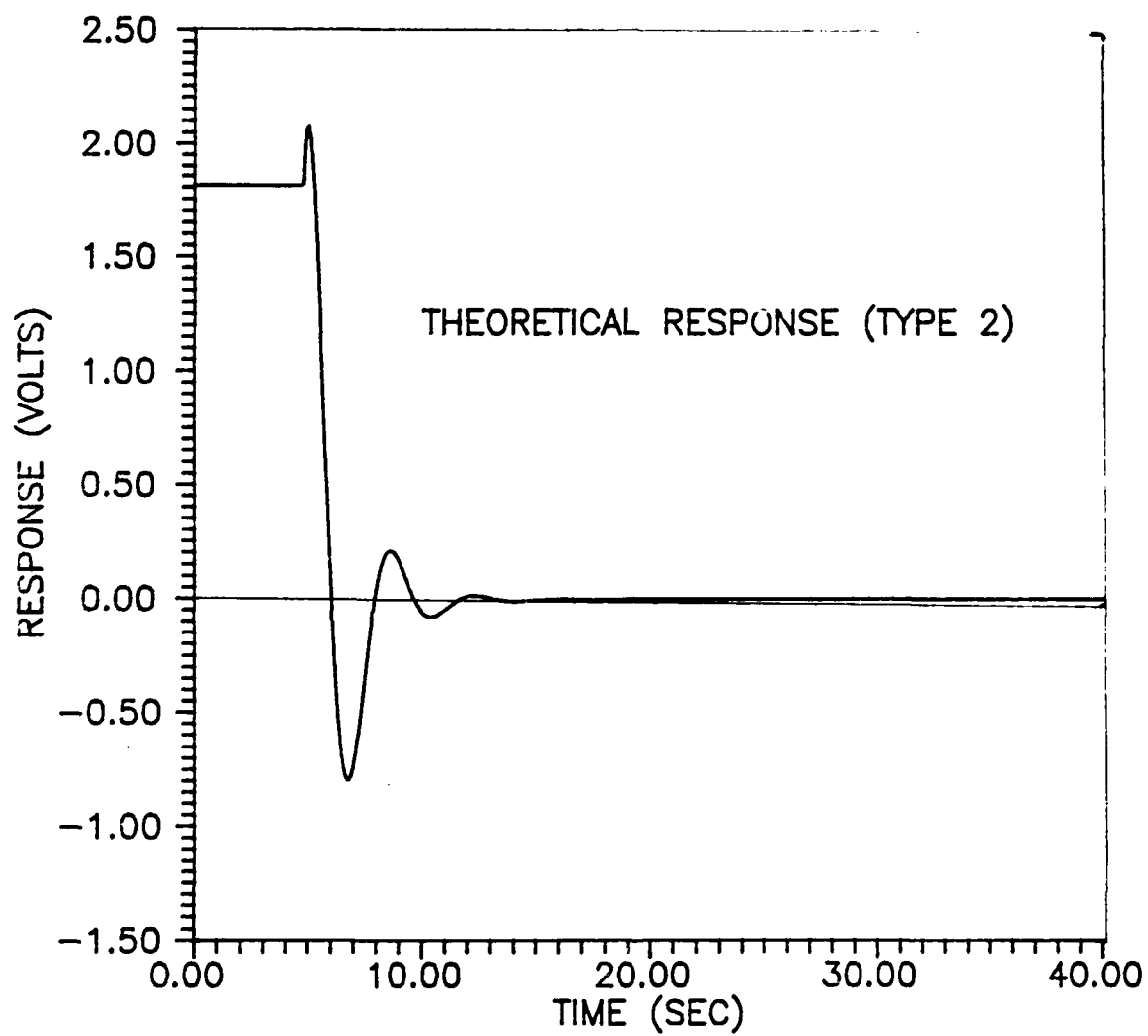


Figure 39. Theoretical Response Without the $s^{-1/2}$ Initial-Value Terms

The first thought was that the circuit and experimental methods were incorrect. The second thought was that the $s^{-1/2}$ terms in the Laplace transform method were invalid. After looking at several possibilities, it appeared that the problem centered on the method of applying the initial conditions and an understanding of the definition of a zero initial condition on the half-order circuits.

Two specific applications of initial conditions were in question. During the gain evaluation phase a decision was made to isolate the one-half derivative's input until the 'OP' button was pressed. Figure 40 shows the response of the one-half derivative when not isolated. It appears to require four or five cycles to adjust to the correct amplitude. Comparison of this response with that of Figure 41, in which the one-half derivative was isolated with a comparator, led us to believe that a zero initial condition on the half-order circuits meant isolation. When isolated, the one-half derivative attains the correct amplitude in one cycle. For this reason the decision was made to isolate both the three-halves and one-half derivatives. Secondly, when a system is at rest at some displacement value, it is expected that the acceleration would be zero. In the simulation, the \ddot{x} initial condition of 2.0 volts appeared as -2.0 volts at the summer, indicating the system was not at rest.

Two test cases were devised to address the problem. In both cases, the initial displacement was set to zero. In the first case, a harmonic oscillator with $\omega = 1.585$ rad/sec served as the input to the \ddot{x} summer as a forcing function for the circuit $\ddot{x} + x = 0$. The one-half

derivative was connected to the displacement (x) output. The response of the one-half derivative and displacement were recorded.

If a 45 degree phase lag and an amplitude of $(1.585)^{1/2}$ was observed for the one-half derivative, the circuit was working correctly. After one complete cycle, this was the case (Figure 42). This test verified the circuit and methods used; therefore, the initial required further investigation. The comparators were removed from the half derivatives and $x(0)$ was set equal to zero. The "Total-Cycle simulation", as described in the Section IV, was then run. Figures 30 and 31 are examples of this procedure for the open-loop system and Figure 32 is an example for the closed-loop. On one of the runs the "HD" (hold) key was used to hold the values of the displacement (x) operational amplifier at the upper stationary position. The summer value displayed on the Digital Volt Meter (DVM) at this point was 0.0000 volts. With the circuit still on hold, the function switch was then opened, the value of \ddot{x} changed immediately to the negative of the value of the step function. The "OP" button was pressed and the circuit duplicated the second half of the total-cycle simulation. Armed with this information \ddot{x} was isolated from all inputs until pressing the "OP" button closed the comparator contacts. Neither of the half-order circuits was isolated. The circuit was reconfigured so the initial condition was again applied through the IC jack in the x operational amplifier. Figures 35 and 36 depict the final experimental/analytic comparisons for both the open- and closed-loop simulations.

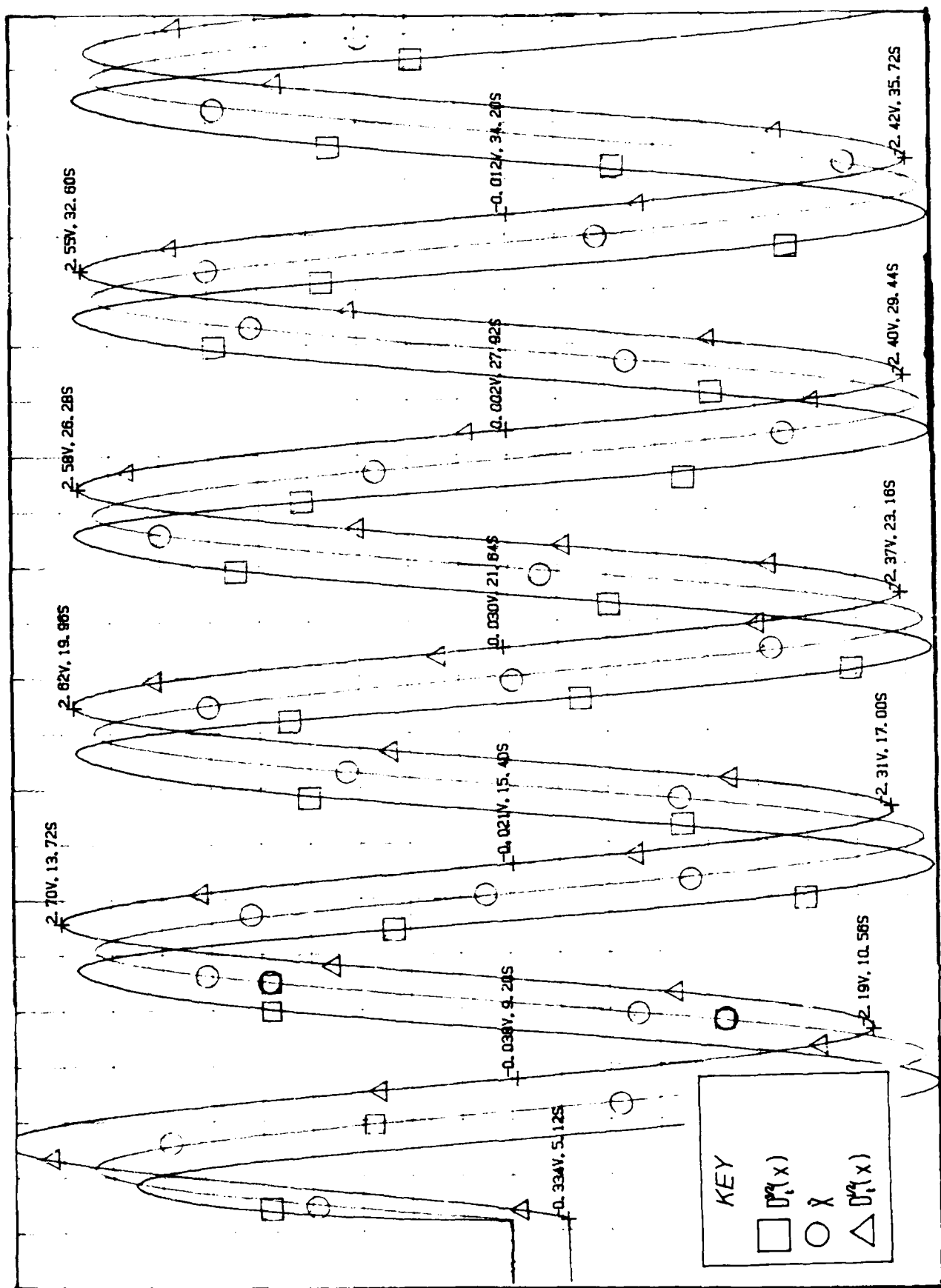


Figure 40. Half Derivative Response with the Input Not Isolated at $t=0$

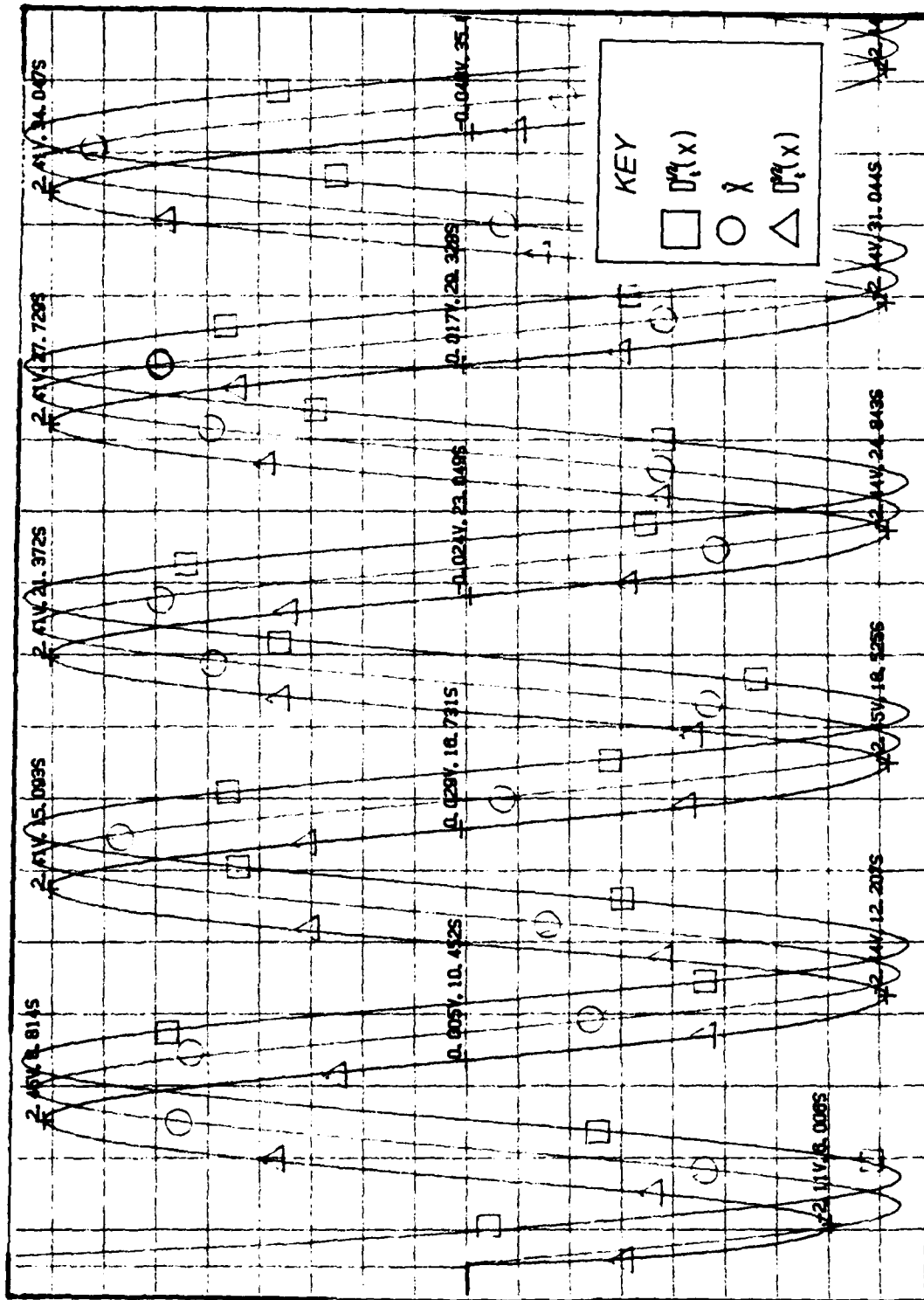


Figure 41. Half Derivative Response with the Input Isolated at $t=0$

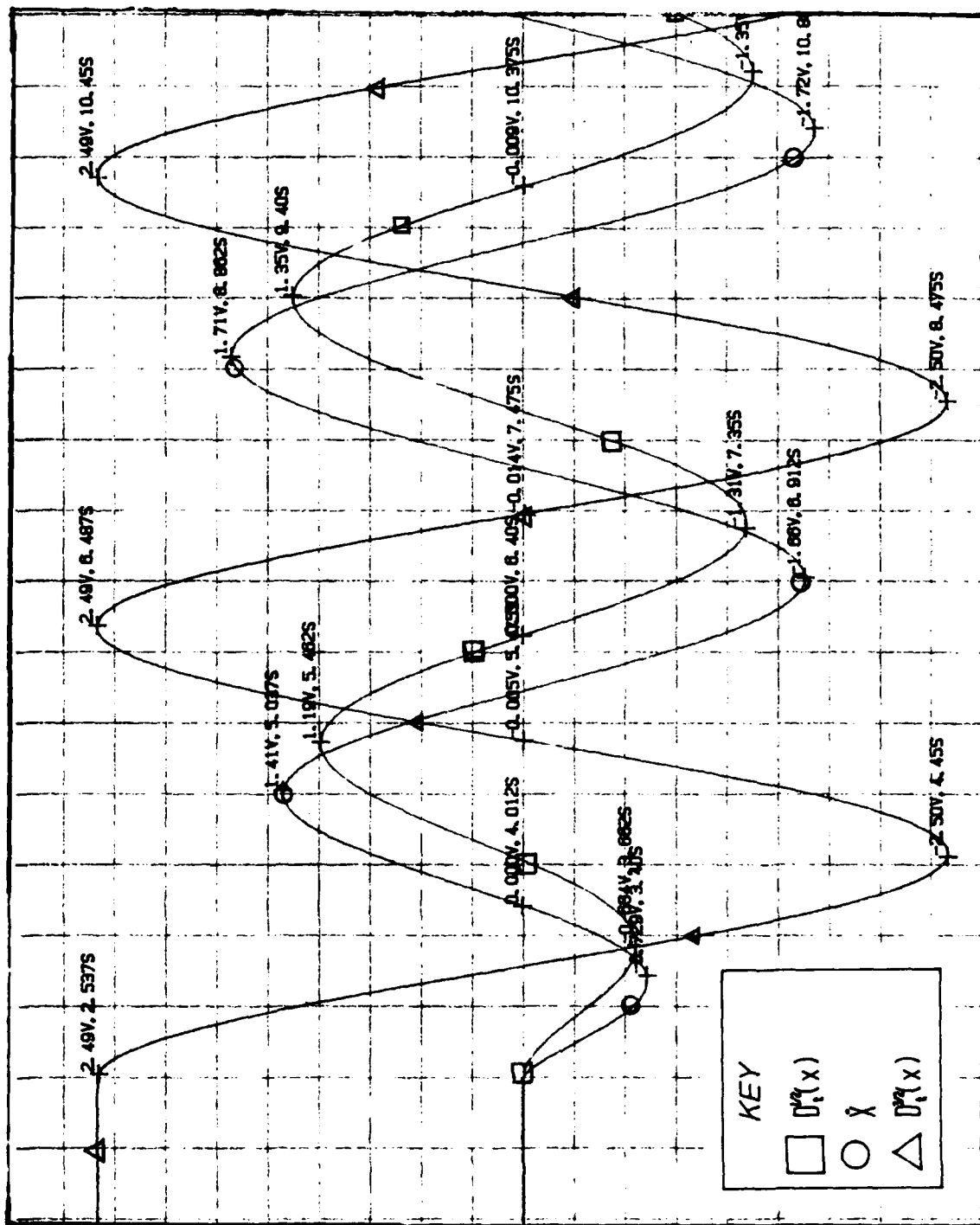


Figure 42. Response to a Sinusoidal Forcing Function
with $\omega_2 = 3.5$

It appears that to function properly in an initial-value problem simulation the capacitors in the fractional-order circuits must be charged to a voltage consistent with the initial value of their input signal. If the initial value of the input to the half-order circuit is zero, zero initial voltage on the half-order circuit is consistent. If the initial value of the signal input to the fractional-order circuit is other than zero, then the initial voltage of the circuit must assume a voltage consistent with that input voltage.

There was a small, apparently constant, displacement in the experimental value when compared with the analytical results. If the absolute value of the displacement varied as the ratio of c_3 to k in the equations, it would indicate a relationship between the displacement and one-half derivative. However, the magnitude of the displacement does not seem to vary from the open-loop to the closed-loop situation; it only changes signs. When not isolated, the $D_t^{1/2}(x)$ initial value is 0.143 volts in the open-loop case and 0.135 volts in the closed-loop configuration. The net displacement between the experimental and analytical results is approximately 0.07 volts. This value is nearly the same magnitude as the circuit bias, but if the bias is the cause, the value of the displacement should change by a factor of two due to the change in c_3 . However, the OZ circuit is only an approximation to an $s^{1/2}$ transfer function over the frequency range of its design. Therefore, the long term accuracy of the circuit is dependent on its

lower frequency limit. Consequently, the results observed are likely to be the best possible for a circuit with this set of design parameters. These displacements, in both cases, make the circuit more responsive and approach zero faster than predicted. This anomaly will be left as an open issue for follow-on research.

Theoretical Tools

Mittag-Leffler Expansion (Appendices C and D)

The program MITLEFR.DAT, an executable file in Matrix[®]_x, expands the roots of the characteristic equation in an infinite series to provide the response of the open-and closed-loop systems in the time domain. For this case the solution was obtained for a second-order system involving multiples of the half derivative $[x, D_t^{1/2}(x), \dot{x}, D_t^{3/2}(x)]$. However, it can be used to expand a second-order equation made up of any 1/nth fractional-order terms by entering $(N = 2 \times n)$ when prompted. Input parameters are upper and lower time limits for calculation, actual response start time, coefficients of the differential equation, and initial conditions for $x, \dot{x}, D_t^{1/2}(x)$, and $D_t^{3/2}(x)$. The method is effective for approximately 15 seconds from the time the response starts. For extended lengths of time, the number of terms required to obtain convergence of the expansion becomes excessive. For example, it required 2 hours of run time to evaluate 100 points using 200 terms in the series for the open-loop system. It required nearly the same amount of time to evaluate 50 points using 400 terms in the closed-loop case.

Laplace Transform (Appendices A and B)

The program RESPONSE is written in Fortran and performs a contour integration in the complex plane to calculate the time response (20:818-824). The current method requires manual calculation of the residues. In addition, asymptotic approximations to the integrand must be made to simplify the inversion process. Figure 43 shows a comparison of five different selections for the asymptotic limits. Three of the five trials required twenty minutes of computational time; the other two required two hours.

The results of the five trials are remarkably close, yet the processing time can be increased unnecessarily by an improper selection of limits. Each time an analysis is accomplished for a different set of coefficients, the equations for four derivatives of three functions must be inserted into the proper function routine in the program. The supporting function routines must be recompiled and then linked with the main program for each specific set of equation coefficients (m, c_1, \dots, c_n, k). The Laplace transform method is not limited with respect to time. If it is necessary to characterize the entire response of a specific system, and that system's response lasts longer than 15 seconds, the Laplace method is viable. However, the Laplace transform method is limited with respect to responses which have Laplace transforms.

Additional Comments - Deciding Which Method to Choose

Figure 44 shows a comparison of the two methods; they are identical. For initial characterization of a system the Mittag-Leffler should

be used since it's easy to implement. For extensive time-domain analysis the Laplace transform method is preferred.

Why use the analytic tools, if the analog computer is available? It was the Laplace transform method which identified the problem with invalid initial conditions. Figure 45 illustrates a preliminary analog simulation of the closed loop-system. The sign on the three-halves derivative was incorrect. Had it not been for the analytical prediction, this situation would not have been identified. In the future, if someone develops a generalized Laplace transform method that solves the problem in terms of the coefficients (m, k, \dots, c_n) , receives them as input parameters, and then calculates the residues, the solution for a given system could be available in twenty minutes. This tool is probably quicker than the analog simulation technique. However, both analog and theoretical methods have special tasks that they're more efficient at. It's best to improve both methods.

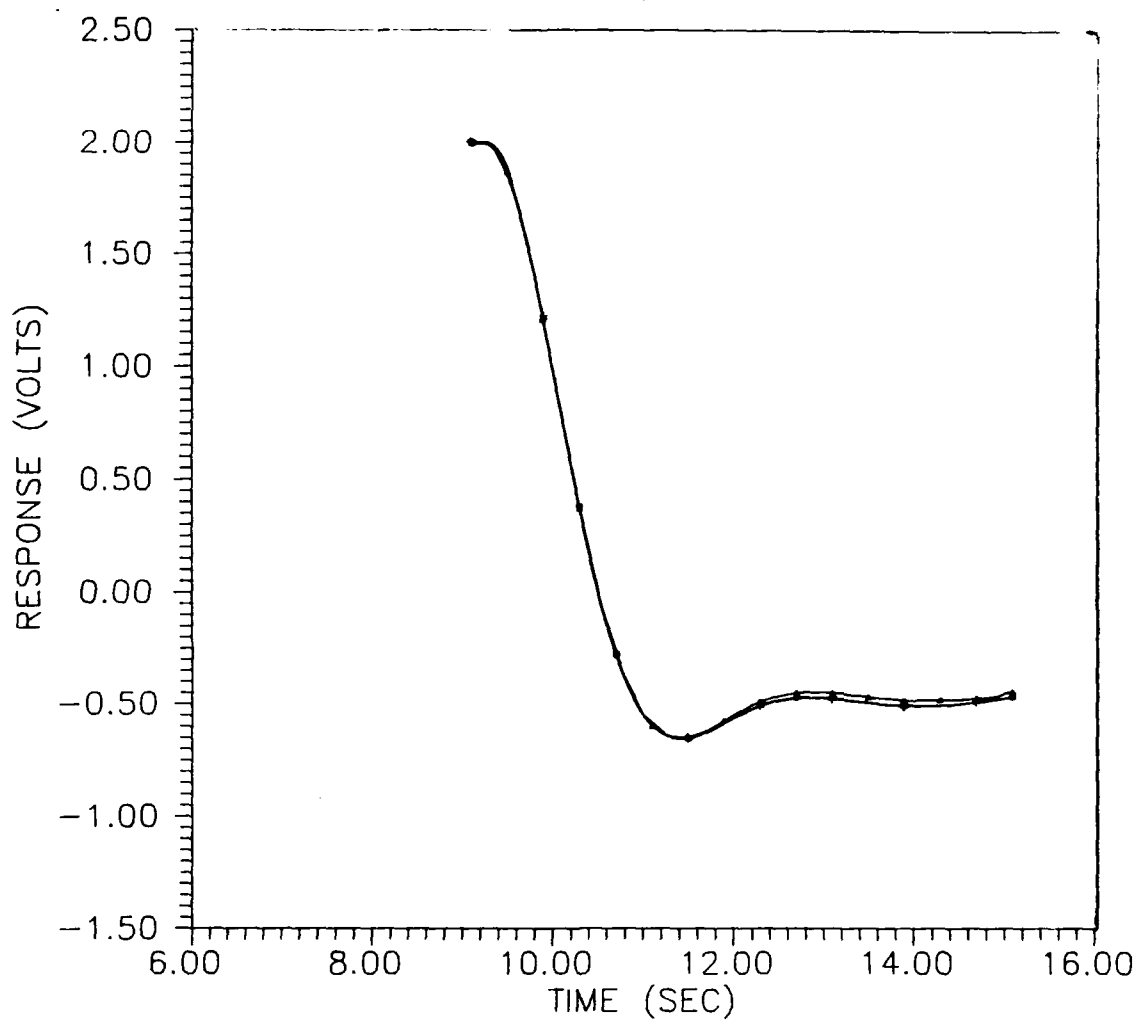


Figure 43. Comparison of Asymptotic Limit Selection for the Laplace Transform Response Method

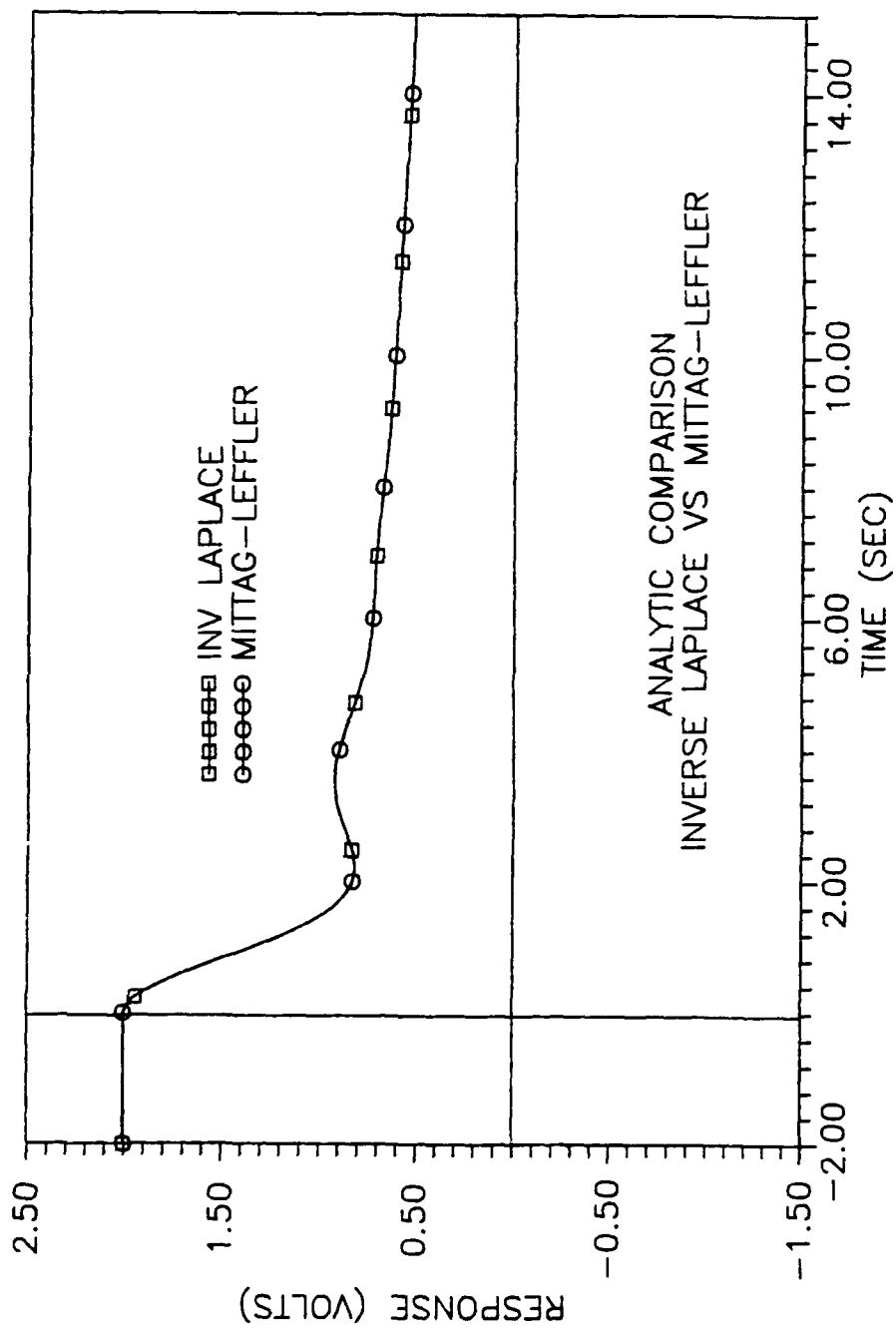


Figure 44. Comparison of Mittag-Leffler Expansion and Laplace Transform Response Predictions

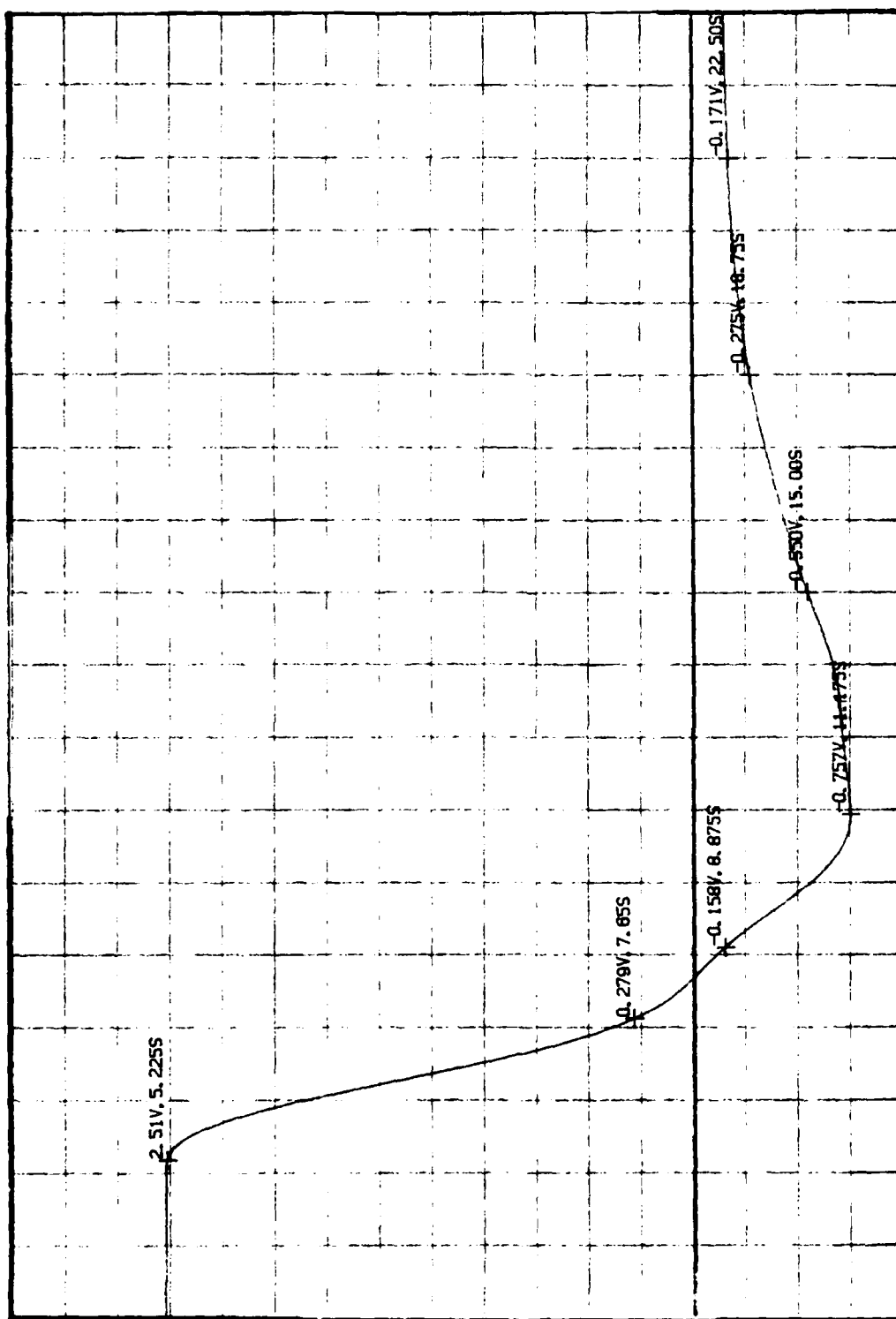


Figure 45. Circuit Response with Improper Coefficient Set-up

VI Conclusions and Recommendations

Summary

This thesis demonstrated that analog simulation of differential equations involving fractional-order derivatives can be performed. Fractional-order feedback in linear systems is feasible, and the response is predictable with computer methods. This feedback is stable and improves system performance. The methods developed are directly applicable to systems whose behavior can best be described by fractional derivatives. These methods could provide additional degrees of freedom for control engineers to improve system performance (12). With the additional fractional-order time derivatives available for feedback, response can be tailored to precisely fit the needs of the application without a loss of system stability.

The Oldham-Zoski circuit provides the $1/n$ th fractional derivative of an input signal. Previous research indicated the circuit functioned for constant and ramp input signals, for any fractional integral or derivative. This investigation demonstrated that this circuit also performs with a sinusoidal input. Therefore, it is anticipated that general fractional-order circuits can be designed and fabricated to cover the frequency range and functional type required by a specific application.

The circuits designed and fabricated can not only function as tools to simulate processes involving fractional derivatives, but they can also be used to modify traditional sensors for active control systems.

Two analytic tools were developed to predict the experimental response. Fully functional computer programs were developed for both methods. Even though the two methods were totally unrelated, the results generated were indistinguishable. A high degree of confidence is merited for these analytic tools as they not only described the response, but they also predicted it.

Areas for Further Study and Development

1) Perform simulation and feedback including higher orders of fractional derivatives as well as the one-half and three-halves. Compare the response to the results presented here. Investigate if the added degrees of freedom produce better system response.

2) Electrical circuit development. Investigate designing and fabricating the fractional-order circuits using current IC methods. Determine if the circuit bias is inherent in the design or can be removed. If it can be compensated for, a single fractional-order micro-circuit could supply the $1/n$ th and $n+1/n$ th derivative. In addition, define interface requirements for the circuits, that is power consumption, impedance matching, etc. If added degrees of freedom are beneficial, determine the number that can be designed into one integrated circuit.

3) Investigate the steady-state offset of the experimental values. Determine if a designing a circuit for operating at lower frequencies produces an improved steady-state response or if the steady-state offset observed was a function of the initial charge on the capacitors. One possibility of testing for this is to run a simulation with a higher initial charge on the capacitors, and then observe the results.

4) Continue development of the Laplace inversion program. Automate the calculation of residues. Solve in terms of general coefficients (k, m, c_1, \dots, c_n); use the general coefficients as input to the function routines.

5) Combine the circuit with an active control system and logic to control the response of an actual structure. One possibility - see if the AFIT/ENG (Department of Electrical and Computer Engineering) robotics laboratory is interested.

6) Investigate the practical limits of frequency range available. Determine if a circuit designed to operate over two decades of frequency functions as effectively over those two decades as one designed for six.

7) Within the design frequency range of the circuit the transfer function's slope is 10 dB/decade with a 45 degree phase shift. Determine the operating characteristics of the circuit outside its design range.

8) Without scaling on the analog computer the voltage limits restrict the magnitudes of voltage that can be used at high frequencies. Research the necessary modifications to the circuit for t^* operating times, where t^* is a fraction of the actual time.

Equipment Improvements

1) A Hewlett-Packard, or similar PC, with an IEEE-488-bus compatible interface card for connecting to the Hewlett-Packard analog-digital recorder (model 7090A). Data from the recorder could be directly transferred to the PC for analysis. Likewise theoretical plots could be done on the recorder. The Hewlett-Packard recorder (model 7090A) has additional capabilities when it is interfaced with a PC than it has in its stand-alone mode.

2) If it is determined to still be more desirable to use discrete components, obtain a supply of 1% components.

3) Investigate the use of the AFIT Department of Electrical and Computer Engineering (AFIT/ENG) hybrid analog computer (SIMSTAR). It is the latest model available, can be programmed through a terminal using Fortran - as opposed to using patchcords, and has an interface for external circuitry.

Appendix A
Laplace Transform Method for Theoretically Predicting Time Response

A general second-order equation for a viscoelastically damped system can be written:

$$m\ddot{x} + c_1 D_t^{3/2}(x) + c_2 \dot{x} + c_3 D_t^{1/2}(x) + kx = f(t) \quad (A1)$$

where \ddot{x} , \dot{x} , and x represent acceleration, velocity, and position. $D_t^{3/2}(x)$ and $D_t^{1/2}(x)$ are the three-halves and one-half fractional derivatives. These fractional derivatives aid in providing simple, causal models of the behavior of analytic systems (2:125-126). ($m\ddot{x}$ is an inertial term, $c_2\dot{x}$ is viscous damping, and kx is stiffness. Therefore, $D_t^{3/2}(x)$ can be defined as a viscoinertial damping term, and $D_t^{1/2}(x)$ as a viscoelastic damping term.)

Open-Loop Example Case

For an example case, let us examine a model of a typical viscoelastically damped system;

$$c_1 = c_2 = f(t) = 0, \quad m = k = 1, \quad c_3 = 2:$$

$$\ddot{x} + 2D_t^{1/2}(x) + x = 0 \quad (A2)$$

The initial conditions are:

$$x(0) = A \text{ and } \dot{x}(0) = 0 \quad (A3)$$

To solve the differential equation, transfer it to the Laplace domain. Integer-order derivatives transform as usual, but fractional-order

derivatives transform slightly differently. The mathematical definition of an m/n_{th} -order derivative contains an integral expression:

$$D_t^{1/2}(x) = [\Gamma(1-1/2)]^{-1} \int_c^t \frac{\dot{x}(t-\tau)}{\tau^{1/2}} d\tau \quad (A4)$$

and in the Laplace domain (12):

$$\mathcal{L}\{D_t^{1/2}(x)\} = s^{-1/2}[sX - x(0)] = s^{1/2} - s^{-1/2}(0) \quad (A5)$$

and the Laplace transform of Eq (A2) becomes:

$$s^2X - As + 2s^{1/2}X - 2As^{-1/2} + x = 0 \quad (A6)$$

and solving for $X(s)$:

$$X(s) = A \frac{(s + 2s^{-1/2})}{s^2 + 2s^{1/2} + 1} \quad (A7)$$

To obtain the response of the system, one must calculate the inverse Laplace transform of $X(s)$ (29:818-824, 14:141-143):

$$\mathcal{L}^{-1}\{X(s)\} = \frac{1}{2\pi i} \int_{\gamma-i\infty}^{\gamma+i\infty} X(s) e^{st} ds \quad (A8)$$

Solving Eq (A8) involves integrating around a closed contour, with Eq (A8) as one of the contours (Figure 46). Again, the $s^{1/2}$ terms make the solution technique slightly different than usual. Mapping the denominator of Eq (A7) into the \hat{s} -plane, where $\hat{s} = s^{1/2}$, permits the characteristic equation to be written $\hat{s}^4 + 2\hat{s} + 1$. The contour integral can then either be performed in the $s^{1/2}$ -plane, or remapped back into the s -plane (21:197-199).

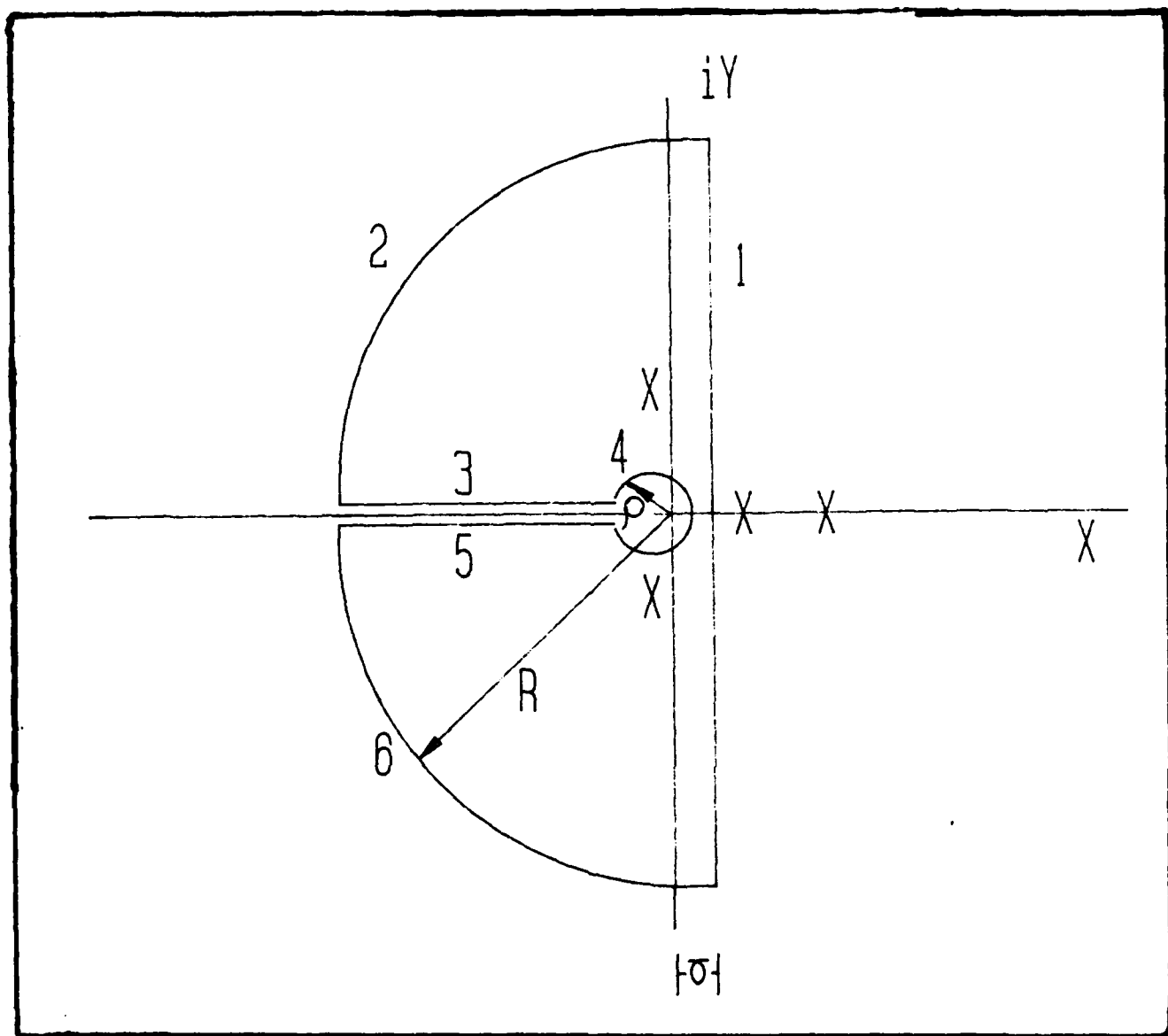


Figure 46. Contour Integral Definition for the Laplace Transform Method

$$\hat{p}_1 = -1, \hat{p}_2 = -0.5437, \hat{p}_3, \hat{p}_3^* = 0.7718 \pm i1.1151 \quad (A9)$$

These are the poles, and are then mapped back into the s-plane by the transformation:

$$\begin{aligned} s &= \sigma + i\omega \\ \hat{s} &= u + iv \\ s &= \hat{s}^2 \\ &= u^2 - v^2 + 2iv \end{aligned} \quad (A10)$$

Equate the real and imaginary parts:

$$\sigma = u^2 - v^2; \quad \omega = 2iv \quad (A11)$$

The poles in the s plane are now:

$$p_1 = 1.0, p_2 = 0.29561, p_3, p_3^* = -0.64777 \pm i1.72127 \quad (A12)$$

Normally, poles on the positive real axis indicate an unstable system. However, in this case, they result from the \hat{s} -to-s mapping. These poles originated in the area of the \hat{s} -plane which did not map onto the principle sheet of the Riemann surface in the s plane. Their effect on the system comes from integrating along the branch cut depicted in Figure 46.

The mathematical expression for the residue theorem is (20:818):

$$\frac{1}{2\pi i} \left[\int_1 + \int_2 + \int_3 + \int_4 + \int_5 + \int_6 \right] = \sum_{i=1}^2 \text{Residue}_{(i)} \quad (A13)$$

The Laplace inversion integral, Eq (A8), is represented by integration along path 1. Therefore:

$$\mathcal{L}^{-1}(X(s)) = -\frac{1}{2\pi i} \left[\int_2 + \int_3 + \int_3 + \int_4 + \int_5 + \int_6 \right] + \sum_{i=1}^2 \text{Residue}_{(i)} \quad (A14)$$

The quantity on the left hand side of Eq (A14) is defined by Eq (A7):

$$X(s)e^{st} = A \frac{(s + 2s^{-1/2})}{s^2 + 2s^{1/2} + 1} e^{st} \quad (A15)$$

Wylie defines the residue (20:818):

$$\text{Residue } (p_n) = R(p_n) = \lim_{s \rightarrow p_n} (s - p_n) X(s) e^{st} \quad (A16)$$

The characteristic equation can be written in terms of its \hat{s} roots:

$$s^2 + 2s^{1/2} + 1 = (s^{1/2} + 1)(s^{1/2} + 0.5437)(s^{1/2} - 0.7718 + i1.1151) \\ * (s^{1/2} - 0.7718 - i1.1151) \quad (A17)$$

The residue at $s = p_3 = -0.647777 + i1.72127$ is:

$$R(p_3) = \lim_{s \rightarrow p_3} \left[\dots \right. \\ \left. \frac{(s + 0.64777 - i1.172127) A (s + 2s^{-1/2}) e^{(-0.64777 + i1.72127)t}}{(s^{1/2} + 1)(s^{1/2} + 0.5437)(s^{1/2} - 0.7718 + i1.1151)(s^{1/2} - 0.7718 - i1.1151)} \right] \quad (A18)$$

The root at p_3 can be written in terms of its half-order factors:

$$(s + 0.64777 - i1.72127) = (s^{1/2} + 0.7718 - i1.72127)(s^{1/2} + 0.7718 + i1.72127) \quad (A19)$$

This results in an expression for the residue:

$$R(p_3) = \lim_{s \rightarrow p_3} \left[\dots \right. \\ \left. \dots \frac{A (s + 2s^{-1/2}) (s^{1/2} + 0.7718 + i1.1151) e^{(-0.64777 + i1.72127)t}}{(s^{1/2} + 1)(s^{1/2} + 0.5437)(s^{1/2} - 0.7718 + i1.1151)} \right] \quad (A20)$$

In the limit, this expression becomes:

$$R_{(p_3)} = A (0.14467 - i0.1122) e^{-0.64777t} [\cos(1.72127t) + i \sin(1.72127t)] \quad (A21)$$

When combined with the residue from the complex conjugate root at

$s = \bar{p}_3 = (-0.64777 + i1.72127)$, the total system residue is:

$$R = 2A [0.14467 \cos(1.72127t) + 0.1122 \sin(1.72127t)] e^{-0.64777t} \quad (A22)$$

Which can be simplified even further through the use of phasor notation:

$$R = 0.73232 e^{-0.64777t} \cos(1.72127t - 0.65966) \quad (A23)$$

For the contour integral (again refer to Figure A1 for the paths):

Along path 2, parameterize $s = \sigma + i\omega$ by $R \exp(i\theta)$, where $R = \sigma^2 + \omega^2$ and $\theta = \tan^{-1}(\omega / \sigma)$:

$$s = R \exp(i\theta) \quad (A24)$$

$$ds = iR \exp(i\theta) d\theta$$

The limits of integration are from $\theta = \alpha$, where $\alpha \equiv \tan^{-1}(\gamma/R)$ to π and the integral can be written:

$$- \frac{A}{2\pi i} \int_{\alpha}^{\pi} \frac{[R \exp(i\theta) + 2R^{1/2} \exp(-i\theta/2)] \exp[Rt \exp(i\theta)] R \exp(i\theta)}{[R \exp(i\theta)]^2 + 2 [R \exp(i\theta)]^{1/2} + 1} i d\theta \quad (A25)$$

Let the integrand be denoted \mathfrak{I} , then:

$$\int |\mathfrak{I}| d\theta \geq \int |\mathfrak{I}| d\theta \quad (A26)$$

also

$$|R \exp(i\theta)| = |R (\cos\theta + i \sin\theta)| \leq |R| \quad (A27)$$

$$|R^{-1/2} \exp(-i\theta/2)| = |R^{-1/2} [\cos(\theta/2) + i \sin(\theta/2)]| \leq |R^{-1/2}| \quad (A28)$$

$$|\exp [R \exp(i\theta t)]| = |\exp [(R \cos \theta) t] [\cos(R t \sin \theta) + i \sin(R t \sin \theta)]| \dots \leq \exp [R \cos(\theta t)] \quad (A29)$$

Employing Eqs (A26) - (A29), an approximation to Eq (A25) for large R is:

$$- \frac{A}{2\pi} \int_{\alpha}^{\pi} \frac{(R^2 + 2R^{-1/2})}{R^2 + 2R^{1/2} + 1} \exp [R \cos(\theta t)] d\theta \quad (A30)$$

Taking the limit as $R \rightarrow \infty$:

$$\lim_{R \rightarrow \infty} - \frac{A}{2\pi} \int_{\alpha}^{\pi} \frac{(1 + 2R^{-3/2})}{1 + 2R^{-3/2} + R^{-2}} \exp [R \cos(\theta t)] d\theta \quad (A31)$$

Examine the $\exp [R \cos(\theta t)]$ term. For $\theta = \pi/2$ to π , $\cos \theta \leq 0$ and in the limit the term goes to $\exp(-\infty)$ or zero. For $\alpha \leq \theta \leq \pi/2$, the term is approximately equal to $\exp(\gamma t)$. As R becomes very large $\alpha \cong \pi/2$ and the integral can be broken into two parts:

$$\lim_{R \rightarrow \infty} - \frac{A}{2\pi} \left[\int_{\pi/2}^{\pi} \exp [R \cos(\theta t)] d\theta + \int_{\pi/2}^{\pi/2} \exp (\gamma t) d\theta \right] \quad (A32)$$

In the limit, the integral on the left disappears because the exponent is negative. The integral on the right disappears due to the path length shrinking to zero in the limit. Thus the contribution of path 2 to the integral is zero. A similar argument can be made for path 6.

On path 4, the radius, ρ , is shrunk to zero in the limit. Along

the path of integration, $s = \sigma + i\omega$ can be parameterized by ρ and θ :

$$\begin{aligned}\rho &= \sigma^2 + \omega^2 \\ \theta &= \tan^{-1}(\omega / \sigma) \\ s &= \rho \exp(i\theta) \\ ds &= i\rho \exp(i\theta) d\theta\end{aligned}\tag{A33}$$

the limits of integration are π to $(-\pi)$ and the path integral is written:

$$\frac{-A}{2\pi i} \int_{\pi}^{-\pi} \frac{[\rho \exp(i\theta) + 2\rho^{1/2} \exp(-i\theta/2)] \exp[\rho \exp(i\theta)] \rho \exp(i\theta)}{[\rho \exp(i\theta)]^2 + 2[\rho \exp(i\theta)]^{1/2} + 1} i d\theta\tag{A34}$$

Again let the integrand be denoted \mathfrak{I} , then:

$$\int |\mathfrak{I}| d\theta \geq \int \mathfrak{I} d\theta\tag{A35}$$

and

$$|\rho \exp(i\theta)| = |\rho (\cos\theta + i\sin\theta)| \leq |\rho|\tag{A36}$$

$$|\rho^{-1/2} \exp(-i\theta/2)| = |\rho^{-1/2} [\cos(\theta/2) + i\sin(\theta/2)]| \leq |\rho^{-1/2}|\tag{A37}$$

$$\begin{aligned}|\exp[\rho \exp(i\theta t)]| &= |\exp[\rho \cos\theta t] [\cos(\rho \sin\theta) + i\sin(\rho \sin\theta)]| \dots \\ &\dots \leq \exp[\rho \cos(t)]\end{aligned}\tag{A38}$$

Applying Eqs (A35) through (A38), Eq (A34) becomes:

$$-\frac{A}{2\pi} \int_{\pi}^{-\pi} \frac{(\rho^2 + 2\rho^{-1/2})}{\rho^2 + 2\rho^{1/2}} \exp[\rho \cos(\theta t)] d\theta\tag{A39}$$

In the limit as $\rho \rightarrow 0$ this expression becomes:

$$- \frac{A}{2\pi} \int_{\pi}^{-\pi} 0 \, d\theta = 0 \quad (\text{A40})$$

and path 4 does not contribute to the integral.

On path 3, s is parameterized by $r \exp(i\pi)$, with the limits on r going from R to ρ . When the appropriate substitutions are made:

$$\begin{aligned} s &= r \exp(i\pi) &= r (\cos \pi + i \sin \pi) &= -r \\ ds &= dr \exp(i\pi) &= -dr \\ s^{1/2} &= r^{1/2} \exp(i\pi/2) &= ir^{1/2} \\ s^{-1/2} &= r^{-1/2} \exp(-i\pi/2) &= -ir^{-1/2} \end{aligned} \quad (\text{A41})$$

and the integral term is then:

$$- \frac{A}{2\pi i} \int_{\rho}^R \frac{(-r^2 - 2r^{-1/2})}{(r^2 + 1) + i2r^{1/2}} \exp(-rt) (-dr) \quad (\text{A42})$$

but, the denominator must be rationalized:

$$- \frac{A}{2\pi i} \int_{\rho}^R \frac{(-r^2 - 2r^{-1/2})[(r^2 + 1) - i2r^{1/2}]}{[(r^2 + 1) + i2r^{1/2}][(r^2 + 1) - i2r^{1/2}]} \exp(-rt) (-dr) \quad (\text{A43})$$

In the limits as $\rho \rightarrow 0$ and $R \rightarrow \infty$:

$$- \frac{A}{2\pi i} \int_{\infty}^0 \frac{(r^3 + r + 4 + i2r^{-1/2})}{r^4 + 2r^2 + 4r + 1} \exp(-rt) \, dr \quad (\text{A44})$$

Dividing through by i :

$$\frac{A}{2\pi} \int_0^{\infty} \left[\frac{i(r^3 + r + 4)}{(r^4 + 2r^2 + 4r + 1)} - \frac{(2r^{-1/2})}{(r^4 + 2r^2 + 4r + 1)} \right] \exp(-rt) \, dr \quad (\text{A45})$$

On path 5:

$$\begin{aligned} s &= r \exp(i\pi) &= r (\cos \pi + i \sin \pi) &= -r \\ ds &= dr \exp(i\pi) &= -dr \\ s^{1/2} &= r^{1/2} \exp(-i\pi/2) &= -ir^{1/2} \\ s^{-1/2} &= r^{-1/2} \exp(-i\pi/2) &= ir^{-1/2} \end{aligned} \quad (\text{A46})$$

and the limits of integration are ρ to R . Following the same procedure as used on path 3 produces:

$$\frac{A}{2\pi} \int_0^{\infty} \left[\frac{i(r^3 + r + 4)}{(r^4 + 2r^2 + 4r + 1)} + \frac{(2r^{-1/2})}{(r^4 + 2r^2 + 4r + 1)} \right] \exp(-rt) \, dr \quad (\text{A47})$$

The limits of integration on paths 3 and 5 are reversed. Combining Eqs (A45) and (A47) and using limits of integration from 0 to ∞ produces:

$$\frac{A}{\pi} \int_0^{\infty} \frac{(2r^{-1/2})}{(r^4 + 2r^2 + 4r + 1)} \exp(-rt) \, dr \quad (\text{A48})$$

The total Laplace inversion is then:

$$\begin{aligned} \mathcal{L}^{-1}\{ \mathcal{X}(s) \} = R &= 0.73232 e^{-0.64777t} \cos(1.72127t - 0.65966) \\ &+ \frac{A}{\pi} \int_0^{\infty} \frac{(2r^{-1/2})}{(r^4 + 2r^2 + 4r + 1)} \exp(-rt) \, dr \end{aligned} \quad (\text{A49})$$

The integral in Eq (A49) does not have a simple closed form solution. Therefore, it becomes necessary to break the integral into three parts and make asymptotic approximations to the upper and lower intervals. For small r , $r^4 + 2r^2 + 4r \ll 1$ and Eq (A48) can be written:

$$\frac{2A}{\pi} \int_0^r r^{-1/2} \exp(-rt) dr \quad (A50)$$

The upper limit of integration is determined by a trial and error process. Agreement between the integrands in Eqs (A48) and (A50) must be accurate to within three significant digits over the interval of integration to favorably compare with the experimental data. (Since the experimental data contained three significant figures). The worst an asymptotic approximation could do over the interval of integration would be to produce a constant error. The difference between the actual integrand and the asymptotic approximation would then be the error at the upper limit of integration multiplied by the interval of integration. If r_1 is chosen to be 0.00025, then:

$$r^{-1/2} = 63.426 \quad \text{and} \quad \frac{r^{-1/2}}{r^4 + 2r^2 + 4r + 1} = 63.1824 \quad (A51)$$

and $r_1 = 0.00025$ produces an estimated error over the interval which is much smaller than three significant digits. Eq (A50) contains an exponential term which can be expanded in an infinite series and combined with the $r^{-1/2}$ term:

$$\frac{2A}{\pi} \int_0^{.00025} (r^{-1/2} - r^{1/2}t + r^{3/2}t^2 + \dots) dr = \frac{2A}{\pi} \int_0^{.00025} \left[\sum_{n=0}^{\infty} (-1)^n r^{(n-1/2)t} \right] dr \quad (A52)$$

Upon performing the integration, Eq (A52) becomes:

$$\frac{2A}{\pi} \sum_{n=0}^{\infty} \frac{(0.00025)^{(n+1/2)t}}{n + 1/2} \quad (A53)$$

This series is convergent for $t < 4000$ seconds and it is not anticipated that the response of the system will last this long.

For large r , an integral which closely approximates the integral in Eq (A48) is:

$$\frac{2A}{\pi} \int_{r_2}^{\infty} r^{-5/2} \exp(-rt) dr \quad (A54)$$

If a value of 30 is selected for r_2 the difference between the integrand of Eqs (A48) and (A50) is less than 10^{-8} . If the same criteria for approximating the lower limit integral error is applied to this upper integral, then 30 is a good choice. Section V contains a discussion of asymptotic limit selection. It's impossible to perform numerical integration on Eq (A54), but if the substitution $u = 1/r$ is made:

$$\frac{2A}{\pi} \int_0^{1/30} u^{5/2} \exp(-t/u) du \quad (A55)$$

and Eq (A50) now becomes:

$$\frac{2A}{\pi} \sum_{n=0}^{\infty} \frac{(0.00025)^{(n+1/2)} t^n}{n+1/2} + \frac{2A}{\pi} \int_{r_1}^{r_2} \frac{r^{-1/2} \exp(-rt)}{(r^4 + 2r^2 + 4r + 1)} dr$$

$$+ \frac{2A}{\pi} \int_0^{1/30} u^{5/2} \exp(-t/u) du \quad (A56)$$

Using a composite Simpson integration algorithm (5:162-167) the value of the two integral terms in Eq (A56) can be determined to within a specified error value. For example, the upper integral:

$$\frac{2A}{\pi} \int_0^{1/30} u^{5/2} \exp(-t/u) du = \frac{h}{3} \left[f(0) + 2 \sum_{j=1}^{m-1} f(x_{2j}) + 4 \sum_{j=1}^m f(x_{2j-1}) + f(1/30) \right]$$

$$- \frac{(1/30 - 0)}{180} h^4 f^4[u^{5/2} \exp(t/u)] \Big|_{u=\mu} \quad (A57)$$

where

- $h \equiv$ integration step
- $\mu \equiv$ some mean value (from the mean value theorem)
- $2m \equiv$ the number of integration steps required
- $f^4() \equiv$ the fourth derivative of the integrand.

The last term in Eq (A57) is the error term. To obtain a conservative integration step for a wide range of times, μ is chosen to be close to the 1/30th end of the interval and t is chosen as small as possible. This selection produces the largest possible error for the interval for all time and appears to be a conservative selection.

The same type of composite Simpson integration routine can be used for the interval from 0.00025 to 30. Appendix B is the Fortran source code for calculating the response using the method detailed here. The

program is liberally commented and a detailed description of the input is included. Using this program, Figure 27 depicts an output plot of these results.

Closed Loop Example

For the closed loop system the equation to Laplace transform is:

$$\ddot{x} - 1.6324 D_t^{3/2}(x) + 2.891 \dot{x} - 1.1156 D_t^{1/2}(x) + 1.4142x = 0 \quad (A58)$$

with initial conditions $\dot{x}(0) = 0$ and $x(0) = A$

The details of the procedure will only be summarized for this case.

$$\begin{aligned} \mathcal{L}\{\ddot{x}\} &= s^2 X - s x(0) - \dot{x}(0) = s^2 X - As \\ \mathcal{L}\{D_t^{3/2}(x)\} &= s^{-1/2}[s^2 X - s x(0) - \dot{x}(0)] = s^{3/2} X - As \\ \mathcal{L}\{\dot{x}\} &= s X - x(0) = s X - A \\ \mathcal{L}\{D_t^{1/2}(x)\} &= s^{-1/2}[s X - x(0)] = s^{1/2} X - As^{-1/2} \end{aligned} \quad (A59)$$

Substituting back into the equation and solving for X :

$$X = \frac{A(s - 1.6324s^{1/2} + 2.891 - 1.1156s^{-1/2})}{s^2 - 1.6324s^{3/2} + 2.891s - 1.1156s^{-1/2} + 1.4142} \quad (A60)$$

The roots of this characteristic equation in the \hat{s} -plane are:

$$\hat{p}_1, \hat{\bar{p}}_1 = 0.7892 \pm i1.2346; \hat{p}_2, \hat{\bar{p}}_2 = 0.0270 \pm i0.8111 \quad (A61)$$

Mapping these roots back into the s -plane :

$$p_1, \bar{p}_1 = -0.65715 \pm i0.0438; p_2, \bar{p}_2 = -0.9014 \pm i1.9487 \quad (A62)$$

The residue at $s = -0.65715 + i0.0438$ is given by the expression:

$$R_{(p_1)} = \lim_{s \rightarrow p_1} \left[\dots \frac{A (s-1.6324s^{1/2}+2.891-1.11156s^{-1/2}) (s^{1/2}+0.027+i0.8111) \exp(-st)}{(s^{1/2}-0.7892+il.2346) (s^{1/2}-0.7892-il.2346) (s^{1/2}-0.027+i0.811)} \right] \quad (A63)$$

Carrying out the calculations and combining the result with the residue obtained at \bar{p} can be shown to produce the residue expression:

$$R_{(p_1, \bar{p}_1)} = 2.25721A \exp(-0.65715t) \cos(0.0438t + 0.74302) \quad (A64)$$

The residue at p_2 is:

$$R_{(p_2)} = \lim_{s \rightarrow p_2} \left[\dots \frac{A (s-1.6324s^{1/2}+2.891-1.11156s^{-1/2}) (s^{1/2}+0.9014-il.94877) \exp(-st)}{(s^{1/2}-0.7892+il.2346) (s^{1/2}-0.7892-il.2346) (s^{1/2}-0.027+i0.811)} \right] \quad (A65)$$

which results in the residue:

$$R_{(p_2, \bar{p}_2)} = 0.82138A \exp(-0.9014t) \cos (1.9487t - 1.15255) \quad (A66)$$

Again, when evaluating the paths for the contour integrals, the only paths which contribute are paths 3 and 5 and the resulting integral:

$$\frac{A}{\pi} \int_0^{\infty} \frac{[2.30854 r^{1/2} - 1.63425 r^{-1/2}] \exp(-rt) dr}{r^4 - 3.11727r^3 + 7.41348r^2 - 6.84149r + 2} \quad (A67)$$

Finally, after calculation of the asymptotic approximations the full equation in the time domain:

$$\begin{aligned}
 x(t) = & 2.25721A \exp(-0.65715t) \cos(0.0438t + 0.74302) \\
 & + 0.2138A \exp(-0.9014t) \cos(1.9487t - 1.15255) \\
 & + \frac{2.30854A}{\pi} \sum_{n=0}^{\infty} \frac{0.00025^{(n+1.5)} (-1)^n}{(2n+3)} \\
 & + \frac{A}{\pi} \int_0^{\infty} \frac{[2.30854 r^{1/2} - 1.63425 r^{-1/2}] \exp(-rt) dr}{r^4 - 3.11727r^3 + 7.41348r^2 - 6.84149r + 2} \\
 & + \frac{2.30854A}{\pi} \int_1^{1/20} u^{7/2} \exp(-tu) du \quad (A68)
 \end{aligned}$$

When substituted into the Fortran program, RESPONSE, with the input parameters listed in Appendix B, the output of this equation is illustrated in Figure 28.

Appendix B

Fortran Source Code - Laplace Transform Method

```

C*-----*
C*
C*              RESPONSE
C*      Programmed by CAPT KEVIN J KLONOSKI
C*              AFIT/ENY/DA/88D
C*      DATE OF LAST UPDATE: 11 MARCH 1989
C*
C*-----*
C*
C*      PURPOSE:  Calculates the residue response and numerically evaluates
C*                an integral which represents a contour integral in the
C*                complex s-plane. The combination of the residue and the
C*                integral response provides the total response of a linear
C*                system in the time domain.
C*-----*
C*
C*      HOW TO RUN: Each system of poles will have its own unique set of inter-
C*                  grants. This program was written modularly to account for
C*                  that through the use of functions. This main program does
C*                  not require recompiling to handle different systems. Modify
C*                  the functions for each system, compile the functions and
C*                  then link them with this main module.
C*-----*
C*
C*      SUBROUTINES CALLED
C*
C*          RESCON - Calculates the residue contribution to the response
C*          HCALC  - Evaluates the numerical integration step size to
C*                  minimize the error
C*          LOWINT - Evaluates the asymptotic approximation integral for the
C*                  interval from 0 to R1
C*          MIDINT - Evaluates the integral for the interval from R1 to R2
C*          UPINT  - Evaluates the asymptotic approximation integral for the
C*                  interval from R2 to infinity
C*-----*
C*
C*      INPUT REQUIRED:  TSTART - Time at which the experimental response
C*                      began (useful for correlating output plots)
C*                      TZERO  - Beginning of the evaluation period (might be
C*                      other than zero, permits evaluation of long
C*                      response times in short interval blocks)

```

```

J*          TMAX      - Time interval response end here          *
J*          XLIMIT    - A vector of three points along the integra- *
C*                  tion interval. From Appendix A of AFIT Thesis *
C*                  AFIT/ENVY/GA-88D-05: XLIMIT(1)=R1, XLIMIT(2)= *
C*                  R2, and XLIMIT(3) represents a point close to *
C*                  zero at which to start the integral evalua- *
C*                  tion. If set to zero, will give a divide by *
C*                  zero. *
C*          LFLAG      - Permits evaluation of the residue response *
C*                  only when set to 0. When set to 1 permits *
C*                  evaluation of the total response. *
C*          N          - Number of points (times) to evaluate in the *
C*                  interval. *
C*          AMP(I)     - Amplitude of sinusoid associated with the *
C*                  ith complex conjugate poles *
C*          FREQ(I)     - Frequency of same sinusoid *
C*          PHASE(I)    - Phase shift associated with the sinusoid *
C*          DAMP(I)     - Damping coefficient associated with poles *
C*          XMULT(I)    - The coefficient multiplying the integral *
C*                  intervals (such as 2.30954A for the closed *
C*                  loop case in Appendix A of GA-88D-05) *
C*          IDB(I)     - Permits troubleshooting of routines when *
C*                  calculating the response for the first time *
C*                  for a given system. Eight possible outputs *
C*                  are available as follows: *
C*                  IDB(1): When set to 0 no debugging. 1 opens *
C*                  the output file *
C*                  IDB(2): Intermediate values for interval 0-R1 *
C*                  IDB(3): Values for interval R1 to 1.0 *
C*                  IDB(4): Values for interval 1.0 to R2 *
C*                  IDB(5): Not used *
C*                  IDB(6): Values for interval R2 to Infinity *
C*                  IDB(7): Not used *
C*                  IDB(8): Values from determining ideal step *
C*                  size - permits preliminary evaluation *
C*                  of program run time when N set to 1 *
C* ***** *
J* *
C*          FILES USED: *
C*          INPUT.DAT   - Input file *
C*          OUTPUT.DAT  - Contains times and associated responses *
C* *

```



```

C*****
C*
C*   COMMON BLOCKS
C*       RPARAM - Contains the information for evaluating residue
C*               response  AMP,FREQ,PHASE,DAMP
C*       INTINT - Integration interval information
C*               XLIMIT,XMULT
C*       H - Integration step size for each interval
C*       M - Number of total subintervals, including the
C*           endpoints, in each interval
C*       IBCONT - Debugging control parameters IDB(1-8)
C*
C*****
C
C   use $DEBUG to help identify reasons for program failure
C
$DEBUG
    IMPLICIT DOUBLE PRECISION (A-H,O-Z)
    COMMON /RPARAM/ AMP(2),FREQ(2),PHASE(2),DAMP(2)
    COMMON /INTINT/ XLIMIT(3),XMULT(3),H(3),PI,M(3)
    COMMON /IBCONT/ IDB(8)
    PI=3.141592654
C
C   open input and output files
C
    OPEN (6,FILE='INPUT.DAT',STATUS='OLD')
    OPEN (7,FILE='OUTPUT.DAT',STATUS='NEW')
C
C   read input parameters
C
    READ (6,*) TSTART,TEERO,TMAX,(XLIMIT(I),I=1,3),LFLAG
    READ (6,*) (AMP(I),FREQ(I),PHASE(I),DAMP(I),I=1,2)
    READ (6,*) (XMULT(I),I=1,3)
    READ (6,*) N,(IDB(I),I=1,8)
C
C   if intermediate values are to be printed open debug output file
C
    IF (IDB(1).EQ.1) OPEN (8,FILE='DEBUG.DAT',STATUS='NEW')

```

```

C
C establish time increments
C
      TINC=(TMAX-TZERO)/ISLEIN)
C
C step through the time period to be evaluated
C
      DO 10 NINC= 0,N
        T=NINC*TINC+TZERO
C
C if the time at which the experimental response starts has not been reached
C set the elapsed time to 0. otherwise calculate the elapsed time from
C start of the response
C
        IF (T.GE.TSTART) THEN
          TCALC= T - TSTART
        ELSE
          TCALC= 0.000
        ENDIF
C
C call subroutine to evaluate the residue response
C
        CALL RESCON TCALC,RES
C
C if desired, calculate the response contribution from the integration paths
C
        IF (LFLAG.NE.0) THEN
          CALL HCALC(TCALC)
          CALL LOWINT (TCALC,XINT1)
          CALL UPINT (TCALC,XINT3)
          CALL MIDINT (TCALC,XINT2)
        ENDIF
C
C sum the responses from the residue and integration intervals for this time
C step
C
      1  RESPNS= RES + XINT1-XINT2+XINT3

```

```

C
C output time to the CRT for tracking purposes
C
C   WRITE (*,*) T
C
C output time and associated response to the output file
C
C   WRITE (7,5) T,RESPNS,RES,XINT0,XINT2,XINT3
5   FORMAT ('5.1X,E14.6')
10  CONTINUE

C
C close files
C
20  CLOSE(6)
    CLOSE(7)
    IF (IDB(1).EQ.1) CLOSE(9)
    STOP
    END

C
SUBROUTINE RESCON(T,RES)
  IMPLICIT DOUBLE PRECISION (A-H,O-Z)
  COMMON /PARAM/ AMP(2),FREQ(2),PHASE(2),DAMP(2)
C
C evaluates the residue contribution (RES) of the response for a
C selected time (T)
C
    RES= AMP(1)*DEXP(DAMP(1)*T)*DCOS(FREQ(1)*T-PHASE(1))
    RES= RES+AMP(2)*DEXP(DAMP(2)*T)*DCOS(FREQ(2)*T-PHASE(2))
C
    RETURN
    END

```

```

SUBROUTINE LOWINT(T,XINT)
IMPLICIT DOUBLE PRECISION (A-H,O-Z)
COMMON (INTINT/ XLIMIT(3),XMULT(3),H(3),PI,M(3)
COMMON (IBOINT/ IIB(8)

```

```

C
C evaluates the series solution for the lower interval 0 to R. terms
C are calculated until the nth term (TERM) is smaller than a test value
C (TERMST). evaluation of the term is done by the function (TERML) which
C is external to the main module and must be change for different systems
C

```

```

C initialize sum parameters
C

```

```

      TERMST=1.0D-4
      PRETRM=1.0D0
      N=0
      SUM=0.0D0
      P=XLIMIT(1)

```

```

C calculate N
C

```

```

5      IF (N.EQ.0) THEN
          FAC=1.0D0
      ELSE
          FAC=FAC*N*(1-1.0D0/P)
      ENDIF

```

```

C use TERML to evaluate term, add term to the sum and if intermediate
C values are desired as output (IIB(2)=1) output the values to debug file
C

```

```

      TERM=TERML(T,R,FAC,N)
      SUM=SUM+TERM
      IF (IIB(2).EQ.1) THEN
          WRITE (8,10)
10      FORMAT('LOWINT')
          WRITE (8,*) N,FAC,TERM,SUM
      END IF

```

```

C test size of term, if larger than test value, repeat term evaluation loop,
C otherwise output the information.
C

```

```

      IF (DABS(TERM).GT.TERMST) THEN
          N=N+1
          PRETRM=TERM
          GOTO 5
      ELSE
          XINT=SUM*XMULT(1)/PI
      ENDIF

```

```

      RETURN
      END

```

```

C
C      SUBROUTINE MIDINT (T,XINT)
C      IMPLICIT DOUBLE PRECISION (A-H,O-Z)
C      COMMON /XINT/ XLIMIT(3),XMCULT(3),H(3),PI,M(3)
C      COMMON /DECONT/ IDB(3)
C
C      evaluates the integrand from R1 to R2 using a Composite Simpson
C      iteration routine (S:164). the interval is divided into two subintervals
C      for the sake of convergence considerations. the lower interval spans
C      the range R1 to 1.0 while the upper interval spans 1.0 to R2. at each
C      integration step, the function VMCALC is used to evaluate the integrand
C
C      XLOW=R1, HIGH=R2
C
C      XLOW=XLIMIT(1)
C      HIGH=XLIMIT(2)
C
C      each subinterval of integration is divided into 2 steps in the Composite
C      Simpson algorithm. there is a sum for the even steps (EVNSUM) and a sum
C      for the odd steps (ODDSUM)
C
C      ODDSUM=0.0D0
C      EVNSUM=0.0D0
C      NSTEPS= M(1)*2-1
C
C      set the initial point in the interval to be R1
C
C      VALUE=XLOW
C
C      evaluate the integrand at the three limits of integration (R1,1.1,R2)
C
C      F0=VMCALC(XLOW,T)
C      F1=VMCALC(1.0D0,T)
C      FX=VMCALC(HIGH,T)
C
C      use of a control parameter (IBIT) allows tracking of even and odd steps
C
C      IBIT=1
C
C      use of a flag (LOWFLG) controls which interval is under evaluation and
C      therefore which step size to use
C
C      LOWFLG= 1
C
C      DO 20 ISTEP=1,NSTEPS

```

C
 C at each step, add the step size to obtain the current value for evaluation
 C by VMTCALC, then depending on whether the step is odd or even, add to
 C the correct sum
 C

```

    VALUE = VALUE + H*(LOWFLG)
    F = VMTCALC(VALUE,T)
    IF (IBIT.EQ.1) THEN
      ODDSUM=ODDSUM + F
      IBIT=0
    ELSE
      EVNSUM=EVNSUM+F
      IBIT=1
    ENDIF
  20 CONTINUE

```

C
 C at the end of the lower interval, calculate the value for the integral
 C (XINT2), reset the control parameters for evaluating the interval from
 C 1.0 to RC, and if intermediate values are desired (IDB(3)=1) output
 C these values, return through the Evaluation loop for the upper interval
 C

```

    IF (LOWFLG.EQ.1) THEN
      XINT2=(F0+F1+3.000*EVNSUM+4.000*ODDSUM)*H*(1+3.000
      VALUE=1.000
      NSTEPS= M(2)*2-1
      LOWFLG=2
      IF (IDB(3).EQ.1) THEN
        WRITE (8,25)
        25  FORMAT ('MIDINT1')
        WRITE (8,*) XINT2,F0,F1,EVNSUM,ODDSUM,H,1)
      END IF
      EVNSUM=0.000
      ODDSUM=0.000
      GOTO 10
    ENDIF

```

```

C
C at the end of the second interval, calculate the value of the integral
C for the entire interval. if intermediate values are required IIB=4=1
C output these values
C
      KINT2=(KINT1*(F1-FX+0.000*EVNSUM-4.0*ODDSUM)*H(2)+3.010)
      *(XMULT(2)/PI)
      IF (IIB=4) THEN
        WRITE (9,26)
26      FORMAT ('MIDINT2')
        WRITE (9,*) KINT2,F1,FX,EVNSUM,ODDSUM,H(2)
      END IF
C
      RETURN
      END
C
      SUBROUTINE UPINT T,KINT3)
      IMPLICIT DOUBLE PRECISION (A-H,O-Z)
      COMMON /INTINT/ XLIMIT(3),XMULT(3),H(3),F1,M(3)
      COMMON /DECONT/ IDB(3)
C
C slightly offset from zero the lower limit of the interval (XLOW)
C and define the upper limit of the interval to be 1/R2
C
      XLOW=XLIMIT(3)
      HIGH=(1.000-XLIMIT(3))
C
C identify the step size for the interval determined in HCALC
C
      VINC=H(3)
C
C same definition for even and odd sums as in MIDINT
C
      ODDSUM=0.000
      EVNSUM=0.000
C
C evaluate the integrand at the lower and upper limits
C
      F0=HICALC(XLOW,T)
      FX=HICALC(HIGH,T)
C
C again use IBIT to keep track of evens and odds
C
      IBIT=1

```

```

C
C assign the initial value to be the lower limit and determine the number
C of steps required
C
      VALUE=XLOW
      NSTEPS=2*M(3)-1
C
C at each step, add the step size to obtain the current value for evaluation
C by HICALC, then depending on whether the step is odd or even, add to
C the correct sum
C
      DO 20 I=1,NSTEPS
      VALUE=VALUE+VINC
      F=HICALC(VALUE,T)
      IF (IBIT.EQ.1) THEN
        ODDSUM=ODDSUM+F
        IBIT=2
      ELSE
        EVNSUM=EVNSUM+F
        IBIT=1
      ENDIF
20 CONTINUE
C
C at the end of the interval calculate the value of the integral
C for the entire interval. if intermediate values are required (IDB(6)=1)
C output these values
C
      XINT3=((F0-FX-2.000*EVNSUM-4.000*ODDSUM)*H/3./3.1400)
      *XWULT 30,PI
      IF (IDB(6).EQ.1) THEN
        WRITE (9,35)
35      FORMAT ('UPINT')
        WRITE (9,*) XINT3,F0,FX,EVNSUM,ODDSUM,H/3
      END IF
C
      RETURN
      END
C
SUBROUTINE HICALC (T)
IMPLICIT DOUBLE PRECISION (A-H,O-Z)
COMMON /INTINT/ XLIMIT(3),XWULT 30,H/3,PI,XMAG
COMMON /DECONT/ IDB(6)

```



```

C
C calculates the integration step size for each interval of integration.
C an acceptable error of integration is specified (ERROR). The step size
C is then calculated, using the error definition for the composite Simpson
C method (5/164). This method involves calculating the fourth derivative
C of the integrands (FQVAL). All of the integrands evaluated for a typical
C Laplace inversions are of the form (AB/C) where A and C are polynomial
C expressions and B is an exponential expression. Function subprograms
C are used to evaluate the functions A, B, and C and their first four
C derivatives. These terms are then combined to form the fourth derivative
C of the expression (AB/C).
C
C define the size of the error (half the size of the least significant
C digit of experimental data)
C
      ERROR=5.00E-4
C
C for each interval of integration define the interval size, and select
C an intermediate value at which to calculate the error term
C
      DO 10 N=1,3
        IF (N.EQ.1) THEN
          XBAR= XLIMIT(1) + 2.50E1*XLIMIT(1)
          XINT=1.00E0-XLIMIT(1)
        ELSEIF (N.EQ.2) THEN
          XBAR= (1.00E0+XLIMIT(2))/2.00E1
          XINT=XLIMIT(2)-1.00E0
        ELSE
          XBAR=XLIMIT(3)
          XINT= 1.00E0/XLIMIT(3)-XBAR
          IF ((1/XBAR).GT.7.50E2) THEN
            XINT=XINT/2.00E0
            M(N)=1
          GOTO 20
        ENDIF
      ENXIF

```

C
 C call the function routines to evaluate A, B, and C and the first through
 C fourth derivatives A1, A2, A3, A4, etc
 C

```

    A=ACALC(XBAR,N)
    A1=APCALC(XBAR,N)
    A2=ADCALC(XBAR,N)
    A3=ATPCALC(XBAR,N)
    A4=AQCALC(XBAR,N)
    B=BCALC(XBAR,T,N)
    B1=BPICALC(XBAR,T,N)
    B2=BDCALC(XBAR,T,N)
    B3=BTICALC(XBAR,T,N)
    B4=BQICALC(XBAR,T,N)
    C=CCALC(XBAR,N)
    C1=CPICALC(XBAR,N)
    C2=CDICALC(XBAR,N)
    C3=CTICALC(XBAR,N)
    C4=CQICALC(XBAR,N)
  
```

C
 C the chain rule is used to combine the A,B, and C derivatives into the
 C fourth derivative for the expression (A*B/C)
 C

```

    T1=(4.0D0*A3*B1/C)-(4.0D0*A3*B*(C1**2)/(C**3))
    T2=(1.2D1*A2*B*(C1**2)/(C**3)-(6.0D0*A2*B*C2/(C**2))
1      -(1.2D1*A2*B1*C1/(C**2))-6.0D0*A2*B2/C)
    T3=(2.4D1*A1*B*C1/C2/(C**3)-(2.4D1*A1*B*(C1**3)/(C**4))
1      -(4.0D0*A1*B*C3/(C**2))-(2.4D1*A1*B1*(C1**2)/(C**3))
2      -(1.2D1*A1*B1*C2/(C**2))-(1.2D1*A1*B1*C1/(C**2))
3      -(4*A1*B3/C)
    T4=(2.4D1*A*B*(C1**4)/(C**5))-(3.6D1*A*B*(C1**2)*C2/(C**4))
1      +(6.0D0*A*B*C1*C3/(C**3))+(6.0D0*A*B*(C2**2)/(C**3))
2      -(A*B*C4/(C**2))-(A*B4/C)-(4.0D0*A*B3*C1/(C**2))
    T5=(2.4D1*A*B1*C1*C2/(C**3))-(2.4D1*A*B1*(C1**3)/(C**4))
1      -(4.0D0*A*B1*C3/(C**2))
    T6=(A4*B/C)-(6.0D0*A*B2*C2/(C**2))-(1.2D1*A*B2*(C1**2)/(C**3))

    FQUAD=T1-T2-T3-T4-T5-T6
  
```

```

C the step size is calculated using Eq(4.43) of reference 5. the
C calculation for M(N) rounds the # of intervals to the next highest
C integer. the step size is then determined to be one-half the
C interval size
C
      H(N)=(DABS(ERROR*1.8187/(FQUAD*XINT))**.5*.125)
      M(N)=IDNINT(XINT/H(N))+1
      H(N)=XINT/(DBLE(M(N))+2.0D0)
C
C if output of the intermediate values is desired (IIB 9)=1) output those
C values
C
      IF (IIB(9).EQ.1) THEN
          WRITE (8,10)
          FORMAT('HOCALC')
          WRITE(9,*) XEAR,N,T
          WRITE(9,*) A,A1,A2,A3,A4
          WRITE(9,*) B,B1,B2,B3,B4
          WRITE(9,*) C,C1,C2,C3,C4
          WRITE(9,*) T1,T2,T3,T4,T5,T6
          WRITE(9,*) X,H(N),FQUAD,XINT,M(N)
      END IF
C
      20 CONTINUE
C
      RETURN
      END

```

C the following functions are for the open-loop case. they are contained in
 C file F4FUNC.FOR. this file is compiled, then linked with the main module
 C RESPONSE.FOR

C
 C DOUBLE PRECISION FUNCTION ACALC(XBAR,N)
 C IMPLICIT DOUBLE PRECISION (A-H,O-Z)

C
 C this function evaluates the numerator polynomial of the integrand at a
 C selected intermediate value in the interval. n=3 indicates the
 C middle interval (R1 to R2) integrand is to be evaluated. n=3
 C indicates the upper interval (R2 to infinity) is to be evaluated.
 C NOTE: when changing to a different linear equation this function
 C must be changed to accurately reflect the integrand being
 C evaluated

C
 C IF (N.LT.3) THEN
 C ACALC= 1.010
 C ELSE
 C ACALC= XBAR**2.5
 C ENDIF

C
 C RETURN
 C END

C
 C DOUBLE PRECISION FUNCTION APCALC(XBAR,N)
 C IMPLICIT DOUBLE PRECISION (A-H,O-Z)

C
 C this function evaluates the first derivative of the numerator polynomial
 C of the integrand at a selected intermediate value in the interval.
 C n=3 indicates the middle interval (R1 to R2) integrand is to be evaluated.
 C n=3 indicates the upper interval (R2 to infinity) is to be evaluated
 C NOTE: when changing to a different linear equation this function
 C must be changed to accurately reflect the integrand being
 C evaluated

C
 C IF (N.LT.3) THEN
 C APCALC= 0.00
 C ELSE
 C APCALC= 2.500*XBAR**1.5
 C ENDIF

C
 C RETURN
 C END

```

C
C      DOUBLE PRECISION FUNCTION ADCALC(XBAR,N)
C      IMPLICIT DOUBLE PRECISION (A-H,O-Z)

```

```

C      this function evaluates the second derivative of the numerator polynomial
C      of the integrand at a selected intermediate value in the interval.
C      n=3 indicates the middle interval (R1 to R2) integrand is to be evaluated.
C      n=3 indicates the upper interval (R2 to infinity) is to be evaluated.
C      NOTE: when changing to a different linear equation this function
C             must be changed to accurately reflect the integrand being
C             evaluated

```

```

C      IF (N.LT.3) THEN
C         ADCALC= 0.00
C      ELSE
C         ADCALC= (1.5D1/4.0D0)*XBAR**0.5
C      ENDIF

```

```

C      RETURN
C      END

```

```

C
C      DOUBLE PRECISION FUNCTION ATCALC(XBAR,N)
C      IMPLICIT DOUBLE PRECISION (A-H,O-Z)

```

```

C      this function evaluates the third derivative of the numerator polynomial
C      of the integrand at a selected intermediate value in the interval.
C      n=3 indicates the middle interval (R1 to R2) integrand is to be evaluated.
C      n=3 indicates the upper interval (R2 to infinity) is to be evaluated.
C      NOTE: when changing to a different linear equation this function
C             must be changed to accurately reflect the integrand being
C             evaluated

```

```

C      IF (N.LT.3) THEN
C         ATCALC= 0.0D0
C      ELSE
C         ATCALC= (1.5D1/8.0D0)*XBAR**(-0.5)
C      ENDIF

```

```

C      RETURN
C      END

```

```

C
C      DOUBLE PRECISION FUNCTION AQCALC(XBAR,N)
C      IMPLICIT DOUBLE PRECISION (A-H,O-Z)

```

```

C      this function evaluates the fourth derivative of the numerator polynomial
C      of the integrand at a selected intermediate value in the interval
C      n=3 indicates the middle interval (R1 to R2) integrand is to be evaluated.
C      n=3 indicates the upper interval (R2 to infinity) is to be evaluated

```

```

C      NOTE: when changing to a different linear equation this function
C      must be changed to accurately reflect the integrand being
C      evaluated

```

```

C      IF (N.LT.3) THEN
C          AQCALC= 0.000
C      ELSE
C          AQCALC= -1.000*(1.501/(1.001)*XBAR**(-1.5)
C      ENDIF

```

```

C      RETURN
C      END

```

```

C      DOUBLE PRECISION FUNCTION BCALC(XBAR,T,N)
C      IMPLICIT DOUBLE PRECISION (A-H,O-Z)

```

```

C      this function evaluates the numerator exponential term of the integrand
C      at a selected intermediate value in the interval. n=3 indicates the
C      middle interval (R1 to R2) integrand is to be evaluated. n=3
C      indicates the upper interval (R2 to infinity) is to be evaluated)

```

```

C      NOTE: when changing to a different linear equation this function
C      must be changed to accurately reflect the integrand being
C      evaluated

```

```

C      IF (N.LT.3) THEN
C          BCALC= DEXP(-1.000*XBAR*T)
C      ELSE
C          BCALC= DEXP(-1.000*T/XBAR)
C      ENDIF

```

```

C      RETURN
C      END

```

```

C
C
C      DOUBLE PRECISION FUNCTION BFCALC(XBAR,T,N)
C      IMPLICIT DOUBLE PRECISION (A-H,O-Z)
C
C      this function evaluates the first derivative of the numerator exponential
C      term at a selected intermediate value in the interval.  n=3 indicates the
C      middle interval (R1 to R2) integrand is to be evaluated.  n=3 indicates
C      the upper interval (R2 to infinity) is to be evaluated)
C
C      NOTE:  when changing to a different linear equation this function
C              must be changed to accurately reflect the integrand being
C              evaluated
C
C      IF (N.LT.3) THEN
C          BFCALC= -1.000*T*DEXP(-1.000*XBAR*T)
C      ELSE
C          BFCALC= (T/XBAR**3)*DEXP(-1.000*T/XBAR)
C      ENDIF
C
C      RETURN
C      END
C
C      DOUBLE PRECISION FUNCTION BDCALC(XBAR,T,N)
C      IMPLICIT DOUBLE PRECISION (A-H,O-Z)
C
C      this function evaluates the second derivative of the numerator exponential
C      term at a selected intermediate value in the interval.  n=3 indicates the
C      middle interval (R1 to R2) integrand is to be evaluated.  n=3 indicates
C      the upper interval (R2 to infinity) is to be evaluated)
C
C      NOTE:  when changing to a different linear equation this function
C              must be changed to accurately reflect the integrand being
C              evaluated
C
C      IF (N.LT.3) THEN
C          BDCALC= T**2*DEXP(-1.000*T*XBAR)
C      ELSE
C          BDCALC= (T**2/XBAR**4)*DEXP(-1.000*T/XBAR)
C      ENDIF
C
C      RETURN
C      END

```

```

C
C      DOUBLE PRECISION FUNCTION BTCALC(XBAR,T,N)
C      IMPLICIT DOUBLE PRECISION (A-H,O-Z)

```

```

C      this function evaluates the third derivative of the numerator exponential
C      term at a selected intermediate value in the interval.  n=3 indicates the
C      middle interval (R1 to R2) integrand is to be evaluated.  n=3 indicates
C      the upper interval (R2 to infinity) is to be evaluated.

```

```

C      NOTE:  when changing to a different linear equation this function
C              must be changed to accurately reflect the integrand being
C              evaluated

```

```

C      IF (N.LT.3) THEN
C          BTCALC= T**3*DEXP(-1.000*T*XBAR)
C      ELSE
C          BTCALC= (T**3/XBAR**6)*DEXP(-1.000*T/XBAR)
C      ENDIF

```

```

C      RETURN
C      END

```

```

C
C      DOUBLE PRECISION FUNCTION BQCALC(XBAR,T,N)
C      IMPLICIT DOUBLE PRECISION (A-H,O-Z)

```

```

C      this function evaluates the fourth derivative of the numerator exponential
C      term at a selected intermediate value in the interval.  n=3 indicates the
C      middle interval (R1 to R2) integrand is to be evaluated.  n=3 indicates
C      the upper interval (R2 to infinity) is to be evaluated.

```

```

C      NOTE:  when changing to a different linear equation this function
C              must be changed to accurately reflect the integrand being
C              evaluated

```

```

C      IF (N.LT.3) THEN
C          BQCALC= (T**4)*DEXP(-1.000*T*XBAR)
C      ELSE
C          BQCALC= (T**4/XBAR**9)*DEXP(-1.000*T/XBAR)
C      ENDIF

```

```

C      RETURN
C      END

```



```
DOUBLE PRECISION FUNCTION CCALC(XBAR,N)
IMPLICIT DOUBLE PRECISION (A-H,O-Z)
```

```
C
C this function evaluates denominator polynomial of the integrand at a
C selected intermediate value in the interval. n=3 indicates the
C middle interval (R1 to R2) integrand is to be evaluated. n=3
C indicates the upper interval (R2 to infinity) is to be evaluated
C NOTE: when changing to a different linear equation this function
C must be changed to accurately reflect the integrand being
C evaluated
```

```
C
C IF (N.LT.3) THEN
C   CCALC= XBAR**4.5+2.0D0*XBAR**2.5+4.0D0*XBAR**1.5-XBAR**0.5
C ELSE
C   CCALC= 1.0D0
C ENDIF
```

```
C
C RETURN
C END
```

```
DOUBLE PRECISION FUNCTION CPCALC(XBAR,N)
IMPLICIT DOUBLE PRECISION (A-H,O-Z)
```

```
C
C this function evaluates the first derivative of the denominator polynomial
C of the integrand at a selected intermediate value in the interval.
C n=3 indicates the middle interval (R1 to R2) integrand is to be evaluated.
C n=3 indicates the upper interval (R2 to infinity) is to be evaluated
C NOTE: when changing to a different linear equation this function
C must be changed to accurately reflect the integrand being
C evaluated
```

```
C
C IF (N.LT.3) THEN
C   CPCALC= 4.5D0*XBAR**3.5+5.0D0*XBAR**1.5-6.0D0*XBAR**0.5
C   +5.0D-1*XBAR**(-0.5)
C ELSE
C   CPCALC= 0.0D0
C ENDIF
```

```
C
C RETURN
C END
```

DOUBLE PRECISION FUNCTION CDCALC(XBAR,N)
 IMPLICIT DOUBLE PRECISION (A-H,O-Z)

this function evaluates the second derivative of the denominator polynomial
 of the integrand at a selected intermediate value in the interval.
 n=3 indicates the middle interval (R1 to R2) integrand is to be evaluated.
 n=5 indicates the upper interval (R2 to infinity) is to be evaluated)

NOTE: when changing to a different linear equation this function
 must be changed to accurately reflect the integrand being
 evaluated

IF (N.LT.3) THEN
 CDCALC=(6.3D1/4.0D0)*XBAR**2.5+(1.5D1/2.0D0)*XBAR**0.5+
 3.0D0*XBAR**(-0.5)-(1.0D0/4.0D0)*XBAR**(-1.5)
 ELSE
 CDCALC= 0.0D0
 ENDIF

RETURN
 END

DOUBLE PRECISION FUNCTION CTCALC(XBAR,N)
 IMPLICIT DOUBLE PRECISION (A-H,O-Z)

this function evaluates the third derivative of the denominator polynomial
 of the integrand at a selected intermediate value in the interval.
 n=3 indicates the middle interval (R1 to R2) integrand is to be evaluated.
 n=5 indicates the upper interval (R2 to infinity) is to be evaluated)

NOTE: when changing to a different linear equation this function
 must be changed to accurately reflect the integrand being
 evaluated

IF (N.LT.3) THEN
 CTCALC=(3.15D2/8.0D0)*XBAR**1.5-(1.6D1/4.0D0)*XBAR**(-0.5)
 -1.8D0*XBAR**(-1.5)-(3.0D0/8.0D0)*XBAR**(-2.5)
 ELSE
 CTCALC= 0.0D0
 ENDIF

RETURN
 END

```

DOUBLE PRECISION FUNCTION QQCALC(XBAR,N)
IMPLICIT DOUBLE PRECISION (A-H,O-Z)

```

```

C
C this function evaluates the fourth derivative of the denominator polynomial
C of the integrand at a selected intermediate value in the interval.
C n=3 indicates the middle interval (R1 to R2) integrand is to be evaluated.
C n=5 indicates the upper interval (R2 to infinity) is to be evaluated.
C

```

```

C NOTE: when changing to a different linear equation this function
C must be changed to accurately reflect the integrand being
C evaluated
C

```

```

IF (X.LT.3) THEN
  QQCALC= (9.4500/1.600)*XBAR**(-0.5)-(1.500/8.000)*XBAR**
1      (-1.5)-(9.000/4.000)*XBAR**(-2.5)-(1.500/1.600)*
2      XBAR**(-3.5)
  ELSE
    QQCALC= 0.000
  ENDIF

RETURN
END

```

```

DOUBLE PRECISION FUNCTION TERMLO(T,R,FAC,N)
IMPLICIT DOUBLE PRECISION (A-H,O-Z)

```

```

C
C this function evaluates a term in the series solution for the lower
C interval (0 to R1)
C NOTE: when changing to a different linear equation this function
C must be changed to accurately reflect the integrand being
C evaluated
C

```

```

TERMLO=0.000*((T**N)*(R**((DBLE(N)+5.00-10)**-1)/(2.000*DBLE(N)
1      +1.000)*FAC)

RETURN
END

```

```

DOUBLE PRECISION FUNCTION VMCALC(X,T)
IMPLICIT DOUBLE PRECISION (A-H,O-Z)
COMMON /IBCONT/ IIB(8)

```

this function evaluates a term at a selected step location for the middle interval (R1 to R2)

NOTE: when changing to a different linear equation this function must be changed to accurately reflect the integrand being evaluated

```

VMCALC=DEXP(-1.000*X*T)/(X**4.5)+2.000/(X**2.5)
-4.000*(X**1.5)-X**1.5
IF (IIB(6).EQ.1) THEN
  IF (NCOUNT.GT.5) GOTO 10
  WRITE (8,5)
  FORMAT ('VMCALC')
  WRITE (9,*) X,T,VMCALC
  NCOUNT=NCOUNT+1
END IF
10 RETURN
END

```

```

DOUBLE PRECISION FUNCTION HICALC(X,T)
IMPLICIT DOUBLE PRECISION (A-H,O-Z)
COMMON /IBCONT/ IIB(8)

```

this function evaluates a term at a selected step location for the upperinterval (R2 to infinity)

NOTE: when changing to a different linear equation this function must be changed to accurately reflect the integrand being evaluated

```

HICALC=DEXP(-1.000*T/X)*(X**0.5)

IF (IIB(7).EQ.1) THEN
  IF (NCOUNT.GT.5) GOTO 10
  WRITE (8,5)
  FORMAT ('HICALC')
  WRITE (9,*) X,T,HICALC
  NCOUNT=NCOUNT+1
END IF
10 RETURN
END

```

The following is the input data for the opening simulation:

```
4.0 0.0 0.0 0.0 0.0025 0.0 0.000000 1  
0.000000 0.000000 -0.000000 -0.000000  
0.0 0.000000 0.0 0.0  
4.0 4.0 4.0  
0.0 0.0 0.0 0.0 0.0 0.0
```

Appendix C

Mittag - Leffler Expansion Method for Predicting Time Response

The Laplace inversion method for analytical prediction of closed- and open-loop system response agrees closely with experimental results. The method has drawbacks which make alternative methods requiring less up-front work attractive. Up-front work refers to hand calculation of the residues, calculation of four derivatives of three functions, then programming these derivatives into the function routines, and finally making engineering judgments on the points at which to apply the asymptotic limit expansions. There are many points at which errors can be made in this process. Is there a simpler analytic tool to use?

The Mittag-Leffler expansion method (12) employs a time-domain solution technique. Identity relations for $D_t^{3/2}(x)$, $D_t^1(x)$, and $D_t^{1/2}(x)$ exist as follows:

$$\begin{aligned} D_t^{1/2}(x) &= D_t^{1/2}x \\ D_t^{1/2}[D_t^{1/2}(x)] &= D_t^1x = \dot{x} \\ D_t^{1/2}[D_t^1(x)] &= D_t^{3/2}x \\ \text{and} \quad D_t^{1/2}[D_t^{3/2}(x)] &= D_t^2x = \ddot{x} \end{aligned} \tag{C1}$$

The entire second-order equation can then be written:

$$mD_t^{1/2}[D_t^{3/2}(x)] + c_1D_t^{1/2}[D_t^1(x)] + c_2D_t^{1/2}[D_t^{1/2}(x)] + c_3D_t^{1/2}(x) = kx = u(t) \tag{C2}$$

Eqs (C1) and (C2) can be put together into a set of linear equations in matrix form:

$$D_t^{1/2}(x) \begin{bmatrix} 0 & 0 & 0 & 1 \\ 0 & 0 & 1 & 0 \\ 0 & 1 & 0 & 0 \\ m & c_1 & c_2 & c_3 \end{bmatrix} \begin{Bmatrix} D_t^{3/2}x \\ D_t^{1/2}x \\ D_t^{1/2}x \\ x \end{Bmatrix} + \begin{bmatrix} 0 & 0 & -1 & 0 \\ 0 & -1 & 0 & 0 \\ -1 & 0 & 0 & 0 \\ 0 & 0 & 0 & k \end{bmatrix} \begin{Bmatrix} D_t^{3/2}x \\ D_t^{1/2}x \\ D_t^{1/2}x \\ x \end{Bmatrix} = \begin{Bmatrix} 0 \\ 0 \\ 0 \\ u(t) \end{Bmatrix} \quad (C3)$$

If the fractional derivative operator, $D_t^{1/2}(x)$, is replaced by λ ,

Eq C3 becomes:

$$\left\{ \lambda \begin{bmatrix} 0 & 0 & 0 & 1 \\ 0 & 0 & 1 & 0 \\ 0 & 1 & 0 & 0 \\ m & c_1 & c_2 & c_3 \end{bmatrix} + \begin{bmatrix} 0 & 0 & -1 & 0 \\ 0 & -1 & 0 & 0 \\ -1 & 0 & 0 & 0 \\ 0 & 0 & 0 & k \end{bmatrix} \right\} \begin{Bmatrix} \lambda^3 \\ \lambda^2 \\ \lambda \\ 1 \end{Bmatrix} = \begin{Bmatrix} 0 \\ 0 \\ 0 \\ u(t) \end{Bmatrix} \quad (C4)$$

and if $u(t) = 0$, the zero state response of the system is characterized:

$$\begin{bmatrix} 0 & 0 & -1 & \lambda \\ 0 & -1 & \lambda & 0 \\ -1 & \lambda & 0 & 0 \\ m\lambda & c_1\lambda & c_2\lambda & c_3\lambda + k \end{bmatrix} \begin{Bmatrix} \lambda^3 \\ \lambda^2 \\ \lambda \\ 1 \end{Bmatrix} = \begin{Bmatrix} 0 \\ 0 \\ 0 \\ 0 \end{Bmatrix} \quad (C5)$$

Now this is an eigenvalue problem and has the same characteristic equation of the system posed in terms of $D_t^{1/2}$:

$$m\lambda^4 + c_1\lambda^3 + c_2\lambda^2 + c_3\lambda + k = 0 \quad (C6)$$

Using a root solving routine, such as that contained in Matrix_x[®], the eigenvalues are simply the roots of the characteristic open- or closed-loop differential equation. The system response can now be posed in eigenvalue/eigenvector format:

$$\begin{Bmatrix} D_t^{3/2} x(t) \\ D_t^1 x(t) \\ D_t^{1/2} x(t) \\ x(t) \end{Bmatrix} = \begin{bmatrix} \lambda_1^3 & \lambda_2^3 & \lambda_3^3 & \lambda_4^3 \\ \lambda_1^2 & \lambda_2^2 & \lambda_3^2 & \lambda_4^2 \\ \lambda_1 & \lambda_2 & \lambda_3 & \lambda_4 \\ 1 & 1 & 1 & 1 \end{bmatrix} \begin{Bmatrix} a_1(t) \\ a_2(t) \\ a_3(t) \\ a_4(t) \end{Bmatrix} \quad (C7)$$

or symbolically:

$$\{ D(t) \} = [\Lambda] \{ A(t) \} \quad (C8)$$

Total system response is the sum of the characteristic behavior belonging to each root of the differential equation:

$$x(t) = \sum_{i=1}^4 a_i(t) \quad (C9)$$

and the $a_i(t)$ is a series expansion:

$$a_i(t) = a_i(0) E_{1/2}(\lambda_i t^{1/2}) \quad (C10)$$

The expansion, $E_{1/2}$ is defined:

$$E_{1/2}(z) = \sum_{n=0}^{\infty} \frac{z^n}{\Gamma(1 + n/2)} \quad (C11)$$

Γ is the gamma function or generalized factorial. The total solution is then:

$$x(t) = \sum_{i=0}^4 \sum_{n=0}^{\infty} a_i(0) \frac{(\lambda_i t^{1/2})^n}{\Gamma(1 + n/2)} \quad (C12)$$

The $a_i(0)$ terms arise from the initial condition vector, $\{ D(0) \}$. From Eq (C8):

$$\{ A(0) \} = [\Lambda]^{-1} \{ D(0) \} \quad (C13)$$

The $a_i(t)$ terms can be complex numbers. The solution can be implemented on a mainframe computer using any type of programming language. However, to implement it on a Z248 PC, one must use the

macro-programming routines in Matrix_x[®] to be able to work with complex numbers. These macro-routines are portable to the Matrix_x[®] version contained on the AFIT Vax mainframes. Appendix D contains the Matrix_x[®] routines, files, and instructions for their use. It is programmed so the expansion $E_{1/n}$ can be done for any 1/nth order value desired. This is accomplished by responding to the prompt for system dimension with (2*n). For example, if the second order equation involved quarter derivatives instead of halves the response would be [(2)(4)] = 8.

Appendix D

Matrix_x[®] Code for Mittag - Leffler Expansion

Page 141 contains the code for MITLEFR.DAT which is an executable file.

To run, execute Matrix_x, ensure MITLEFA.DAT (page 142) and MITLEFB.DAT (page 143) are present on disk, then enter "EXECUTE ['MITLEFR.DAT']".

Follow the prompts.

```

// define the two subroutines to be run
//
DEFINE 'A:MITLEFA.IAT'
DEFINE 'A:MITLEFE.IAT'
//
// prompt for the dimension of the system: (0 smallest
// fractional order)
//
INQUIRE N 'INPUT N: '
//
// call executable file invert to obtain the eigenvector matrix
// and the the a-sub-zero (1) vector
//
[AZERO,A]=CONVERT(N)
//
// call rspral (response calculation) to perform the M-L
// expansion
//
[ITOUT,XOUT]=RSFICAL(AZERO,A,N)

```

```

//
// the routine for calculating the a-sub-zero vector
//
// AZERO,AM=CONVERT(M)
//
// prompt for system coefficients
//
INQUIRE COEFF 'ENTER SYSTEM COEFFICIENTS: '
//
// obtain initial conditions
//
INQUIRE AZ 'ENTER INITIAL CONDITIONS: '
//
// solve for the characteristic roots of the differential
// equation
//
A=ROOTS(COEFF);
//
// form the eigenvector matrix
//
FOR I=1:N,...
  FOR J=1:N,...
    AM(I,J)=A(I,J)** N-I;END,END
//
// form the inverse of the eigenvector matrix
//
AINVRS=INV(AM);
//
// calculate the a-sub-zero(t) vector
//
AZERO=AINVRS*AZ;
//
// return control to mitlefr.dat
//
RETF

```

```

//([TOUT,XOUT,XERR]=RSPCAL(AZERO,A,N)
//...
//... accept routine control input
//...
INQUIRE TSTART 'INPUT START TIME: '
INQUIRE TZERO 'INPUT START TIME OF DESIRED INTERVAL: '
INQUIRE TMAX 'INPUT MAX TIME: '
INQUIRE NUMPTS 'INPUT NUM OF POINTS TO CALCULATE: '
INQUIRE NUMITS 'NUM OF TERMS IN MITTEF SERIES: '
//...
//... calculate time increment & setup to correctly define initial time
//...
TINC=(TMAX- TZERO)/NUMPTS;
T=TZERO-TINC;
FOR INC=0:NUMPTS....
//...
// establish matrixx compatible storage index and initial increment values...
//...
    INDX=INC+1;...
    ZX=0;...
    T=T+TINC;...
//...
// if interval start prior to response start set calculation time to zero...
//...
    IF T<TSTART,TCALC=0;ELSE TCALC=T-TSTART;END,...
//...
// set up initial values for gamma function...
//...
    PRE1=1.0;PRE2=0.5;LBIT=1;...
//...
// calculate the first 2 terms in the Mittag-Leffler (ML) series...
// ... use these terms as multipliers of the integer and...
// non-integer gamma function terms of the M-L series...
//...
    FOR I=1:N,...
        Z(I)=-A(I)*SQRT(TCALC);...
        ELAST1(I)=1.0/PRE1;...
        ELAST2(I)=Z(I)/(SQRT(P1)*PRE2);...
        ZX=ZX+AZERO(I)*(ELAST1(I)+ELAST2(I));END,...
//...
// set up the correct denominator for the next non-integer gamma term...
//...
    PRE2=PRE2+1

```

```

//...
// LBIT controls the use of the integer or non-integer gamma function terms...
// ...the next loop calculates the j+2 term of the M-L series for each of...
// the n roots...
//...
  FOR J=1:NUMITS,...
    R=0+JAY*0;...
//...
// calculate the gamma function term and set up for the next loop...
//...
  IF LBIT=1,DEN=PRE1;PRE1=PRE1+1;LBIT=2;...
  ELSE DEN=PRE2;PRE2=PRE2+1;LBIT=1;...
  END,...
  FOR I=1:N,...
//...
// multiply the last integer/non-integer term by z**2/n-1 to get the...
// correct M-L term for the ith root...
//...
    IF LBIT=2, ELAST1(I)=(ELAST1(I)*Z(I)**2)/DEN;...
    R=R+AZERO(I)*ELAST1(I);...
    ELSE ELAST2(I)=(ELAST2(I)*Z(I)**2)/DEN;...
    R=R+AZERO(I)*ELAST2(I);...
  END,...
  END,...
//...
// ZX represents the sum of the i roots for each term...
//...
  ZX=ZX+R;...
  END,...
//...
// store the output for each time step...
//...
XOUT (INDX)=REAL(ZX);XERR(INDX)=IMAG(ZX);TOUT(INDX)=T;...
END
//...
// save the data file in a format readable by grapher...
//...
FSAVE 'MITAPP.DAT' TOUT XOUT
RETF

```

Appendix E

Oldham - Zoski Circuit Design Parameters

A summary of the design and fabrication process involved in realizing the Oldham-Zoski resistor/capacitor domino-ladder circuit, which will perform the operation d^{ν}/dt^{ν} on an input electrical signal is presented. The valid range for ν :

$$-1 < \nu < 1 \quad (E1)$$

where ν less than zero indicates integration.

The basic circuit is referred to as a domino ladder and consists of a chain of resistors and capacitors, the two chains being connected at each node as in Figure 3. Each resistor is a constant factor multiple of its predecessor as is each capacitor giving the relationship:

$$R_j = R_0 g^{-j} \quad \text{and} \quad C_j = C_0 a^{-j} \quad (E2)$$

where both g and a are greater than unity.

To proceed select a value of ν ; then

$$\ln a \leq 3/2 \nu^{2/3} \quad (E3)$$

$$\text{and } \ln g = (1-\nu) \nu^{-1} \ln a \quad (17:31) \quad (E4)$$

The rest of the method follows the basic guidelines established in (17). However, the derivation is put in terms of frequency instead of time, as was done in the original Oldham-Zoski article. First, a minimum frequency, f_m , is selected for the application (f_m is in Hz). The time constant of the first resistor-capacitor pair is then:

$$R_O C_O = \frac{111 \exp(-3\nu^{2/3})}{f_m G g} \text{ sec} \quad (E5)$$

Any combination of resistors and capacitors which produces this time constant is acceptable. As explained in the analysis section, the smaller the capacitance values the better. This must be balanced, on the other hand, by the values of the largest resistors and smallest capacitors available. If $|\nu|$ is $\cong 1$, or the frequency range is large, the design will require more cells than if $|\nu|$ is small. This could possibly put a limit on the initial resistance and capacitance values used. It is also wise to make the tolerance on the components less than 2%. This appears to guarantee good performance.

To calculate the number of cells required in the domino-ladder, select a desired upper frequency limit, f_M . The number of cells required, N , is then:

$$N + 1 \geq [5.5 + \ln(f_M/f_m) - 3\nu^{2/3}] [\ln(gG)]^{-1} \quad (E6)$$

Some enhancements for the high- and low-frequency performance are available (17:33). To increase the accuracy at high frequencies, modify the final resistor capacitor pair:

$$\begin{aligned} \text{from } R_N &= R_O g^{-N} & \text{to } 1/2 R_O g^{-N} \\ C_N &= C_O G^{-N} & \text{to } 2 C_O G^{-N} \end{aligned} \quad (E7)$$

and introducing a final resistor at the output of the circuit:

$$R_{N+1} = R_O g^{-N} (\ln g)^{-1} \quad (E8)$$

Low-frequency performance can be improved by adding an additional resistor-capacitor pair at the start of the circuit :

$$R_{-1} = \left(\frac{1}{2} + \frac{1}{\ln G} \right) R_O \quad \text{and} \quad C_{-1} = \frac{C_O G}{\left[\frac{1}{2} + \frac{1}{\ln G} \right]} \quad (E9)$$

While circuits produced using this method possess the correct Bode magnitude slope and phase response, the actual gain value at $\omega = 1$ requires adjustment to 0 dB. This adjustment depends on:

- $\nu \equiv$ fractional order
- $C \equiv$ Capacitance of the analog circuit interface component
- $R \equiv$ Resistance of the analog circuit interface component
- $R_O \equiv$ Resistance of the Oldham-Zoski base resistor
- $C_O \equiv$ Capacitance of the Oldham-Zoski base capacitor

On the Pace analog computer (model TR48) there are two possible interface resistor values, 10K Ω and 100K Ω . The two interface capacitor values are 0.02 μ F and 10.0 μ F. Figure 47 shows the possible configurations available to obtain specific fractional differentiator or integrator values and the corresponding equations to calculate the gains required for a given circuit. Table 2 contains the calculations of the gains for the two circuits built for this thesis and compares predicted and actual gains required. Table 3 details the method of configuring the operational amplifiers and capacitors to take advantage of the four different interface components. For further information on the Oldham-Zoski circuit refer to reference 17.

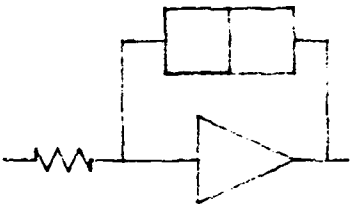
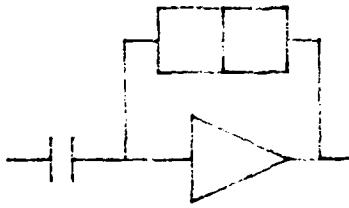

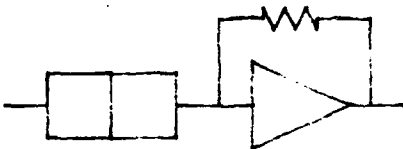
Config #		Equation
1		$\frac{\Pi R_o^{1/2}}{RC_o^{1/2} \ln(Gg)} E_{out} = \frac{d^{-1/2}}{dt^{-1/2}} E_{in}$
2		$\frac{\Pi CR_o^{1/2}}{C_o^{1/2} \ln(Gg)} E_{out} = \frac{d^{1/2}}{dt^{1/2}} E_{in}$
3		$\frac{C_o^{1/2} \ln(Gg)}{\Pi CR_o^{1/2}} E_{out} = \frac{d^{1/2}}{dt^{-1/2}} E_{in}$
4		$\frac{RC_o^{1/2} \ln(Gg)}{\Pi R_o^{1/2}} E_{out} = \frac{d^{1/2}}{dt^{1/2}} E_{in}$

Figure 47. Analog Interface Configurations for the Oldham-Zoski Circuit for Different Fractional Operators

Table 2. Circuit Gains - Predicted Versus Experimental
Oldham-Zoski--Analog Interface Configuration 4

Predicted	$\left[\frac{\pi R_o^{1/2}}{RC_o^{1/2} \ln(Gg)} \right]$	Experimental
Circuit 1	26.52	25.06
Circuit 2	13.26	11.47

Table 3. Details for Realizing the Four Different Analog Computer
Interface Configurations for the Oldham-Zoski Circuit

CONFIGURATION 1	Input signal to either a x10 terminal on an operational amplifier (R=10k) or a x1 input terminal (R=100k). Output of the amplifier is input to the OZ circuit, output of the OZ circuit is connected to the x10 input terminal on the amplifier (10KΩ must be removed from the last OZ resistor before connecting).
CONFIGURATION 2	Remove T plug from one of the integrator modules. Insert 2 pin bottle plugs in the '0.1/3' and 'SPEC' terminals, and a 4 pin bottle plug in the 'OPR/RESET' bus. In this configuration C=10μF. Removing the bottle plug from the '0.10/3' area gives C=1μF. The OZ circuit is connected to the amplifier as in Configuration 1. The input to the capacitor is connected to the 'SJ' input terminal, the output is then available at the 'O' terminal. Connect this terminal to an input terminal on the operational amplifier. Use only a 2 pin bottle plug on the operational amplifier to connect the 'B' and 'SJ' terminals.
CONFIGURATION 3	Configure the integrator as in Configuration 2 with the following exception - the input to the integrator (capacitor) is the output signal of the operational amplifier. The input signal is connected to the input terminal of the OZ circuit. The output terminal of the OZ circuit is then connected to the input of the amplifier.
CONFIGURATION 4	Configure the operational amplifier with a 4 pin bottle plug (R=100KΩ). If R=10K is desired, use two 2 pin bottle plugs - one connecting 'SJ' and 'B' and one connecting an output terminal to a x10 input terminal. The input signal is connected to the input terminal of the OZ circuit. The output terminal of the OZ circuit is connected to the input of the amplifier.

Appendix F:
Detailed Experimental Procedure

For each task listed in Section IV this appendix details the instrumentation configuration used to experimentally gather the data. It also provides references to equipment manuals should additional information concerning the equipment be of interest.

Circuit Build

The Tektronix Digital Multimeter (model DM501) (28) and Dynascan Capacitance Meter (model 820) are required for this step. The scale on the multimeter should be set to ohms and the proper range selected for the resistor being measured. A note of caution on the capacitance meter: as the capacitances get smaller, the offset error becomes large. Take this into consideration when measuring pF capacitors.

Circuit Test

Equipment Used

The criteria for a fractional derivative of order one-half is a Bode plot with a slope of 10dB/decade and a constant phase shift of 45 degrees. To determine if this criteria was satisfied by the circuits fabricated, a function generator, counter/timer, and oscilloscope were used .

Tektronix Function Generator (model FG506) (24:1-1,1-3).

Capable of producing a 10 volt peak-to-peak sine wave at frequencies from .001 to 50 MHz when shunted across a 50Ω impedance load.

Tektronix Universal Counter/Timer (model DC509) (25:2-1,2-13).

Two channel input, with adjustable trigger voltage for each channel.

Capable of measuring frequency to within 1×10^{-6} Hz for the frequencies of interest; period to within 1×10^{-5} sec; and phase difference between channels to within 1×10^{-5} sec when triggers are set correctly.

Tektronix Oscilloscope (model SC504) (26:1.1-2.29). Two channel display, graticule on the screen capable of representing 0-100% of 5 times the magnitude of the volts/division setting. Resolution is $\pm 2\%$ of this range. Volts/division settings spanning 5mV to 10V. The unit has adjustable horizontal sweep frequencies.

Using BNC T fittings and coax cables, the function generator output is connected to Channel A of the counter/timer, Channel 1 of the oscilloscope, and the input of the Oldham-Zoski circuit. This circuit produces an output current which is the fractional derivative of the input voltage. The voltage across the last resistor is just the value of this current multiplied by the value of the resistor. This voltage is the voltage to be compared with the input voltage. (It is important to place the output measurement device in parallel with this last resistor. Since they are high-impedance devices, very little current will be required to produce the measurement, whereas a series measurement would seriously affect the circuit current). The voltage

across the last resistor is connected to Channel B of the counter/timer and Channel 2 of the oscilloscope.

Procedure

The gain of the circuit is defined, in dB, as:

$$20 \log_{10}(v_{out}/v_{in}) \quad (F1)$$

It is not necessary to maintain the same input amplitude over the range of frequencies tested. However, it leads to the conclusion that the voltage input to the circuit is not frequency dependent. Since the performance of the circuit is necessarily dependent on frequency, it makes the calculation of gain straight forward if the input voltage is constant.

Without the circuit attached to the function generator, a 50Ω resistor should be shunted across the output of the function generator, and then a common connection should be made to ground; this matches the impedance of the function generator. A sweep across the frequency band to be investigated (0.01 to 1000 Hz) should be made. The amplitude of the input voltage on Channel 1 of the oscilloscope should be observed. If no changes are evident then the assumption can be made that the OZ circuit input voltage remains constant. The circuit should be connected in parallel with the 50Ω resistor. Since the impedance of the Oldham-Zoski circuit is several orders of magnitude higher than the 50Ω resistor, the parallel combination will appear as a 50Ω impedance to the function generator.

Amplitude Ratio Determination

The procedure is as follows:

1. Set function generator to a desired test frequency (record)
 2. Set counter/timer to frequency and validate the frequency.
 3. Ground both channels of the oscilloscope and adjust the zero position of each channel.
 4. Set both channels to DC input coupling
 5. Adjust the volts/division reference for each channel to give the maximum deflection without exceeding the 100% mark on the graticule.
 6. If a volts/division change was made, repeat step 2 for the appropriate channel.
 7. Use the chop display mode to look at both signals at once.
 8. Use the percent values listed on the left side of the graticule to record each channel's amplitude as a given percentage of 5x the value of the volts/division setting for that channel.
- Divisions on the left hand side of the graticule are 4% per minor division, giving accuracies of $\pm 2\%$ Use Eq (F1) to determine the gain for the frequency just tested.

Phase Determination

After calculating the gain at a given frequency the following procedure will determine the phase angle:

1. On the counter/timer select the 'PERIOD A' function.
2. Select the desired number of cycles to be averaged together on the 'Averages' selector. Select 1 for frequencies less than 0.1 Hz, 'Auto' for frequencies up to 1 Hz, and adjust to stabilize the reading for higher frequencies. Record the period in the data table being made.
3. Adjust the trigger voltages to provide an accurate evaluator of the phase shift.

3a) For both channels, ensure the following configuration:

'SLOPE': both the same

'ATTEN': 'x1'

'SOURCE': 'Ext'

'COUPL': AC

Ensure the button on the timer/counter marked 'AUTO TRIG LEVEL' is not depressed.

3b) Using the multimeter with needle probes, select

'DC VOLTS' and '200 mV', insert the positive lead into the contact marked 'A - TRIG LEVEL' on the timer/counter and the negative lead into the contact marked 'COM - SHAPED OUT'. Adjust the channel A trigger level to as close to zero as possible on the multimeter readout.

Switch the positive lead to 'B - TRIG LEVEL' and repeat the adjustment for channel B to get the trigger as close as possible to the value for channel A.

- 4) Select the 'TIME A→B' function, the phase shift time will appear in the readout. Record.
- 5) Calculate the phase shift as follows:

$$('TIME A \rightarrow B' / \text{Period}) * 360 = \phi \text{ (degrees)} \quad (F2)$$

- 6) Record values; repeat gain and phase procedure as required.

Hewlett-Packard HP7090A Analog Measurement System

Overall circuit performance depends not only on steady-state performance, but also on start-up transient characteristics. It became clear that observing the startup transient was a necessity. How long did it take the circuit to become an efficient fractional differentiator?

To answer this question, a Hewlett-Packard Analog-Digital Measurement Recording System (model 7090A) was obtained and substituted for the oscilloscope. The recorder is capable of plotting 3 channels of input data, with a sampling rate of 33 kHz. The model 7090A also has three 1000 word-length buffers (one buffer for each channel). Each word represents a time slice of 1000th of the total time window specified prior to data recording. After experimenting with this total time window, it was observed that three to five cycles of the input sine wave

produced a steady-state response of the circuit, and sufficient data to accurately determine gain and phase shift. The equation used as a guide for the total time setting:

$$t_{\text{total}} = 5 \text{ cycles} * [1 / (f_{\text{Hz}})] \quad (\text{F3})$$

Another feature of the model 7090A is the ability to record data prior to the start-up of the system. A trigger function represents the actual start of the measurement. This trigger can be set internally to occur at a specific clock time, or it can be controlled externally. By specifying a duration of pre-trigger recording time, t_{pt} , all events occurring within t_{pt} seconds prior to the actual trigger event are recorded. In addition, if t_{pt} seconds pass after starting to fill the buffers without the trigger event occurring, the oldest pre-trigger data is written over so that only the latest t_{pt} seconds of data are retained in the buffer.. These features allow the actual startup transient of the circuit under test to be recorded (27:3-1,24).

The external triggering system of the model 7090A can be accessed through a BNC fitting on the right-hand side of the unit. The trigger uses TTL logic, and is activated when the signal level is connected to ground. This made fabricating a trigger quite easy. A coax cable was attached to the trigger input. A short piece of insulated wire, with one end stripped of insulation, was inserted into the female connector (signal) of the BNC fitting at the free end of the cable. To activate the trigger, the wire was grounded to the shield of the coax cable. (27:5-1,9).

After the trigger event, the input channels are recorded until the buffers are full at time t_{tot} . Each buffer recorded can then be plotted. A special function allows the buffer to be stepped through, one location at a time. The plotter moves the pen directly over the point on the plot representing the current storage location; its value is observable on the LCD display on the plotter. If the point represents a point of interest, such as a peak in a curve or a zero amplitude, a function can be selected to mark the point with a '+' and annotate it with voltage and time values (27:4-1,10).

Determination of Gain and Phase Angle Using the Model 7090A

To interface input signals with the model 7090A use banana plugs, or a coax cable with a dual banana plug adaptor. Connect the ground of the device or circuit being measured to the ground jack on the recorder. Configure the input signal from the function generator into channel 1 of the recorder, and the output of the Oldham-Zoski circuit into channel 2. Repeat the constant amplitude input voltage check as previously mentioned. Input values can be observed on the LCD display and do not need to be plotted (this was repeated once; the voltage remained constant over the frequency range).

For a given frequency determine the total time from Eq (F1) and the desired pre-trigger time and input to the plotter. Select channels 1 and 2 for recording. Set the expected voltage for each channel. Set the frequency generator to the desired value and verify with the

counter timer. Turn the frequency generator off. This permits recording of the start-up transient of the fractional differentiator. Press the 'FILL BUFFER' switch; after sufficient time has passed to load the pre-trigger buffer, turn on the function generator and ground the trigger wire. After the buffers fill, plot the buffers twice (27:4-7,8). On one annotate the points of interest on the input channel. On the other annotate the points of interest for the circuit output. The points of interest used for the data in Appendix G are the maximum and minimum points of each cycle and the negative slope time axis crossings (the LCD display, in the annotation mode, can be invaluable in selecting these points) (27:4-8).

The period, gain, and phase are calculated as follows:

Period:

$$\frac{\text{FINAL PEAK VOLTAGE TIME (SEC)} - \text{INITIAL PEAK VOLTAGE TIME (SEC)}}{\text{NUMBER OF CYCLES BETWEEN THE PEAK VALUES USED}} \quad (\text{F4})$$

Gain:

$$\frac{\sum [\text{OUTPUT VOLTAGE PEAKS} + |\text{OUTPUT VOLTAGE MINIMUMS}|] / [\# \text{ MAXES} + \text{MINS}]}{\sum [\text{INPUT VOLTAGE PEAKS} + |\text{INPUT VOLTAGE MINIMUMS}|] / [\# \text{ MAXES} + \text{MINS}]} \quad (\text{F5})$$

This method compensates for offsets in the input and output voltages.

Phase Angle (using paired input and output time axis crossings):

$$\frac{\sum [\text{INPUT TIME AXIS CROSSINGS (sec)}] - \sum [\text{OUTPUT TIME AXIS CROSSINGS}]}{\text{NUMBER OF CROSSINGS EVALUATED} * \text{TOTAL PERIOD}} \quad (\text{F6})$$

This method proved much easier and faster than observing the oscilloscope, counter/timer, and continually making the necessary adjustments.

Analog Components and Tasks

Figure 20 shows the PACE[®] analog computer (model TR48), with its three major panel subdivisions - the control and monitoring panel on the left, the component panel in the center, and the potentiometer adjustments on the right.

Control and Monitoring Panel (22:1-11)

There are three items of concern for operating the analog computer on this panel; the multi-colored mode select keys, digital voltmeter (DVM), and the operational amplifier/potentiometer selector keypad. First the mode select keys. There are four of interest for the tasks at hand; 'PS', potentiometer set; 'IC', initial condition; 'OP', operation, and 'HD', hold modes. To select a specific mode, simply depress the appropriate key. The amplifier/potentiometer selector keypad simply selects one of the numbered potentiometers or amplifiers (depending on whether the 'A' or 'P' selector is chosen) for display on the DVM.

To view the value of a specific potentiometer used for establishing the coefficients of the differential equations, depress the 'PS' key. This isolates the potentiometers from their input voltages, giving their true values in the circuit. Depress the black 'P' key, then the appropriate two-digit potentiometer identifier as listed on the component panel. The desired value can now be read off the DVM.

To view the output value of a specific amplifier in any mode, depress the 'A' key and appropriate two digit designator of the desired amplifier as found on the component designator panel. The output of all amplifiers is a varying voltage level. The DVM represents this level as a certain percentage of the computer's reference voltage of 10 volts. Therefore, when the DVM reads 0.2500, the output of a given amplifier is actually 2.5 volts (22:1-11)

When are the different modes used? Use 'PS' mode when setting and rechecking potentiometer values. The potentiometers have a tendency to drift, so after a few data runs switch back into the 'PS' mode and recheck the values. Use 'IC' at the completion of a data run, to abort a run, or to reestablish initial conditions. When in the 'IC' mode, the initial conditions for each operational amplifier and potentiometer can be viewed on the DVM. This capability is ideal for verifying proper circuit configuration. After everything is properly configured, depressing the 'OP' button starts the simulation by activating the integrators. The 'HD' key freezes all computations at the current levels and permits observation of intermediate values (22:1-20).

Located on the center panel of the model TR48 are many components required to simulate control systems and differential equations. Only the ones used for the open- and closed-loop simulations will be described.

Summing, Inversion, and Factor of Ten Multiplication

These functions are provided by the '6.514 Dual DC Amplifier' (22:3-1). All amplifiers on the model TR48 are inverting amplifiers, that is, the output voltage is the negative of the input voltage. A voltage input to the jack labeled '10' produces a negative ten times the input voltage. If more than one voltage is input to the operational amplifier, the output is the sum of the input voltages multiplied by the value of the input jacks used.

Attenuators (Potentiometers)

Without attenuators, precision multiplication would not be possible. The '42.283 Attenuator Module' (22:2-1) consists of 5, wire-wound resistors and whose resistance is established by the setting associated with its control dial. The dials are divided into one ten-thousandths increments. Circuit schematics and flowchart symbols for the potentiometers are shown in Figure 22. To obtain a desired voltage, for example $0.8973 \times_{in}$, the following procedure applies:

1. Patch the input voltage into the upper terminal of the potentiometer
2. Patch the output of the potentiometer to the input of the next device
3. Determine the component identifier of the potentiometer (for example P07)
4. Depress the 'PS' key to go into Potentiometer Set mode
5. Select 'P', '0', and '7', using the selection keys

6. Observe the current value of the pot on the DVM
7. Unlock the 'P07' dial on the right panel and adjust until the DVM reads 0.8973
8. Lock the dial, making sure the potentiometer value remains the same

The output of P07 will now be 0.8973 of the value input.

Integrators

The '12.1322 Dual Integrator Network' (22:4-6) produces the integral of the input voltage with respect to time. Reference the symbol under 'X(0) = 2.0', depicted in Figure 34, for the circuit schematic associated with an integrator. Note the value at the top of the x integrator, this is the initial condition applied to the integrator, and is the output of the integrator when in the 'IC' mode. This value is established with a reference voltage input to the 'IC' jack on the integrator. Again, the integrator is an inverter and the negative value of this voltage is the initial condition. When placed in the 'OP' mode, the output of the integrator is:

$$- \left(\int_c^t [\text{input voltage}(t)] dt + IC \right) \quad (F7)$$

Comparator

To successfully interface the model 7090A with the analog computer, the recorder must receive its input signal at the moment the op button is depressed on the control panel. As previously discussed, the model 7090A activates its trigger when the signal voltage is connected to ground. To correctly patch this logic, the '40.404 Relay Comparator'

(shown schematically in the upper right hand corner of Figure 23 isolating the one-half derivative input) is used. The trigger input signal from the model 7090A recorder is patched into the common terminal of the switching relay, the trigger ground into the comparator terminal marked '-'. The switching voltage required to initiate the trigger signal is provided at the output of the 'OP' bus jack on the 12.132 Dual Integrator when the 'OP' mode is selected. When the computer is in 'IC' mode the output of the 'OP' bus jack $\cong 0$. This makes the output of the comparator positive and the model 7090A trigger signal is isolated from ground. When the 'OP' mode is selected, the output of the comparator is negative, closing the connection between signal and ground.

Function Switches

On the right-hand panel of the model TR48 analog computer, below the potentiometer adjustment dials, are five toggle switches. These switches are three-position, single-pole switches connected to the '12.766 Function Switch Module' (22:2-6). When the switch is moved to the left, the input is connected to the 'L' output jack. Likewise, the 'R' contact is closed when the switch is moved to the right. This switch is useful in connecting different forcing functions to a system model. In this specific case, several $f(t)$ s could be available for switching in and out of the circuit. This switch was used in the 'Total-Cycle Simulation' to apply and remove the input step voltage.

More detailed information on these components can be found in the EAI PACE (model TR48) Analog Computer Reference Handbook (22).

Steps for Programming an Example Simulation (23:84+)

For an example simulation set-up, program a harmonic oscillator $\ddot{x} + x = 0$ with an initial condition $x(0)=2.5$. To run the simulation:

1) Select three operational amplifiers and 3 potentiometers and define as follows:

Component	Purpose
A01	\ddot{x}
A02 } configure as	\dot{x}
A03 } integrators	x
P01	m
P02	k
P03	$x(0)$

2) Make the following patches:

From	To
A01 Output	P01 input
P01 Output	x10 A02 input
A02 Output	x1 A03 input
A03 Output	P02 input
-10 Ref on P00-04 module	P03 input
P03 Output	A03 IC
P02 Output	x10 A01 Input
A03 Output	HP7090A Channel 1 input

3) Patch the ground jacks for A01, A02, and A03 and the model 7090A Channel 1 grounds together to eliminate floating grounds.

4) Configure the '40.404 Comparator' and model 7090A per the description under comparators in this appendix.

5) Depress 'PS' selector on the control console

6) Turn the model 7090A recorder and the model TR48 analog computer on

7) Press 'Restore Setup' on the model 7090A to establish standard values. Make desired changes to

Channel 1 Range
Channel 1 Offset
Trigger Value
Total Time

8) For each potentiometer, press the appropriate component selection keys. Unlock the associated potentiometer set dials, and establish the following values on the DVM for each potentiometer:

<u>Potentiometer</u>	<u>Value</u>
P01	0.1000
P02	0.1000
P03	0.2500

9) Depress the 'IC' mode select button.

10) Select 'A03' for display on the DVM. It should read $\cong 0.2500$
(whatever the setting on P03 was)

11) Press 'BUFFER FILL' on the model 7090A, and allow adequate time for the pre-trigger buffer to fill

12) Depress 'OP' on the model TR48 analog computer

13) When the 'Buffer Full' light comes on on the model 7090A:

- a) Press 'IC' on the model TR48 to end the run
- b) Insert paper in the model 7090A

- c) If a grid is desired on the plot
 - 1) Select a pen color with the 'PEN SELECT' button
 - 2) Press 'Grid'
- 14) When plotting is complete, annotate the points of interest as previously mentioned.

The resulting output should be a cosine function with amplitude 2.5 volts and period ($\pi/2$) Hz. This circuit can be used for the analog/half-order compatibility verification trial. Similar methods can be used for simulating other second-order equations. In this simulation P01 and P02 were not required to obtain the coefficients m and k since they were both identically equal to 1. The output of A01 and A03 could have been connected directly to the next component with the same results. However, the example provided an exercise for establishing the proper coefficients for each term.

Appendix G

Oldaham - Zoski Circuit Validation Data

Appendix G

Oldaham - Zoski Circuit Validation Data

Table 4. Circuit 1 Performance Validation Data

Frequency (Hz)	Gain (dB)	Phase (deg)
0.0116	-47.85	44.74
0.0505	-41.71	45.81
0.0963	-38.95	45.76
0.1451	-37.26	47.00
0.1934	-36.03	48.04
0.5102	-31.67	46.53
0.9780	-28.88	45.77
5.042	-22.08	44.16
9.750	-19.36	45.40

Table 5. Circuit 2 Performance Validation Data

Frequency (Hz)	Gain (dB)	Phase (deg)
0.0107	-38.96	42.18
0.0503	-32.75	50.35
0.0976	-29.34	48.51
0.1470	-27.61	46.97
0.1944	-26.62	44.08
0.5034	-23.53	40.11
0.9900	-21.03	43.20
5.012	-13.89	46.92
9.670	-10.79	46.19



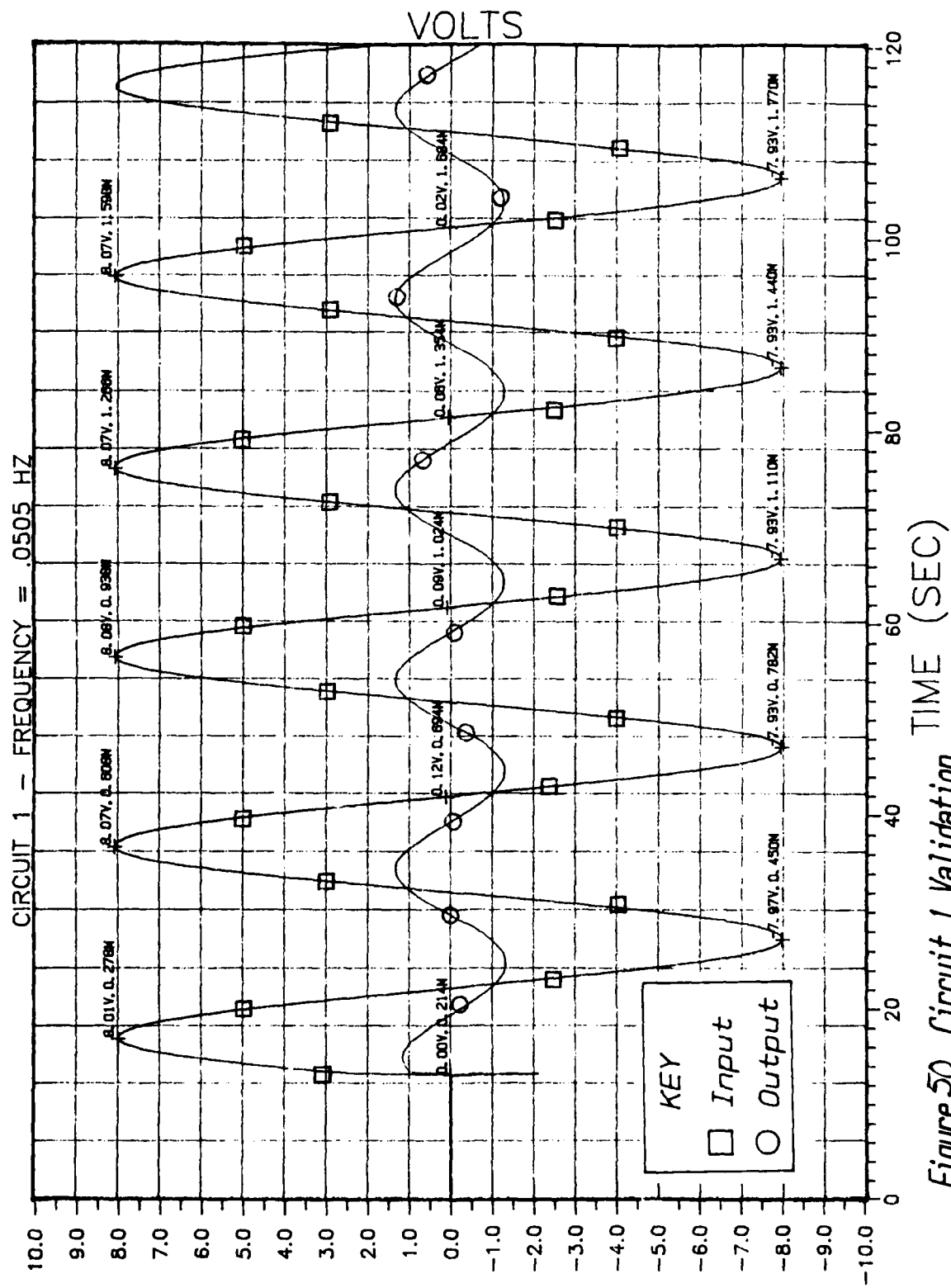


Figure 50. Circuit 1 Validation

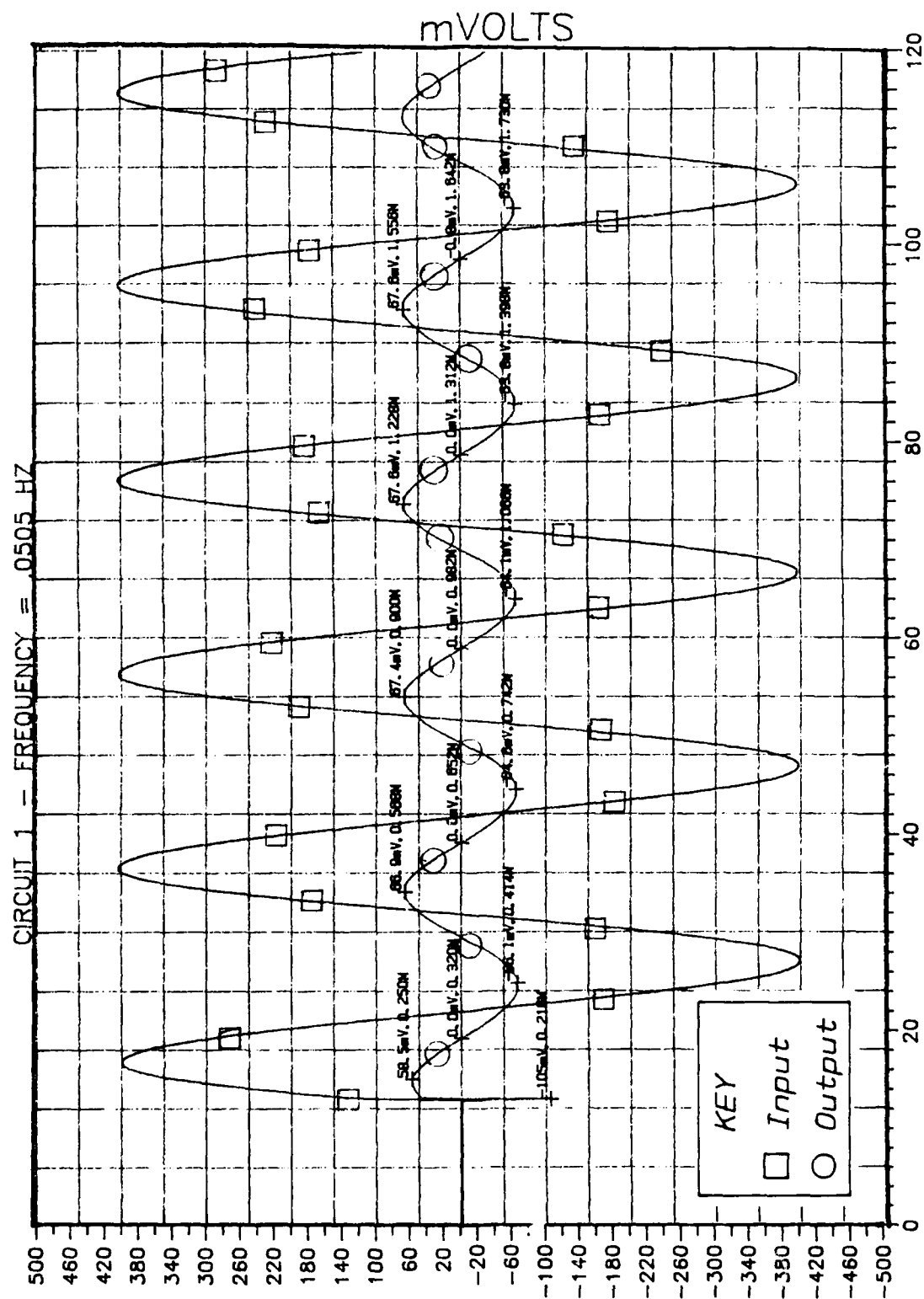


Figure 51. Circuit 1 Validation

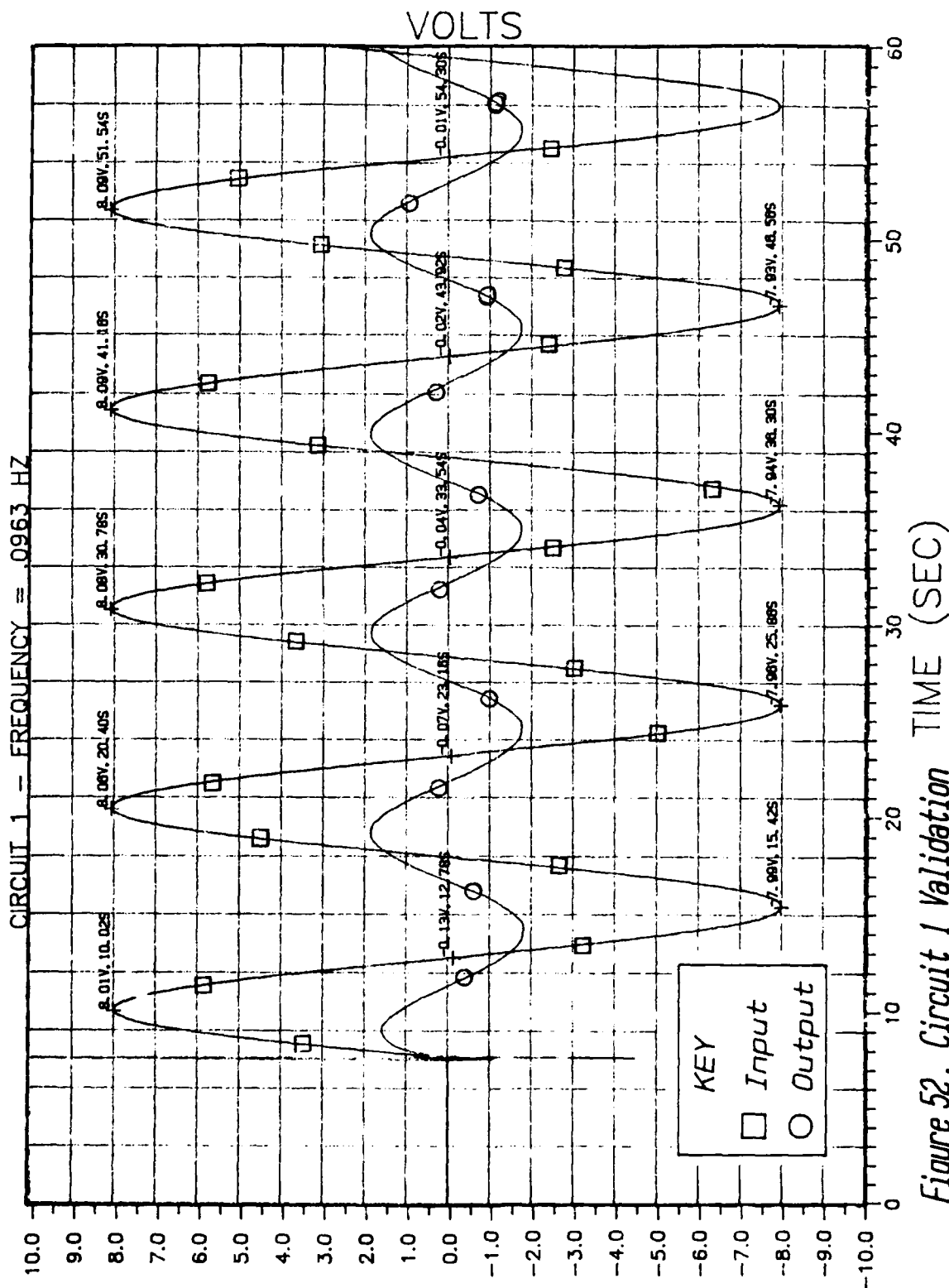


Figure 52. Circuit 1 Validation

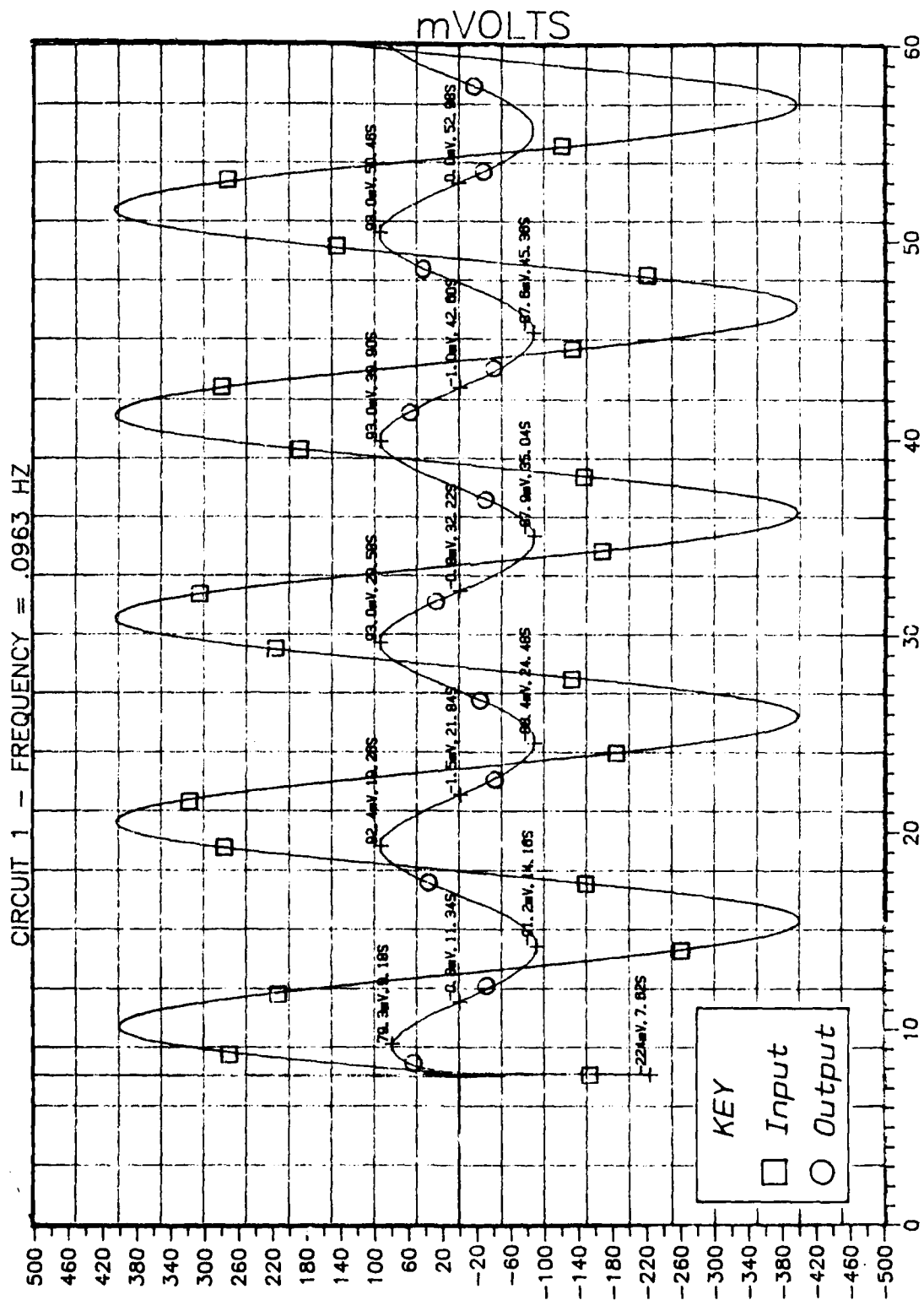


Figure 53. Circuit 1 Validation

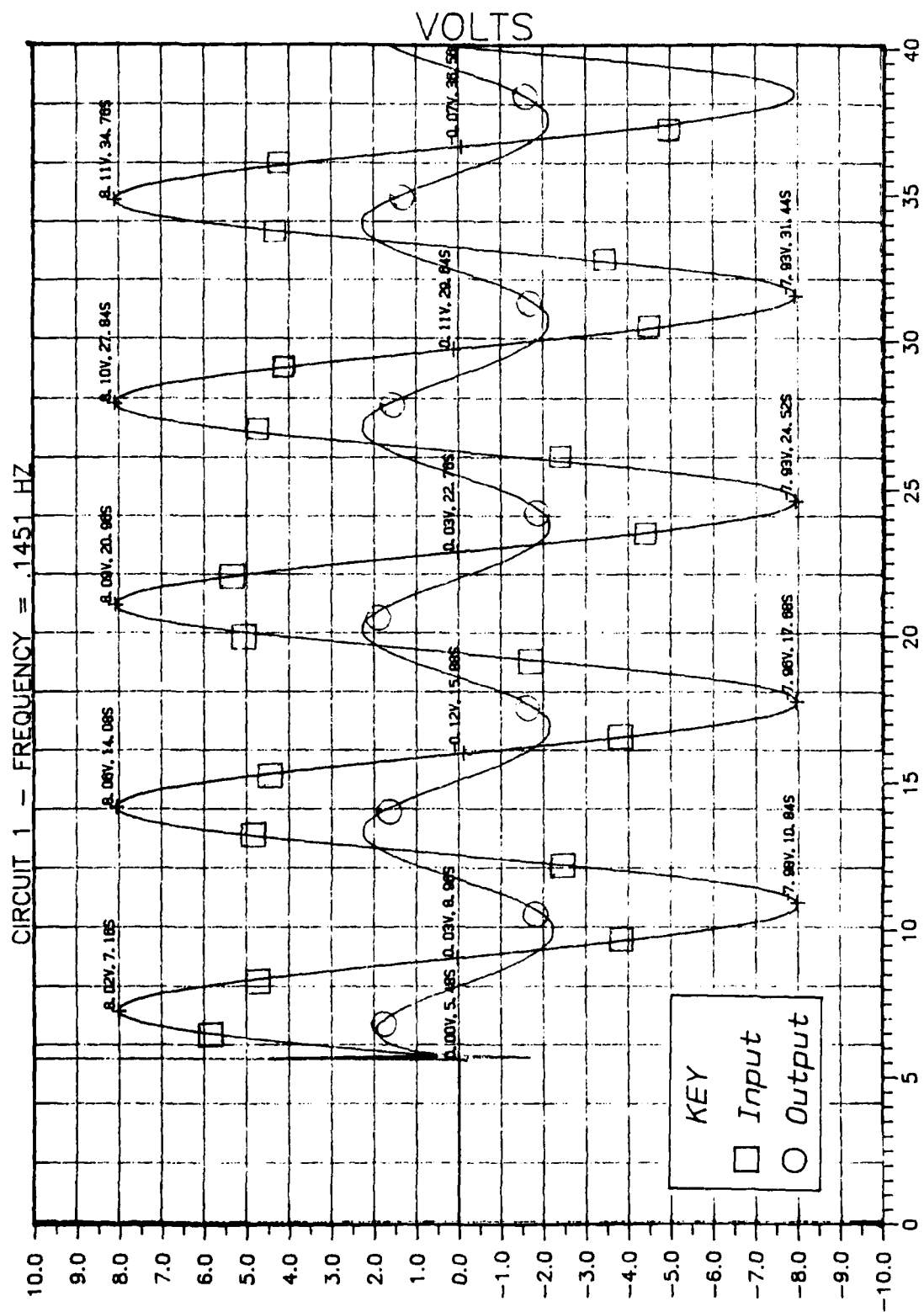


Figure 54. Circuit 1 Validation

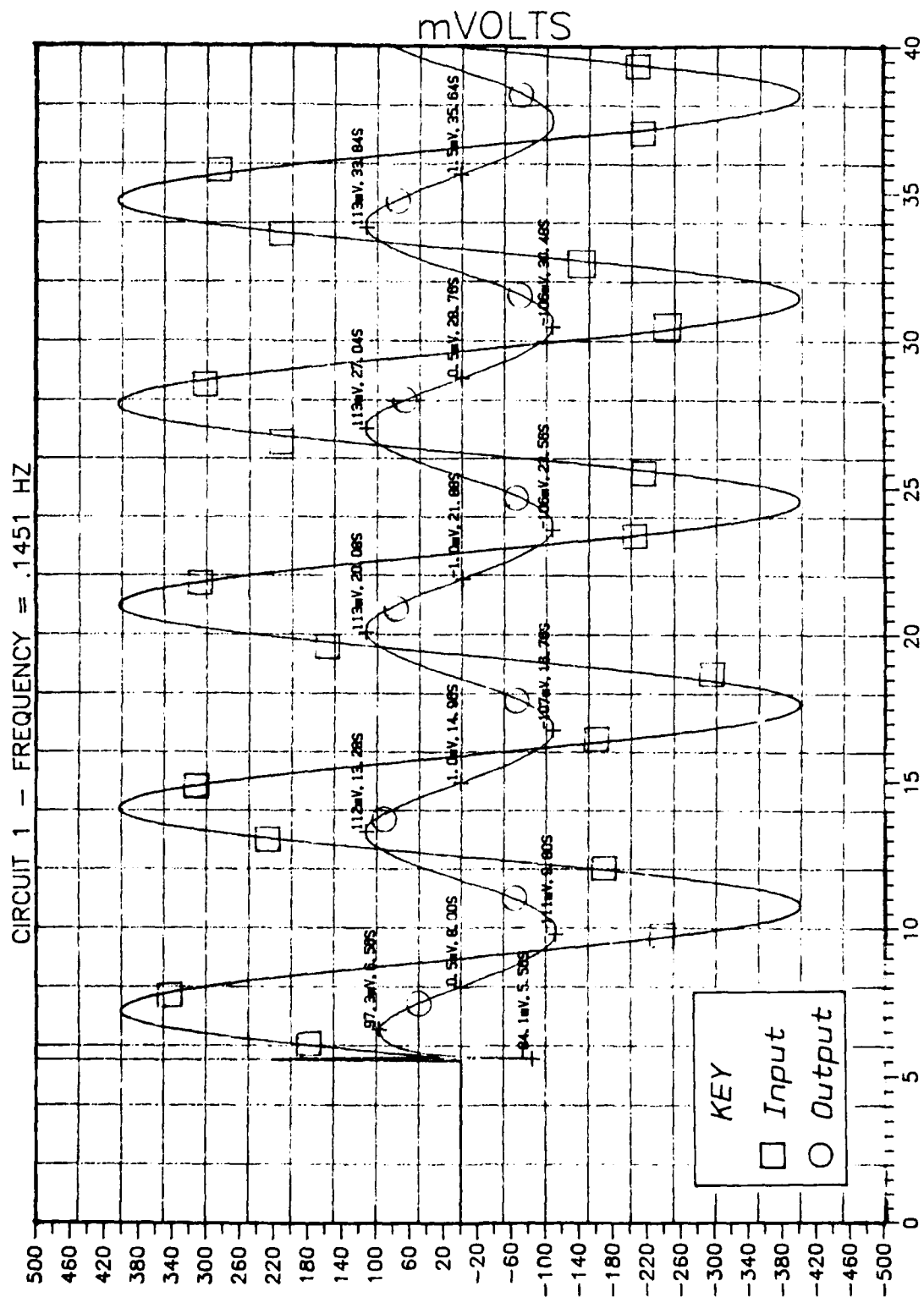


Figure 55. Circuit 1 Validation

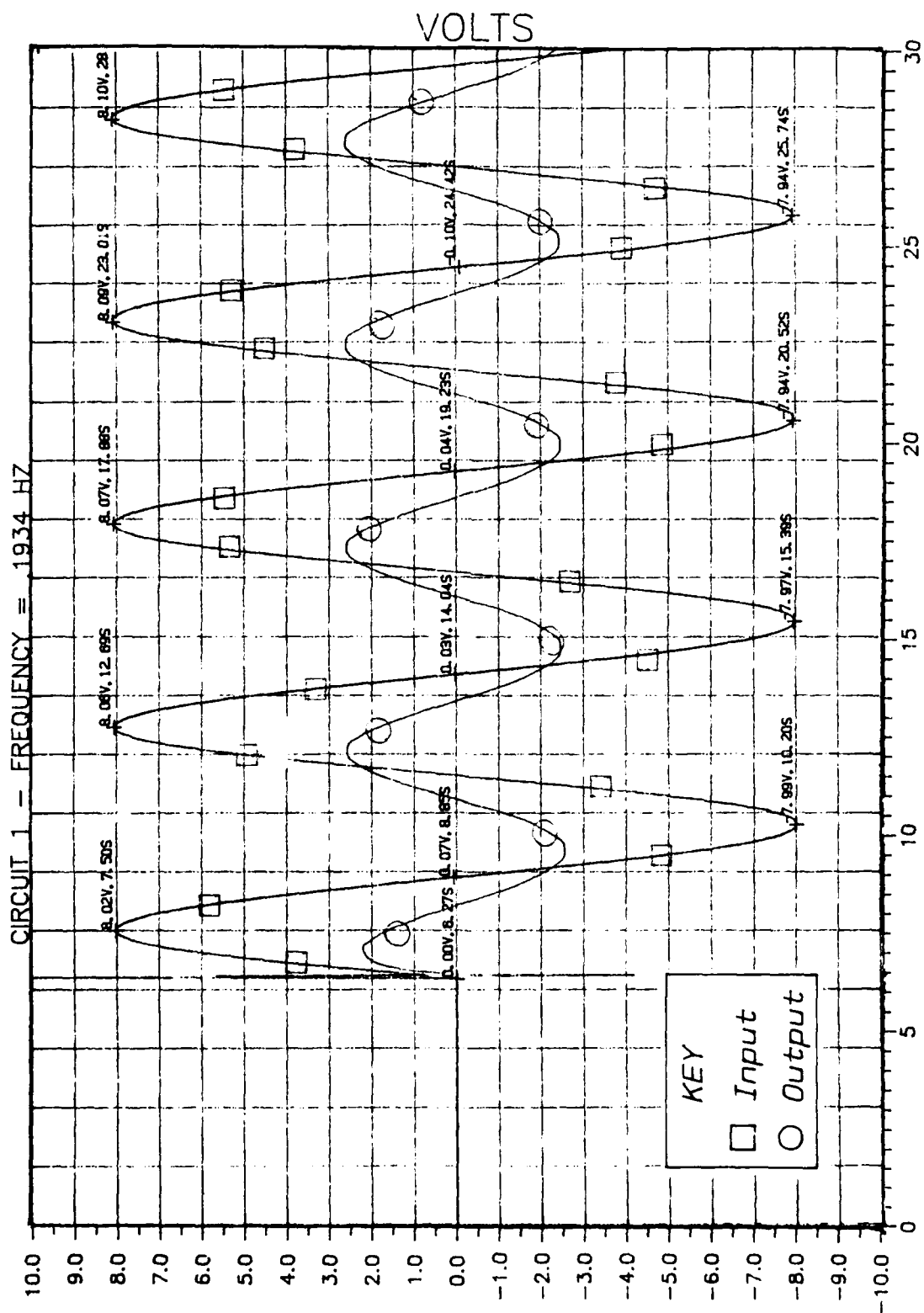


Figure 56. Circuit 1 Validation

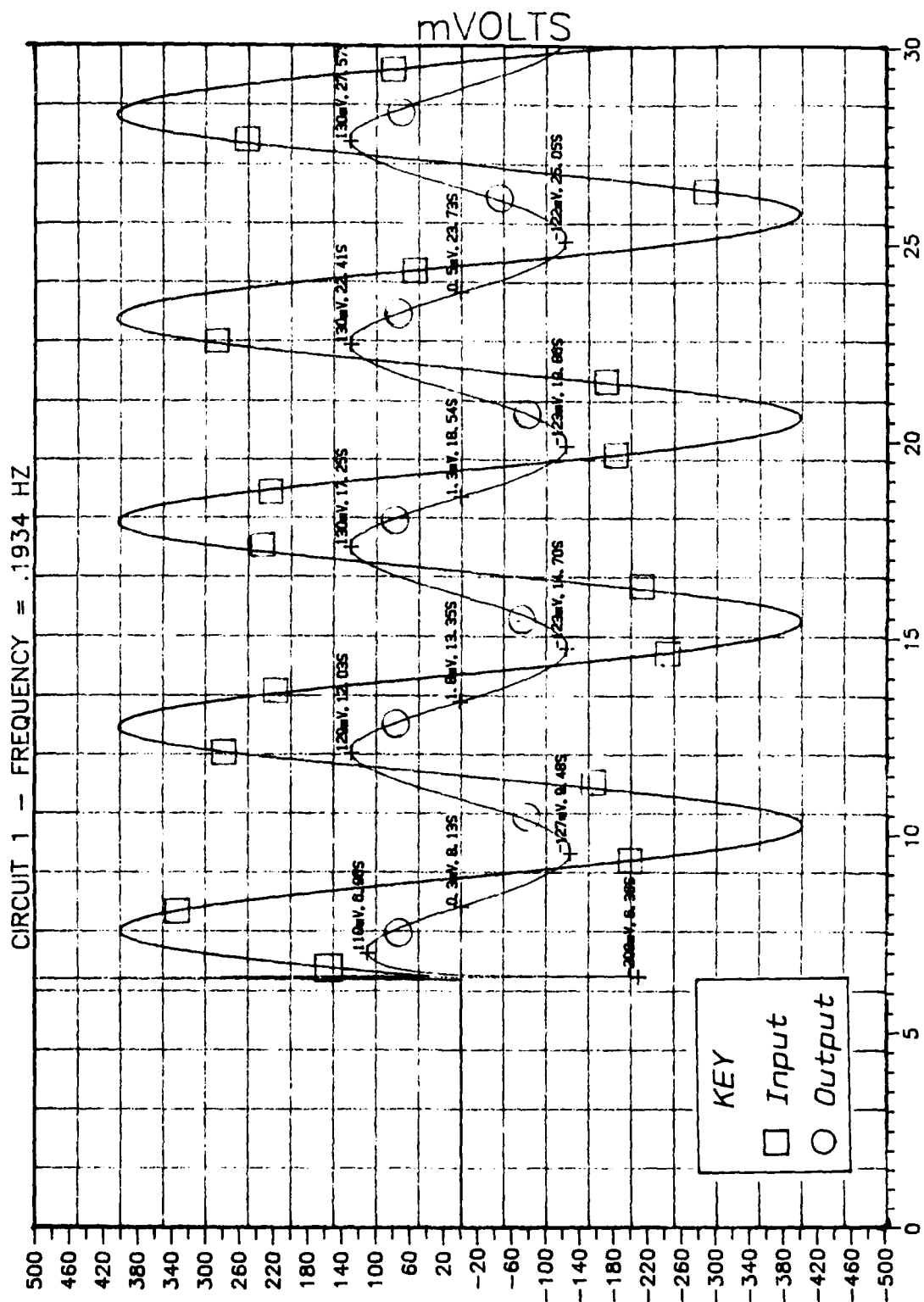


Figure 57. Circuit 1 Validation

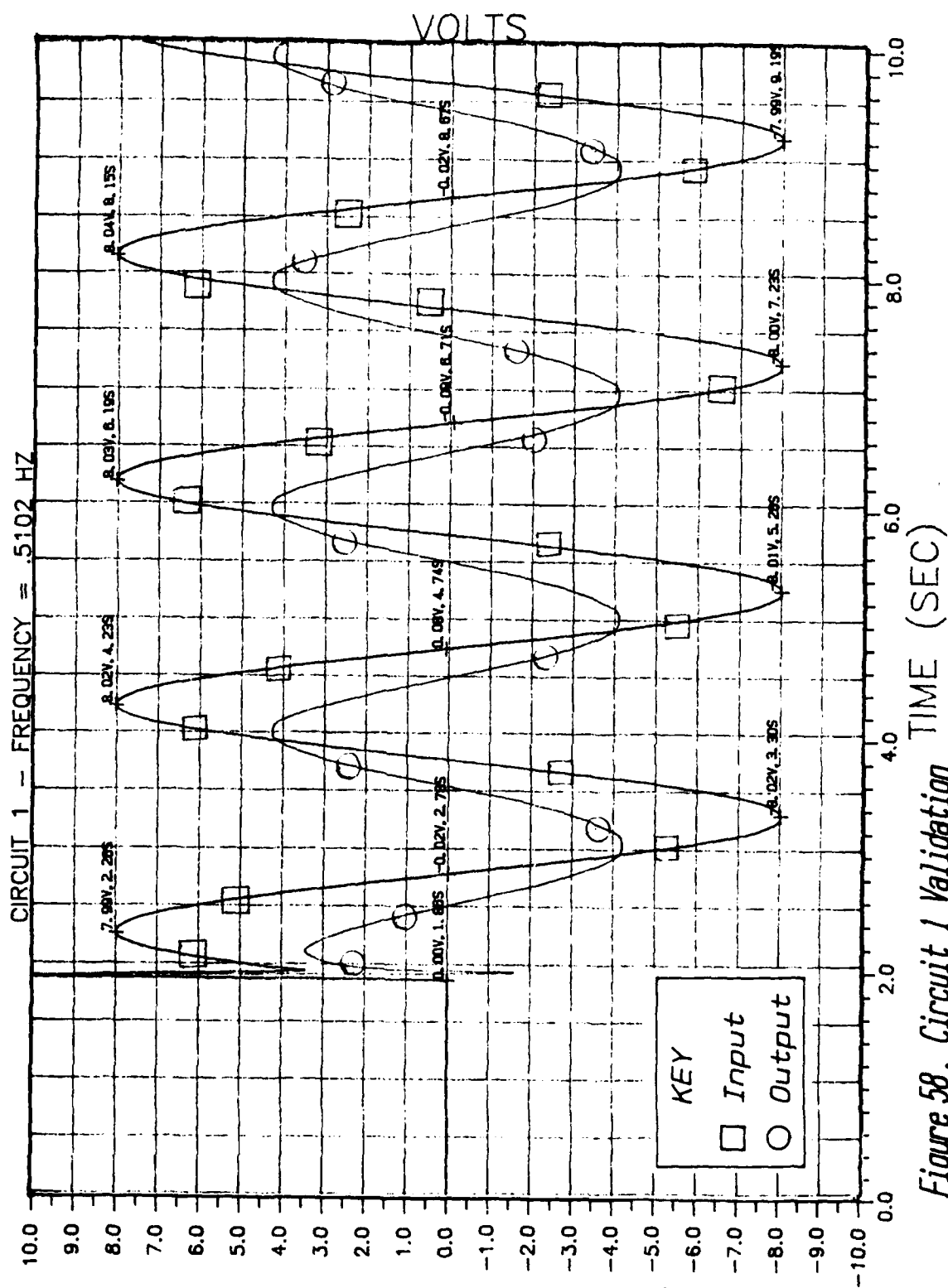


Figure 58. Circuit 1 Validation

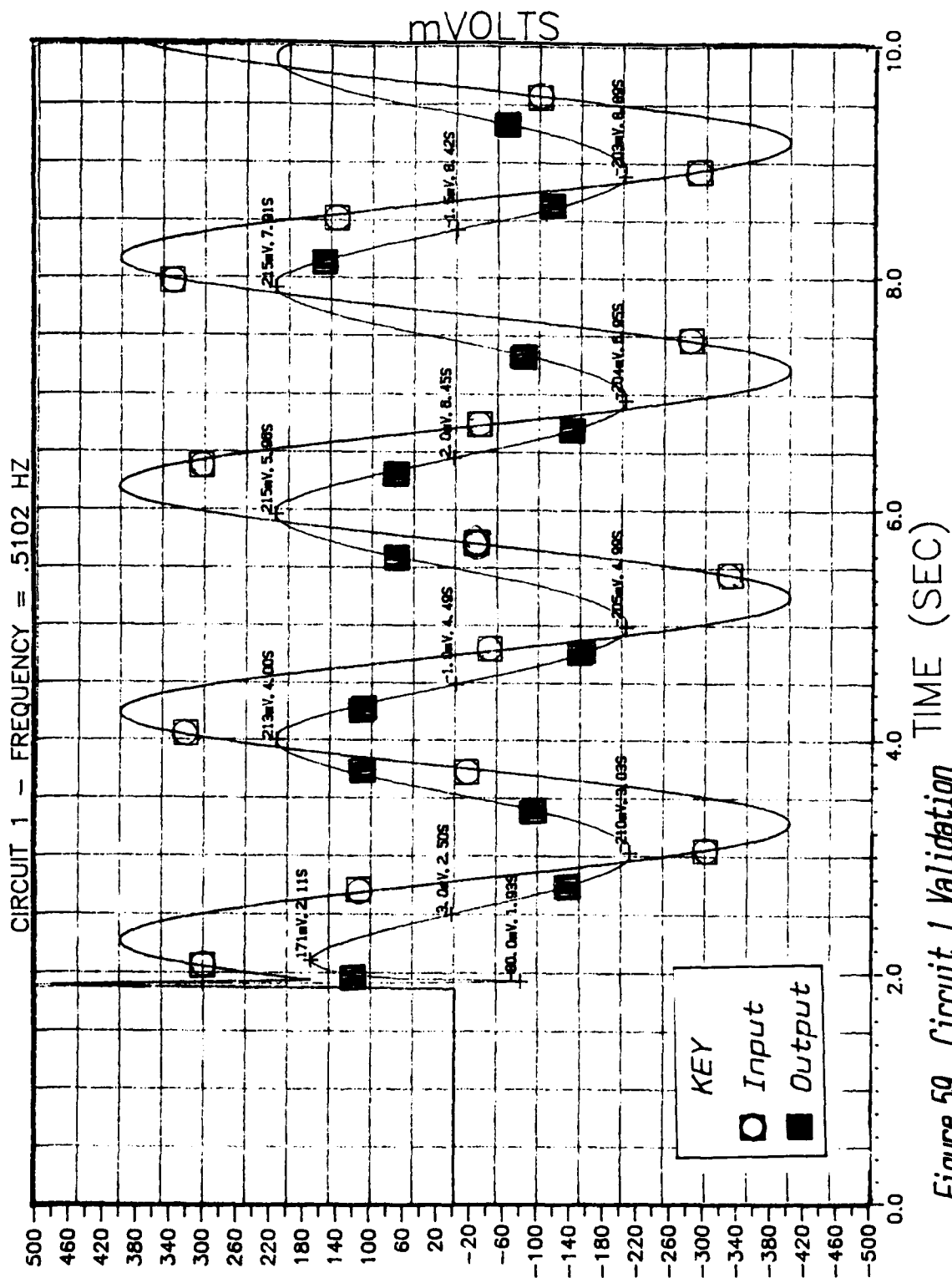


Figure 59. Circuit 1 Validation

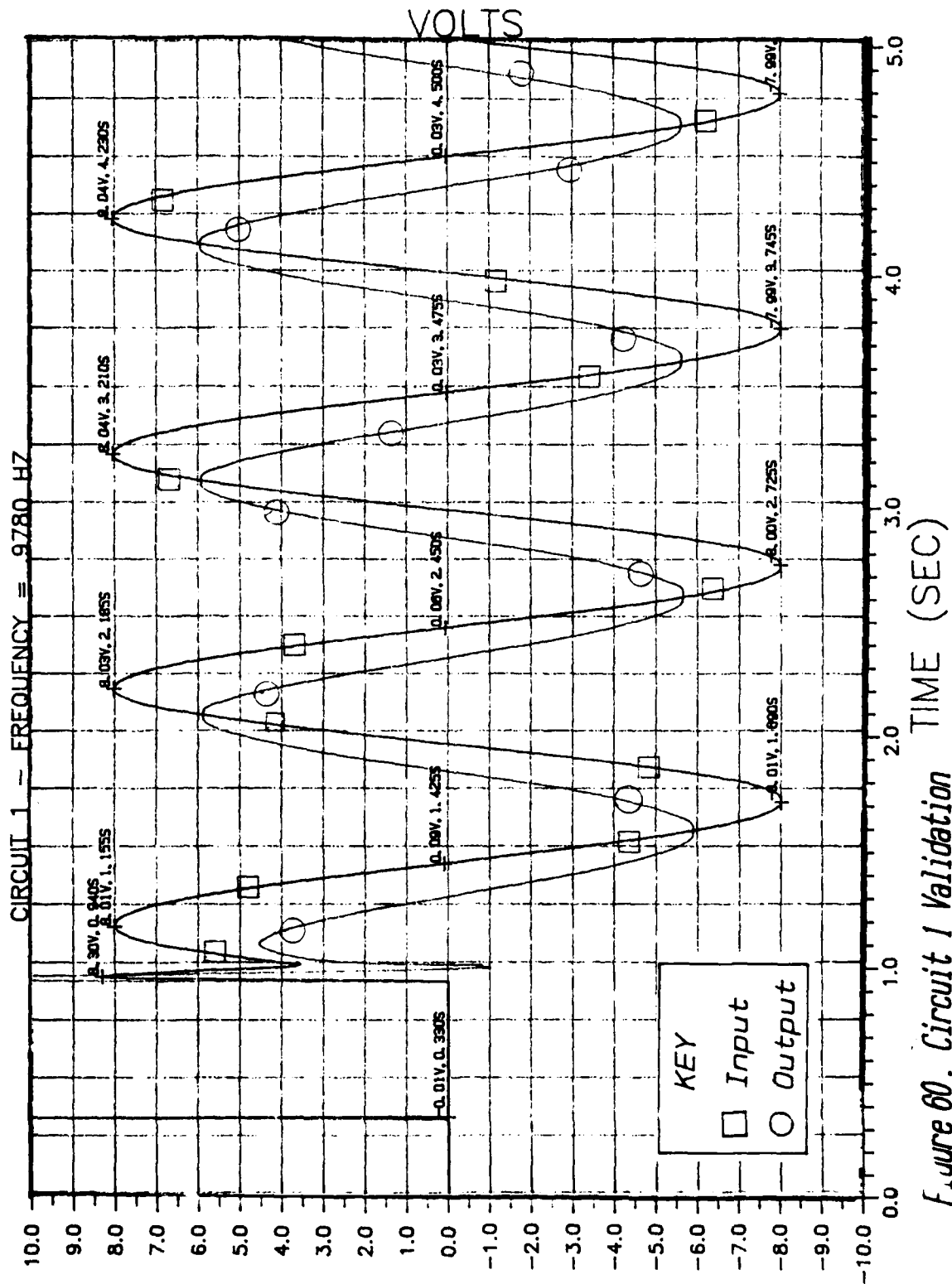
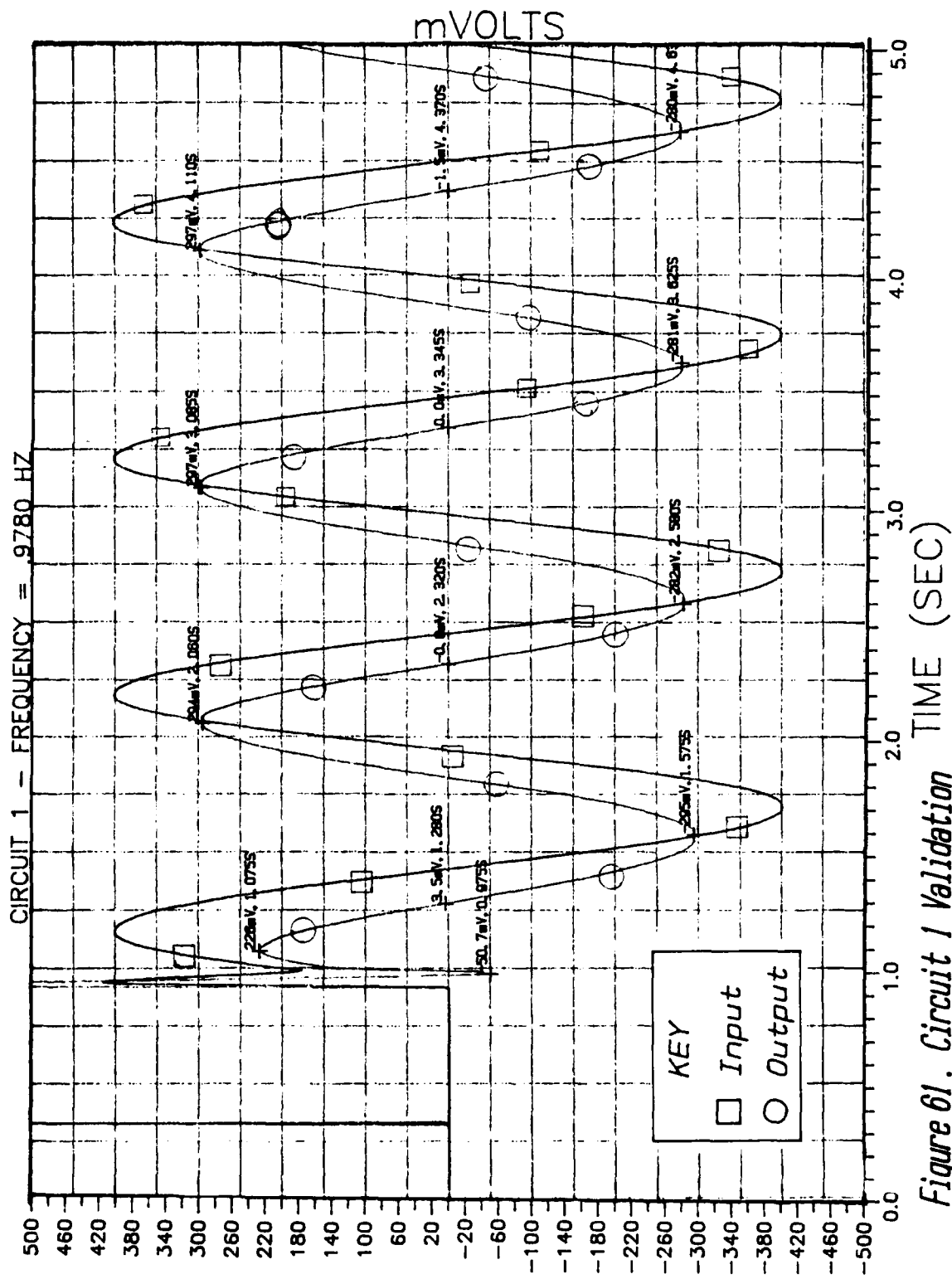


Figure 60. Circuit 1 Validation



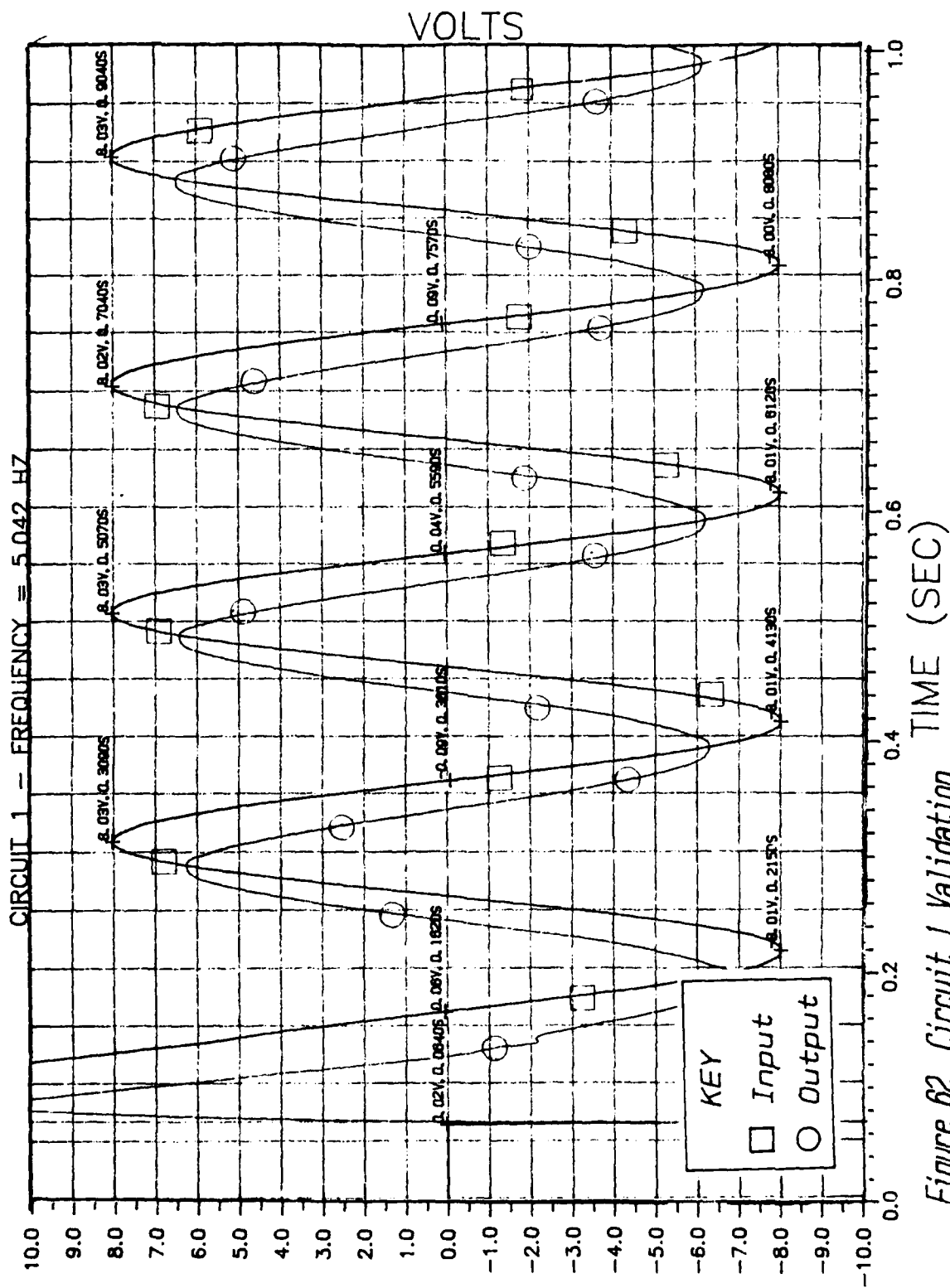


Figure 62. Circuit 1 Validation

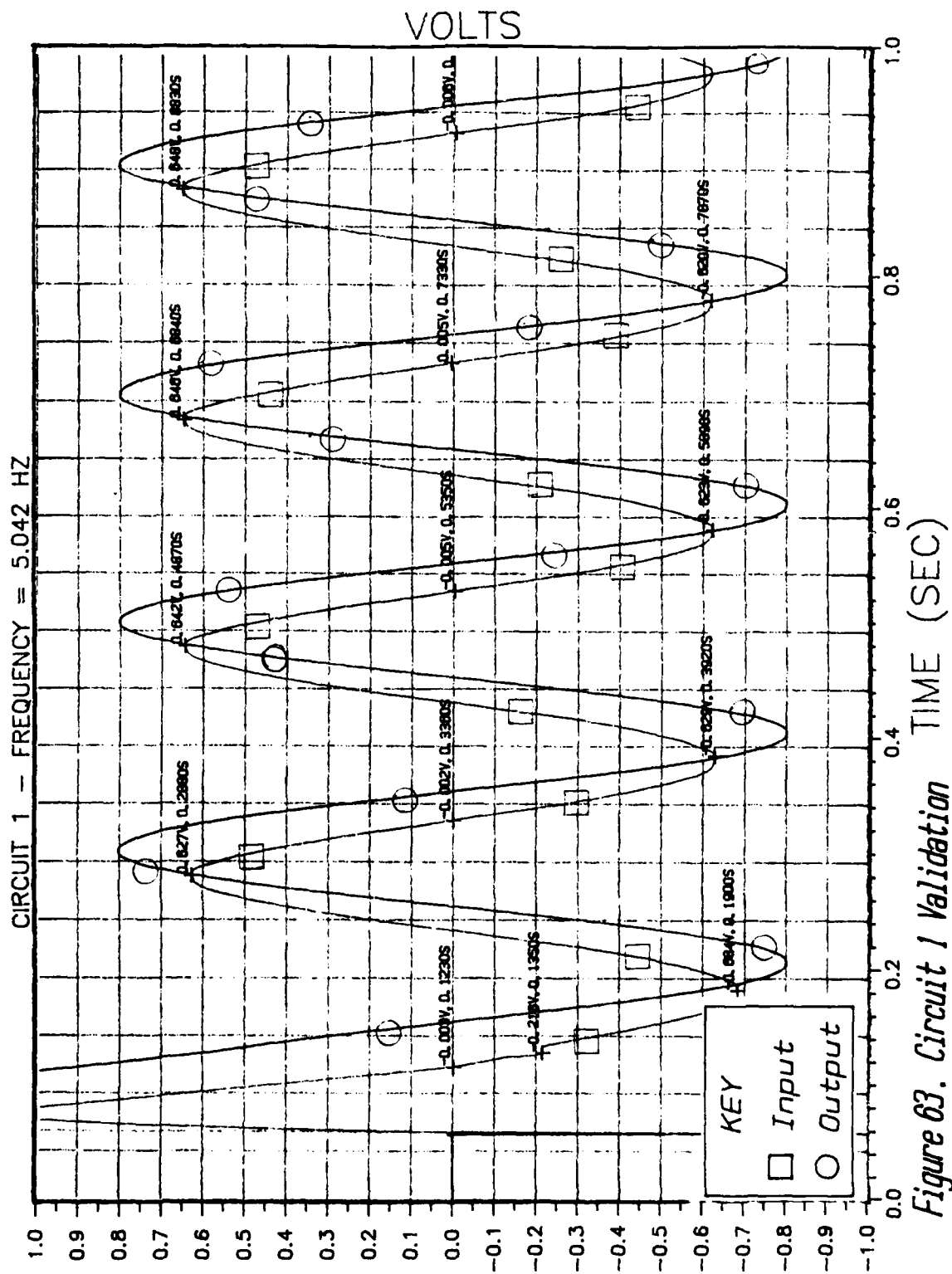


Figure 63. Circuit 1 Validation

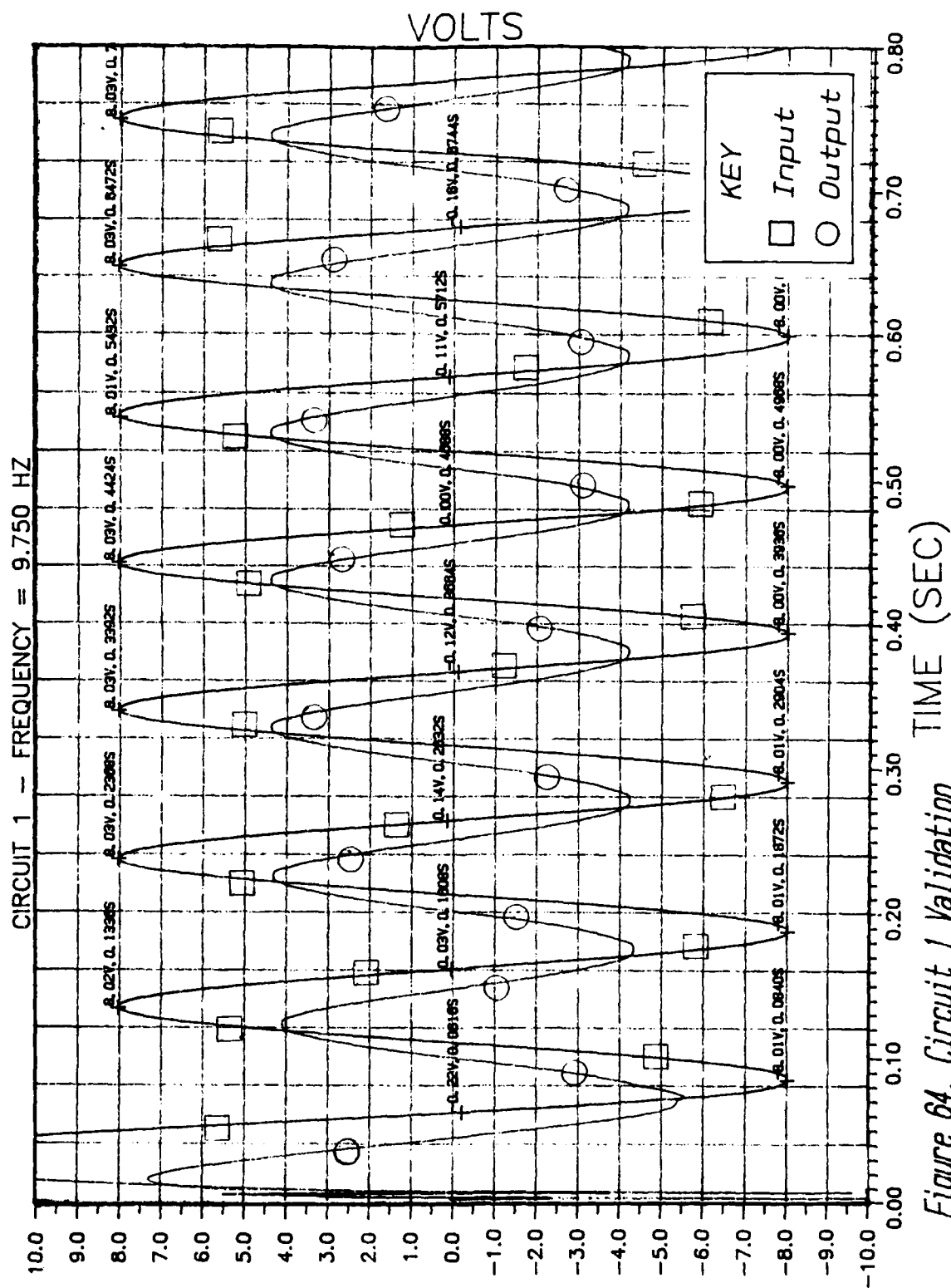


Figure 64. Circuit 1 Validation

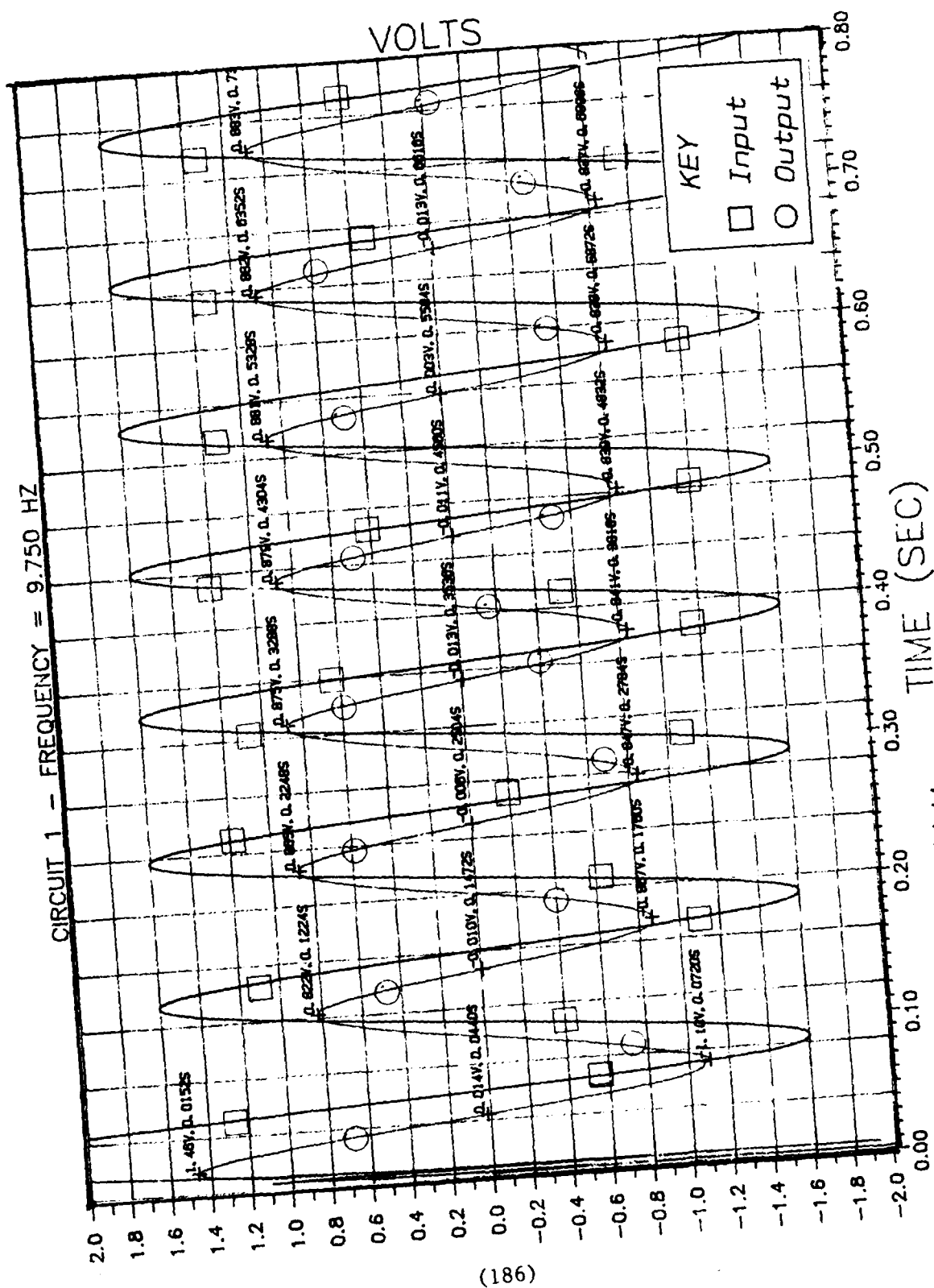


Figure 65. Circuit 2 Validation -

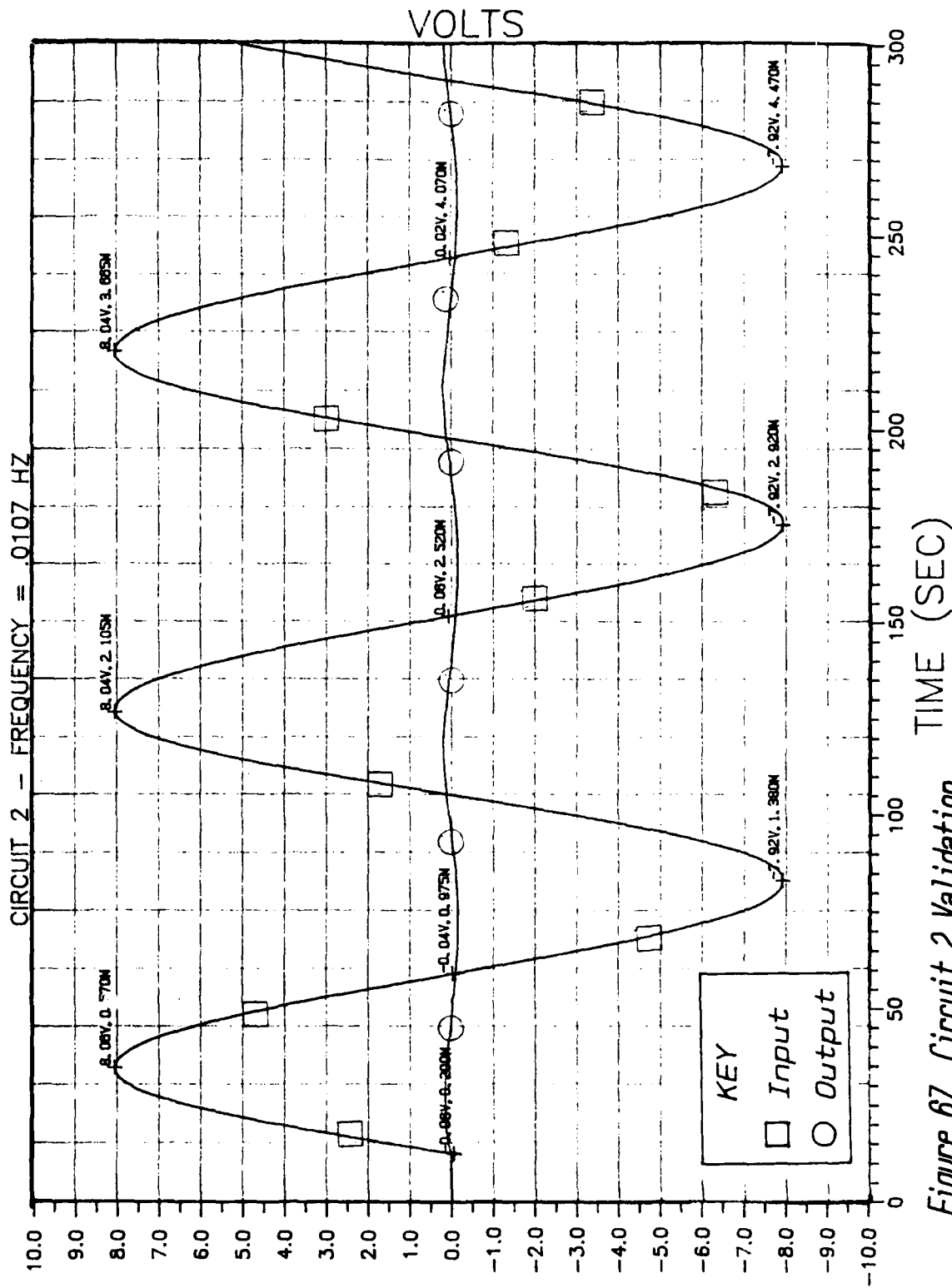


Figure 67. Circuit 2 Validation

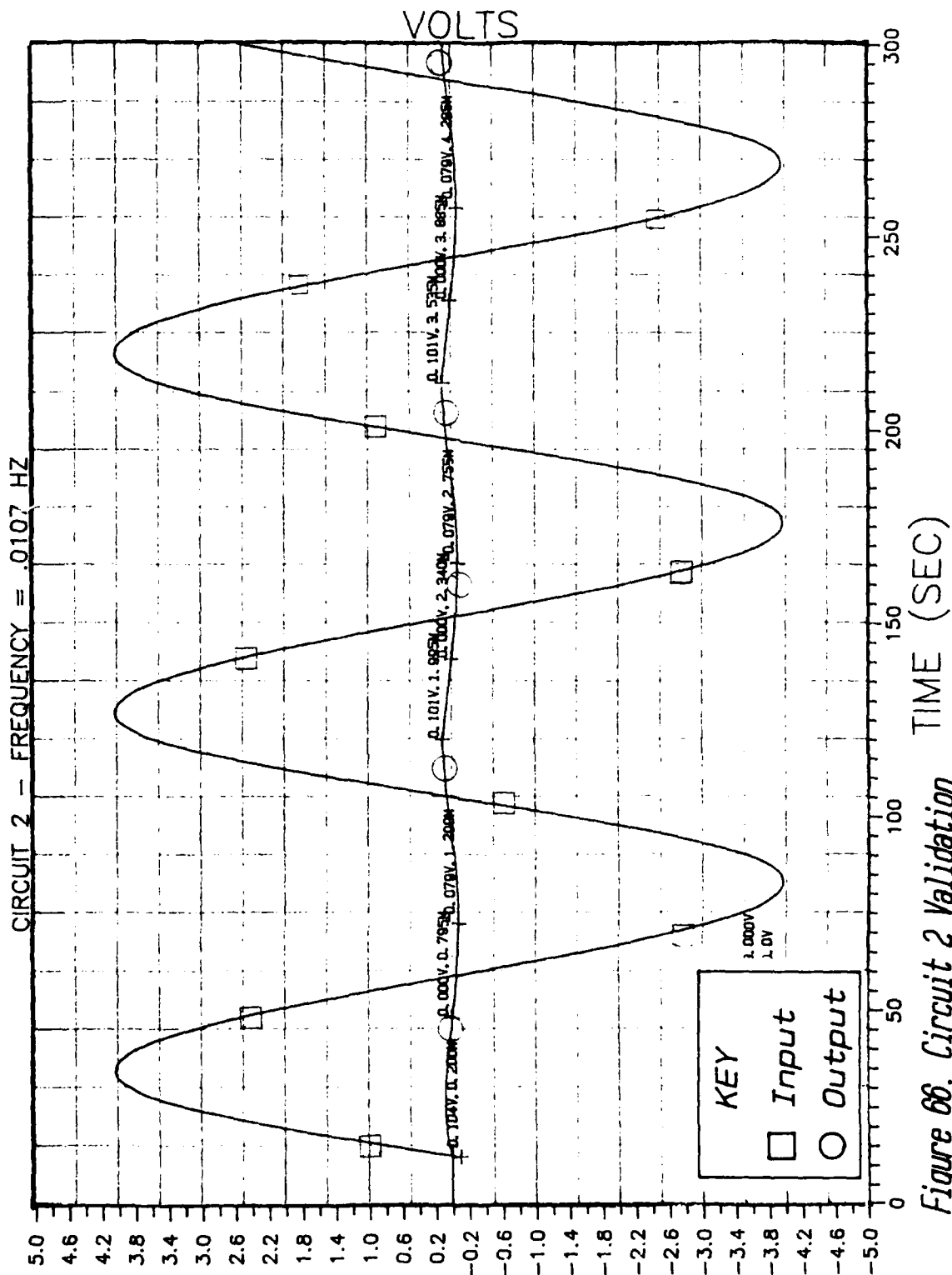


Figure 66. Circuit 2 Validation

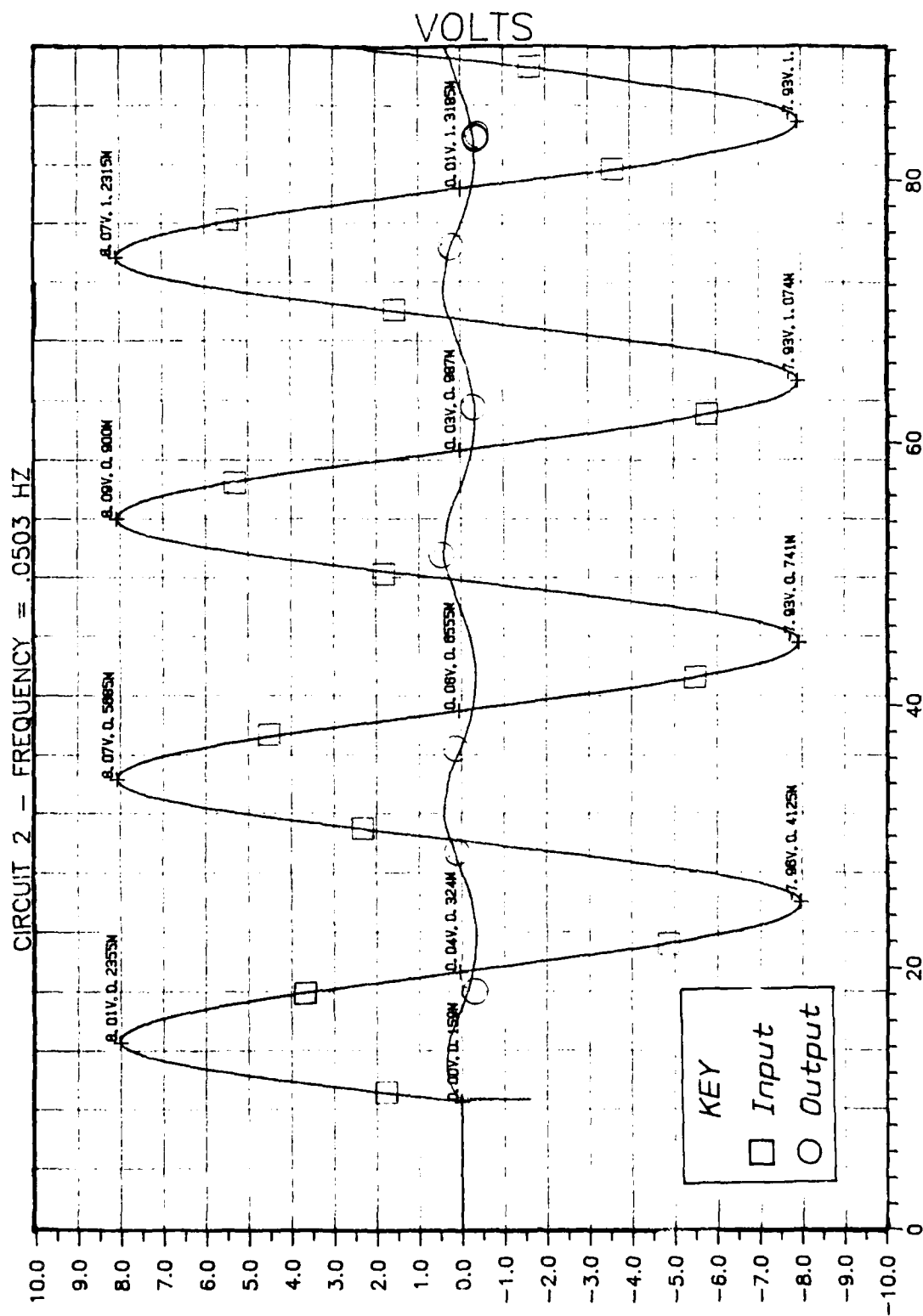


Figure 68. Circuit 2 Validation

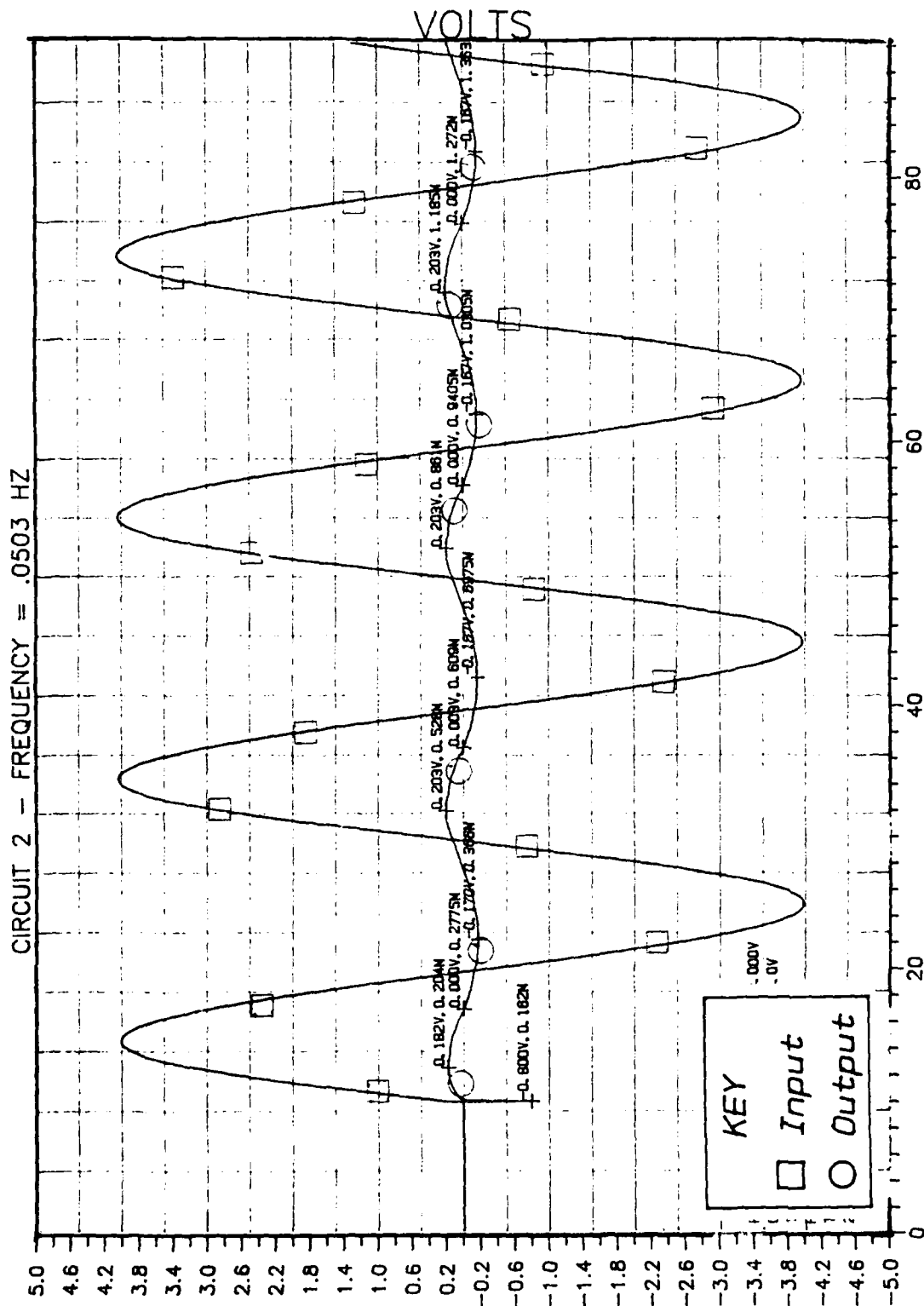


Figure 69. Circuit 2 Validation

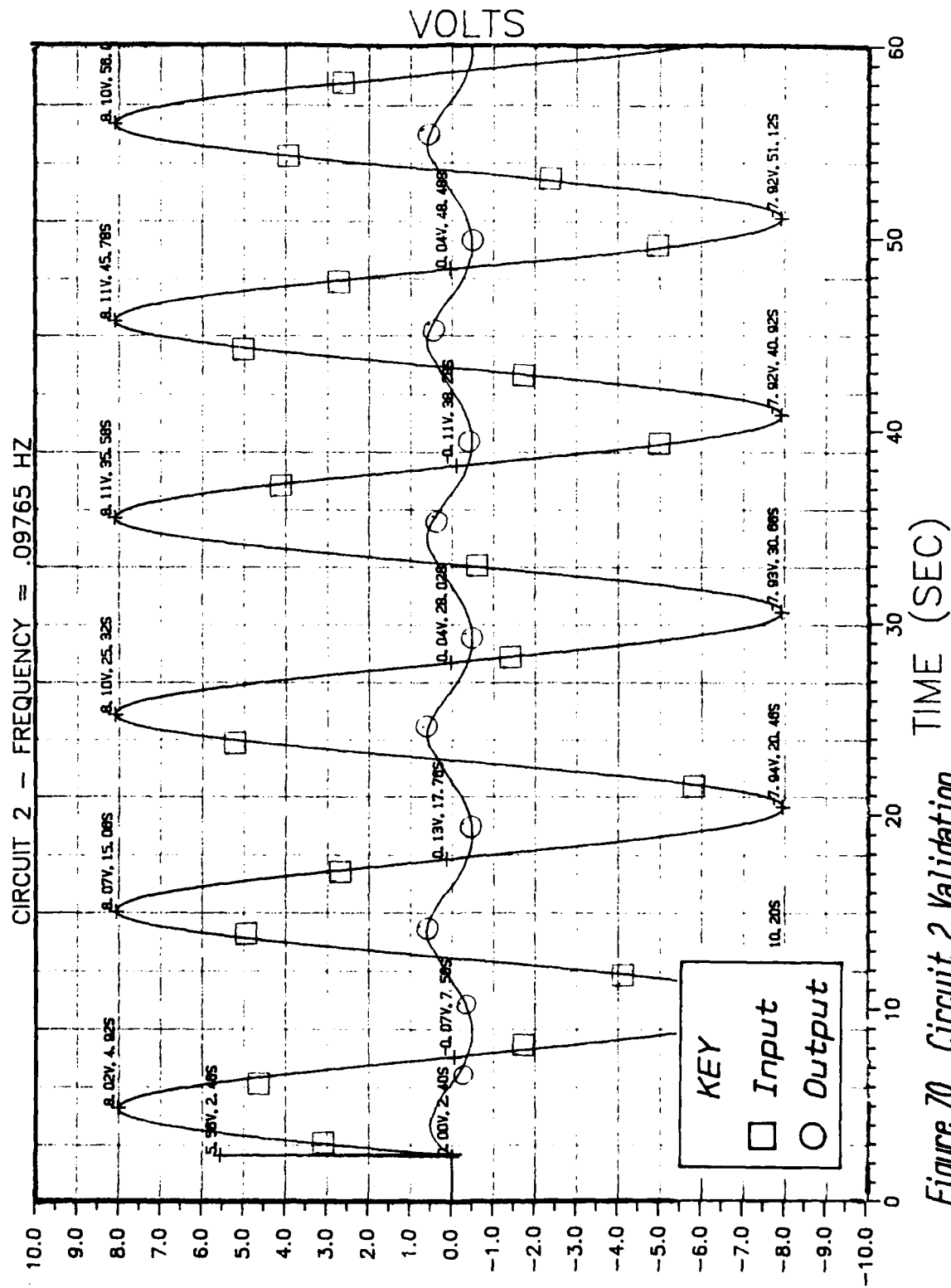


Figure 70. Circuit 2 Validation

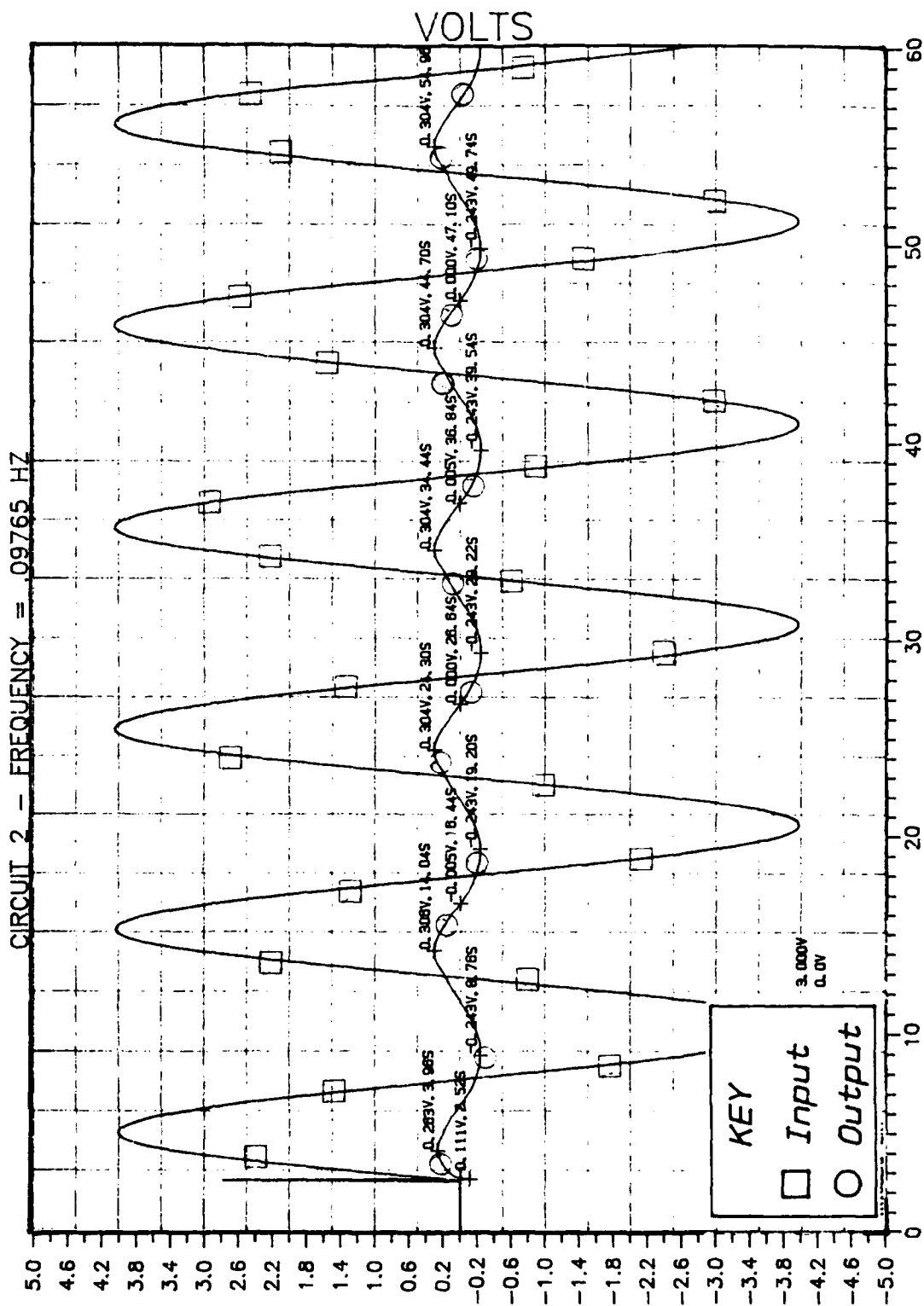
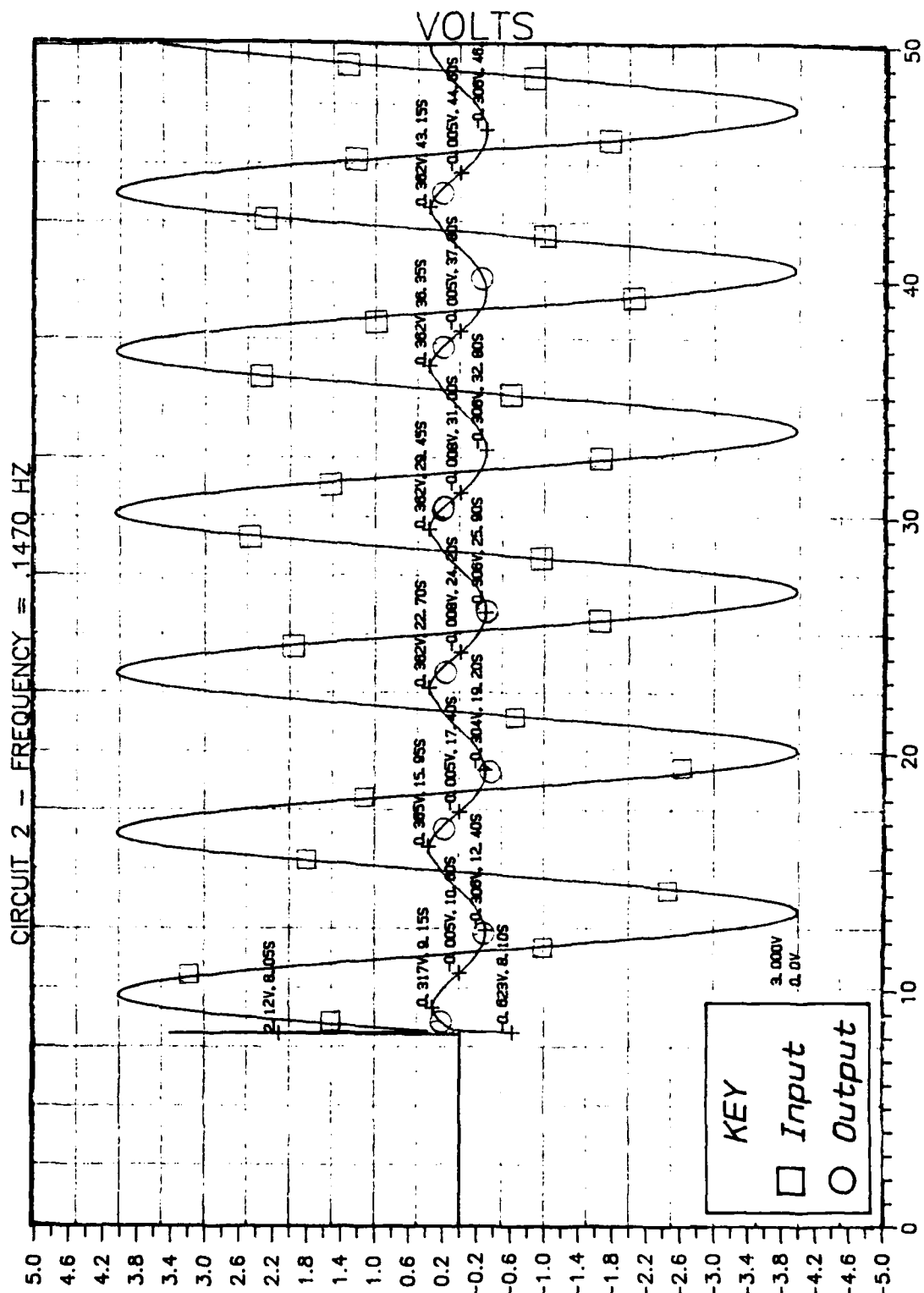


Figure 71. Circuit 2 Validation



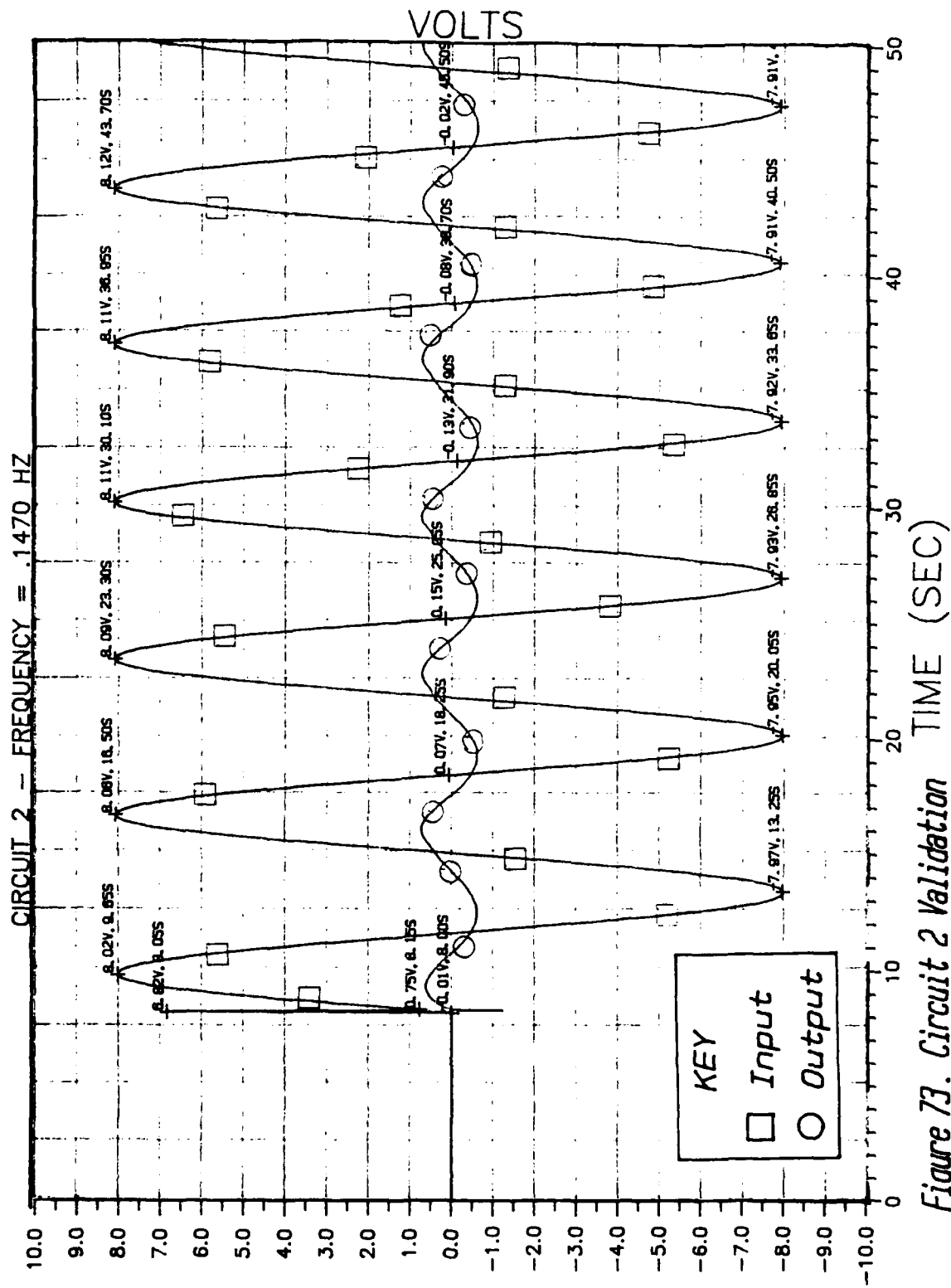


Figure 73. Circuit 2 Validation

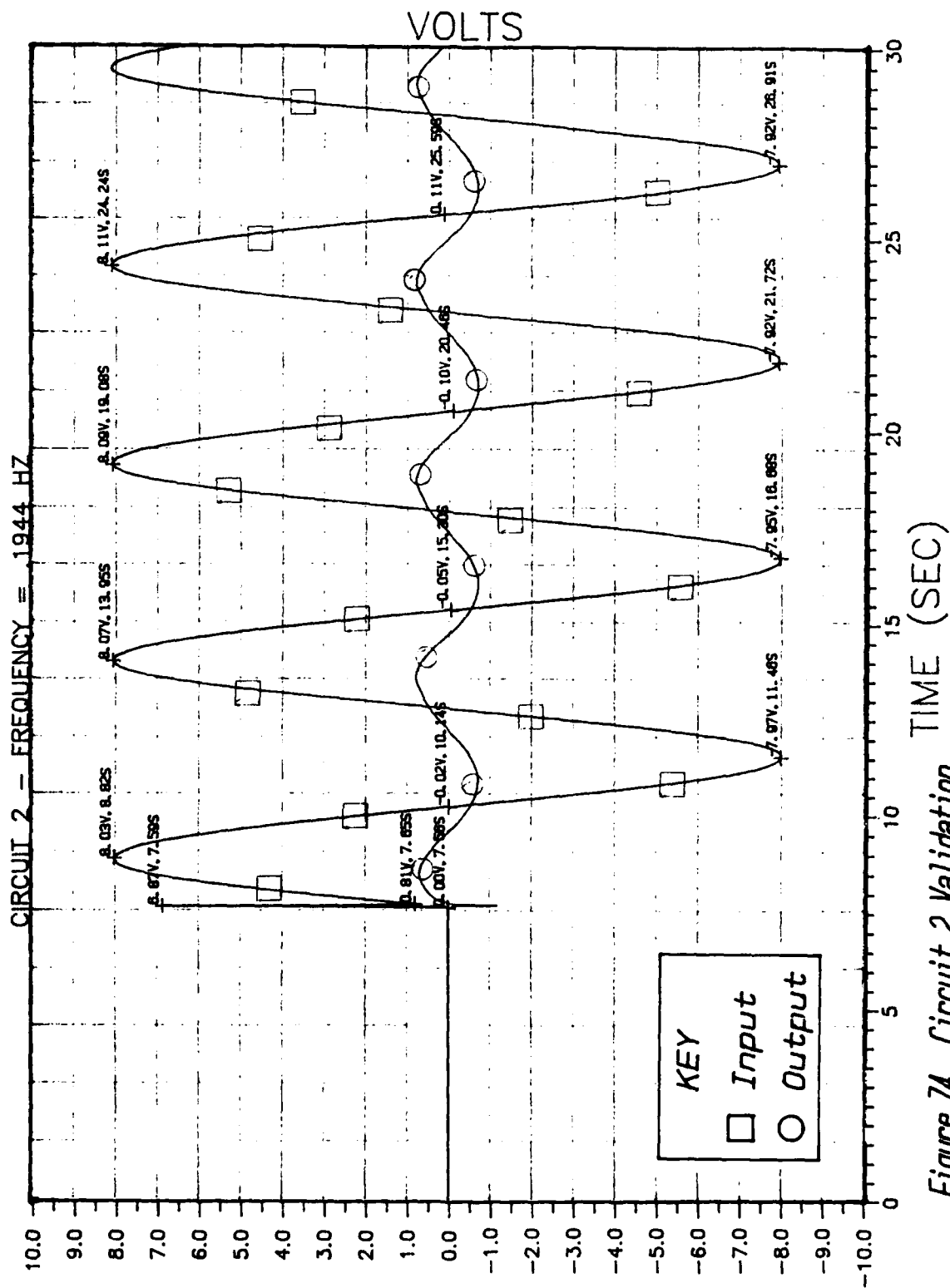


Figure 74. Circuit 2 Validation

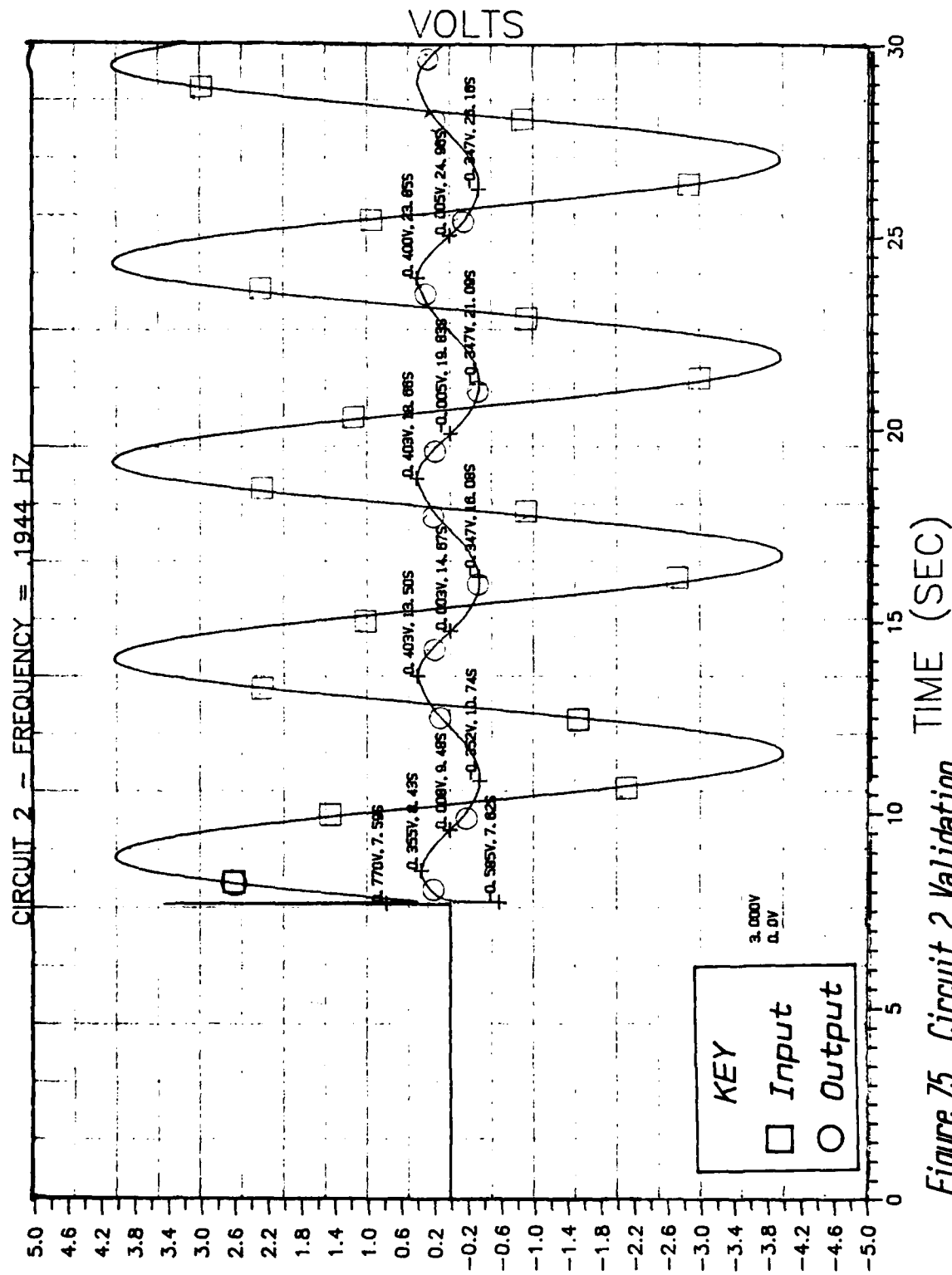


Figure 75. Circuit 2 Validation

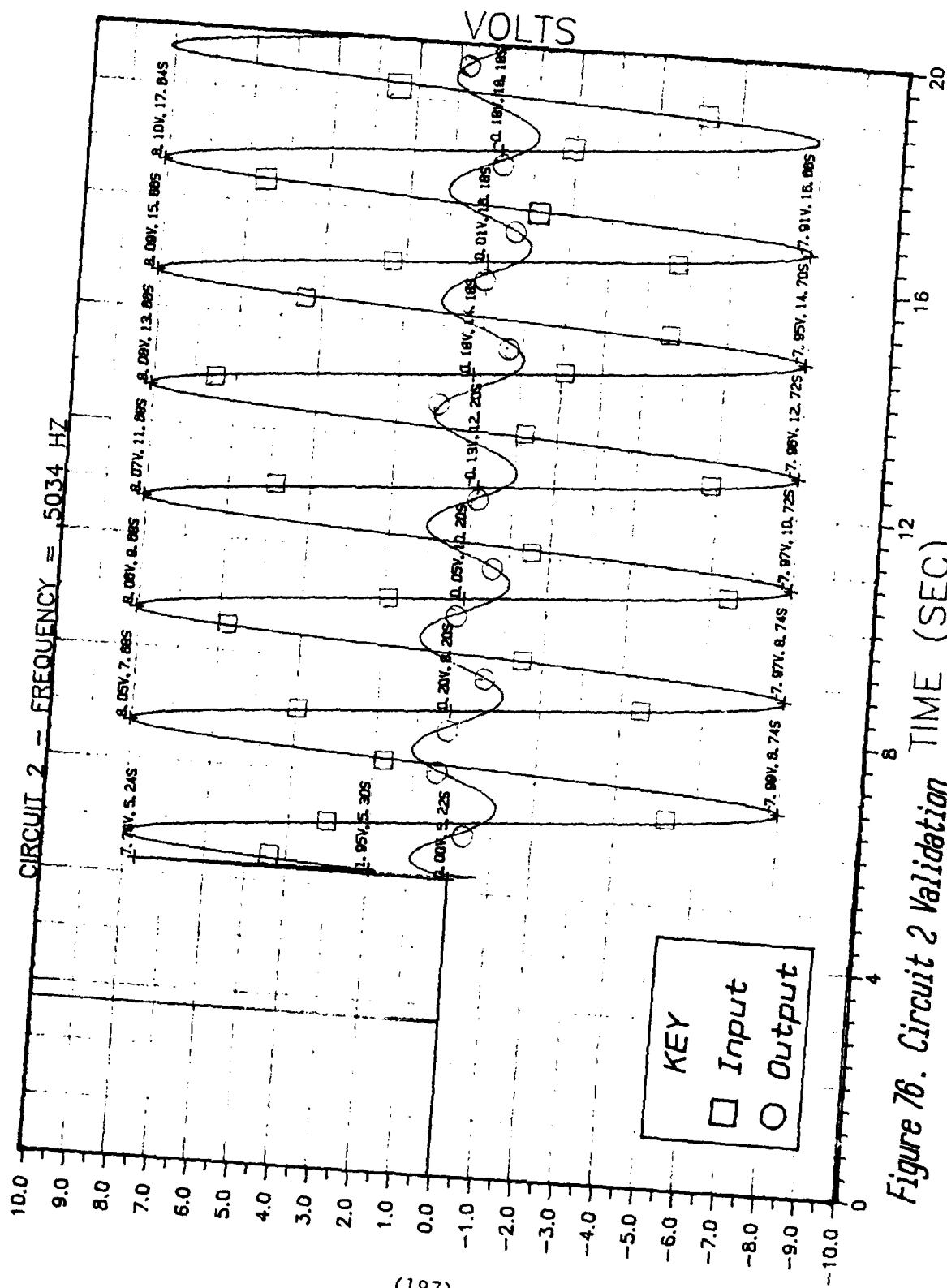


Figure 76. Circuit 2 Validation



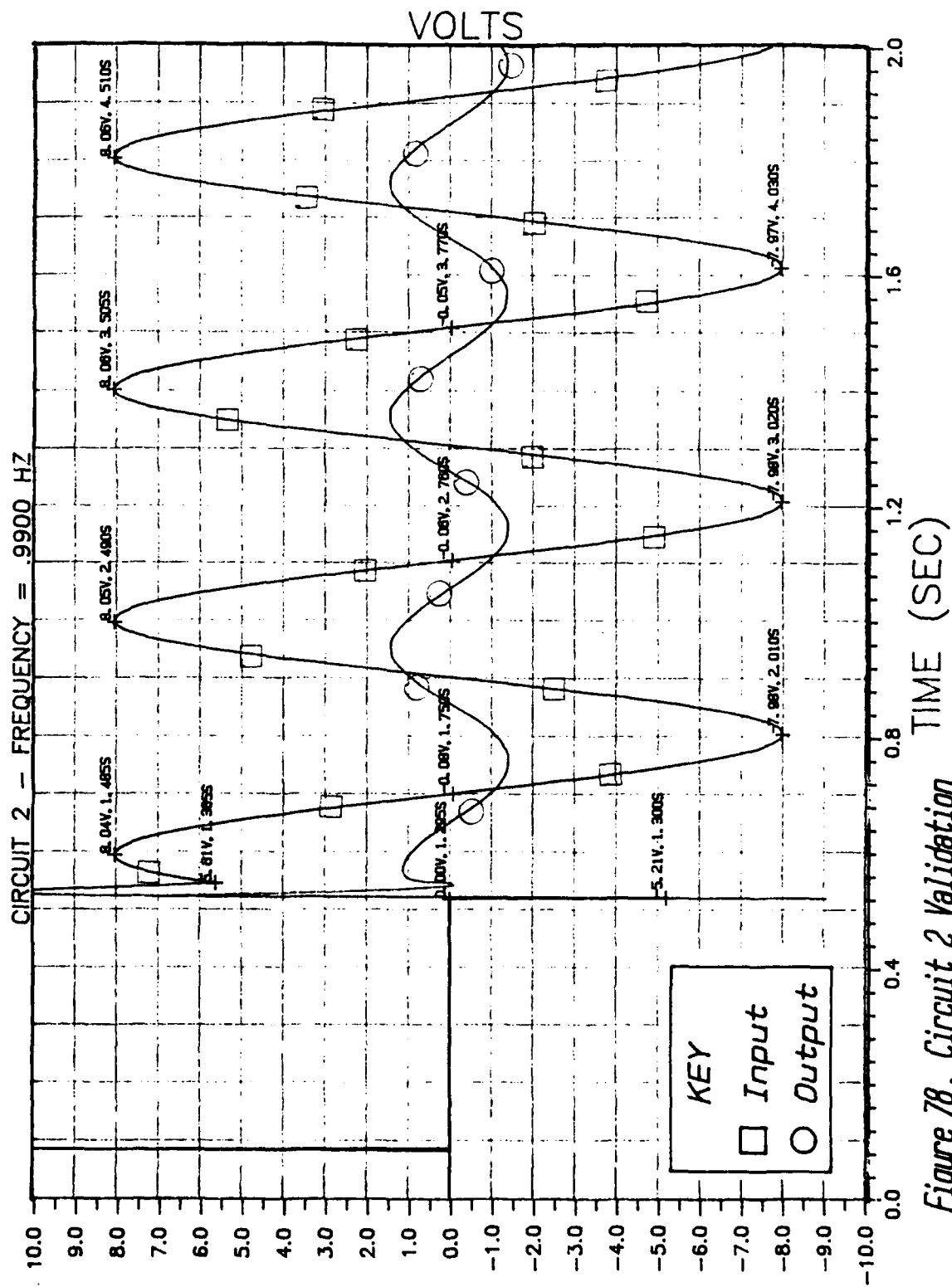


Figure 78. Circuit 2 Validation

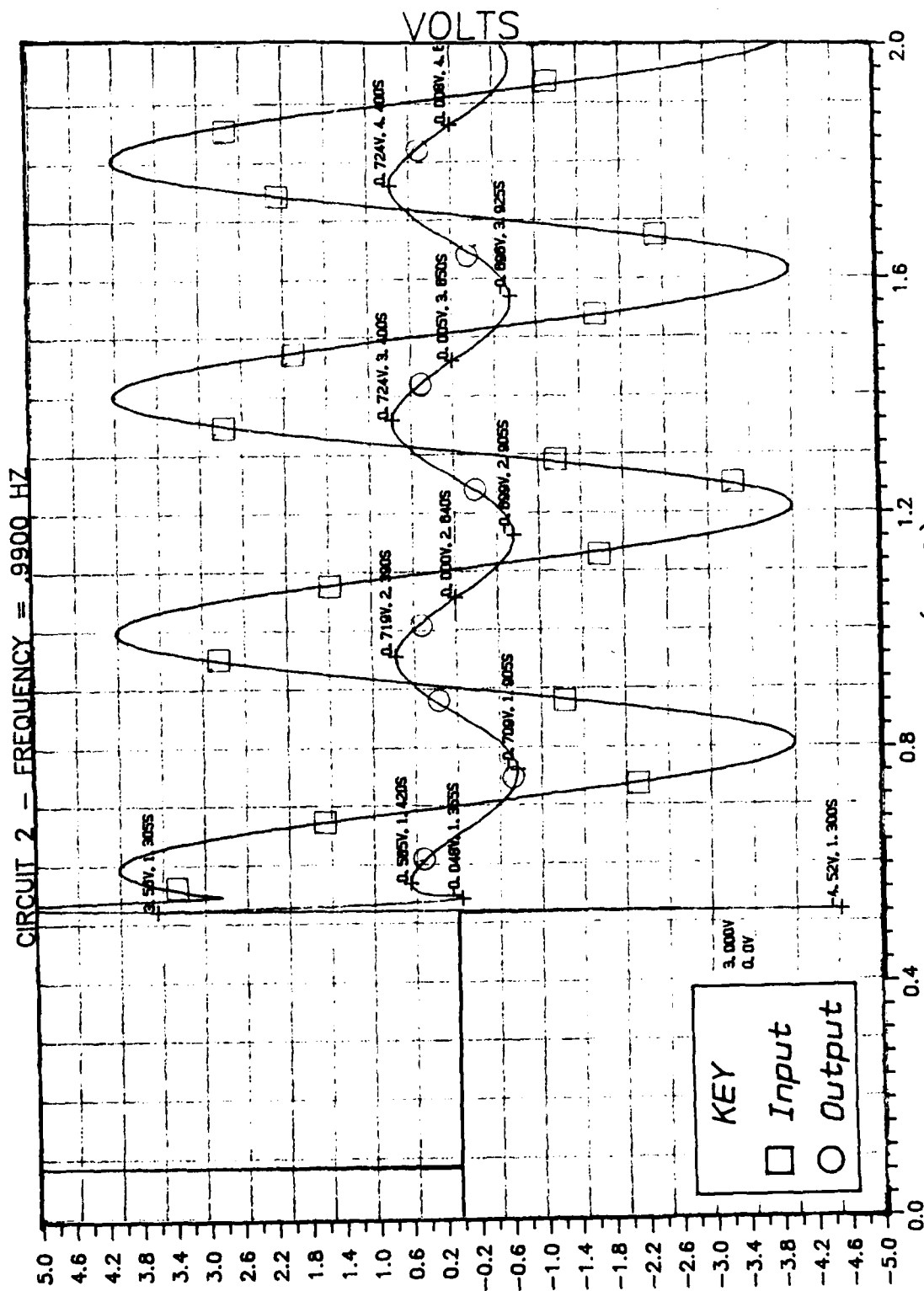


Figure 79. Circuit 2 Validation

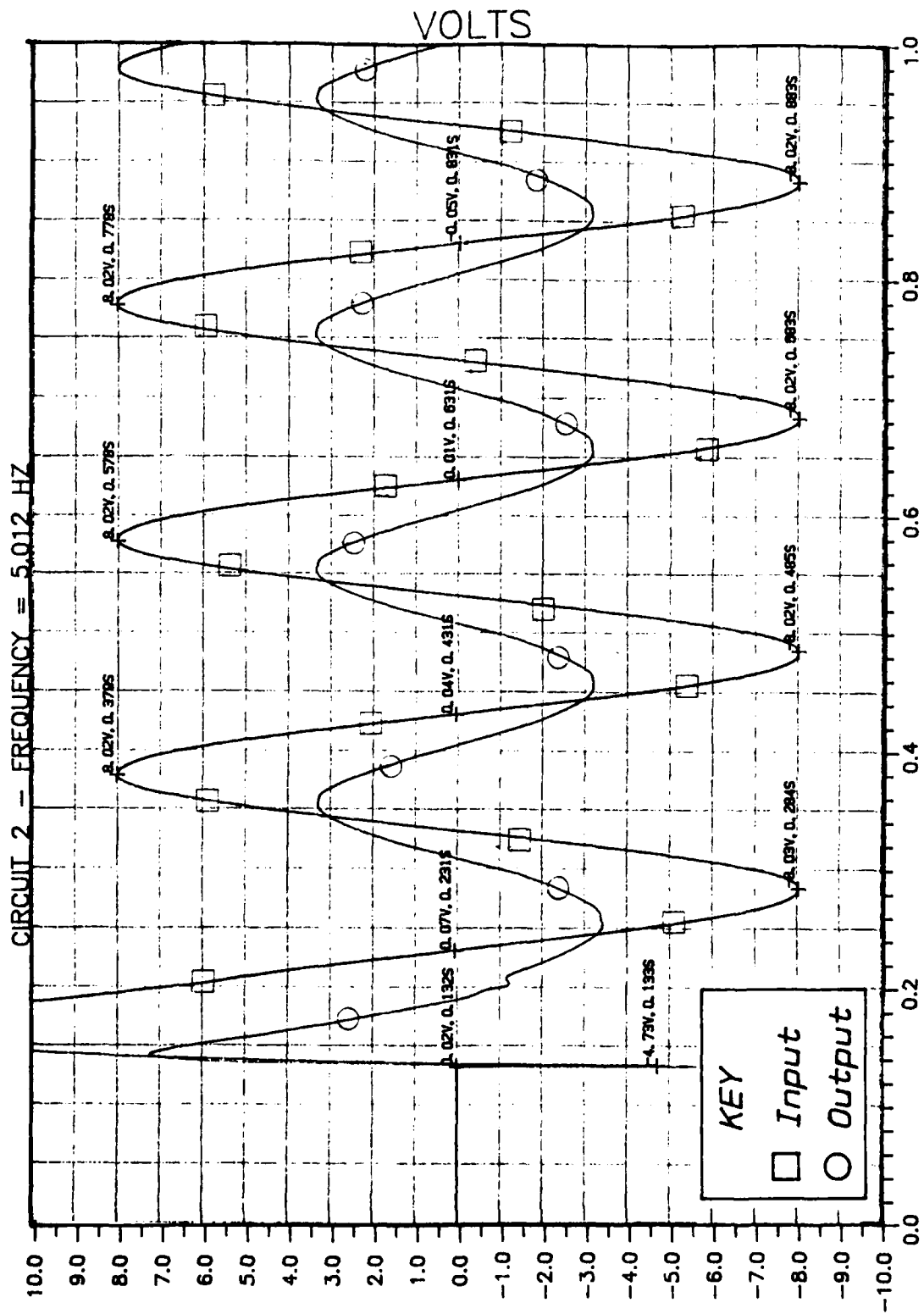


Figure 80. Circuit 2 Validation

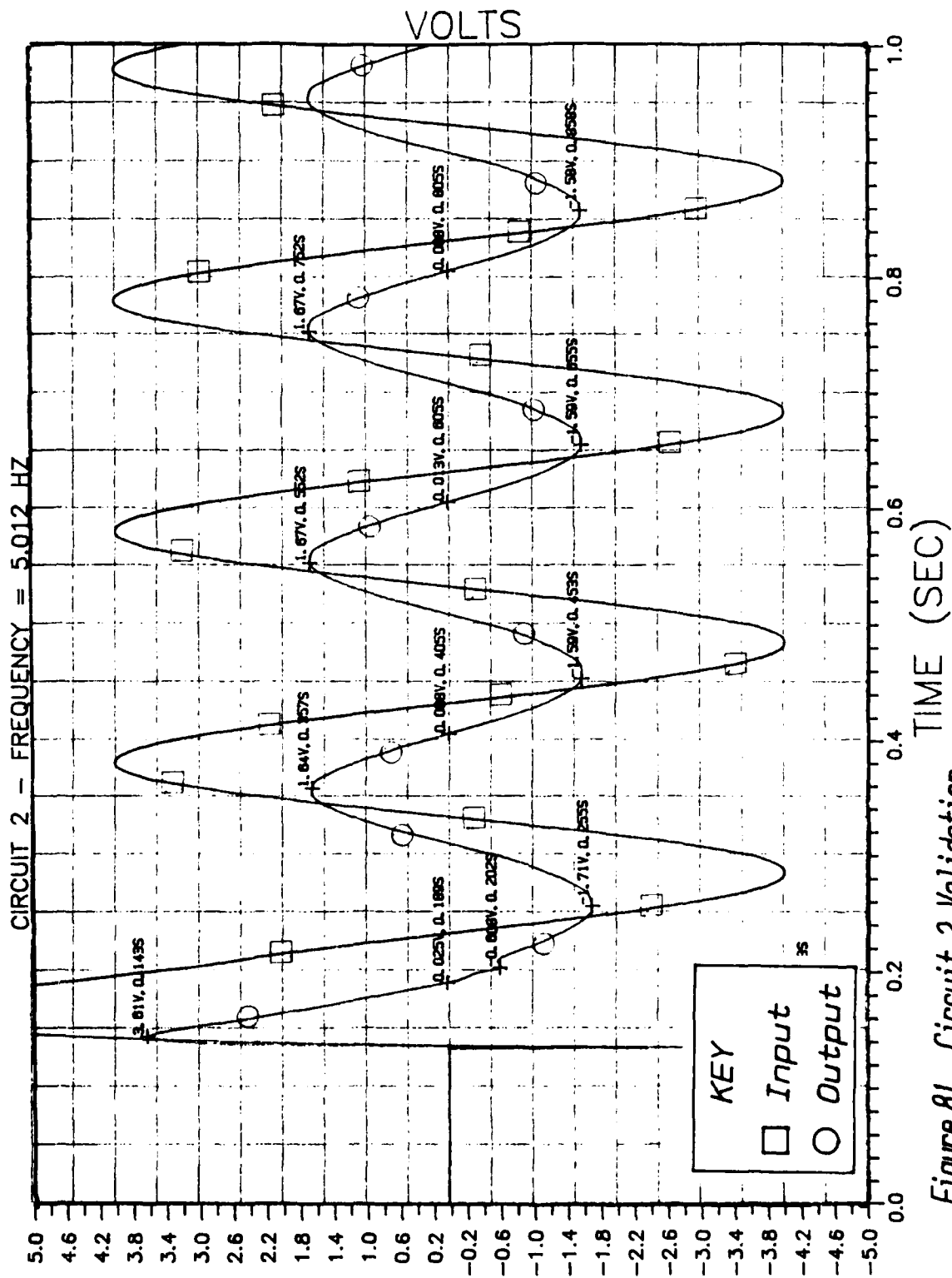


Figure 81. Circuit 2 Validation

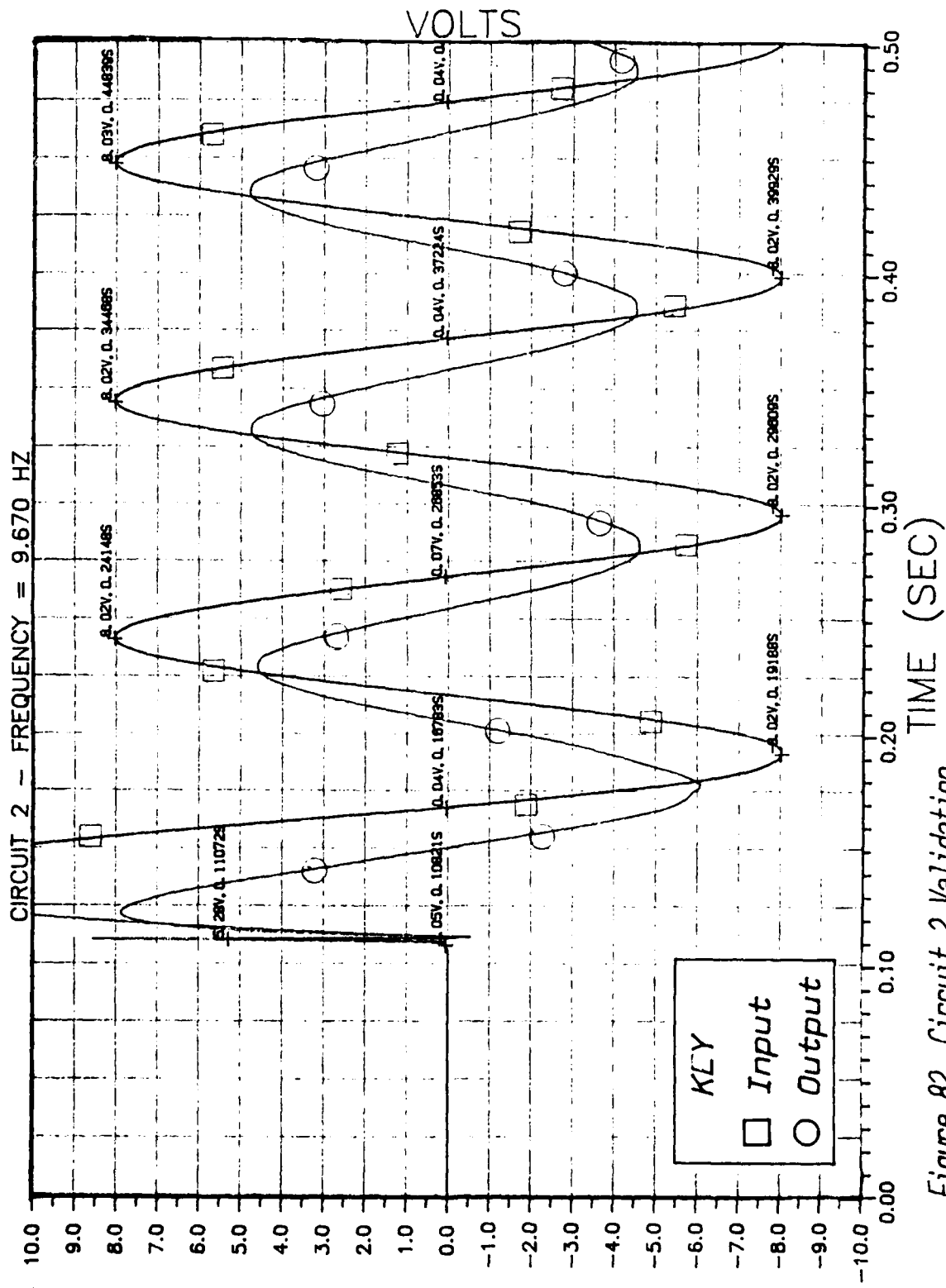


Figure 82. Circuit 2 Validation

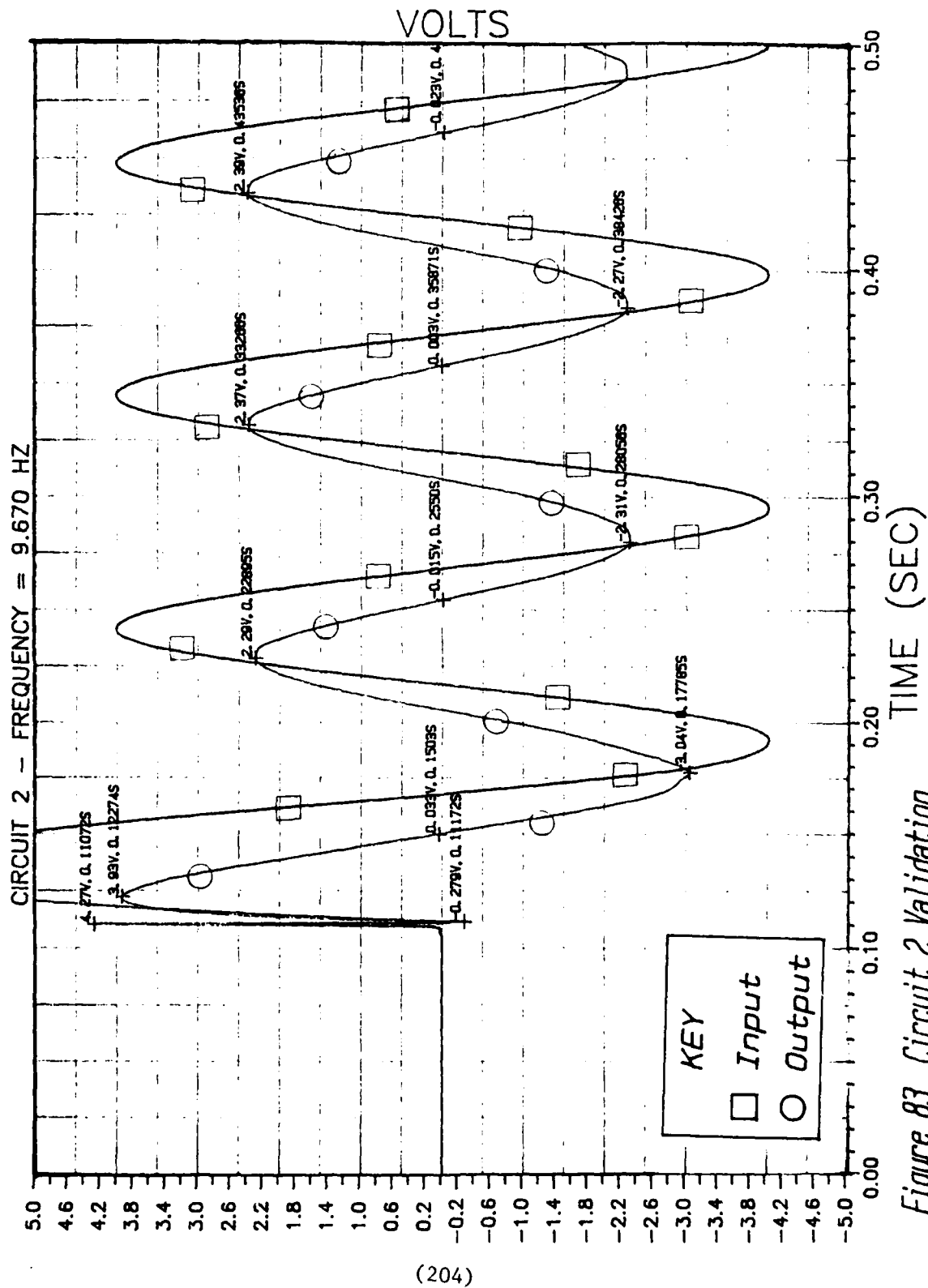


Figure 83. Circuit 2 Validation

Bibliography

1. Ross, Bertram. "Fractional Calculus," Mathematics Magazine, 50:115-122 (May 1977).
2. Torvik, P.J. and R.L. Bagley. "Fractional Derivatives in the Description of Damping Materials and Phenomena," The Role in Damping in Vibration and Noise Control, DE Vol 5, ASME Book No. H00405: 125-135, Edited by L Rogers and J.C. Simonis, NY.
3. Skaar, Steven B, et al. "Stability of Viscoelastic Control Systems," IEEE Transactions on Automatic Control, 33: 348-357 (April 1988).
4. Bagley, R.L. and Peter J. Torvik. "A Theoretical Basis for the Application of Fractional Calculus to Viscoelasticity," Journal of Rheology 27: 201-210 (May 1983).
5. Burden, Richard L. and J. Douglas Fairies. Numerical Analysis (Third Edition): 162-167, PWS Publishers Boston (1985)
6. Walker, Capt Richard. Linear Quadratic Optimal Control Theory for Viscoelastically Damped Structures Using a Fractional-Derivative Viscoelasticity Model, MS Thesis, AFIT/GA/EN/88D-13 School of Engineering, Air Force Institute of Technology (AU), Wright-Patterson AFB, OH (Dec 1988).
7. Oldham, Keith B. "Semiintegral Analysis; Analog Implementation," Analytical Chemistry 45: 39-46 (Jan 1973).
8. Torvik, P.J. and R.L. Bagley. "On the Appearance of the Fractional Derivative in the Behavior of Real Materials," Journal of Applied Mechanics 51:234-238 (1984).
9. Sze, Scott M. Physics of Semiconductors (Second Edition): 54-56.849, John Wiley and Sons, NY (1981).
10. Oldham, Keith B. and Jerome Spanier. The Fractional Calculus: 148-154, Academic Press, NY (1974).
11. Wall, Hubert S. Analytic Theory of Continued Fractions: 349-355, D Van Nostrand, NY (1948).
12. Bagley, R.L. "On The Fractional-Order Feedback In Linear Systems", Article to be Published in 1989.

13. Bagley, R.L. and Peter J. Torvik. "A Generalized Derivative Model for an Elastomer Polymer," The Shock and Vibration Bulletin, No 49: 135-143 (Sep 1979).
14. Bagley, R.L. and Peter J. Torvik. "Fractional Calculus - A Different Approach to the Analysis of Viscoelastically Damped Structures," AIAA Journal 21: 741-748 (May 1983).
15. Bagley, R.L. and Peter J. Torvik. "Fractional Calculus in the Transient Analysis of Viscoelastically Damped Structures," AIAA Journal 23: 918-925 (June 1985).
16. Ichise, S.Y. et al. "Analog Simulation of Non-integer Order Transfer-Functions for Analysis of Electrical Chemistry," Journal of Analytical Chemistry 33: 253-265 (1971).
17. Oldham, Keith B. and Cynthia G. Zoski. "Analogue Instrumentation for the Processing of Polarographic Data," Journal of Electroanalytical Chemistry 157: 27-51 (1983).
18. Franklin, Gene F. et al. Feedback Control of Dynamic Systems: 226-228. Addison-Wesley, Reading MA, (1986).
19. Kolesar, Maj Edward S., PhD, PE. Associate Professor of Electrical Engineering, Air Force Institute of Technology. Personal Interview. (15 Dec 1988).
20. Wylie, Ray C. Advanced Engineering Mathematics (Fourth Edition): 818-824. McGraw-Hill, NY (1975).
21. Churchill, Ruel V. et al. Complex Variables and Applications (Third Edition): 197-199. McGraw-Hill, NY (1976).
22. Electronic Associates Inc. TR48 Analog Computer Reference Handbook: Publication 00 800.200: 8-1. West Long Branch NJ (1966).
23. Electronic Associates Inc. Handbook of Analog Computation, Edited by Alan Curlson, George Hannauer, Thomas Carey, and Peter J. Holsberg Publication 00 800.0001-1: 85+. Princeton NJ (1966).
24. Tektronix, Inc. FG506 Function Generator Instruction Manual: 1-1 to 2-8. Beaverton OR (1986).
25. Tektronix, Inc. DC509 Universal Counter/Timer Instruction Manual: 1-1 to 2-13. Beaverton OR (1986).
26. Tektronix, Inc. SC504 Oscilloscope Instruction Manual: 1-1 to 2-29. Beaverton OR (1986).
27. Hewlett-Packard Company. Hewlett-Packard 7090A Measurement Plotting System Operators Manual: 2-1 to 6-8. San Diego (1984).

28. Tektronix, Inc. DM501A Digital Multimeter: 1-1,1-9. Beaverton OR
(1986)

VITA

Captain Kevin D. Klonoski ~~born [REDACTED]~~

He graduated in 1973 from Flint Kearsley High School. In 1975 he enlisted in the Air Force and spent 4 1/2 years as a computer operator at Charleston AFB SC. During this time he qualified and was accepted for the Air Force Airman Education and Commissioning Program. Beginning in 1980 he attended The Ohio State University, graduating in 1983 with a Bachelor of Science degree in Aeronautical-Astronautical Engineering. He received his commission through OTS, being recognized as a Distinguished Graduate, in September 1983. He was then assigned to the Shuttle Activation Task Force and subsequently Shuttle Test Group at Vandenberg AFB CA. During this time he worked first as Shuttle Launch Accessories engineer, then Orbiter Mechanical Systems engineer, and finally Ground Systems Project engineer. While at Vandenberg he received two NASA awards - The Johnson Space Center Engineering Achievement Award and the Astronaut's Personal Achievement Award. He was the 1986 Space Division nominee for the Air Force System Command's Roland R Obenland Engineering Award for his work in developing a system to eliminate explosive hydrogen buildup in the event of a shuttle launch abort. He entered the Air Force Institute of Technology in June 1987.

~~[REDACTED]~~

~~[REDACTED]~~

REPORT DOCUMENTATION PAGE

Form Approved
OMB No. 0704-0188

1a. REPORT SECURITY CLASSIFICATION UNCLASSIFIED			1b. RESTRICTIVE MARKINGS		
2a. SECURITY CLASSIFICATION AUTHORITY			3. DISTRIBUTION/AVAILABILITY OF REPORT Approved for public release; distribution unlimited		
2b. DECLASSIFICATION/DOWNGRADING SCHEDULE			5. MONITORING ORGANIZATION REPORT NUMBER(S)		
4. PERFORMING ORGANIZATION REPORT NUMBER(S) AFIT/GA/ENY/88D-05			7a. NAME OF MONITORING ORGANIZATION		
6a. NAME OF PERFORMING ORGANIZATION School of Engineering	6b. OFFICE SYMBOL (If applicable) AFIT/ENY	7b. ADDRESS (City, State, and ZIP Code)			
6c. ADDRESS (City, State, and ZIP Code) Air Force Institute of Technology Air University Wright-Patterson, AFB OH 45433-6583		9. PROCUREMENT INSTRUMENT IDENTIFICATION NUMBER			
8a. NAME OF FUNDING/SPONSORING ORGANIZATION	8b. OFFICE SYMBOL (If applicable)	10. SOURCE OF FUNDING NUMBERS			
8c. ADDRESS (City, State, and ZIP Code)		PROGRAM ELEMENT NO.	PROJECT NO.	TASK NO.	WORK UNIT ACCESSION NO.
11. TITLE (Include Security Classification) See Block 19					
12. PERSONAL AUTHOR(S) Kevin D. Klonoski, Captain, USAF					
13a. TYPE OF REPORT MS Thesis	13b. TIME COVERED FROM _____ TO _____	14. DATE OF REPORT (Year, Month, Day) 13 March 1989	15. PAGE COUNT 222		
16. SUPPLEMENTARY NOTATION					
17. COSATI CODES			18. SUBJECT TERMS (Continue on reverse if necessary and identify by block number)		
FIELD	GROUP	SUB-GROUP	Feedback Amplifiers, Circuits, Control Theory		
20	04		Damping, Differential Equations, Derivatives		
12	09		Viscoelasticity		
19. ABSTRACT (Continue on reverse if necessary and identify by block number) Title: Fractional-Order Feedback in Linear Systems Thesis Chairman: Lt Col Ronald Bagley Assistant Professor of Aeronautical Engineering					
20. DISTRIBUTION/AVAILABILITY OF ABSTRACT <input checked="" type="checkbox"/> UNCLASSIFIED/UNLIMITED <input type="checkbox"/> SAME AS RPT. <input type="checkbox"/> DTIC USERS			21. ABSTRACT SECURITY CLASSIFICATION UNCLASSIFIED		
22a. NAME OF RESPONSIBLE INDIVIDUAL Ronald Bagley, Lt Col, USAF			22b. TELEPHONE (Include Area Code) (513)-255-3517	22c. OFFICE SYMBOL AFIT/ENY	

SUMMARY: Feedback of the $1/2$ and $3/2$ derivatives as well as x and \dot{x} is demonstrated for a second-order system defined by the differential equation:

$$m\ddot{x} + c_1 D_t^{3/2}(x) + c_2 \dot{x} + c_3 D_t^{1/2}(x) + kx = u(t)$$

Three methods of producing the fractional derivative or integral of an input signal are investigated. The method selected employs a circuit developed at Trent University, Ontario, Canada for use in electrochemistry research. The circuit performs the mathematical operation $d^{\nu}(\)/dx^{\nu}$ for $-1 < \nu < 1$; negative values of ν represent integration. The results presented show the circuit accurately differentiates a sinusoidal input for a frequency range spanning 0.01 Hz to 10.0 Hz.

The second-order differential equation above is simulated on an analog computer. An optimal $u(t)$ is then used for feedback modification of the original open-loop system. Improved system performance resulted.

A Laplace transform method and a Mittag-Leffler expansion provide analytical predictions of the system's response. The output of the two methods is identical. Comparison of the theoretical predictions with the experimental data shows excellent agreement with respect to the initial transient behavior and asymptotic behavior of the steady-state response for both the open- and closed-loop systems.